(3)

ATTITUDE REFERENCE DEVICES

ATTITUDE REFERENCE DEVICES

FOR

GUN-LAUNCHED ROCKET VEHICLES

BY

WILLIAM BARRY HILL

A Thesis

Submitted To The Faculty of Graduate Studies

in Partial Fulfilment of The Requirements

For The Degree

Master of Engineering

McMaster University

October, 1967

MASTER OF ENGINEERING (1967) (Mechanical)

McMASTER UNIVERSITY Hamilton, Ontario.

TITLE: Attitude Reference Devices for Gun-Launched Rocket Vehicles

AUTHOR: William Barry Hill, B.Eng., McMaster University

SUPERVISOR: Dr. G. Kardos

NUMBER OF PAGES: xiii, 266

SCOPE AND CONTENTS: A proposal is made to extend the present capabilities of gun-launched rocket vehicles to include attitude control during flight. The problems involved are stated and design criteria for possible sensors are listed. A review of presently available sensing devices is made and rejection of unsuitable instruments is based on fundamentals of their design and operation.

A report is made upon the sensors which most adequately fulfil the harsh environmental requirements of gun-launch. These sensors are infared-horizon sensors and a tuning fork vibratory gyroscope. A preliminary design is given for the tuning fork gyroscope as well as a summary of fundamental design considerations.

ACKNOWLEDGEMENTS

The author wishes to express his appreciation for the assistance given him by many people in the preparation of this thesis. He would like to thank particularly Dr. G. Kardos for his advice and guidance at the beginning of the programme. Thanks are also due to Mrs. A. Woodrow for her long hours of careful typing.

The programme was supported by a Ford Foundation Scholarship in Design awarded by the Department of Mechanical Engineering, McMaster University. The author gratefully acknowledges receipt of this award.

LIST OF ILLUSTRATIONS

CHAPTER 7

CHAPTER 8

CHAPTER 9

CHAPTER 10

CHAPTER 11

CHAPTER 12

CHAPTER 13

CHAPTER 14

CHAPTER 16

APPENDIX A

APPENDIX B

TABLE OF CONTENTS

PART I
INTRODUCTION

PART 2

HORIZON SENSING METHODS

PART 3

CELESTIAL SENSING METHODS

PART 4

AMBIENT-FIELD SENSING METHODS

PART 5

INERTIAL SENSING METHODS

PART I

INTRODUCTION

CHAPTER I

DESIGN PROJECT PROPOSAL

1.1 SCOPE OF PROPOSAL

The following proposal was submitted to the Space Research Institute in October, 1966 and its contents initiated the study which resulted in the body of this thesis.

1.2 CONTENTS OF PROPOSAL

GRAPHS AND TABLES

1.3 PART ONE

PROPOSAL INTRODUCTION

The High Altitude Research Programme initiated by McGill University has offered a logical alternative to the conventional sounding rocket for probes into the upper atmosphere. Experiments have shown the gun-fired probe vehicle to be economically superior to present sounding rockets for certain experiments.

In view of the proven feasibility of such a system, and the areas of study in Meteorology, Re-entry and Meteor Physics still untouched, it would seem advantageous to develop a gun-launched research vehicle capable of self control and high altitude manoeuvers such as would be required for the above experiments.

The Department of Mechanical Engineering of McMaster University therefore proposes to the Space Research Institute of McGill University an engineering design study in which known methods of direction references will be examined and their suitability to withstand acceleration rates of the order of 10,000 g will be assessed. The performance of each reference system will be rated on its capacity to provide for vehicles a direction reference after gun launch. The above programme will terminate approximately one year from the date of submission of this proposal. At that time a report will be submitted which will list all direction reference systems considered, a synopsis of the state of the art of each type, and evaluation of feasible types with respect to gun-launch accelerations, and a recommendation for further development of selected reference systems.

1.4 PART TWO

DETAILED DISCUSSION

SECTION ONE

CONSIDERATIONS OF THE DESIGN STUDY PROGRAMME

The system performance requirements of the Martlet II directional and altitude control system will be in accordance with limits outlined by the Space Research Institute. While it is known that a guidance system is presently in development, it is realized that certain limitations are inherent in the components and thus in the utility of the vehicle. Therefore the ideal guidance system would be required to fulfill the following conditions:

(1) ability to function independently of varying meteorological and solar conditions.

(2) adaptability to a wide range of trajectories.

(3) capacity for abrupt change of trajectory while in flight.

(4) capacity to stabilize finless projectiles while in flight.

(5) ability to withstand 10,000 g acceleration forces.

The above requirements are in some cases logical extensions of existing vehicle systems and it is not impractical to expect that such a system could be constructed.

As the proposed system will ultimately be required to conform to the gun-launched vehicle in terms of geometry, weight, and operating characteristics, relevant performance parameters will have to be supplied by the Space Research Institute. The subsequent report will then outline the requirements and modes of operation of the direction reference system so that further development of system components and auxiliary equipment can take place.

1.5 SECTION TWO

WORK STATEMENT AND PROGRAMME SCHEDULE

The programme outlined will be carried out from the time of acceptance of this proposal to October 1st, 1967. The main steps are listed below and their approximate performance schedule is indicated with the bar graph shown in Figure 1. This work programme is geared to the development of a design concept and its analytical characteristics.

The steps in the work programme are:

1. Literature search to determine known methods of direction reference. Radio inertial, full inertial, celestial reference inertial and homing type guidance systems and components will be covered. New developments applicable to attitude reference systems will be noted. The operating characteristics and present applications will be summarized

in a "state of the art" report for each method.

2. Classification according to type (electronic, mechanical), function (external, internal, open or closed loop) and any other operational category necessary will be made. Preliminary elimination of unsuitable approaches will then take place.

3. The most suitable systems will be critically examined for their resistance to high rates of acceleration (10,000 g's). Their structural integrity and reference accuracy will be carefully noted and compared with requirements for gun-launched vehicles. This step will be carried out analytically and experimentally.

4. Based on the above investigations, a direction reference system concept will be proposed, along with the expected operating characteristics. These should coincide with the Space Research Institute's requirements.

1.6 SECTION THREE

COSTS OF THE DESIGN PROGRAMME

To keep this project in line with the Space Research Institute's requirements and to assure that sufficient and accurate information is obtained from suppliers and other research centres, personal visits to places of interest by the research worker will be necessary. Estimated travelling expenses are shown in Table 1. A stipend for the research worker during the months of May to October should bring the total cost to approximately $3,000.00.

1.7 COST TABLE

TABLE NO. 1

ESTIMATED COSTS OF PROGRAMME
PERIOD OF NOV. 1/66 TO NOV. 1/67

ITEM	DESCRIPTION	COST
TRANSPORTATION	1. Montreal (approx. 12 trips)	$ 840.00
	2. U.S. Research Centres (approx. 4 trips of 5 days each)	912.00
SUPPLIES	Equipment, Books, Reprints, Report	125.00
STIPEND	May 1/67 to October 15/67	1,200.00
	TOTAL . . .	$ 3,077.00

Note: Trip estimates based on:

(1) Economy return flight fares from Toronto to points of interest. (prices quoted October 20th, 1966).

(2) Daily expense allowance of $18.00.

1.8 PROGRAMME SCHEDULE GRAPH

FIGURE NO. 1

GRAPH SHOWING SCHEDULE OF PROPOSED WORK PROGRAMME

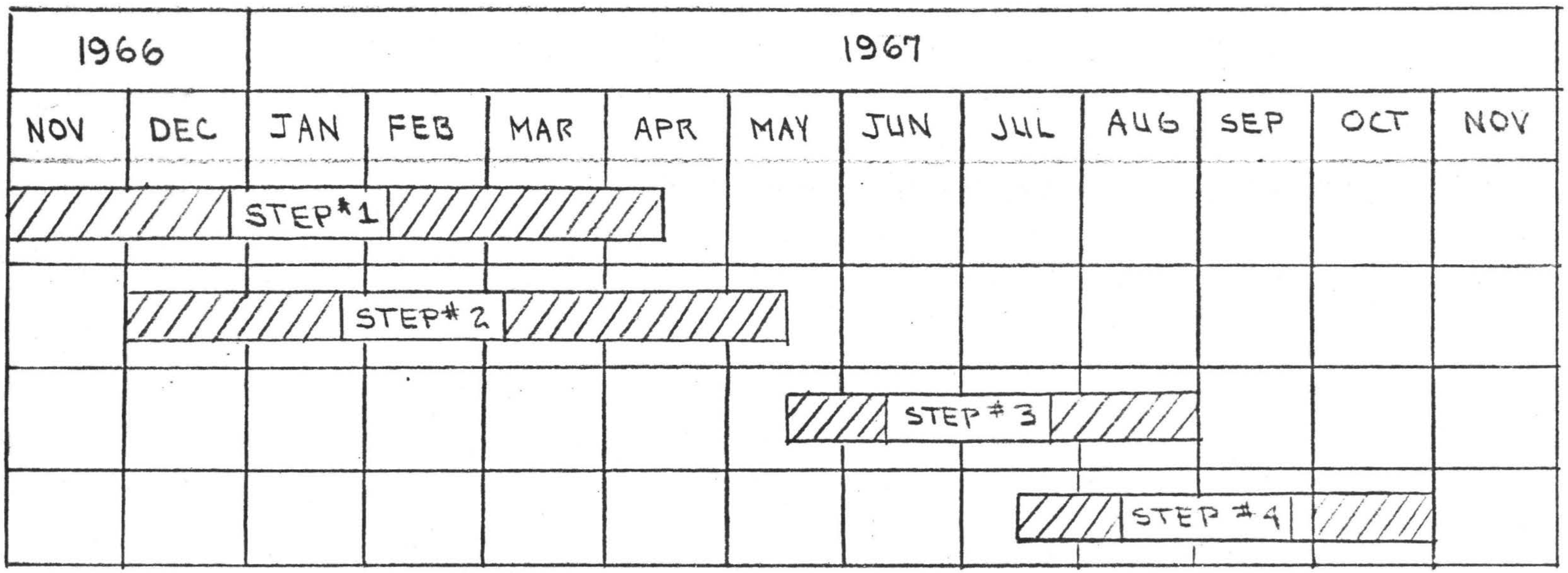

Step No. 1	Literature Search
Step No. 2	Classification of System Types: State of Art Report on each Type
Step No. 3	Evaluation of Selected Systems
Step No. 4	Preparation of Resulting System Proposal

1.9 REFERENCE LIST

PROPOSAL REFERENCES

1. KOELLE - "Handbook of Astronautical Engineering", McGraw-Hill, 1966.

2. BOYD - "Space Research by Rocket and Satellite", Harper, 1960.

3. KARDOS - "Notes on Mechanical Design of Gun Launched Vehicles", TN65-2 Mechanical Engineering Laboratories, McGill University, 1962.

4. S.R.I. - "Project HARP", McGill University Staff Report.

5. A.E.L. - "Martlet IV Orbit Injection Control", Proposal No. 9290, Aviation Electric Ltd., Montreal.

6. A.E.L. - "Progress Report No. 1, Orbit Injection Control", AETR 13484, Aviation Electric Ltd., Montreal.

7. A.E.L. - "Progress Report No. 4, Orbit Injection Control", AETR 13565, Aviation Electric Ltd., Montreal.

1.10 COMMENTS ON PROPOSAL

During the course of the programme the Space Research Institute experienced grave financial difficulties. The support requested for this programme was not available, thus the scope of this project was limited. Security restrictions by both government and industry also prevented detailed studies in certain areas.

That the project be brought to a close in one year was still accepted as a fundamental criterion however. The report that follows is thus a product of the aims stated in the proposal tempered by the developments over the period of investigation.

The system proposed at the end of this report as a solution to the problems outlined in the proposal is considered by the author to be the best choice based on the unclassified information available to him at the time of the investigation. The proposed system satisfies all of the original criteria stated in Part Two, Section One of the Proposal.

It must be realized that other sensors may become more attractive than the ones chosen when more information becomes available. The most likely candidates are thus indicated and sufficient information is included in the report so that it may be used as basic reference material for more advanced work.

CHAPTER 2
DEVELOPMENT OF PROGRAMME FORMAT

2.1 INTRODUCTION

The initial step in any design programme is the determination of system constraints and design criteria. These are subsequently combined with the data on various devices capable of performing the required function. An engineering solution is then sought. Thus, the body of this thesis begins with a statement of the mission characteristics and vehicle behaviour. General design and performance criteria are then developed for attitude sensors. A listing of various modes of approach to attitude sensing is made as the closing section of this chapter.

2.2 THE MISSION

The vehicle, in which the proposed sensors must operate, is a small spinning rocket of the type illustrated in Figure (2.1). This rocket is the second stage of a ballistic vehicle which is fired from a large bore naval cannon. The control system, of which the sensors are a part, must successfully steer the second stage into a predetermined earth orbit. The payload to be orbited would be a small instrument package used for upper atmosphere research. The mission profile is outlined in Figure (2.2).

2.3 THE LAUNCH ENVIRONMENT

The ballistic two stage vehicle is fired from a 16.4 inch bore cannon having a 100 foot long barrel. The launch acceleration would be of the order of 7000 g's and acceleration time would be around 30 milliseconds. The launch shock would be semi-sinusoidal.

After the vehicle leaves the barrel it would experience and acceleration near 2000 g's in the direction opposite to the direction of travel. This latter acceleration is due to the relaxation of strains imposed upon vehicle structure during launch.

When the second stage engine is fired the system experiences an additional acceleration of 30 g's. The time of flight for this second stage is 10 minutes. This is also the operation time for the control system. Thus the sensors need not be operating during the actual gun firing period.

The temperatures to be experienced by the sensors and associated electronics has been taken as 25°C ± 15°C. Altitudes would range from sea level to 350 nautical miles.

At this stage of development, one would be content with the best accuracy obtainable. As a cutoff point, however, the previous specification of ± 1° at 0° pitch (injection) given by Space Research Institute to Aviation Electric Ltd. (August 1965) will be used.

2.4 THE CONTROL SYSTEM

The large pitch angle precession that is required for orbit injection combined with the short operating time of the system precludes the use of small natural forces associated with natural phenomena as actuation mechanisms. Such natural phenomena are the earth's gravitational and magnetic fields, and the sun's radiation field. Aerodynamic pressures are also insignificant at the altitudes near 200,000 feet, where the system would be operating. A reaction control system is thus required.

The mathematical study of control systems for spinning bodies usually employs the well-known Euler's equations describing the rotational motion of a body subjected to body torques. Euler's general equations can be approximated for spin axis symmetrical bodies by the two equations

$$A\dot{\omega}_1 + (C-A)\,\omega_2\,\omega_3 = M_1 \qquad (1)$$

$$A\dot{\omega}_2 - (C-A)\,\omega_1\,\omega_3 = M_2 \qquad (2)$$

where C is the moment of inertia about the axis of symmetry and A is the moment of inertia about the cross-body axes. Figure (2.3) illustrates the orientation.

Figure (2.3) also shows two Euler angles θ and ψ required to determine an attitude for the vehicle. By designing a reaction control system within the rocket, whose servo-null conditions are satisfied only when it has achieved the attitude representing the desired rotations, the essential elements for attitude control are provided.

The spinning body control system mechanization requires that torques, given as M_1 and M_2 above, be applied to the body with such time and spatial phasing as to cause the rocket to proceed through the desired rotations to the required attitude. The spinning vehicle behaves according to the gyroscopic law when the torques are applied about its centre of gravity.

Cold gas reaction control systems for spinning vehicles have been developed by Aviation Electric Limited, Montreal, and the Whittaker Corporation, California. The AEL system employs four nozzles mounted at the rear of the vehicle and is used for both spin speed control and orientation. The Whittaker system employs one nozzle and can be used only for attitude control. Figure (2.4) is a detailed block diagram of the Whittaker system and is included to illustrate the components required for a typical system. Such systems as Whittaker's have proven themselves feasible for vehicle control in "low g" vehicles and there is no fundamental reason why they would not work in "high g" vehicles provided sensors can be found which will survive the gun launch conditions.

It should be noted that for spinning vehicles two Euler rotations can achieve any desired pointing in space. Thus only two attitude sensors are needed, one for pitch and one for yaw. Finally, only two channels of computational electronics are needed.

2.5 SYSTEMS IN WHICH THE SENSORS ARE USED

Care must be taken to distinguish between control techniques and sensing techniques and the manner in which these numerous methods may be combined to achieve an overall vehicle guidance system. Some space is thus devoted here to describing the general design philosophies of injection guidance.

Orbit injection guidance can be accomplished using one of three fundamental system concepts; programmed attitude, radio or inertial.

Programmed-attitude systems cause the vehicle to precess itself through predetermined angles as a function of time rather than as a function of its environment. The sensing of angular

$$A\omega_1 + (C-A)\,\omega_2\,\omega_3 = M_1$$

movement is necessary to generate cutoff signals to the precession rockets. In conventional rockets this has been accomplished by

$$A\dot{\omega}_2 - (C-A)\,\omega_1\,\omega_3 = M_2$$

state-of-the-art rate gyros. The control system is open loop. No decision processes are carried out on board.

Radio control systems are of two main types; those which sense the vehicle orientation with radar methods and those which use on-board sensors and relay their pickoff signals to the ground. In both cases actual reference information and computational facilities are located on the ground. Actuation signals are relayed back to the vehicle.

Inertial systems are usually completely self contained. An inertial platform provides a coordinate system which is stable in space. Additional inertial sensors, mounted on this platform detect rotations and accelerations in this co-ordinate system. An on-board computer obtains position and velocity by numerical integration of the acceleration indicated by the inertial platform's sensors. Only the initial conditions and constants loaded into storage prior to launch are required from a ground-based computer after the airborne computer has been programmed. Advantages of this guidance system lie in its great flexibility in trajectory selection and its closed loop design. It is not necessary to predict beforehand the disturbing forces that might act on the vehicle. A great disadvantage is the large number of inertial sensors required to stabilize the platform and detect vehicle motion.

A new development in inertial systems has been the elimination of the stable platform arrangement. Recent advances in the speed and capacity of airborne computers has made it feasible to maintain the inertial reference in the computer and mount the sensors directly to the frame of the vehicle. Such systems are termed "strapped-down" and will be discussed further later.

The control system described in Section (2.4) could be adopted to any of the programmed-attitude radio or inertial concepts. From a hardware point-of-view, the programmed-attitude systems have the least number of components, the lowest range costs and the lowest accuracy requirements for sensors and computers. They also, as a consequence, have the lowest accuracy for orbit injection.

Programmed attitude systems have an adaptibility to varied trajectories which is equal to the adaptibility of inertial systems. While these considerations are not in the same category as design criteria, they are important factors to be noted for future consideration.

2.6 ATTITUDE REFERENCE SYSTEM ALIGNMENT

The initial alignment of the attitude reference co-ordinate system is an important design consideration. For self contained and radio-aided inertial systems alignment is accomplished before launch and the attitude sensors are in operation throughout the lift-off period.

For gun-launched vehicles it is not likely that the sensors can be expected to operate during the period of gun launch. This approach may result in a situation in which the sensors begin to operate after a large vehicle misalignment has already occurred. If body rate sensing methods were used, the sensor could not detect this inital misalignment. The same is true for displacement gyroscopes. References to fixed points in space (stars,planets) may be made instead. However, their observation may be prevented by cloud conditions or by movement from the sensor's field of view.

It is therefore apparent that tradeoffs will be made between system concepts and allowable accuracy in the final selection.

2.7 DESIGN CONSTRAINTS

From the foregoing discussions one can determine general guidelines to aid in subsequent sensor evaluation. The most important characteristics are listed below.

LIST OF DESIRED SENSOR CHARACTERISTICS

1. Sensor must withstand gun launch (7000 g) without loss of sensitivity.
2. Support equipment (electronics) must be capable of surviving gun launch in working order.
3. Sensors and related equipment must be compact and light in weight to increase payload (i.e. less than 10 lbs. and 200 cu. in.).
4. Acceleration sensitive drifts should be small as device operates during boost phase.
5. Operation time need not exceed 15 minutes.
6. The device must function in a spinning vehicle.
7. Initial system alignment should be simple and easy to accomplish (especially during flight).
8. The system must be able to function at any hour of the day or night.
9. Weather conditions (up to the capabilities of the vehicle itself)should not affect the attitude sensor's operation.
10. The device chosen should have a proven feasibility and use proven components and proven design techniques as much as possible. Design and development of new highly specialized component items should be kept to a minimum.

NOTE: As the primary concern of Space Research was to obtain a system capable of just surviving the launch environment while fulfilling the above ten conditions and since no real criteria exist to judge whether or not a gun-launched system is good or bad, considerations of accuracy and power will be left to a further analysis, beyond the scope of this initial survey.

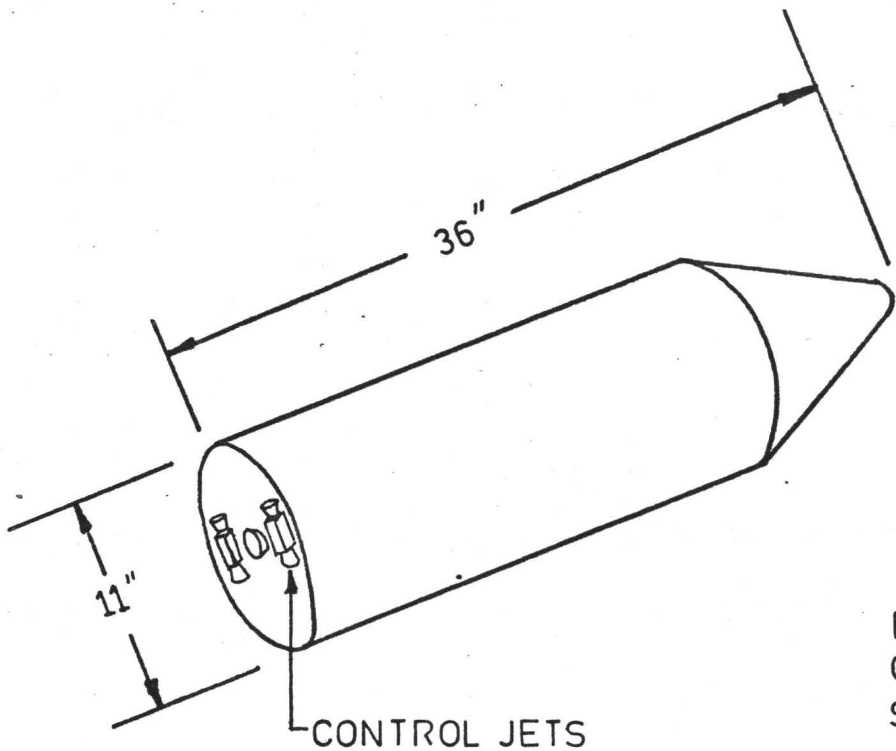

DIMENSIONS ON THE DRAWING ARE GIVEN TO ILLUSTRATE RELATIVE SIZE ONLY.

SPIN SPEED - 5 REV/SEC
WEIGHT ≃ 100 LBS.(WITHOUT FUEL)

TITLE: TYPICAL VEHICLE	
SCALE: NONE	SOURCE: REF. 1 & 2
DRAWN BY: HILL	FIGURE NO: 2-1

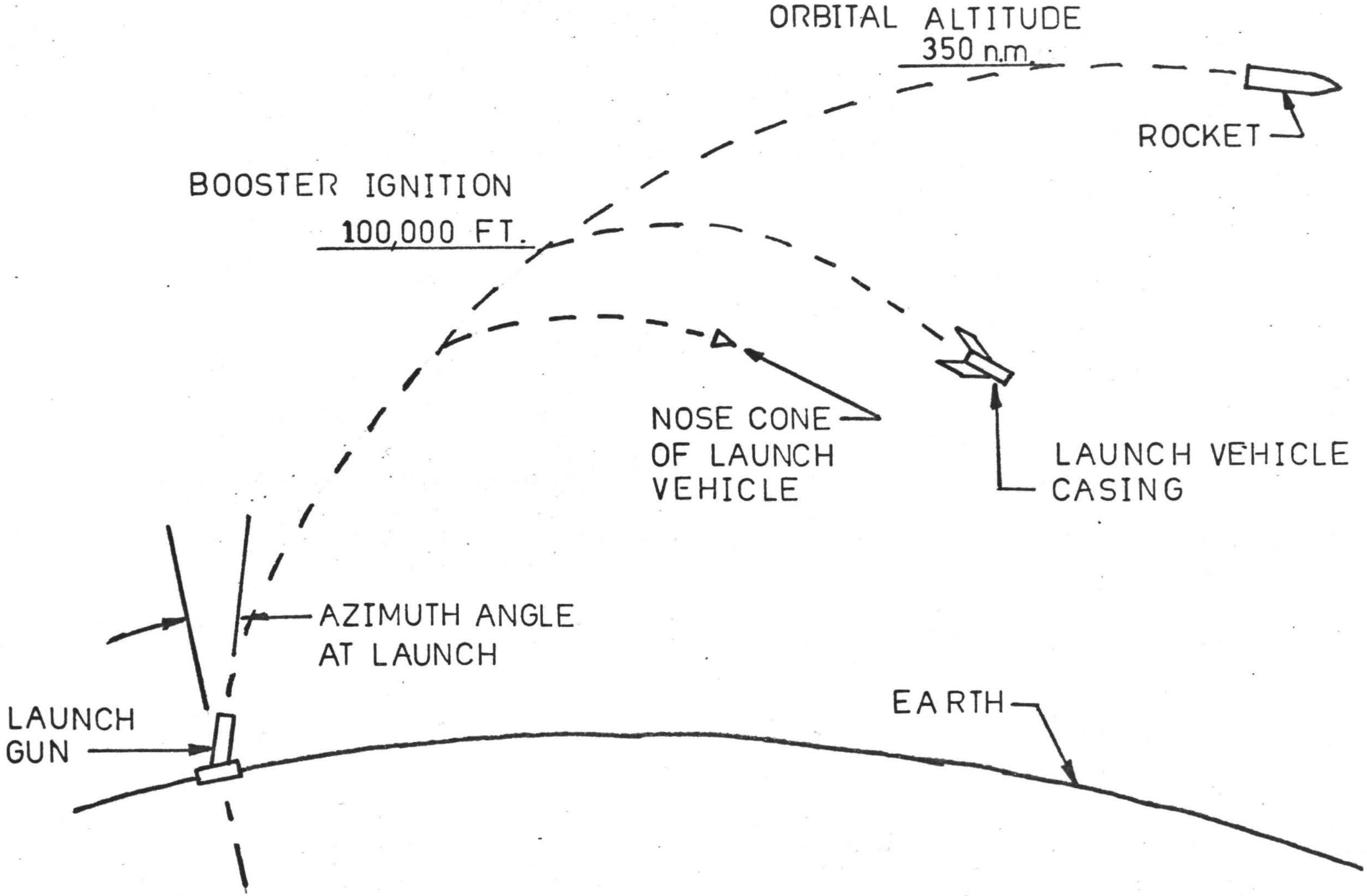

TITLE: TYPICAL MISSION PRÔFILE	
SCALE: NONE	SOURCE: REF. 2
DRAWN BY: HILL	FIGURE NO: 2-2

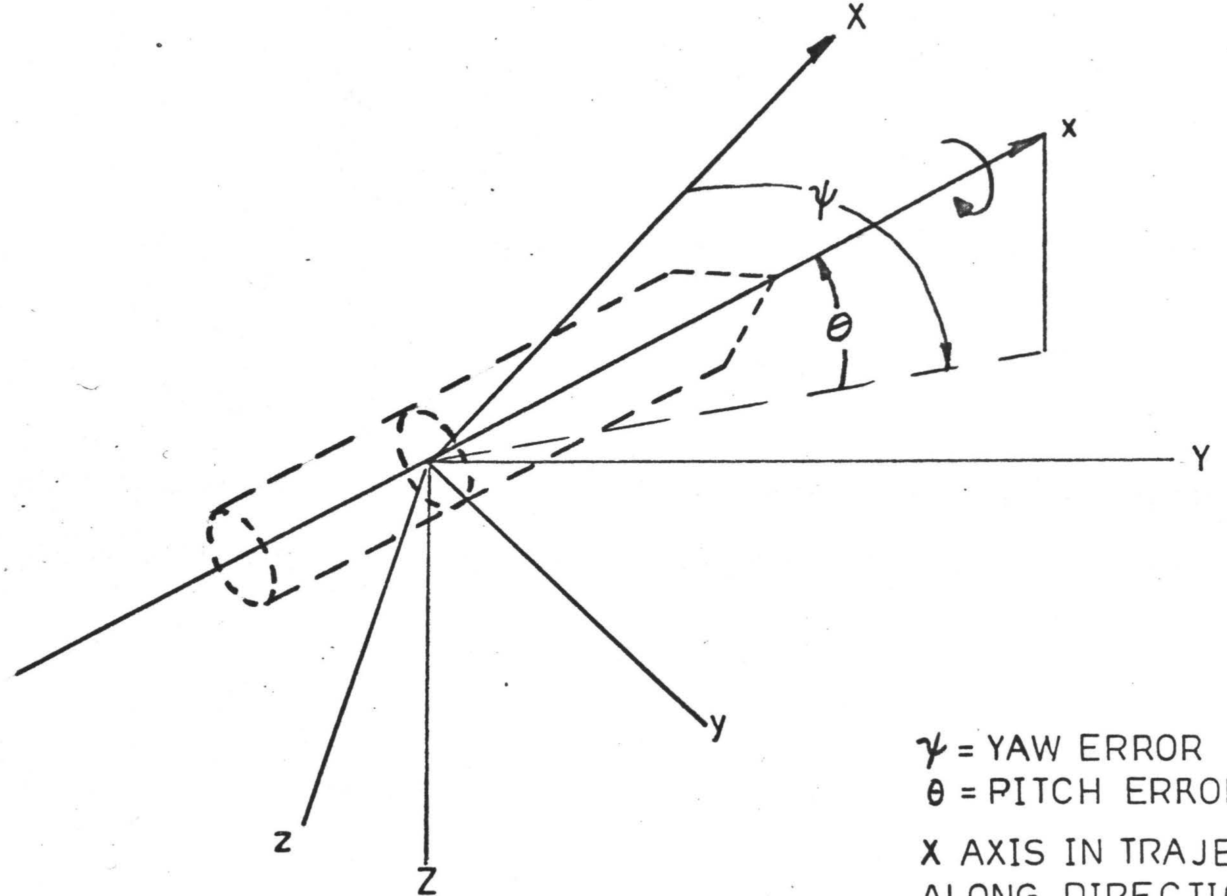

ψ = YAW ERROR
θ = PITCH ERROR

X AXIS IN TRAJECTORY PLANE, ALONG DIRECTION OF TRAVEL
x AXIS IS VEHICLE ROLL AXIS

TITLE: ERROR ANGLES	
SCALE: NONE	SOURCE: NONE
DRAWN BY: HILL	FIGURE NO: 2-3

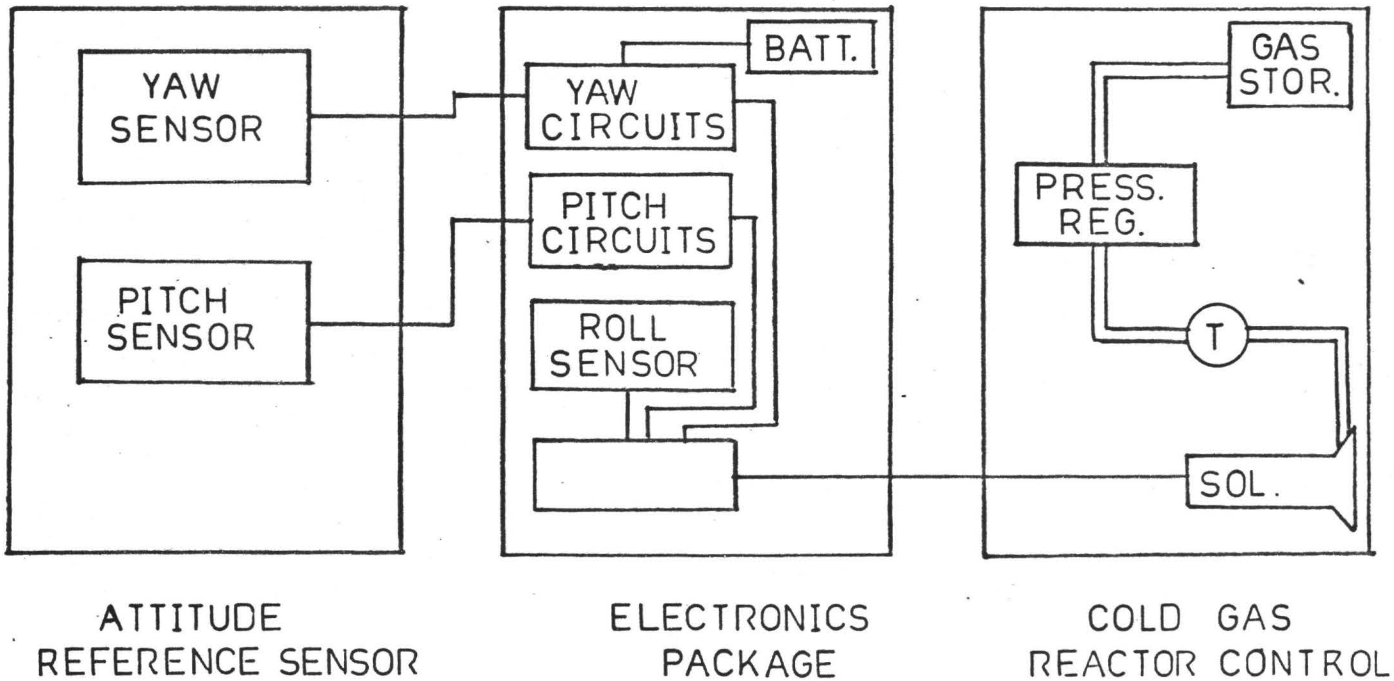

TITLE: WHITTAKER SYSTEM DIAGRAM	
SCALE: NONE	SOURCE: REF. 3
DRAWN BY: HILL	FIGURE NO: 2-4

REFERENCES

1. Aviation Electric Limited, Proposal No. 9290, Martlet IV Orbit Injection Control System, June 12, 1964.

2. Aviation Electric Limited, AETR 13565, Martlet IV Orbit Injection Control System, Progress Report No. 4, August 30, 1965.

3. Whittaker Corporation, Controls and Guidance Division, "Attitude Control of Spinning Payloads", 1966.

4. Thomson, W. T., Introduction to Space Dynamics, Wiley, New York, 1961.

5. Freed, L. E., "Attitude Control System for a Spinning Body", ARS Journal, March, 1962, pp. 396-401.

6. Space Research Institute, McGill University, Analysis of Orbital Injection Control System, prepared by M. Delfow and H. L. Brants, August 25, 1965.

CHAPTER 3

A SURVEY OF ATTITUDE SENSORS

3.1 INTRODUCTION

This chapter investigates the manner in which attitude may be sensed. The various sensing methods applicable to the problem of orbit injection are listed. A preliminary examination of these approaches is made and a selection of those methods most worthy of closer inspection is presented.

3.2 DETERMINATION OF ATTITUDE

Vehicle attitude can be established by direct observation or by the on-board determination of any two non-colinear lines in space. Because of the multiple ground stations that would be required for adequate coverage of a variety of trajectories, line of sight systems such as radar tracking and radio control must be eliminated due to high range costs.

Various physical phenomena can be sensed and used to define a reference line in space against which the vehicles orientation can be referred. These various sensing modes are listed below.

METHODS AVAILABLE FOR ORIENTATION DETERMINATION

1. Determination of Earth Line by Infared Horizon Sensing.
2. Planet Tracking
3. Star Tracking
4. Determination of Earth Line by Gravity Field Determination

5. Earth's Magnetic Field Sensing.

6. Sun Line Sensing.

7. Orbital Plane Determination by Inertial Methods (e.g. Body Rate Sensing).

Many of the methods listed above are not included in discussions of state-of-the-art rocket control systems for orbit injection. In fact, except for inertial sensors, the above methods are generally considered for satellite or space vehicle orientation systems. This limitation is shown to be quite arbitrary however, when the fundamentals of operation are considered.

3.3 SENSOR CATEGORIES

Because of similarities in operation or in system design many of the methods listed in Section 3.2 may be grouped together for easier discussion. These groupings will be as follows.

Celestial sensing methods will include planet and star sensors Sun detection schemes will be described in detail.

Ambient Field Sensing Techniques will describe current methods of detecting gravity field and magnetic field of the earth.

Horizon sensing methods are treated separately because their development has been greatest among the scanning methods. The literature on infared scanning techniques is extensive. Their application to spinning vehicles is comparatively easy.

The final grouping covers the various types of inertial sensors presently considered to be the most worthwhile for development. Details of their operation and design are included.

PART 2

HORIZON SENSING METHODS

CHAPTER 4

HORIZON SENSING FOR ATTITUDE DETERMINATION

4.1 INTRODUCTION

Horizon sensing is a procedure which can be employed in attitude reference systems for determining the vehicles orientation with respect to a planet-centered local vertical. The basic method for determining the local vertical involves the detection of the discontinuity between space and each side (or horizon) of the planet. Horizon sensors are radiation detectors that sense the sharp increase in radiation between the earth and deep space at the horizon.

4.2 PHENOMENA TO BE DETECTED

There are several physical phenomena which may be used to define the earth's horizon. Singer [1]*, Holler [2], Hanel [3] and Plass [4] discuss the several alternatives.

(1) The albedo of the earth: The horizon is seen as the gradient between the apparent surface of the earth, which reflects sunlight, and the blank space beyond, which does not.

(2) The air glow around the earth: The upper portion of the earth's atmosphere radiates energy owing to excitation by the sun. The intensity is low, varies with time and position and very little data is available.

---

* Numbers denote the references at the end of this chapter.

(3) Infared Radiation from the Earth: The earth's horizon may be defined as the sharp gradient of infared radiation which exists at the limb or border between it and outer space.

As a first approximation, if one looks at the earth-space interface from a sufficiently high altitude, the earth appears to radiate as a black body having a temperature of approximately 270°K, in contrast with the surrounding space which is at 0°K. Thus if a transducer is capable of detecting this difference in radiation, it will generate a signal proportional to the difference in radiation. Figure (4.1) is an example of a scan signal from Tiros III shows the wave form to be expected. Because the earth has a fairly uniform temperature, this gradient can be used for navigation during either day or night conditions.

The actual radiation processes involved in the atmosphere is beyond the scope of this report. Details are available in references by Howard [5], Plass [4,6] and Wark [7]. In brief, however, it will be said that background of natural infared vibration emitted by the ground and atmosphere is determined by the absorption bands of the atmsopheric molecules and by the emission characteristics of emitting surfaces such as the ground, oceans or clouds. The same absorption bands determine the radiative flux in the atmosphere and its variation with altitude.

In the infared range of spectral emission, the sharpness of the horizon depends upon the vertical temperature and pressure profiles and on the distribution of absorbing (and therefore emitting) matter in the atmosphere. Hanel, Bandeen and Conrath [3] have carried out investigations on the radiance emitted by the earth in five spectral intervals. Calculations were made for various latitudinal, seasonal, climatic and meteorological conditions.

Curves of radiance in the 15 micron CO_2 band versus distance about the horizon are shown in Figure (4.2). These curves were chosen for illustration because they show the most consistency with respect to radiance and cut-off values. The final results of the above report [3] are shown in the table in Figure (4.3).

This table points out the advantages of the long wavelength high absorption regions between 14 and 16 and beyond 21 microns. Uncertainties in the horizon (Δh) caused by meteorological and seasonal effects are lower, radiance values are higher and the contrast across the disk of the Earth is low compared to values in the shorter wavelength region. Experimental values of radiance from Tiros 7 show that these calculated values are quite accurate.

Instrument techniques for wavelengths longer than 30 microns are not as highly developed as those for the shorter wavelengths. The 15 micron CO_2 band, however, is well within the convenient operating range of thermal detectors. These facts, coupled with the relative stability of the 15 micron band during meteorological disturbance make the choice of a 14-16 micron horizon scanner a most logical one.

4.3 RADIATION SENSORS

The various types of radiation detectors that could be employed are discussed in detail by Howell [9], Powell [10], Leybourne [11], Dewaard and Wormser [12]. The main ones are listed below.

1. Radiation Thermocouples
2. Pneumatic Type Detectors

   The incident radiation produces a temperature (and thus a pressure) change in a confined gas sample. The pressure change is sensed.
3. Bolometer Type Detectors

   The two main possibilities here are the metal strip and the thermistor instrument.

Hanel [13], Gedance [14] and Astheimer [15] report that the most highly developed device and the one which has already been subjected to the gun launch environment is the thermistor bolometer [16]. This device will now be discussed.

4.4 THERMISTOR BOLOMETERS

A. Design and Operation

Thermistor bolometers, according to Jones [17] and

Wormser [18] are fast, sensitive infared detectors with good responsivity from 1 to 15 microns. The detectors consist of a thin flake of thermistor material mounted on a thermal sink. The active element is a thin semiconductor film usually composed of oxide mixtures of manganese, nickel and cobalt. A thermistor bolometer cross-section is shown in Figure (4.4). A schematic bridge circuit is illustrated in Figure (4.5).

The thermistor detector operates by virtue of a resistance change produced by incident radiation.

In order to achieve fast response, thermistor films or "flakes" are attached to good heat conducting thermal sinks. These may range from quartz or glass backings for the flakes, to miniature coolers employing the Joule-Thompson effect described by Goodenough [19]. The refrigerant is a gas, bottled at high pressure. Typical time constants range from 3 to 8 milliseconds.

The minimum signal levels which can be detected by thermistor flakes are in the order of 10^{-8} to 10^{-9} watts. These radiation signals cause temperature changes of the order of 10^{-6} to 10^{-7} degrees centigrade in the flake and produce output signals in the order of one microvolt.

B. Performance Criteria

For infared systems in general the major criterion for good performance is the minimum signal that can be detected. Since this is always limited by extraneous signals (noise) that mask the desired signal, the important factor then is the ratio of signal to the noise, rather than the output response produced by the signal.

Goetze [20] and Jones [21] derive the relationship between signal to noise ratio and attitude alignment errors in terms of optical design parameters. The intrinsic errors of the system are supposed to be paramount in this case and avoidable. Potter [22] and Jones [23] treat the uncontrollable error inherent in horizon sensing proper. These are mainly due to variabilities in atmospheric phenomena over which no control is possible.

The main figures of merit of radiation detectors are generally considered to be the following:

(1) $\text{Responsivity} = \dfrac{\text{Output}}{\text{Input}}$ (over linear range)

(2) $\text{Noise Equivalent Power} = \dfrac{\text{RMS Voltage of the Noise}}{\text{Responsivity}}$

(3) Detectivity = Reciprocal of the Noise Equivalent Power

Other figures of merit exist which are related to the detectivity in a reference noise power spectrum condition and divide detectors into two groups according to their dependence on the dectivity time constant. Detective quantum efficiency is also an important parameter in image detection ratings , but such topics are beyond the scope of this discussion.

4.5 DETERMINING ROLL AXIS ATTITUDE

A typical system for determining the pitch angle of a moving vehicle using horizon sensors will be described.

A fundamental requirement for successful operation of infared sensors is an adequate scanning mechanism. For a spinning vehicle the sensors may simply be mounted directly to the frame.

As the vehicle spins the sensor scans both the earth, where the intensity of the infared radiation is almost a constant value, and space, where the intensity is practically zero. The result of this periodic scanning of the earth is a train of pulses, similar to the one shown in Figure 1. A Schmitt Trigger circuit can be used to square each pulse.

The sensors are mounted on the vehicle inclined to the spin axis at an angle α. Figure (4.6) shows this arrangement. Figure (4.7) shows the geometry of the sensor scan cone and earth sphere intersection.

From Figure 6, η_f is the angle subtended by the front horizon sensor's sweep on the earth's surface, perpendicular to the roll axis. The front sensor sweeping time t_f can be determined by finding η_f as a function of pitch and then

$$t_f = \eta_f / \dot{\varphi}$$

where $\dot{\varphi}$ is the vehicle spin rate. Tait [24] has shown that the sweep times are also a function of vehicle pitch angle, earth radius and vehicle altitudes because η_f depends on these quantities.

The front and rear earth pulses and the resulting error pulses are shown in Figure (4.8). The widths of the two error pulses are added to obtain a pulse of width $t = t_1 + t_2$. A transfer function for the sensor for a particular scan speed, altitude and sensor alignment is needed to make this information useful. A typical transfer function graph is shown as Figure (4.9). For a final pitch attitude of θ degrees the control system would keep reducing the sum of the two error pulses t_1 and t_2 to within a certain limit Δt about t. Δt depends upon $\Delta\theta$ which determines the zone of permissible final pitch attitudes about the required value.

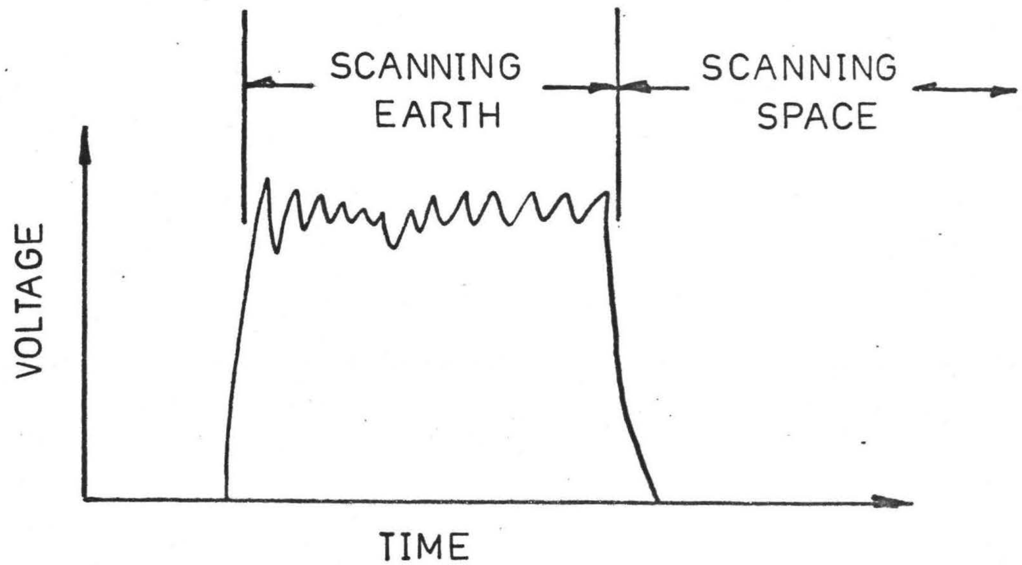

TITLE: HORIZON SCANNING SIGNAL	
SCALE: NONE	SOURCE: REF. 1
DRAWN BY: HILL	FIGURE NO: 4-1

CURVES OF RADIANCE IN THE 15 MICRON CO_2 BAND VERSUS h_o FOR FOUR MODEL ATMOSPHERES

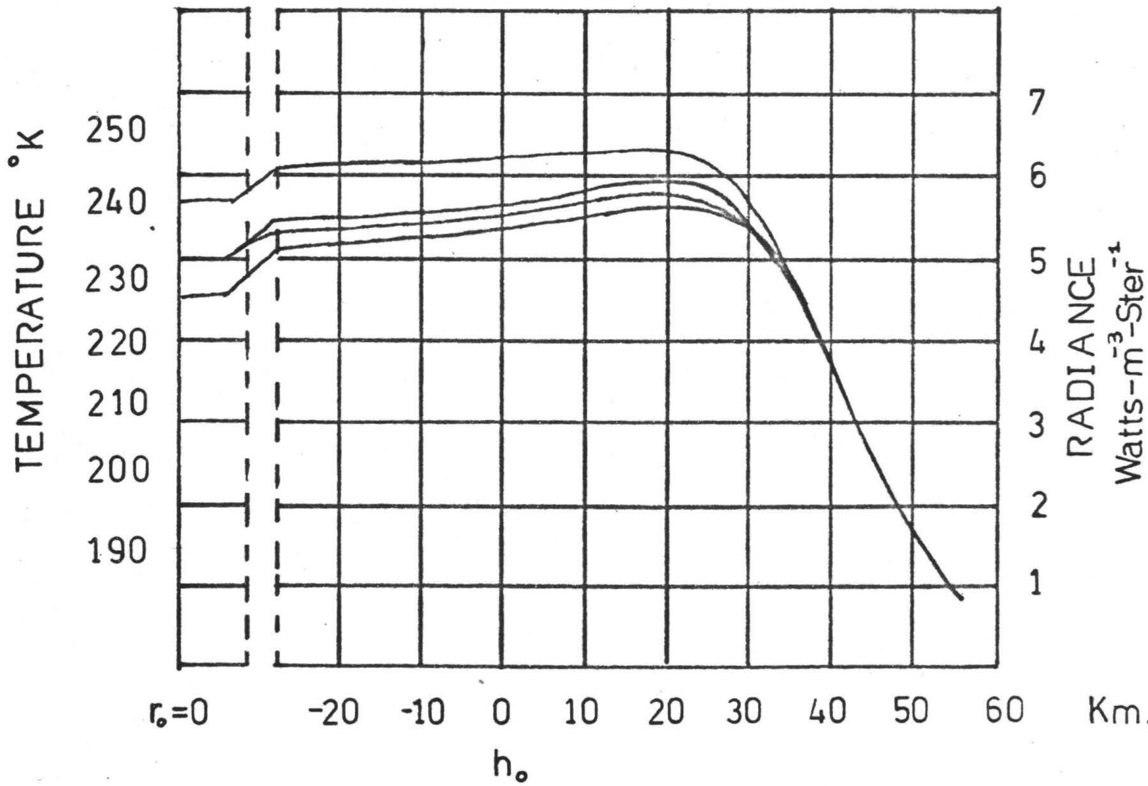

NOTE: 1) h_o= DISTANCE ABOVE HORIZON

2) 15 MICRON CO_2 BAND SHOWS THE LEAST VERTICAL DISPERSION FOR THE FIVE STANDARD ATMOSPHERES

TITLE: GRAPH OF INFARED RADIATION	
SCALE: NONE	SOURCE: REF. 3
DRAWN BY: HILL	FIGURE NO: 4-2

AMOUNT OF RADIATION IN
VARIOUS SPECTRAL BANDS COMPOSING
THE RADIATION NEAR EARTH

WAVELENGTH (microns)	N_{min} (r_o=o)	N_{min} (h_o=o)	N_{max}/N_{min} (r_o=o)	N_{max}/N_{min} (h_o=o)
6.33 - 6.85	0.102	0.201	5.69	2.05
8.9 - 10.1	1.09	1.57	8.95	2.75
10.75 - 11.75	0.86	0.86	14.3	10.9
14 - 16	3.54	3.69	1.69	1.68
21-125	13.3	14.7	1.75	1.37

NOTE N=RADIANCE IN WATTS-M^{-3}-$STER^{-1}$
r_o=o=CENTER OF EARTH'S DISK
h_o=o=OUTER EDGE OF EARTH'S DISK
=HORIZON LINE

TITLE: RADIANCE VALUES	
SCALE: NONE	SOURCE: REF. 3
DRAWN BY: HILL	FIGURE NO: 4-3

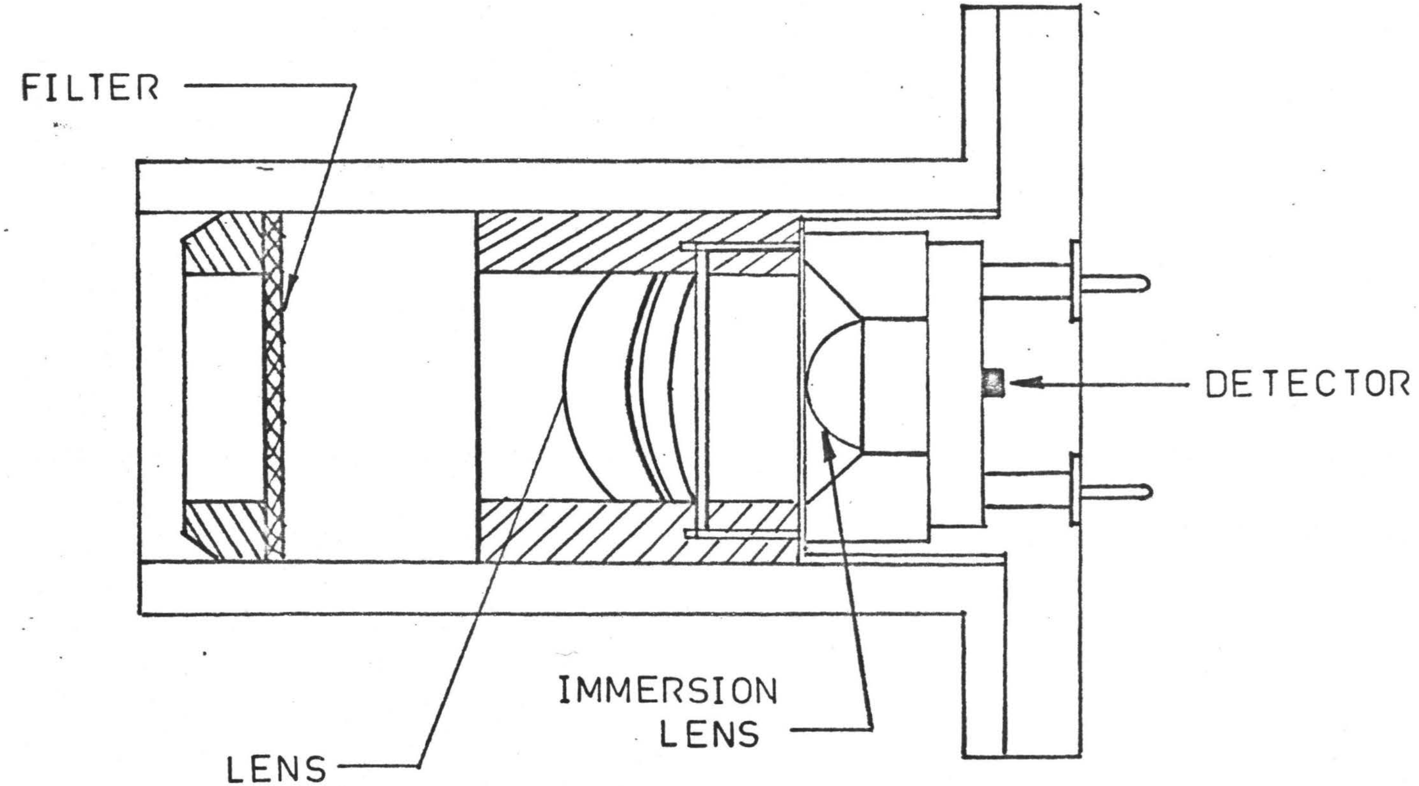

TITLE: BOLOMETER INFARED DETECTOR	
SCALE: NONE	SOURCE: REF. 2
DRAWN BY: HILL	FIGURE NO: 4-4

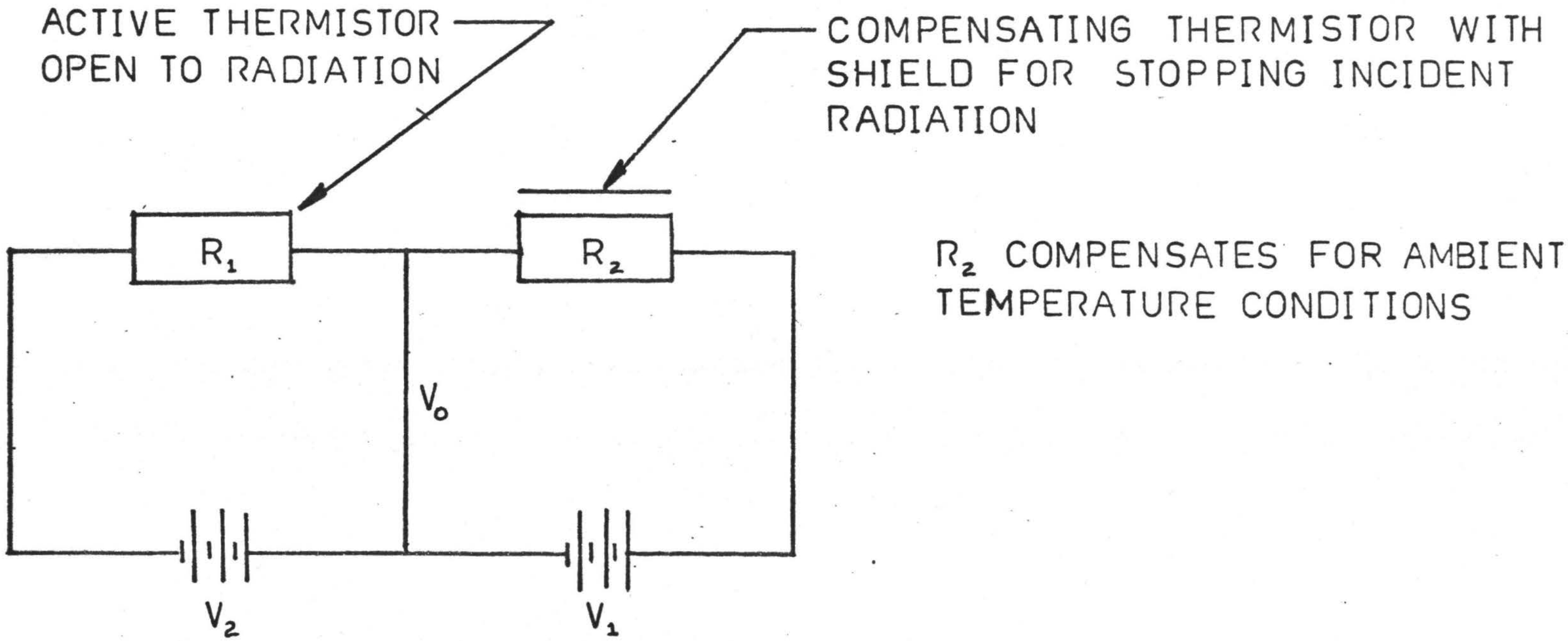

R_2 COMPENSATES FOR AMBIENT TEMPERATURE CONDITIONS

TITLE: BOLOMETER BRIDGE CIRCUITS	
SCALE: NONE	SOURCE: N/A
DRAWN BY: HILL	FIGURE NO: 4-5

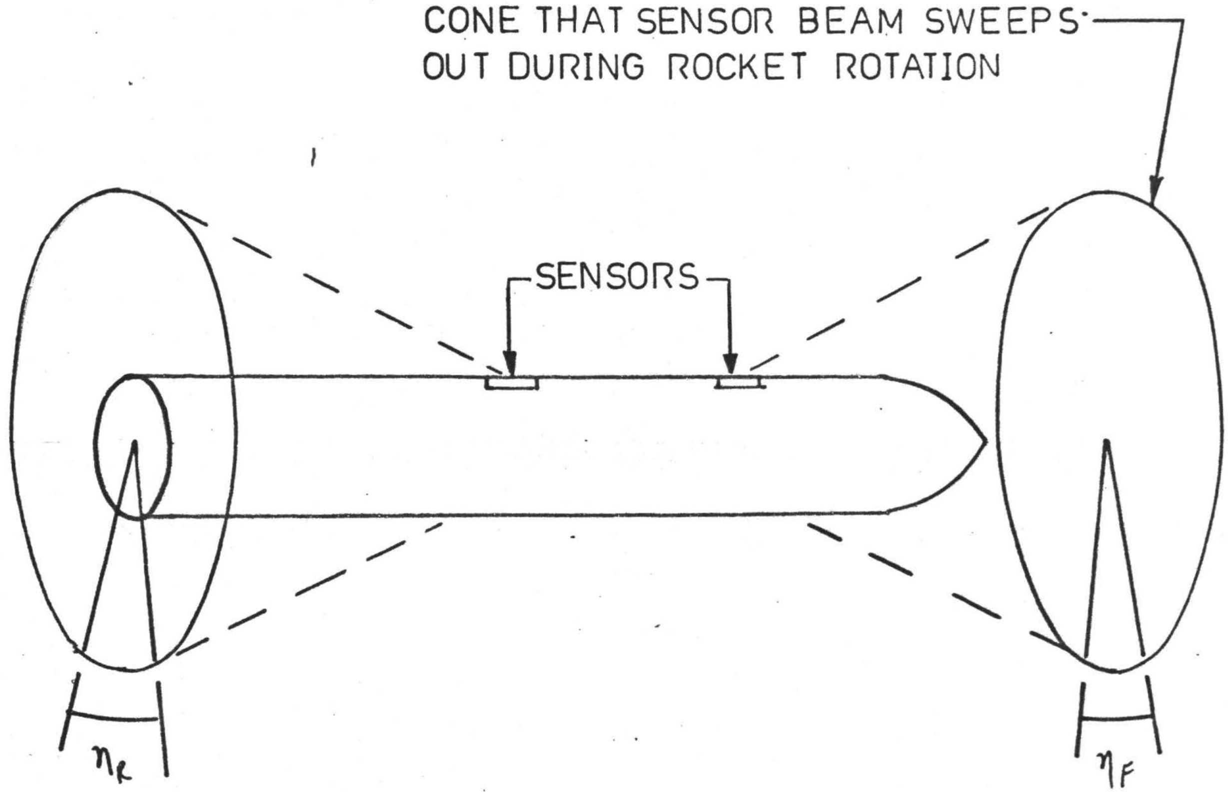

NOTE: ARRANGEMENT OF SENSOR PAIR ON SPINNING VEHICLE ABOUT C.G.
η_F = WIDTH OF SWEEP ANGLE OF FRONT SENSOR WHEN VIEWING THE EARTH

TITLE: HORIZON SCANNER MOUNTING	
SCALE: NONE	SOURCE: REF. 16
DRAWN BY: HILL	FIGURE NO: 4-6

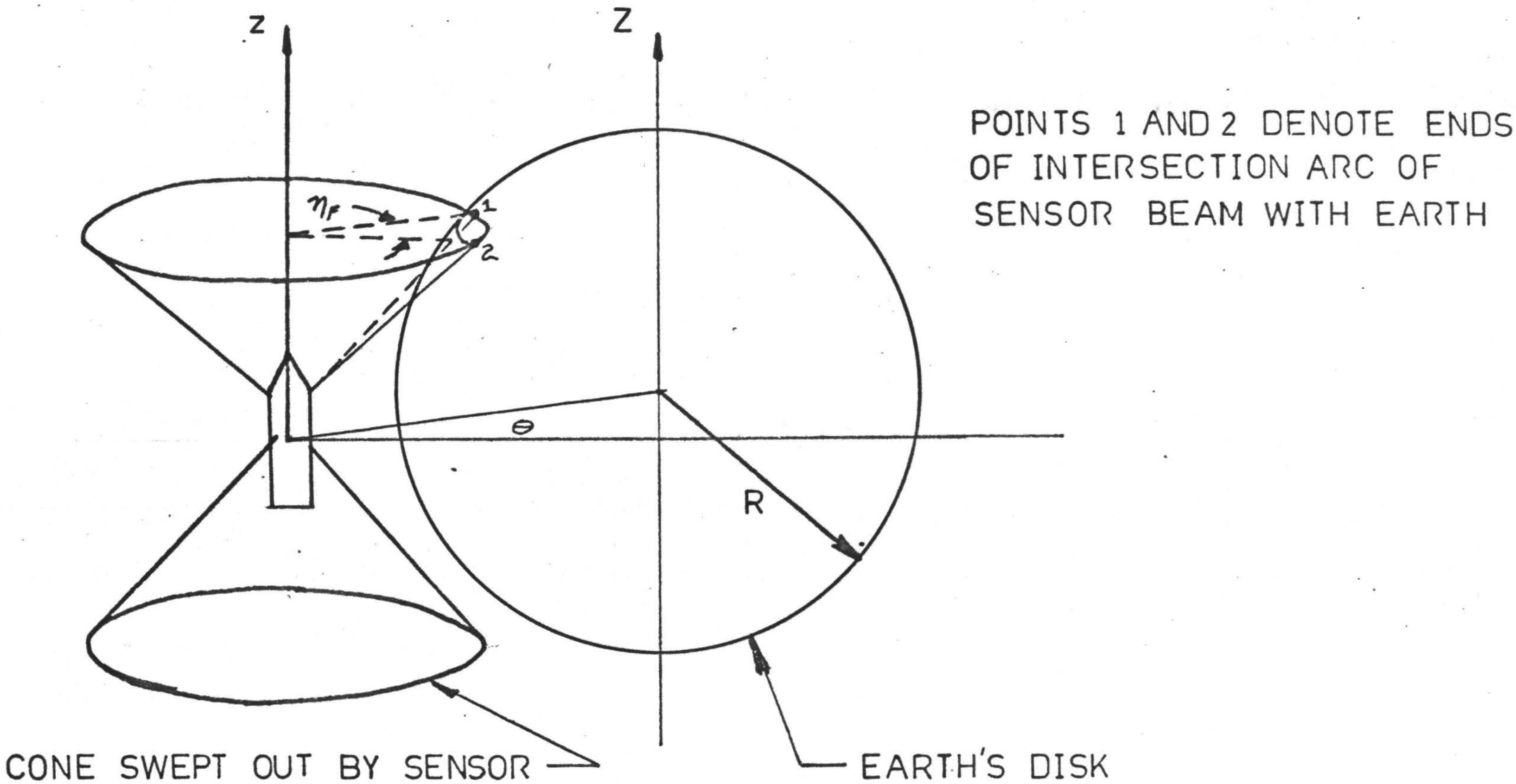

TITLE: EARTH-SENSOR GEOMETRY	
SCALE: NONE	SOURCE: REF. 24
DRAWN BY: HILL	FIGURE NO: 4-7

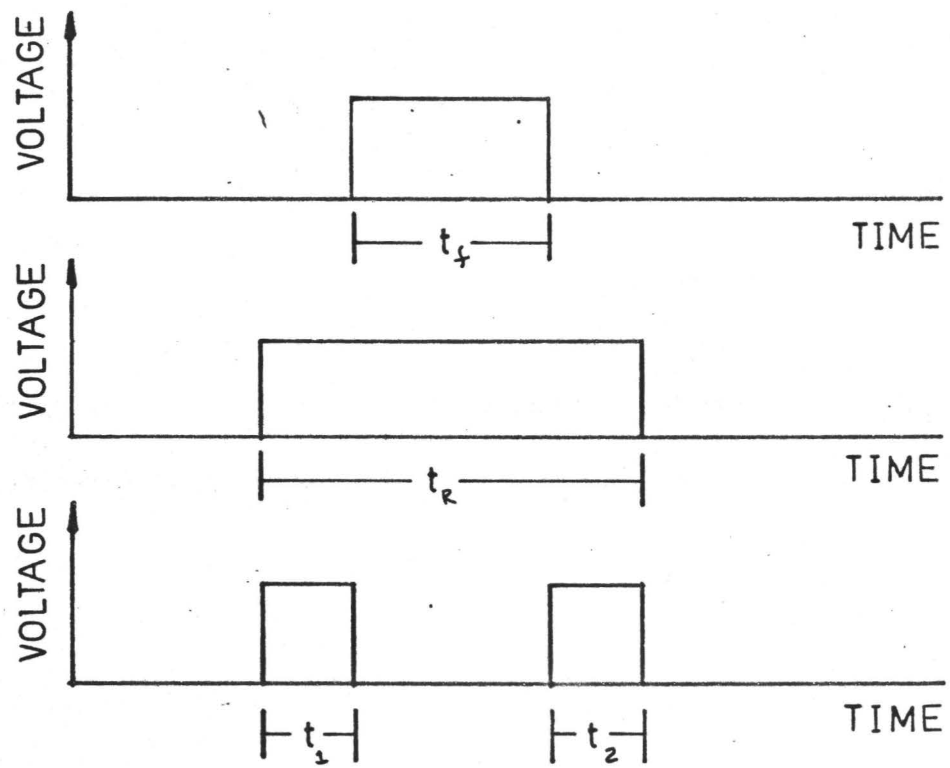

NOTE: t_1 & t_2 ARE ERROR PULSES

TITLE: DETERMINATION OF PITCH ERROR	
SCALE: NONE	SOURCE: REF. 16
DRAWN BY: HILL	FIGURE NO: 4-8

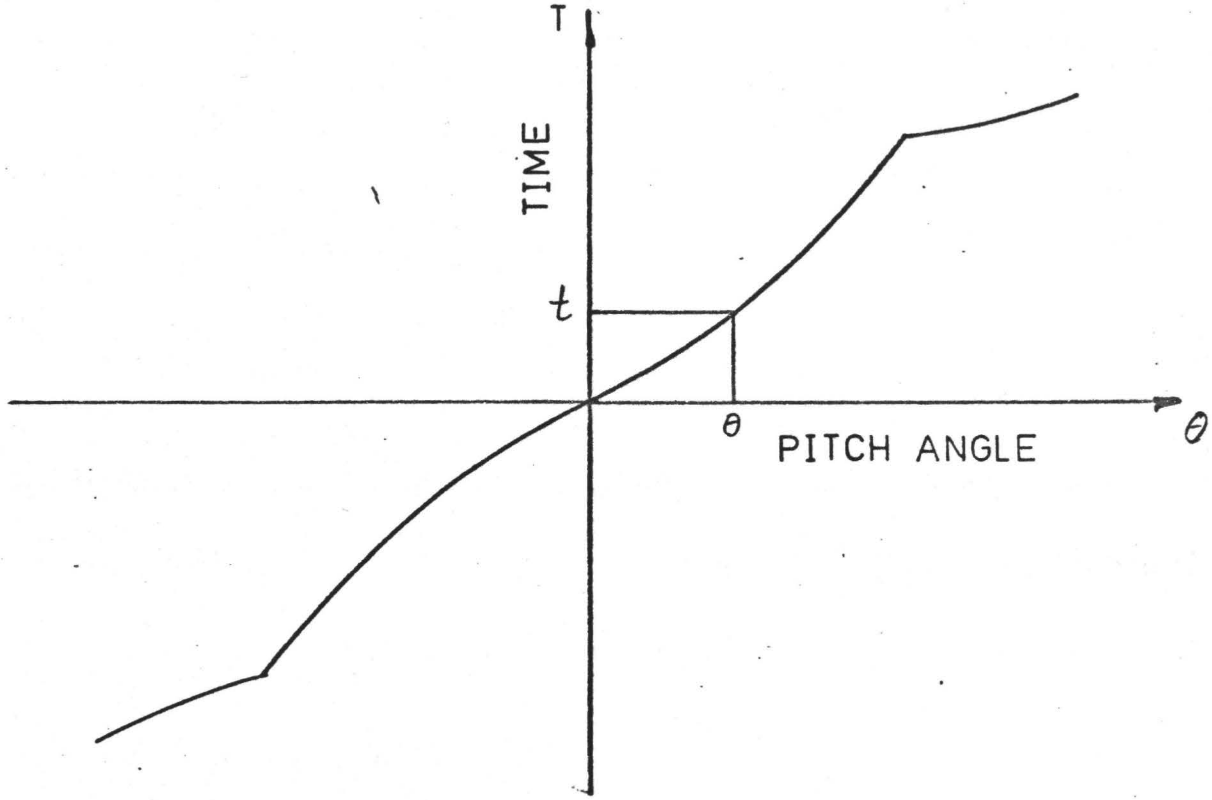

NOTE: 1) TIME = DURATION OF OUTPUT SIGNAL
2) THESE GRAPHS DEPEND ON
a) SCAN SPEED
b) ALTITUDE
c) RADIUS OF PLANET

TITLE: HORIZON SENSOR TRANSFER F'N	
SCALE: NONE	SOURCE: REF. 16
DRAWN BY: HILL	FIGURE NO: 4-9

REFERENCES

1. Singer, S. F., ed., Torques and Attitude Sensing in Earth Satellites, Academic Press, New York, 1964.

2. Holler, M. R. et al, Fundamentals of Infared Technology, MacMillan, New York, 1962.

3. Hanel, R. A., W. R. Bandeen and B. J. Conrath. "The Infared Horizon of the Planet Earth". Journal of the Atmospheric Sciences, Vol. 20, March 1963. References.

4. Plass, G. N., "The Infared Radiation Flux in the Atmosphere", Proceedings of the IRE, September, 1959

5. Howard, J. N., "The Transmission of the Atmosphere in the Infared". Proceedings of the IRE, September, 1959.

6. Plass, G. N., "Selective Radiators", Proceedings of the IRE, September, 1959.

7. Wark, D. Q., G. Yamamoto and J. H. Lienesch, "Methods of Estimating Infared Flux and Surface Temperature from Meteorological Satellites", Journal of the Atmospheric Sciences, Vol. 19, September, 1962, References.

8. Burn, James W. "The Application of the Spectral and Spatial Characteristics of the Earth's Infared Horizon to Horizon Scanners", IEEE Transactions on Aerospace-Support Conference Procedures.

9. Howell, B. J. "A Review of Infared Developments", Sperry Engineering Review, December, 1959, 11 pp.

10. Powell, R. W., "Infared Tracking", ARS Journal, December 1959, 8 pp. References.

11. Leybourne, J. L., "Scientific Sensors for Space Vehicles", Astronautics, November, 1961.

12. DeWaard, R. and E. M. Worser, "Description and Properties of Various Thermal Detectors", Proceedings of the IRE, September 1959, 6 pp.

13. Hanel, Rudolf A., "Dielectric Bolometer: A New Type of Thermal Radiation Detector", Journal of the Optical Society of America, Vol. 51, No. 2, February 1964.

14. Gedance, Alan R., "Comparison of Infared Tracking Systems", Applied Optics, Vol. 51, October 1961.

15. Astheimer, R. W., R. DeWaard, and E. A. Jackson, "Infared Radiometric Instruments on TIROS II, Applied Optics, December 1961.

16. Aviation Electric Limited, "Progress Report No. 4, Orbit Injection Control", AETR 13565, August 30, 1965.

17. Jones, R. Clark, "The General Theory of Bolmeter Performance", Journal of the Optical Society of America, Vol. 43, No. 1, January 1953.

18. Wormser, Eric M., "Properties of Thermistor Infared Detectors", Journal of the Optical Society of America, Vol. 43, No. 1, January 1953.

19. Goodenough, J. G., "Cooling Techniques for Infared Detectors", Proceedings of the IRE, September 1959.

20. Goetze, Dieter, "Accuracy and Range of Infared Horizon Sensors as Limited by Detector Noise", ARS Journal, July 1962, 6 pp. References.

21. Jones, R. C. "Phenomenological Description of the Response and Detecting Ability of Radiation Detectors", Proceedings of the IRE, September 1959, 8 pp.

22. Potter, R. F., J. M. Pernett and A. B. Naugel, "The Measurement and Interpretation of Photodetector Parameters", Proceedings of the IRE, September 1959, 5 pp.

23. Jones, R. Clark, "Noise in Radiation Detectors", Proceedings of the IRE, September 1959.

24. Tait, G. R., "Analysis of Orbital Injection Control System, Space Research Institute, McGill University, August 25, 1965.

PART 3

CELESTIAL SENSING METHODS

CHAPTER 5

CELESTIAL SENSING

5.1 DESCRIPTION OF CATEGORIES

This chapter will describe briefly the three main types of celestial methods for determining attitude of a vehicle in flight. These methods, planet tracking, star tracking and sun sensing, are all basically the same method. The intensity and sharpness of the object sensed affects system accuracy and its variation with time and position in space determines to what application the object serves as reference. It is obvious that for interplanetary navigation certain fixed stars and distant planets are more useful than the sun for trajectory corrections and proper alignment.

5.2 SYSTEM IMPLEMENTATION

There are three main types of star scanning systems that can be used. The first of these, the simplest, is the type of device proposed by Aviation Electric to the Space Research Institute in 1964 [1].

This first device consisted of two silicon photocells mounted directly to the frame of the moving vehicle and inclined to each other, as shown in Figure (5.1). The device was to sense the sun. The angle between the axis of the vehicle and the sun could be measured by comparing the outputs from the two sensors. Because of their inclination, their outputs would always be unequal for any direction of the sun away from the prependicular to the axis. The sensor is calibrated beforehand and a reference computer programmed to relate the sensor outputs to angles. This approach can be quite useful for detecting yaw angles for rocket and space vehicles. The angle to the sun from the plane of the trajectory must be approximately known as no active scanning device is employed. If the vehicle is spinning a scanning is accomplished, but only in the plane normal to the trajectory plane.

A second approach to the use of stellar references is usually employed for realignment of stable platforms in long range aircraft and interplanetary space vehicles. The stellar monitor usually consists of a telescope mounted on a gimbal system.

The telescope has a small aperture and contains an optical lens system which focuses the starlight beam to a point on a photosensitive scanning system. Frequently some type of optical filtering is used. With a very narrow field of view the system can find and track stars even in the daylight.

The gimbals are usually provided with angular readout devices which established the platforms (or vehicles) orientation with respect to a known star at a given time. The platform (or vehicle) may then have to be realigned to the proper attitude as required.

The elements of a gimballed optical tracker are shown in Figure (5.2). The photosensitive device is, typically, a photomultiplier tube. Location of the required star is carried out by searching and tracking operations.

In the search mode the telescope is made to scan a raster pattern, similar to that used in television tubes, in which the tracker may cover a field of 1 degree in azimuth and 10 minutes in elevation [2]. When the star is acquired, the computer controlling the gimbals automatically switches to the tracking mode. The tracking pattern is usually characterized by circular symmetry. A typical one is shown in Figure (5.3). The tracking field may be of the order of 3 minutes of arc in diameter. An off-center condition is detected in the computer as a function of time at which the star signal appears, during the movement through the predetermined tracking pattern. The computer supplies signals to the gimbal drives to restore the telescope to the centered condition.

The searching and tracking operations can both be performed without moving the telescope gimbals. A sensing element may be used which is essentially a television tube such as the image orthicon or vidicon. The "flying-spot" type of scanning employed with such tubes is the equivalent of mechanically moving a restricted field stop over the area containing the star.

Until recently no star tracking device had the ability to locate a designated star by merely "glancing" at the sky. Some method of approximate alignment had to be used to point the device in the general direction of the chosen star. Attitude data was stored on board in relation to the chosen star. This has been eliminated, however, by the recent development of a new system.

Recent work by Farrell and Lillestrand [3] and Lillestrand, Carroll and Newcomb [4] has resulted in an all celestial inertial guidance system with no moving parts such as gyros or gimbals. The system is designed to recognize stars from their position in the sky, just as human observers do, and knowing the stars in the field of view, decide what the orientation of the vehicle is. Experiments have shown that the approach is feasible but no test flights have yet taken place. The future is considered bright for this system, however, as the accuracies are extremely good (pointing errors near 5 seconds of arc are expected) and the number of components required is small. Only a coffee-cup size computer and a sensor together only 3 inches in diameter and 10 inches long will be required [3].

5.3 PROBLEMS WITH CELESTIAL SENSING

While celestial reference methods have proven quite adequate for interplanetary and human space travel, there are certain drawbacks when the concept is used close to the earth.

Celestial references are generally prescribed for use above 100,000 feet of altitude. Below this level, clouds can seriously affect the utility of the device by obscuring completely the star to be sensed. The atmosphere can also affect the sensors operation in two ways. One is to produce the twinkling effect of the stars and thus limit the precision of the star's angular determination. At night, lights from the earth's surface can be reflected in the atmosphere. The noise produced in the scanner may obscure the required star signal.

There is also a possibility that the celestial body to be sensed may be out of the field of view at the required time of operation. A parametric study by Tait [5] for the Martlet IV gun-launched rocket showed that for the launch taking place at Barbados, the only time that the sun would be in the field of view to permit its use as a yaw reference would be at 5:30 a.m. during the months of May to September, and at 5:30 p.m. during the months of November to February inclusive. This fact rather restricts the ultility of the vehicle.

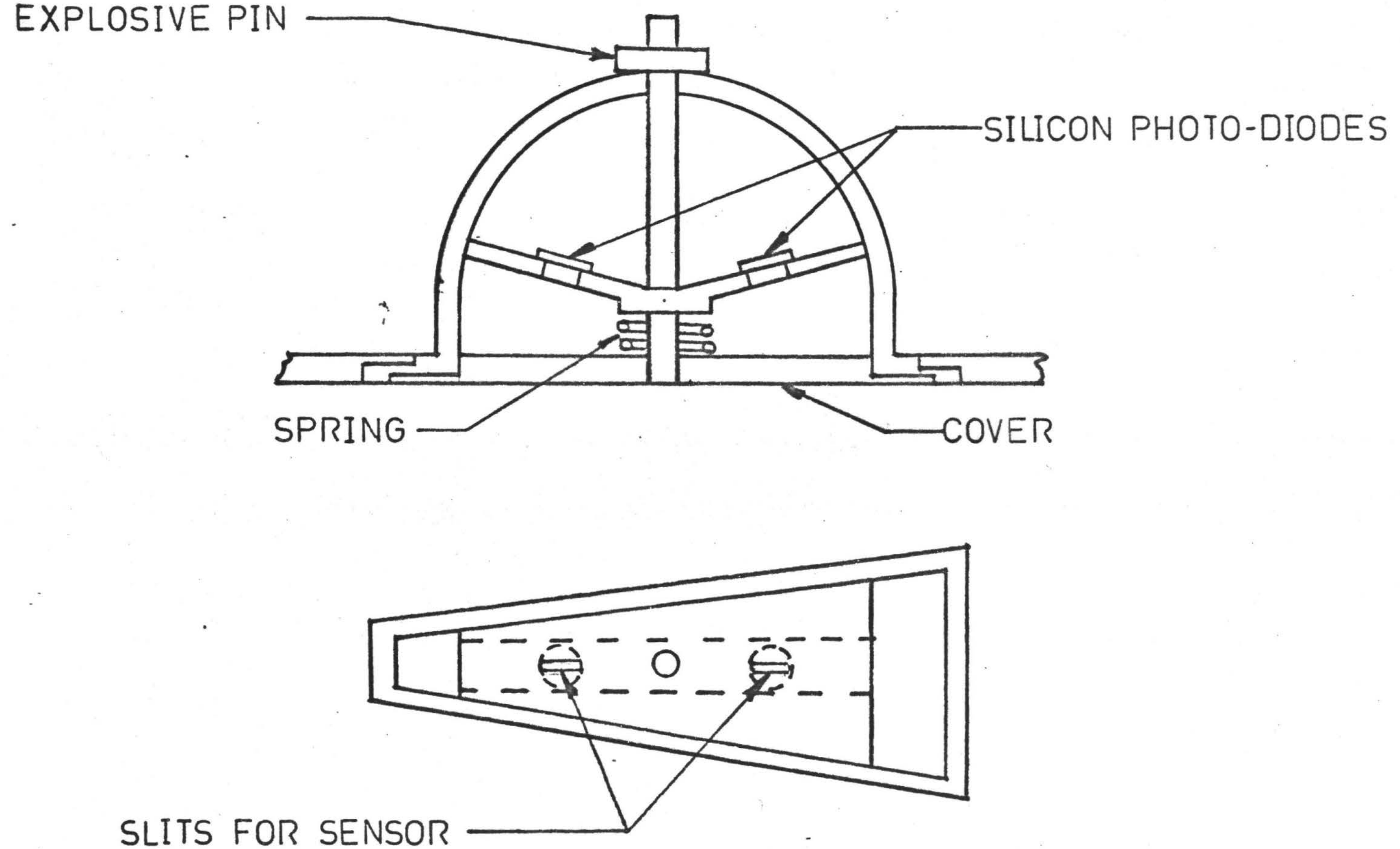

NOTE: PIN AND SPRING CAUSE PROTECTIVE COVER TO BE BLOWN AWAY AFTER LAUNCH

TITLE: PHOTOCELL SUN SENSOR	
SCALE: NONE	SOURCE: REF. 1
DRAWN BY: HILL	FIGURE NO: 5-1

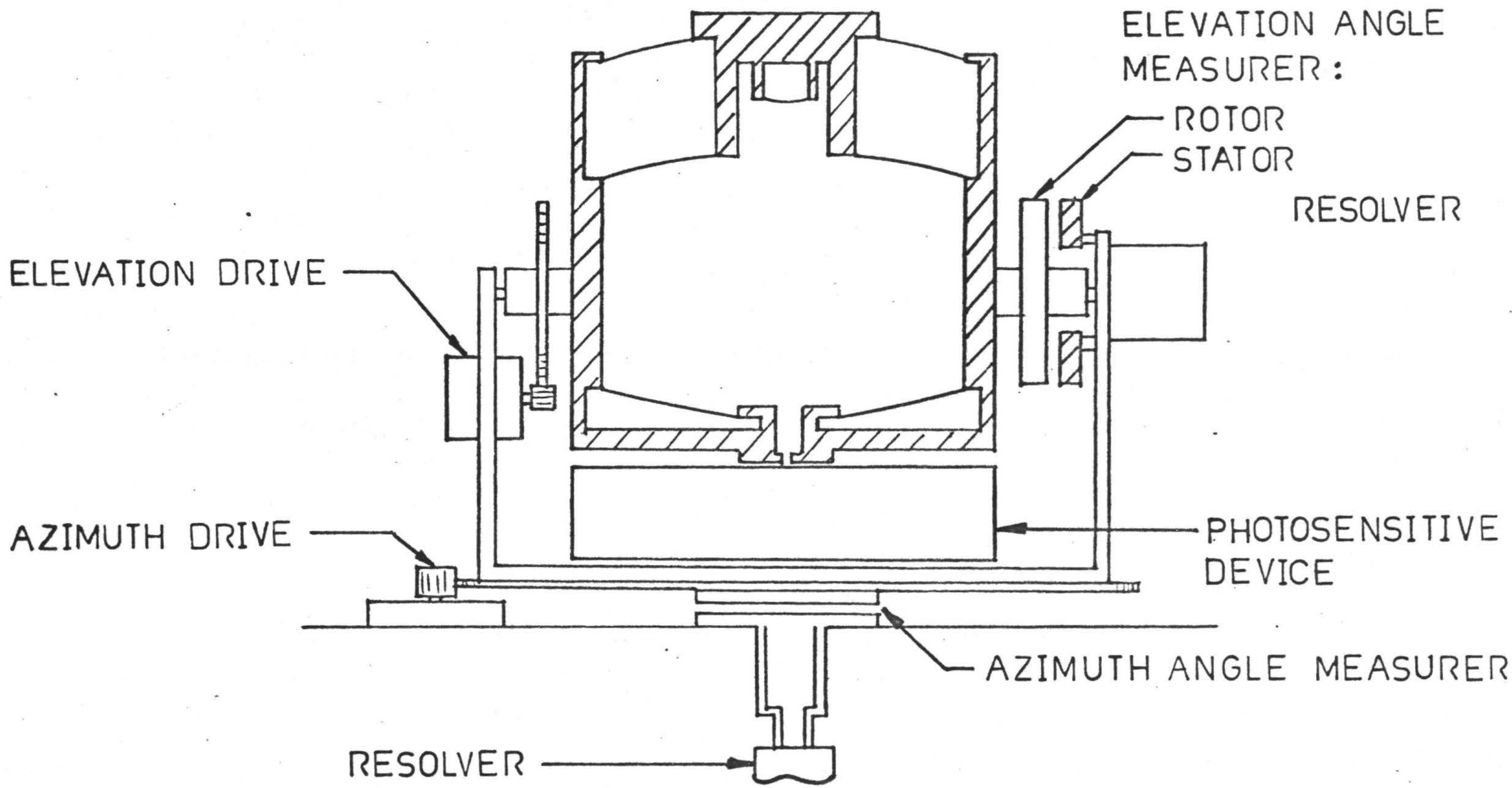

TITLE: GIMBALLED OPTICAL TRACKER	
SCALE: NONE	SOURCE: REF. 2
DRAWN BY: HILL	FIGURE NO: 5-2

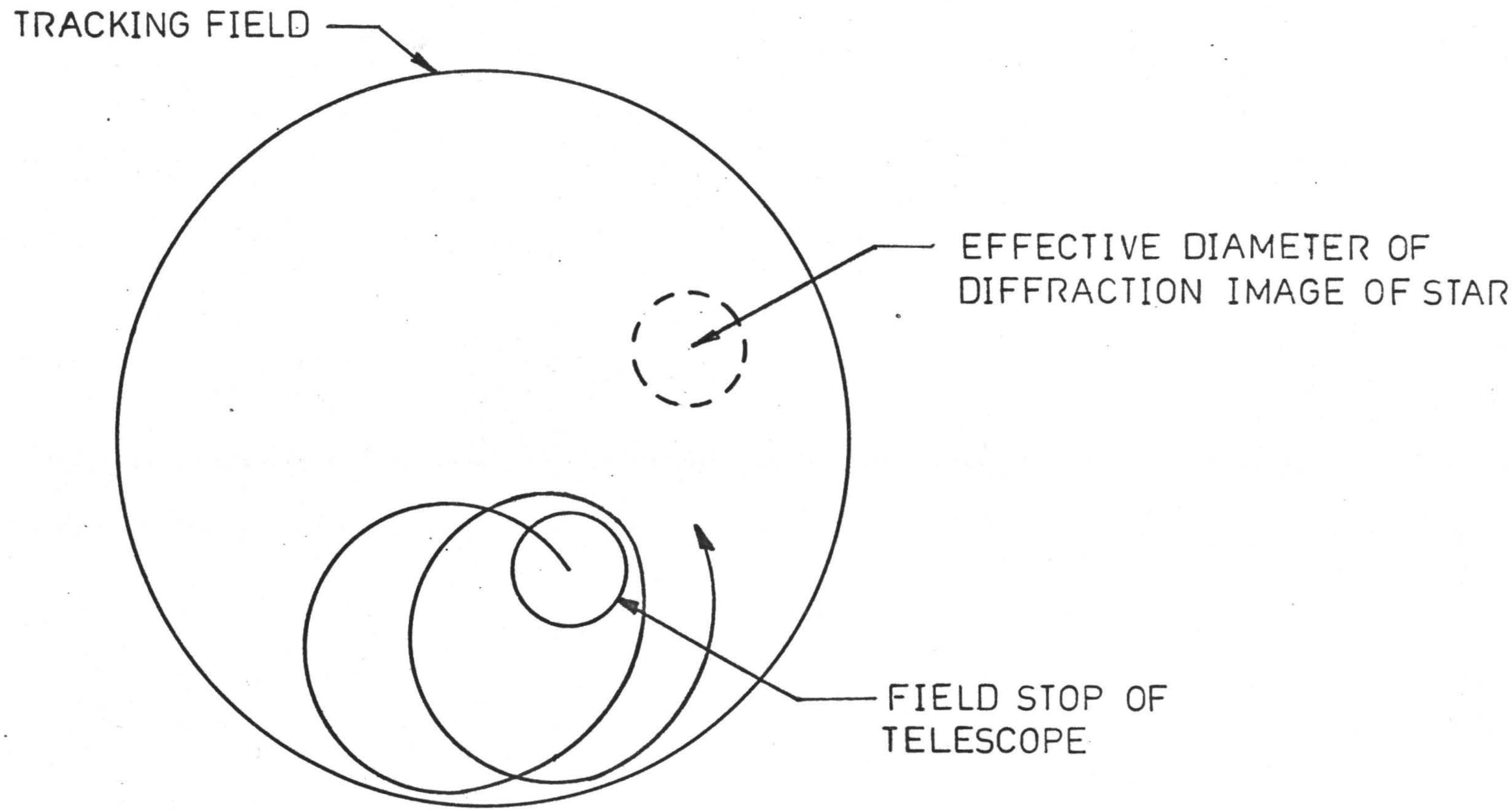

TITLE: SCANNING PATTERN	
SCALE: NONE	SOURCE: REF. 2
DRAWN BY: HILL	FIGURE NO: 5-3

REFERENCES

1. Aviation Electric Limited, Proposal No. 9290, Martlet IV Orbit Injection Control Systems, 1964.

2. Leondes, C. T. (ed), Guidance and Control of Aerospace Vehicles, McGraw-Hill, 1963, Chapter 3.

3. Farell, E. J., and R. I. Lillestrand, "Celestial Successor To Inertial Guidance", Electronics, Vol. 39, No. 6, March 21, 1966.

4. Lillestrand, R. L. , J. E. Carroll and J. S. Newcomb, "Automatic Celestial Guidance", Electronics, Vol. 39, No. 7, April 4, 1966.

5. Tait, G. R., "Analysis of Orbital Injection Control System", Space Research Institute, McGill University, August 25, 1965.

PART 4

AMBIENT-FIELD SENSING METHODS

CHAPTER 6

GRAVITY GRADIENT METHODS

6.1 BACKGROUND

One method suggested for determining the vertical from space vehicles has been the sensing of the gravity field of the earth, or other heavenly body, as the case may be. The concepts proposed to date are based on the gravity gradient phenomena. Crowley, Kolodkin and Scheider [1] and Roberson [2] have investigated the feasibility of sensing the gravity gradient with either a pair or a triad of accelerometers mounted inside an orbiting vehicle. An alternate method proposed by Diesel [3] uses a single rotating accelerometer.

Up to the present time the gravity gradient phenomena has largely been disregarded for actual applications in space vehicles as the inherent accelerometer errors and extraneous vehicle motion have prevented a practical system from being developed. Diesel's approach [3] is designed to circumvent many of these problems.

6.2 A SIMPLE MODEL OF THE GRAVITY GRADIENT

By referring to Figure (6.1) one can become acquainted with a straight forward model of the gravitational field. If point 0 is taken as a reference point and test points P are taken on the circumference of a small reference circle, center 0, then for all points P

$$g = G - G_0 \qquad (6.A)$$

where G = Gravitation at any point P

G_0 = Gravitation at reference point 0

The tangential component, shown in Figure (6.1C) varies sinusoidally with position θ around the circle. The magnitude of this variation, at normal orbital altitudes is 0.5×10^{-7} g/foot of test circle radius. From this diagram it can be seen that the vertical can be determed as one of the directions for which this component goes to zero.

It should be noted also that the radial component varies sinusoidally (with a d.c. component) and reaches its maximum value in the direction of the vertical.

6.3 SYSTEM CONCEPTS

There are really only two main system types. The first, the conventionally proposed approach is illustrated in Figure (6.2). There are two accelerometers paired together a fixed distance apart. The outputs of the two accelerometers are summed. The output error signal could be used to rotate the boom through an angle toward the vertical. The error signal would be nulled at the vertical. Analysis has shown [3] that for an accelerometer separation of 1 foot, an accelerometer bias error of 10^{-11} g would cause an error in the vertical of 10^{-1} milliradians. To obtain an error signal in the first place the two accelerometers should measure gravity to exactly the same precision. Such accuracy is beyond the present state of the art.

The method developed by Diesel [3] is illustrated in Figure (6.3). A single accelerometer is rotated at a constant angular rate is used to sense the sinusoidal variation in g . The vertical is then defined by the phase of this signal. Since the same accelerometer is used to detect g at all points around the circle, bias errors and scale factor errors will cancel when determining the phase angle e_ϕ which determines the vertical. A device has been developed [3,4] which will destroy the effect of translatory motions and bias errors. Other devices are under development to sense the same phenomenon [4] but information is scarce.

6.4 FUNDAMENTAL PROBLEMS

Aside from the problems encountered in getting an acceptable accelerometer, such as bias errors, instrument compliance, and so on, there is one fundamental limitation on gravity gradient sensors for orbit injection control. According to Diesel, the variation of g (0.5×10^{-7} g/foot of radius) is ordinarily not observable when the vehicle is within the atmosphere because the effect represents an extremely small part of the gravitational field. Only in orbiting vehicles will the effect become conspicuous.

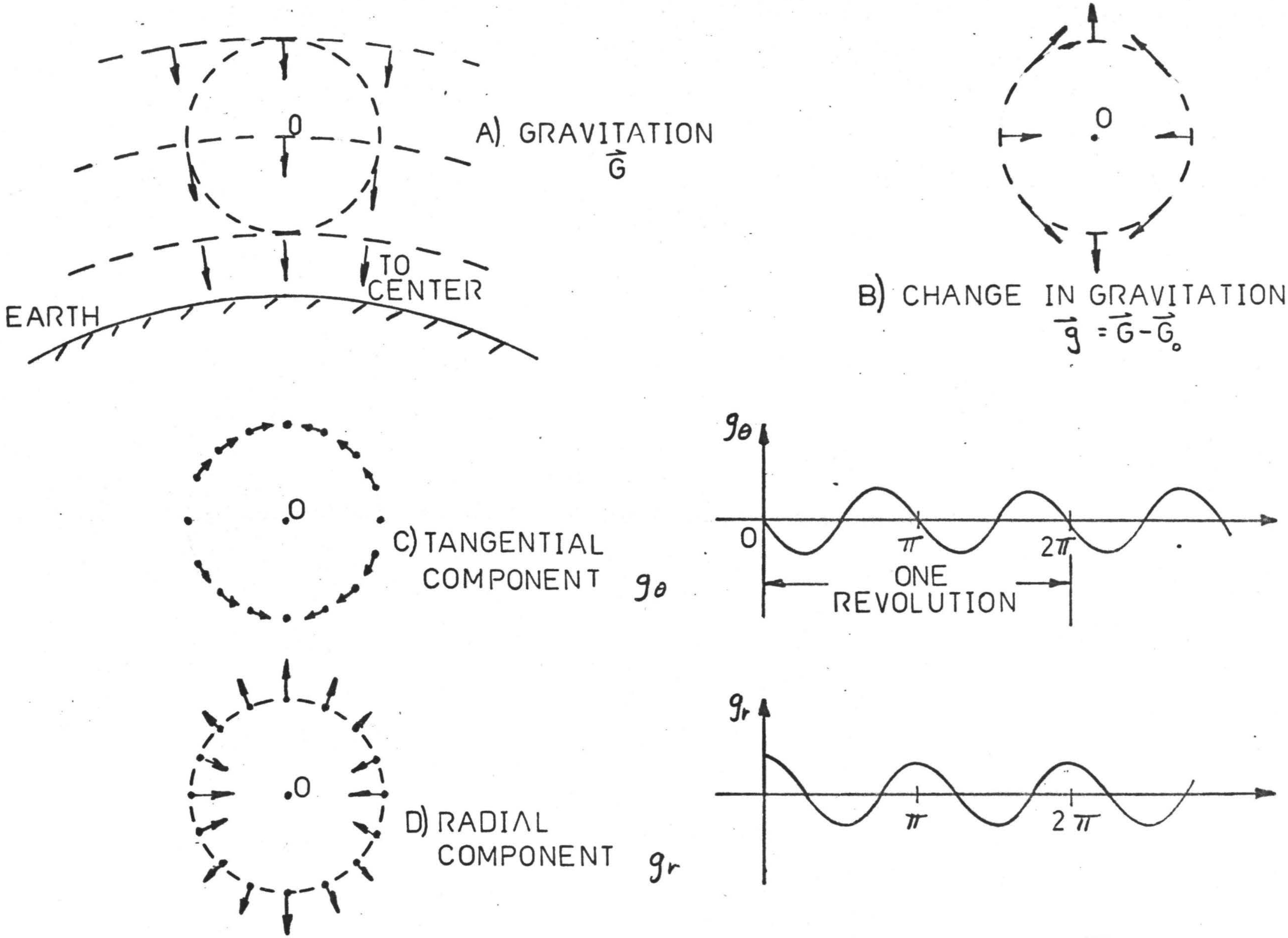

TITLE: GRAVITY FIELD MODEL	
SCALE: NONE	SOURCE: REF. 3
DRAWN BY: HILL	FIGURE NO: 6-1

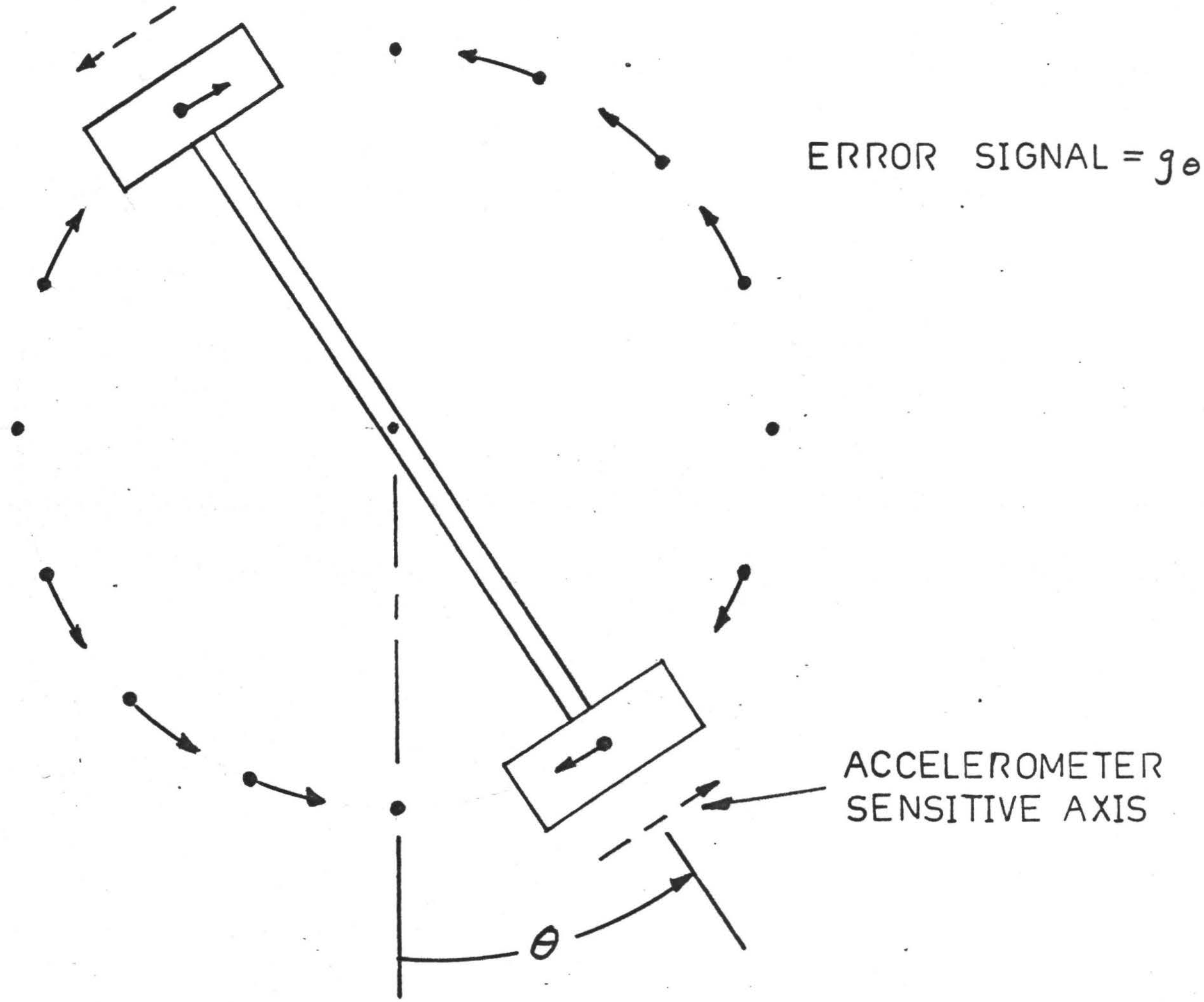

TITLE: CONVENTIONAL SYSTEM	
SCALE: NONE	SOURCE: REF. 3
DRAWN BY: HILL	FIGURE NO: 6-2

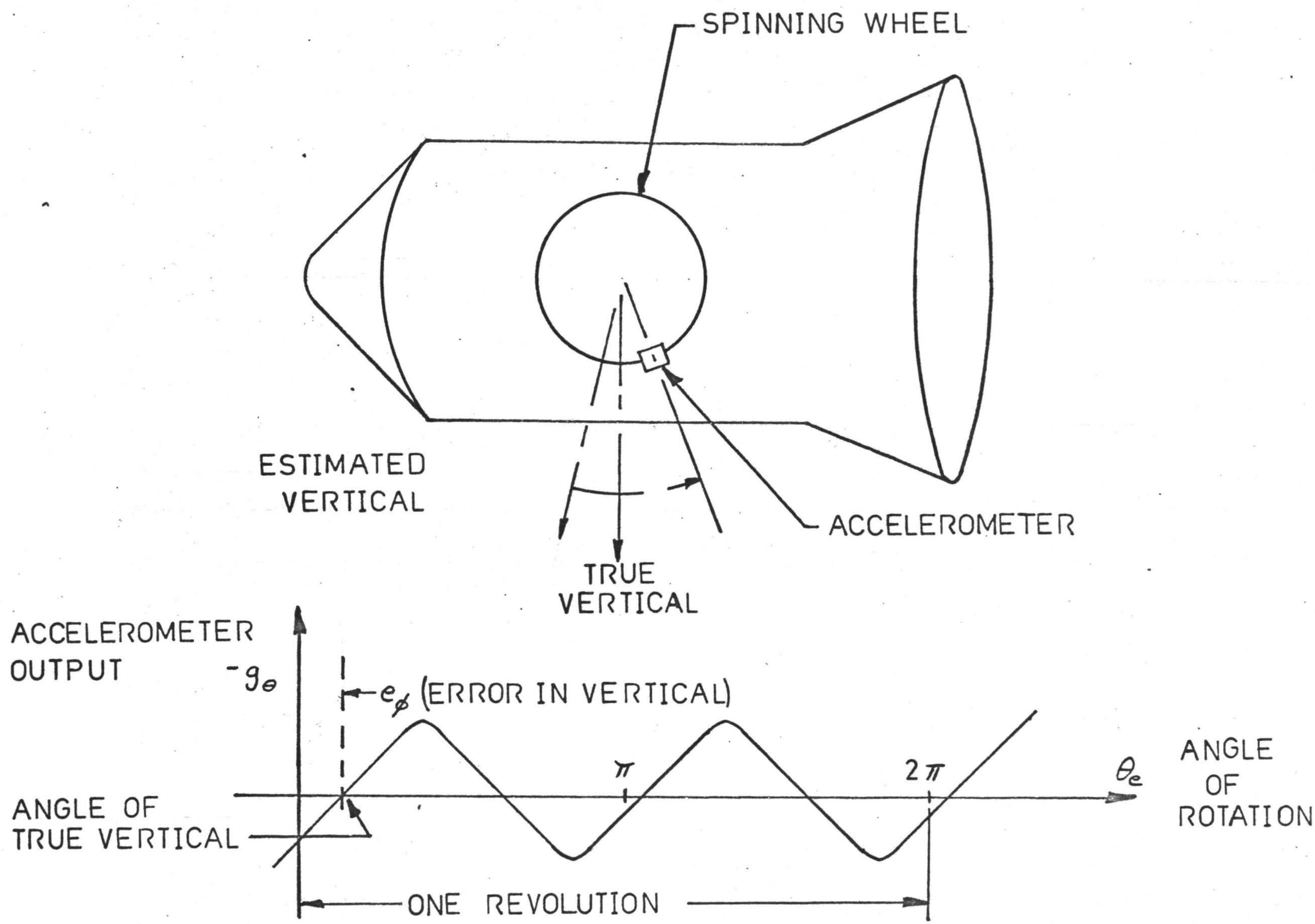

TITLE: VERTICAL INDICATING SYSTEM	
SCALE: NONE	SOURCE: REF. 3
DRAWN BY: HILL	FIGURE NO: 6-3

REFERENCES

1. Crowley, J. C., S. S. Kolodkin and A. M. Schneider, "Some Properties of the Gravitational Field and Their Possible Application to Space Navigation", IRE Trans. on Space Electronics and Telemetry, Set 5, No. 1, March 1959.

2. Roberson, R. E., "Gravity Gradient Determination of the Vertical", ARS Journal, Nov. 1961.

3. Diesel, J. W, "A New Approach to Gravitational Gradient Determination of The Vertical", AIAA Journal, Vol. 2, No. 7, July 1964.

4. Langford, R. C., "Unconventional Inertial Sensors", Astronautica Acta, Vol. 12, No. 4, 1966.

CHAPTER 7
MAGNETIC FIELD SENSING

7.1 MODE OF APPLICATION

Celestial, Gravity Gradient and Horizon Sensing methods have been shown to have modes of operation which could be called direct. That is, they present directly information about pitch error with respect to the local vertical or yaw error with respect to the line of sight to a particular heavenly body. The methods employing magnetometers are not as closely defined. Very recently, systems for the attitude determination of a spinning rocket have been developed by two separate groups. These systems, designed by Conley [1] and Ott [2] have been shown to be feasible and moderately accurate ($\pm$ 1 deg.).

The above designs use as sensors a single axis, flux gate magnetometer and a solar sensor to determine vehicle orientation. These devices are commerically available and quite simple in construction. One additional component of the system not required by other ambient field sensing methods is a large digital computer.

The system proposed by Conley [1] has been conceived specifically for low cost sounding rockets. Because it has fewer components than Ott's system [2] and the available information is more complete Conley's approach will be reviewed as a typical attitude determination system.

7.2 FUNDAMENTALS OF OPERATION FOR A TYPICAL MAGNETOMETER SYSTEM

A flux gate magnetometer and a solar cell are shown in position inside a rocket shell in Figure (7.1). The magnetometer is orthogonal to the sun sensor. The output of the magnetometer in volts (E) is proportional to the component of the geomagnetic field parallel to the sensor axis. That is

$$E = 4.0 \, |H| \cos \lambda \qquad (7.A)$$

where λ = angle between the geomagnetic field vector H and the sensor positive axis M.

For a rocket with spin frequency much greater than pitch frequency the transverse aspect magnetometer produces a modulated sinusoidal output signal, the instantaneous amplitude of which defines the cone about the geomagnetic field, shown in Figure (7.2). Now, if a solar cell is used which will generate a pulse whenever it is swept past the sun, the phase of this sun pulse relative to the magnetometer signal will be a function of the position of the rocket on the cone.

Because it is necessary to obtain a sun pulse during the course of the rocket's rotation, for phase reference rather than for an accurate determination of sun angle, a fan shaped acceptance beam is used for the solar sensor.

7.3 THE COMPUTING PRECEDURE

The attitude of the vehicle is assumed to remain constant during one revolution, but variable from one revolution to another.

Pulses from the solar cell define the time interval of one revolution. In addition to the solar pulses only two observations from the magnetometer are required to compute a pair of angles that completely describe the attitude of the missile.

The method of computation consists of a fitting procedure in which a set of approximations for the aspect angles is improved by successive differential corrections. Mathematically, the magnetometer output information is reduced to a relation between the direction cosines of the earth's magnetic field and the magnetometer itself. After normalization, the data consitutes measurement of cos λ_i where λ_i is the angle between the magnetometer and magnetic field vectors. The system of equations is thus

$$l_H l_{m_i} + m_H m_{m_i} + n_H n_{m_i} = \cos \lambda_i \quad (7.B)$$

The direction cosines of the earth's field are considered known. From the transformation relations between the inertial reference co-ordinates and the vehicle co-ordinates it can be shown that the magnetometer direction cosines depend on the angles θ and ϕ which determine vehicle pitch and yaw. (Roll can be described in terms of pitch and yaw angles).

The procedure is to approximate the unknown angles θ and ϕ, use them to find direction cosines and then keep improving the approximation by a series of differential corrections.

The procedure devised by Conley has been shown to converge quickly for a permissible range of pitch and yaw angle valves.

7.4 DESCRIPTION OF APPARATUS

The magnetometer signal is direct coupled into a standard subcarrier oscillator (10.5 kc) of an FM/FM telemetry system as shown in Figure (7.3). The common base amplifier used with the solar cell sets the signal magnitude for solar illumination of normal incidence above the atmosphere. The sun signal was A.C. coupled into the same oscillator as the magnetometer. The resulting output signal was a slowly varying sinusoidal waveform for the magnetometer output, with sharp pulses superimposed to indicate the sun-vectors position.

The solar sensors was a commercial unit 5 mm x 5 mm mounted 25 mm behind the longitudinal aperature in the rocket skin. The length of the slit was 3 inches, yielding an angular coverage of +66° to -41°.

A brief description of the operation of a typical flux-gate magnetometer shows that there are no moving parts and that the device has great potential for ruggedness of design.

A ring-core flux-gate device is shown in Figure (7.4). It is composed essentially of two half-wave flux gate magnetometer circuits with a common mixing resistor network and a center tapped power-supply transformer. The power supply is A.C. and the graphical symbols indicate the system operation during the first half cycle (solid dots on arrow stem) and during the second half cycle (open dots on arrows).

The principle of operation of this device can be best understood by referring to Figure (7.5). The field to be measured is Φ_x and the path of the flux lines through the flux gate or saturable reactor is shown as dotted lines.

The gate windings N_1 and N_2 are connected with diodes D_1 and D_2 in such a manner that the d-c flux components Φ_1 and Φ_2 produced by the ampere turns I_1N_1 and I_2N_2 in the respective semicircular portions of the core have the directions shown by the solid dots on the arrow stems. Φ_1 and Φ_2 combined with Φ_x, will be additive in one direction and subtractive in the other. Now because the effective impedance of each of the gate windings is varied in accordance with the resultant d.c flux component in the particular semi-circular portion of the core, the measuring instrument R_L indicates the differential effect of currents I_1 and I_2. Thus, for a given supply voltage the instrument can be calibrated for output current as a function of external magnetic field intensity.

When the components are connected as in Figure (7.4) the effects of the external field on the flux gates FG_1 and FG_2 are additive and the sensitivity of the magnetometer system is correspondingly increased.

7.5 PROBLEMS OF THE MAGNETOMETER SYSTEM

The main problem with magnetometer systems is that the elimination of magnetic inteference is tedious. On-board electrical equipment is the main source of these disturbances.

Another source of magnetic disturbance is the attentuation and rotations of the geomagnetic field within the payload due to currents induced by the field in a spinning conducting vehicle shell.

For satisfactory operation over a wide range of trajectories the magnitude and direction of the earth's magnetic field must be known. While this is often not possible, one of the theoretical models could be used. Additional computational facilities would have to be provided, however.

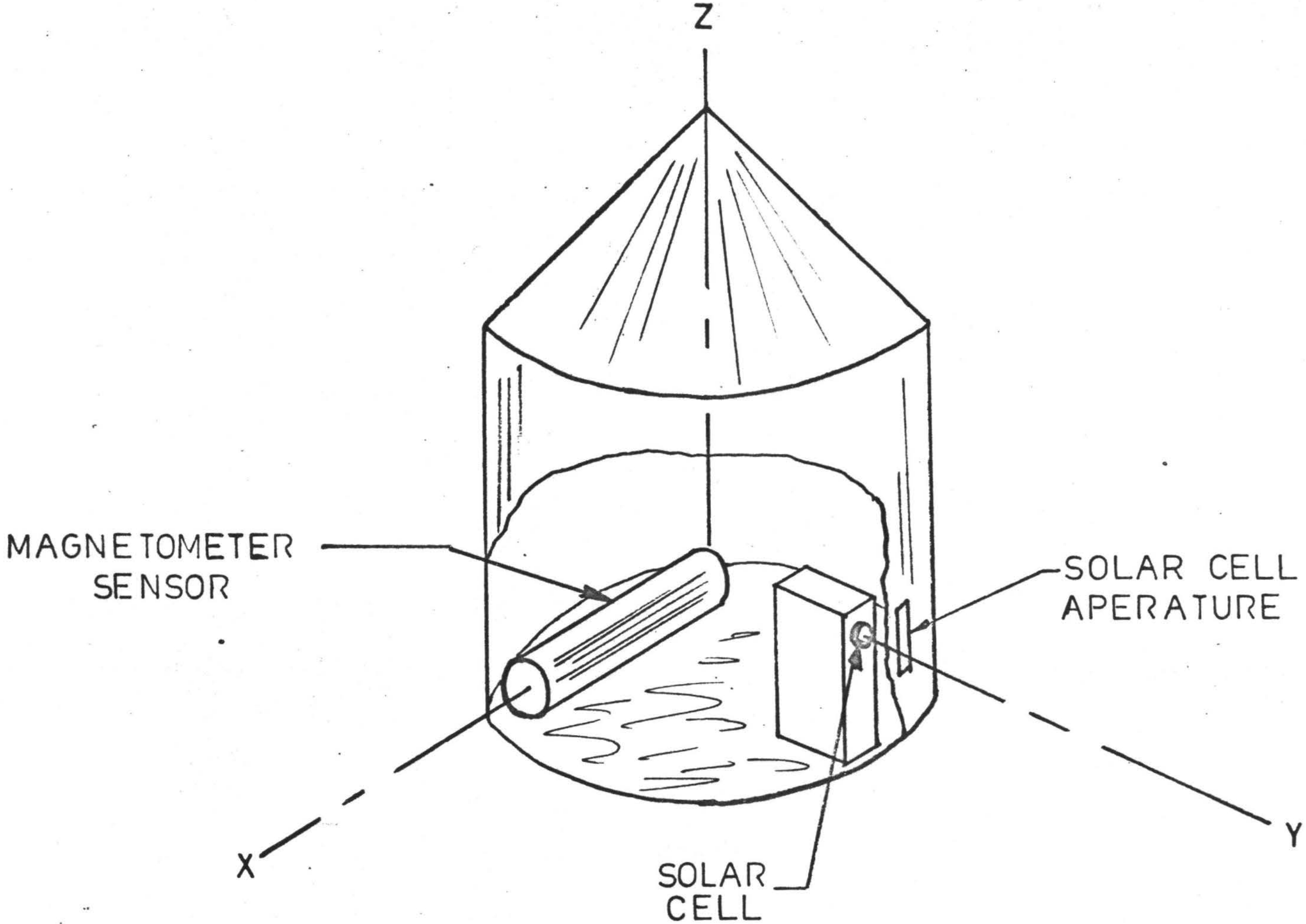

TITLE: SENSOR ORIENTATION	
SCALE: NONE	SOURCE: REF. 1
DRAWN BY: HILL	FIGURE NO: 7-1

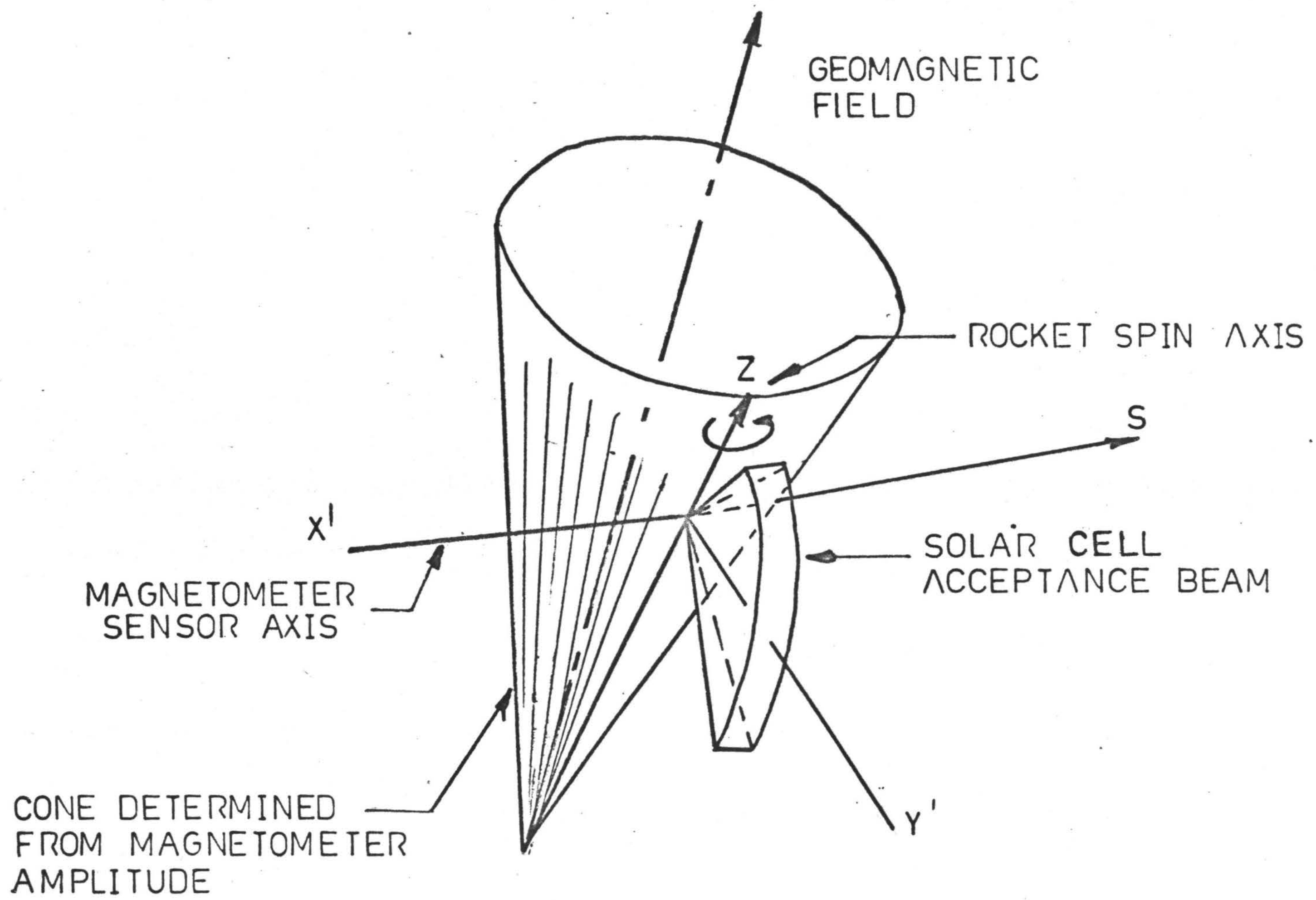

TITLE: SYSTEM GEOMETRY	
SCALE: NONE	SOURCE: REF. 1
DRAWN BY: HILL	FIGURE NO: 7-2

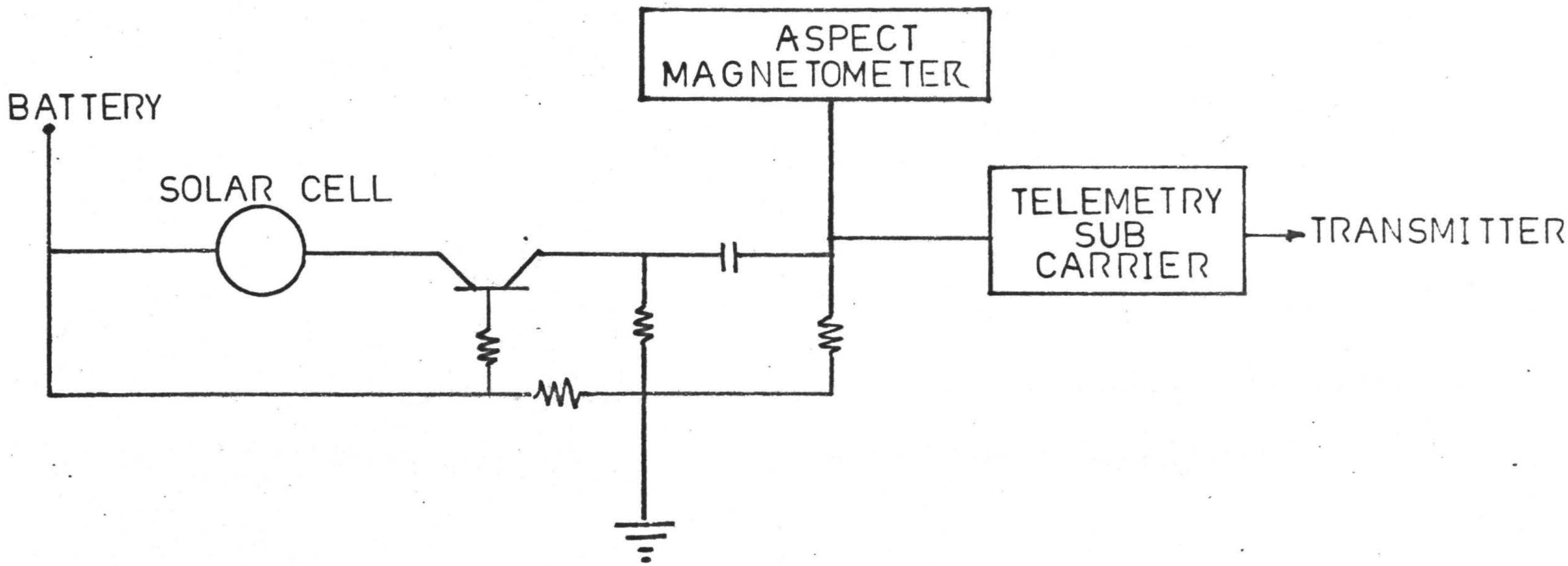

TITLE: TELEMETRY CIRCUIT	
SCALE: NONE	SOURCE REF. 1
DRAWN BY: HILL	FIGURE NO: 7-3

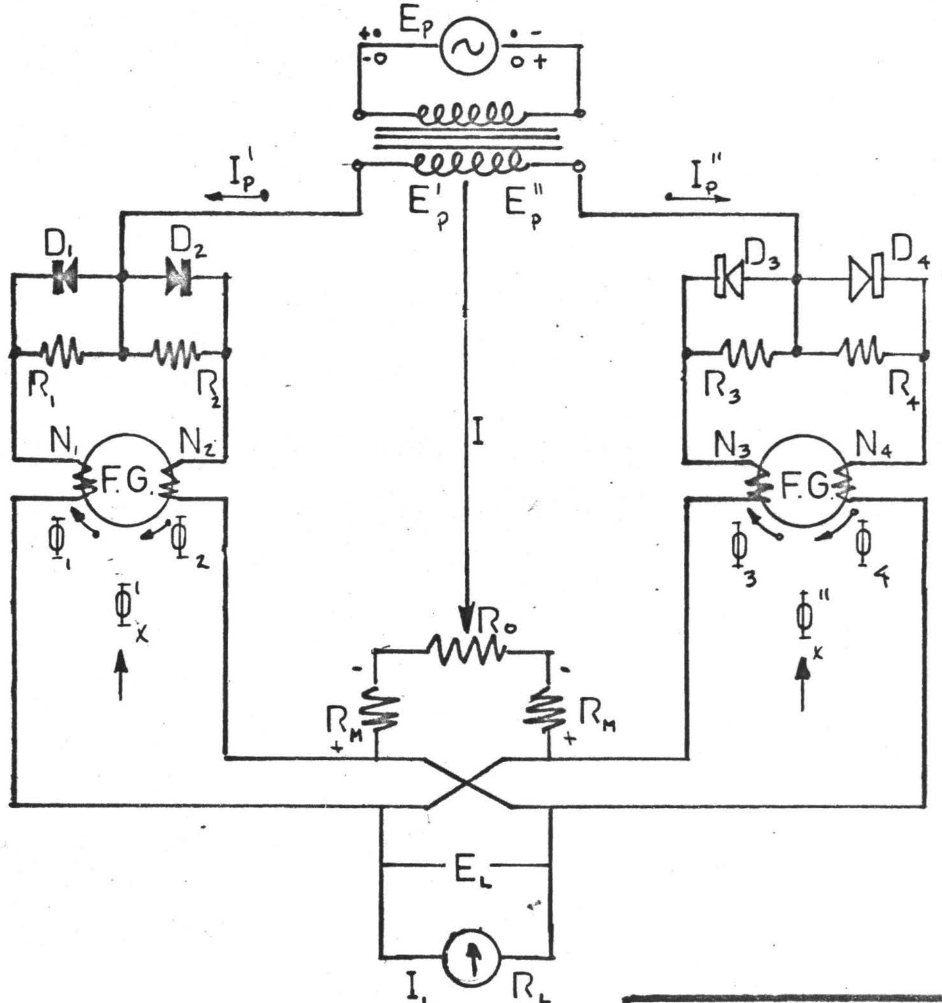

TITLE: MAGNETOMETER CIRCUIT	
SCALE: NONE	SOURCE: REF. 3
DRAWN BY: HILL	FIGURE NO: 7-4

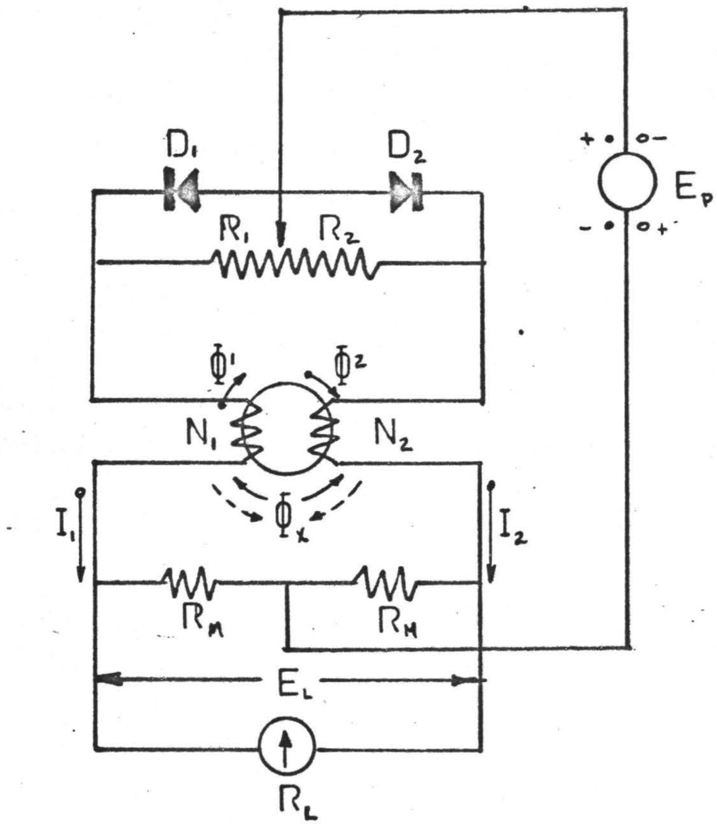

TITLE: BASIC MAGNETOMETER CIRCUIT	
SCALE: NONE	SOURCE: REF. 3
DRAWN BY: HILL	FIGURE NO: 7-5

REFERENCES

1. Conley, J. M. and R. B. Patton Jr., "An Altitude Determining System for Spinning Rockets", Report No. 1291, BRL, Aberdeen Proving Ground, Maryland.

2. Ott, R. H., H. M. Horstman and R. M. Lahn, "The Determining of the Orientation of a Uniformly Rotating or Rapidly Rotating Vehicle Utilizing the Outputs from Solar Sensors and a Lateral Magnetometer", NASA TMX-55424, March, 1966.

3. Geyger, W. A., "Ring-Core Flux-Gate Magnetometer with Self-Saturating Circuits", AIEE Transactions, part 1, (Communications and Electronics), Vol. 81, March 1963.

4. Ito, M., "Analysis of the Output of Rocket-Borne Magnetometers", Can. Journal of Physics, Vol. 41, 1963.

PART 5

INERTIAL SENSING METHODS

CHAPTER 8

CONCEPTS IN INERTIAL SENSORS AND SYSTEMS

8.1 INTRODUCTION

Inertial sensors can be described generally as devices which detect either displacement (angular or linear) or rate (angular or linear). Accelerometers are used for linear movement applications and gyroscopic sensors are employed for angular motion detection. As spinning rocket attitude can be specified by two Euler angles, gyroscopic devices for monitoring these angles should be reviewed.

8.2 PRESENT DEVELOPMENTS IN GYROS

The basic intelligence of an inertial component is provided by the inertial properties of mass. All gyroscopes operate on the principle that a moving-mass system, in the abscence of an external forces, will maintain a fixed attitude in inertial space.

Conventional gyro design has concentrated on developing a low drift instrument employing a spinning metal rotor supported on ball bearings. Recently, gas bearings have been employed in some applications.

In recent years the emphasis on increased accuracy at reduced cost has caused several new avenues to be explored. Lund [1]* and Langford [2] describe instruments which are based on operating principles different from those of conventional gyroscopes. Many of these devices do not require precision of parts and assembly to meet their performance objectives. The most recent listing of concepts in gyroscopy is given by Langford [2] and is given below.

LIST OF GYROSCOPY CONCEPTS

Vibratory	Motion within Fluid
Solid State Vibratory	Electrostatic
All Vibratory Type	Electromagnetic
Rotary Drive, Vibratory Output	Dynamically Tuned
Nuclear	Cryogenic
Nuclear Magnetic Resonance	Low Frequency Electromagnetic
Magnetic Induction	Wave
Solid State Nuclear	Ball
Laser	Spinning Mass
Optical	Non Floated Free
Optical Orientation	Phase Sensitive Field
Vortex	Two Degree of Freedom
Rotating Fluid	Non Floated Modulation
Liquid Filled Rotor	Non Floated Precision
New Fluid Rotor Inertial Sensor	Multirotor unsupported

The problems of achieving stable performance can be just as difficult to solve as those of conventional gyros. Therefore, in addition to conventional gyros, Land and Langford both report that those concepts generally considered as most suitable for development are:

1. Electrically Suspended Gyros
2. Fluid Gyros
3. Vibratory Gyros
4. Laser Gyros
5. Nuclear Gyros
6. Cryogenic Gyros

In actual fact, of the above devices the only two which have not reached the practical stage are the Nuclear and Cryogenic Gyros. The open literature on these devices is limited. Those papers which are available deal with fundamental problems in physics, not operational problems. For these reasons their treatment in later chapters is not undertaken.

The state of the art of the most prominent new devices was summarized by Lund [1] and is given here as Figure (8.1).

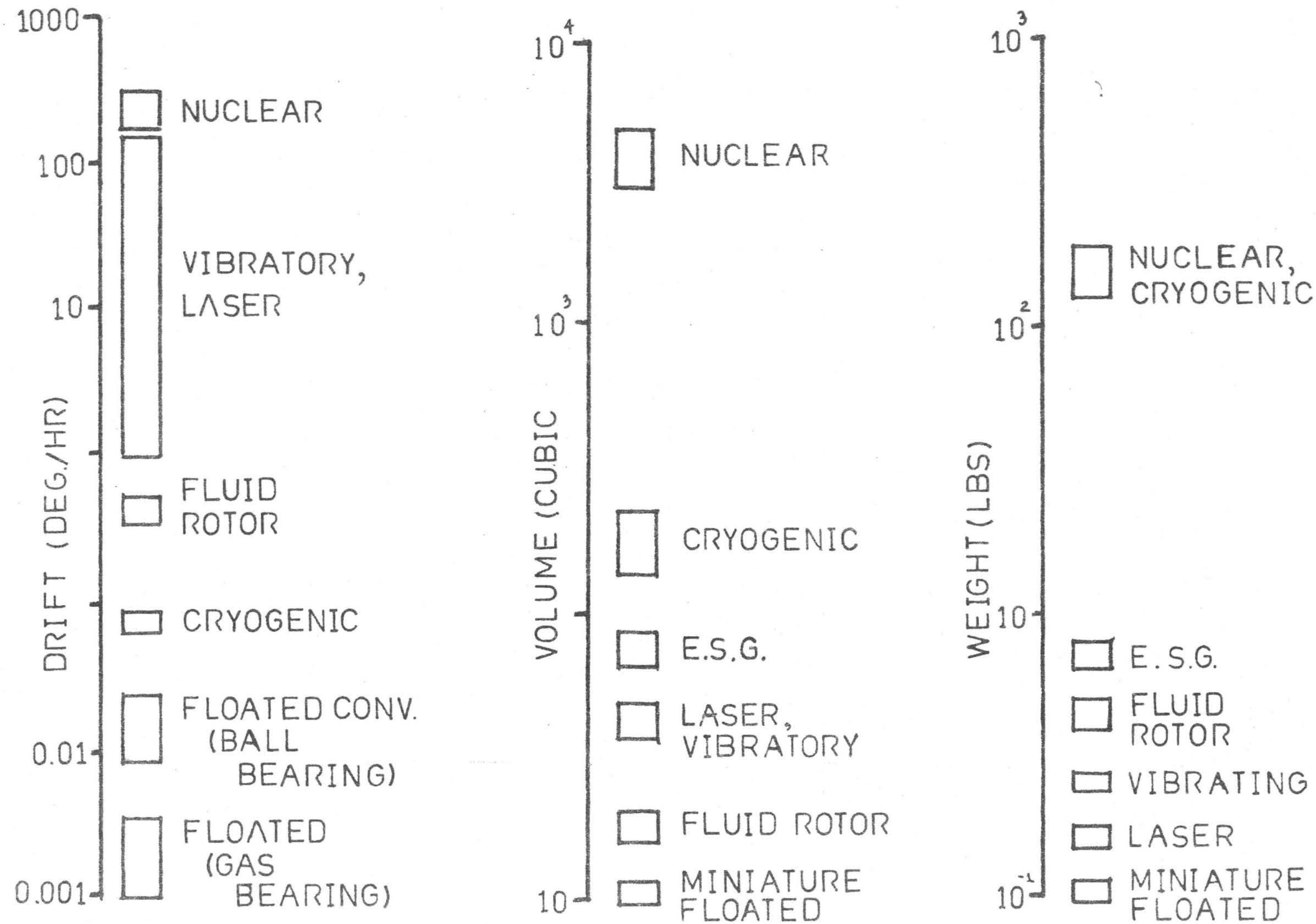

NOTES:
1) RANDOM 3) THRESHOLD 5) NULL STABILITY
2) SYSTEMATIC 4) RUNAWAY

TITLE: SUMMARY OF GYROS	
SCALE: NONE	SOURCE: REF. 1
DRAWN BY: HILL	FIGURE NO: 8-1

REFERENCES

1. Lund, P. S., "The Changing Emphasis and Future Trends in Navigational Gyros", SAE Trans., Paper No. 650586, 1966.

2. Langford, R. C., "Unconventional Inertial Sensors", Astronautica Acta, Vol. No. 6, 1966.

3. Savet, P. H. (ed.) Gyroscopes: Theory and Design, McGraw-Hill, New York, 1961.

4. Puckett, A. E. and S. Ramo, Guided Missile Engineering, Chapter 10, McGraw-Hill, New York, 1961.

CHAPTER 9

CONVENTIONAL GYROSCOPES

9.1 INTRODUCTION

Gyroscopes are considered to be conventional in this report if they have a solid metal rotor supported by bearings (ball or gas). One to three degrees of freedom for this device are permitted by gimbals. In some devices the sensitive element may actually float in a viscous fluid. Pickoffs may be one of several electromagnetic or electromechanical devices, the actual device having no bearing as to the classification of the gyro.

Slater [1] has defined the ranges of accuracy required for different gyro applications as follows.

TYPE OF GYRO	DRIFT RATE REQ'M'TS DEG./HR.
Rate Gyro for Fire & Flight Control	10 - 150
Directional Gyro & Gyro Horizon for Auto Pilots	1 - 15
Marine Gyro Vertical	1 - 5
Polar Direct. Gyro (used at polar regions)	0.1 - 1
Gyrocompass (ship-borne)	0.03 - 0.4
Gyroscope - Inertial Navigator	0.0005 - 0.1

9.2 TWO DEGREE-OF-FREEDOM GYROS (T.D.F. GYROS)

Two degree-of-freedom gyros are also called "free" gyros or amount gyros. It is essentially an orientation measuring device with inputs and outputs both angles. Performance of a typical off-the-shelf unit (Whittaker FF10) is tabulated below.

Example: Miniature Two Degree of Freedom Floated Gyro [2]

Performance:	Drift Rate	- (Vibration, Static)	- 0.5°/min.
	Run-Up Time		- 30 sec. (max.)
	Life		- 1000 hrs.
	Angular Momentum	1.3×10^6 gm-cm^2/ sec.	
Environmental:	Acceleration	30 g's	
	Shock	250 g's	
	Vibration	20 g's	10 - 20,000 c.p.s. (sinusoidal)
	Temperature Range	- 65°F to + 165°F	
General:	Length	-4.200 in.	
	Body Diam.	-3.540 in.	
	Weight	- 4 lbs.	
	Motor	- A. C. Induction, 200 V, 115 V Or 26 V, 400 c.p.s.	

Two axis gyros are employed mainly in aircraft attitude sensing devices such as vertical and directional gyros. Drift levels are from 20 to 40 degrees per hour. There are more sophisticated two axis gyros using spherical gas bearings but these have limited freedom about either axis. Random drift levels of around 0.01 degrees per hour are acceptable for guidance systems and the better gyros accomplish this quite easily.

9.3 THEORY OF OPERATION (2 D.F. GYROS)

The mathematical theory underlying the operation of the free gyroscope has been treated in detail by many authors. It is often included in formal courses on rigid body dynamics. For these reasons it will not be dealt with here. The reader is therefore referred to the excellent treatment given by Savet [3], Arnold and Maunder [4] and Thomson [5].

9.4 GYRO MECHANIZATION

The two-degree-of-freedom displacement gyro consists of the basic gyro rotor and a pair of gimbals or cardans which are simply frames which support the rotor. These frames provide the two degrees of angular freedom required to rotate the gyros case into almost any orientation without forcing the spin axis to rotate away from its original direction or orientation in space.

The main elements of a two-degree-of-freedom gyro are shown in Figure (9.1). This is a schematic drawing to illustrate basic principles and problems. No matter how sophisticated the design may be, the fundamental elements shown must be included.

The majority of two axis gyros use ball bearings for rotor and gimbal support although some gas bearing work is being done on this device. Axis pickoffs can be potentiometers, synchros, E-Bars, rotatary differential transformers or optical pickoffs. The two axis gyro has not received as much attention as the single axis gyro, however.

9.5 TWO-DEGREE-OF-FREEDOM GYRO APPLICATION

(i) The Gyrovertical

A single T.D.F. gyro may be used to define the vertical in a moving vehicle. The spin axis is held in the "vertical" position by servodriven gimbals.

(ii) The Gyrocompass

This device is often called the Directional Gyro or Azimuth Gyro. The spin axis is horizontal and is made to maintain a given direction in a moving vehicle.

(iii) Gyro Stabilized Platform

Two free gyros can be used to stabilize a platform that must maintain a fixed attitude with respect to inertial space. However, in spite of the benefit of only two gyro units being required, there are certain drawbacks.

Caging of each gyro in two angles is required. If a gyro passes through gimbal lock or strikes a mechanical stop it will tumble and lose reference completely. If reference is lost due to tumbling, it can't be regained without external stable balance. Actual gyro balancing and other production difficulties are approximately four times as great as those for a single degree of freedom gyro.

The above devices are dealt with in greater detail by Thomson [5], Puckett and Ramo [6] and Wrigley and Hollister [7].

9.6 PROBLEMS OF THE TWO GIMBAL GYRO

Two problems which plague the operation of the free gyro are "gimbal lock" and "gimbal errors". When the spin axis becomes co-linear with the outer gimbal axis the gyro can no longer be precessed by applying torques about the gimbal axis. The gyro is effectively stuck or locked in this position, a situation described as "gimbal lock".

If the gyro spin axis is displaced about one of the gimbal axes, this off balance condition can result in a motion about the second gimbal axis. This uncertainty in alignment is termed "gimbal error".

In addition to the above, precise balance of the unit is difficult to achieve about the several axes of permitted movement.

9.7 SINGLE-DEGREE-OF-FREEDOM GYROS (S.D.F.)

The single-degree-of-freedom gyros are the most highly developed of modern gyro devices. Accuracies are becoming extremely good and reliable lifetimes have been extended with the advent of gas bearings used on gyros for space applications.

Due to extensive development work these gyros are now capable of drift levels of less than 0.003 deg./hour in miniature size units which weigh less than one pound. [8]. Volumes can be low as one cubic inch.

Given below are performance figures for a typical off-the-shelf rate gyro supplied by the Whittaker Corporation [9]

Example: Rate Gyro

	Characteristics	Values	Units
Performance:	Maximum Rate	6 to 1000	deg./sec.
	Threshold	0.02	% full scale
	Linearity Limits	(to half scale) ± 0.2	% full scale
		(to full scale) ± 0.2	% full scale
Environmental:	Vibration	25 @ 20 to 2,000	(g's and freq. range,cps)
	Shock	100	g's - peak
	Acceleration	100	g's
	Life (A.C. Motor)	2000	hrs.
	Temperature	-65 to 212	°F

9.8 THEORY OF OPERATION (S.D.F. GYROS)

The mathematic theory underlying the operation of the single axis gyroscope has been treated in detail by many authors. The references given in Section (9.3) are excellent reference sources. No attempt will be made here to review general free-body dynamics.

Single axis gyros are usually employed as rate gyros or rate integrating gyros. Referring to Figure (9.2), if the gyro were to be subjected to a input rate $\dot{\psi}$, the rate of change of the angular momentum vector Cn is $Cn\dot{\psi}$, which requires a moment equal to it about the output axis to balance the developed torque. This moment may be supplied by a torsional spring of stiffness k as the output axis tilts by a small angle θ. Equating the two moments we have

$$Cn\dot{\psi} = k\theta$$

or

$$\theta = \frac{Cn\dot{\psi}}{k} \tag{9.A}$$

Thus the output angle θ is proportional to the rate of turn $\dot{\psi}$ of the input axis.

The single axis gyro may also be employed as a rate integrating gyro. If the torsional spring restraining the output is replaced by a viscous damper, the instrument becomes an integrating gyro. If c_d is the damping constant, equating the rate of change of angular momentum to the viscous damping torque will give

$$Cn\dot{\psi} = c_d\dot{\theta}$$

or

$$\theta = \frac{Cn}{c_d}\int\dot{\psi}\,dt = \frac{Cn}{c_d}\psi \tag{9.B}$$

Thus the output angle is proportional to the integral of the input angular rate, which is the input angle itself.

9.9 SINGLE-DEGREE-OF-FREEDOM GYRO MECHANIZATIONS

A single-degree-of-freedom gyro consists of a rotor, a single gimbal and a restraint device which acts to restrain angular motion about the gimbal axis. This contrasts with the two-degree-of-freedom gyro, which, if it has gimbals at all, must have at least two, and which, usually, has no interval restraints to gimbal motion. Figure (9.2) illustrates schematically the construction of a typical floated rate integrating gyro.

The gimbal element is usually in the shape of a cylinder and is floated in a viscous fluid. This floation concept permits excellent threshold and low drift levels. The shock capabilities are also improved. The Newtonian damping characteristics provide for both damping of oscillations in the spring restrained rate gyro and integration of rate inputs in rate-integrating gyros.

The torsion springs on the output axis of the gyro are usually small diameter torsion bars which provide both the spring effect and help to locate the inner gimbal within the fluid filled container. Beryllium-copper alloy is often used for the spring rods because of its low internal hysterisis properties [10].

The motion of the output axis is usually sensed in modern units by a rotary differential transformer. These devices can be made extremely compact by their pancake design. Excellent resolution and accuracy is achievable.

9.10 SINGLE-DEGREE-OF-FREEDOM GYRO APPLICATIONS

The single axis gyro can be used in the same situations as the two axis gyro. The main difference is that two single axis gyros are needed where one two axis gyro is used. Three single axis gyros must be used on stable platforms. In practise, however, the single axis gyro is preferred for reasons now to be stated.

9.11 ADVANTAGES OF SINGLE AXIS GYRO OVER TWO AXIS GYRO

Because of its single gimbal design the gyro inherently avoids the phenomenon of gimbal lock. The gyro is easier to cage (only one mechanism required) and easier to realign in operation should the reference be lost [3,6].

An additional benefit occurs from the adaptibility of the gyro to the floatation principle. High accuracy and ruggedness are both possible in these units.

9.12 PROBLEMS WITH SINGLE-DEGREE-OF-FREEDOM GYROS

These problems are of two types - fundamental, concerned with the concept itself, and practical, concerned with the mechanical hardware presently available.

The single axis gyro is subject to coupling effects. The gyro may become sensitive to angular velocity about its spin reference axis when there is any angular velocity about the input axis. The primary sensitivity of the device to angular velocity about the input axis and the coupling sensitivity stated above are proportional to the sine and cosine respectively, of the angle of deflection of the gimbal about the output axis. What this means is that to increase sensitivity and to prevent the coupling of the spin into the input, output deflections should be kept as small as possible.

The gyro spin bearing has long been a factor limiting the performance of conventional gyros. Rotor speeds greater than 24,000 r.p.m. are considered impractical because of the excessive power required to overcome windage and friction. Lower speeds are not favoured because angular momentum is lost. According to Whitcomb [11] in the typical 2×10^6 gram-cm^2/sec. gyro of normal proportions, motion of the rotor of the order of a fraction of a billionth of an inch per hour produces a torque change about the input axis large enough to cause the instrument to be rejected. The best ball bearings made cannot stabilize the rotor's center of mass to this extent.

The development of the self lubricated gas bearing has solved many of the mass stability problems and contributed to long life.

These advantages result directly in improved random and anisoelastic drift rates and consistent drift repeatability. Domini, Mott and Squillante [12] report that the Sperry S16-4200 gas bearing gyro should have a life of five years of continuous operation. It has withstood 70 g of centrifugal acceleration without touchdown. Lund [8] reports that a miniature gas bearing gyro (momentum 2×10^3 gm.cm^2/sec., rotor mass 3 gms) is capable of withstanding 100 g's.

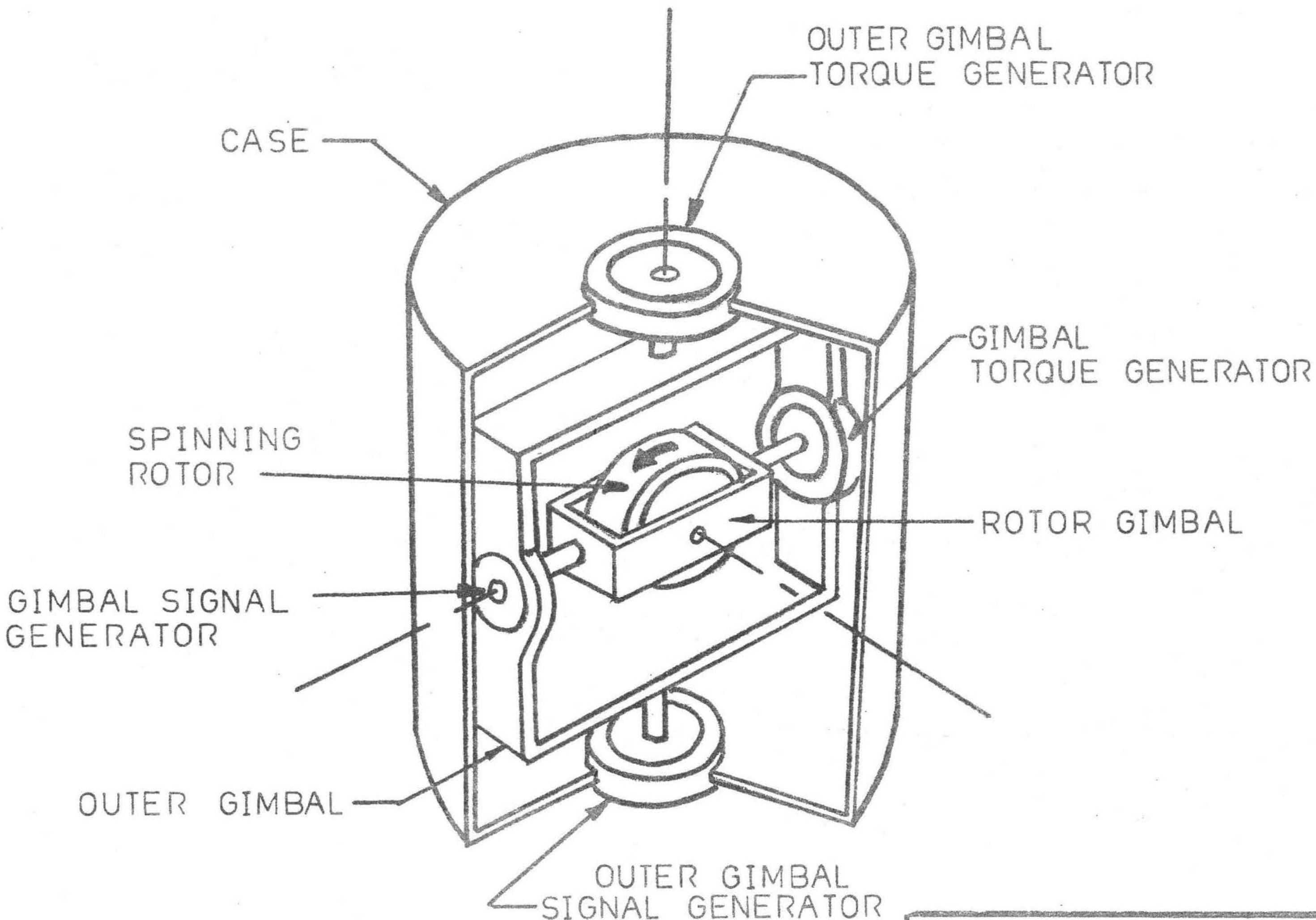

TITLE: TWO-AXIS GYRO	
SCALE: NONE	SOURCE: REF.
DRAWN BY: HILL	FIGURE NO: 9-1

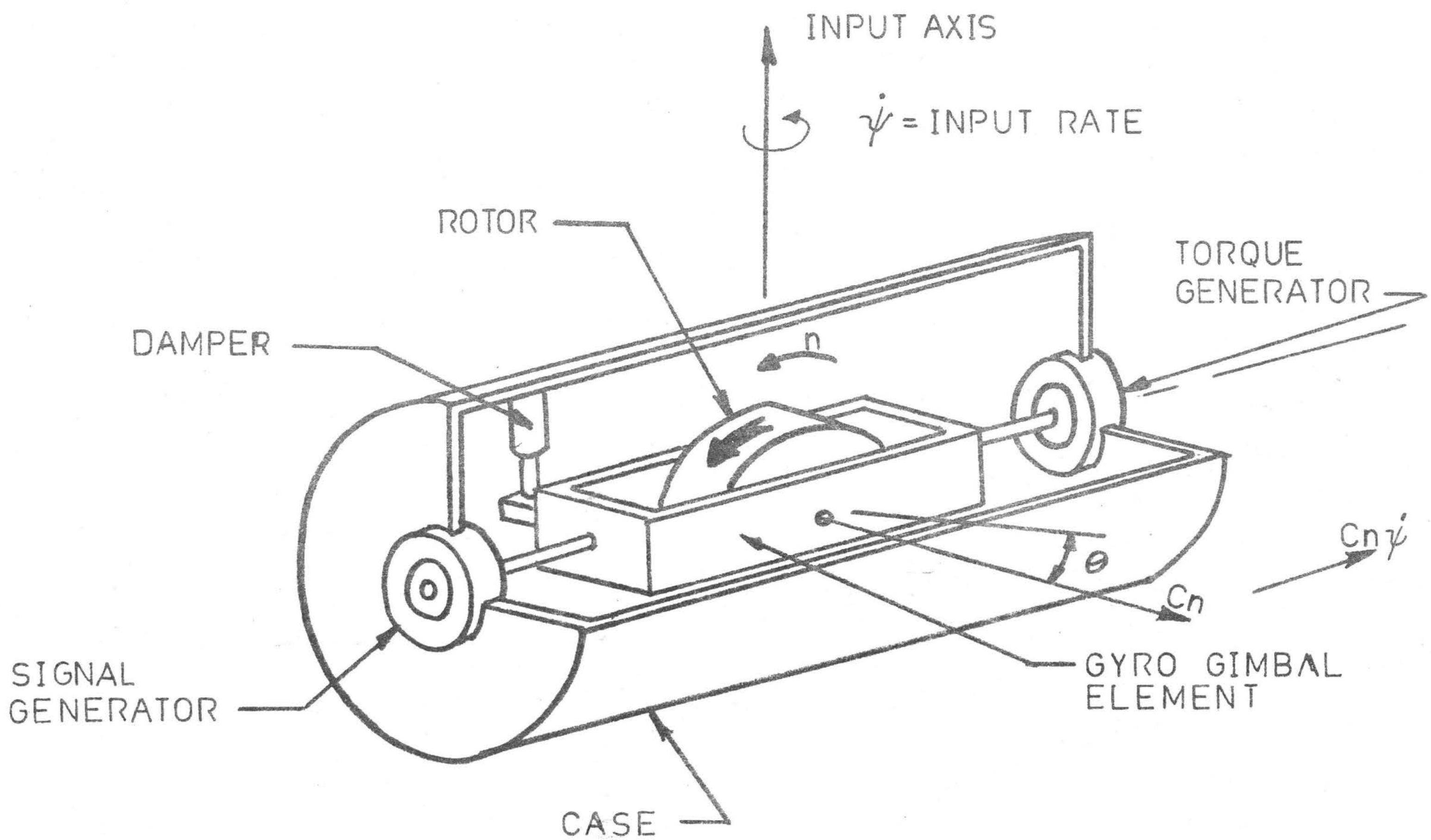

NOTE: THE MOMENT OF INERTIA OF ROTOR
ABOUT SPIN AXIS = C
n = ROTOR SPIN

TITLE: SINGLE AXIS INTEG. GYRO	
SCALE: NONE	SOURCE: REF.
DRAWN BY: HILL	FIGURE NO: 9-2

REFERENCES

1. Slater, J. M., "Gyroscopes for Inertial Navigators", Mechanical Engineering, September, 1957.

2. "Descriptive Data", Specifications for FF10 Series Gyros, Whittaker Controls and Guidance, California, 1966.

3. Savet; P.H., Gyroscopes: Theory and Design, McGraw-Hill, New York, 1961.

4. Arnold, R. N., and L. Maunder, Gyrodynamics, Academic Press, London, 1961.

5. Thomson, W. T., Introduction To Space Dynamics, Wiley and Sons, New York, 1961.

6. Puckett, A. E. and S. Ramo, Guided Missile Engineering, McGraw-Hill, New York, 1959, Chapter 10.

7. Wrigley, W. and W. M. Hollister, "The Gyroscope: Theory and Application", Science, Vol. 149, No. 3685, 1965.

8. Lund, P. S., "The Changing Emphasis and Future Trends in Navigational Gyros", S.A.E. Transactions, Paper No. 650586, 1966.

9. "Descriptive Data", Rate Gyro Performance Characteristics, R20 Series, Whittaker Controls and Guidance, California, 1966.

10. "Technical Data Handbook SA78A", Subminiature Precision Rate Gyroscopes, The United States Time Corporation, New York, 1955.

11. Whitcomb, E. W., "Interial Components", Sperry Engineering Review, Spring 1964.

12. Domini, R. G., J. R. Mott and A. J. Squillante, "Gyroscopes for Space Missions", Sperry Engineering Review, Summer, 1967.

CHAPTER 10

THE ELECTRICALLY SUSPENDED GYROSCOPE

10.1 DESIGN AND PERFORMANCE SUMMARY

The actual performance of the best electrically suspended gyros is classified. Dimensions and power levels required for a typical unit have been reported, by Knoebel [1] and Langford [6]. These are listed below:

TYPICAL SPECIFICATIONS:

Rotor Diameter	- 2.0 in. with 0.020 in. wall thickness
Rotor Weight	- 25 gm.
Total Weight	- 6-7 lbs. (including support electronics)
Operating Speed	- 200 rps.
Electrode Gap	- 0.010 in.
Electrode Area	- 10 cm^2
Container Vacuum	- 10^{-8} mm. Hg.
Applied Voltage	- 3800 RMS
Readout	- by 4 Photomicroscopes
Run Down Time-Constant	- 15,000 to 150,000 days
Drift - (potential)	- 0.0001 deg./hr.

Although the above information is sparse, it does illustrate the inherent compactness of this device, as well as its extremely long life. The very mechanization of the free rotor principle that is employed makes the electrostatic gyro well suited to use in a strapped-down system. Much work has been done recently on this application by the General Electric Company and the Minneapolis-Honeywell Company.

With respect to its physical environment it should be noted for future reference that considerable effort was expended to make the device reliable under 30 g acceleration loads, according to Knoebel [4].

10.2 PRINCIPLES OF OPERATION

The theory of operation of the Electrically Suspended Gyro (ESG) is best given in the thesis of Baker and Harrill [3]. A brief description of the principles of operation will be given here.

The ESG is basically a free rotor gyro. The sphere is supported by the electric forces between the two plates of a capacitor formed between the ball and the walls of the evacuated ceramic enclosure.

From basic physics, the force of attraction between the two plates of a capacitor is given by the equation

$$F = \frac{A e_o}{2} \left(\frac{V}{d}\right)^2 \tag{10-A}$$

where A = Area of a plate

e_o = Permittivity of free space

V = Applied voltage

d = Distance between the plates

From this relation it is seen that as the separation of the plates increases, the force of attraction decreases. This condition is unstable. To make this device operational one technique that is used is to apply an AC voltage to the capacitor through an RLC series circuit such as the one shown in Figure (10.2).

It can be shown that the voltage V_c is given by

$$V_c = \frac{V_i X_c}{R + (X_L + X_c)} \tag{10-B}$$

where $X_L = jωL$, $X_c = 1/jωC$

Now capacitance C can be given as Ae_o/d. Upon substituting for C, X_L and X_c, equation (10-B) can be divided by d to give

$$\left|\frac{V_c}{d}\right| = \frac{V_i}{\sqrt{(d - ω^2 L A e_o)^2 + (ωRAe_o)^2}} \tag{10-C}$$

From (10-C) one can calculate $(V_c/d)^2$ for $V_i = 1$ and substitute into (10-A). Thus

$$F = \frac{Ae_o}{2} \frac{1}{\sqrt{(d - ω^2 L A e_o)^2 + (ωRAe_o)^2}}$$

when a graph of F vs. d is plotted (see Figure (10-4) it will be seen that up to a displacement ϕ the change of force with increasing separation will be positive and the suspension will be "stable". After leviation is accomplished accurate centering of the rotor between electrode pairs is obtained by using a servo loop to control the applied high voltages by sensing the pairs of interelectrode capacitances.

The rotor is spun up by means of induction motor action. A rotating magnetic field is applied using coils A-A$'$ and B-B$'$ (see Fig. 10.1) which are excited by a two phase power supply. Helmholz coils C-c' are used to remove any wobble which may be imparted to the ball during spin up.

Attitude readout is accomplished optically. The exact approach depends upon the configuration in which the instrument is employed. For units used in gimballed systems the spin axis position is monitored and maintained fixed relative to the case with servo driven follow up of the gimballing. Spin axis monitoring is accomplished by having four photomicroscopes scan a zig-zag pattern placed on the rotor. See Figure (10.3).

When both pairs of pickoffs are scanning the center of the zig-zag pattern the wave form occurs at twice the pattern frequency. There is no fundamental component. When the rotor is out of alignment with the case, the pattern will be scanned either above or below its centerline. If the upper half of the pattern is scanned, Figure (10.3) shows that the output signal now has two components; a fundamental and a second harmonic. The magnitude of the fundamental is proportional to the displacement of the scanning line from the center of the pattern. Direction of displacement is obtained by comparing the phase of the fundamental with the phase of the second harmonic. When the scanning line is above the pattern center-line, the two signals will be in phase and out of phase when the scanning line is below center.

In the non-gimballed system of the type described by Christensen, [2], a great circle and a cosine line is placed on the ball. The pickoffs generate a direction cosine matrix. Comparison with reference values from a computer eventually determines the spin axis inclination. This method is quite complicated mathematically and requires careful study to appreciate its elegance. As the purpose of this report is the summarizing of general operating principles, further detail will not be shown. Reference [2], however, is very definitely a required paper should further work be considered in this field.

10.3 DESCRIPTION OF TEST MODEL

As the ESG is classified, no detail drawings are available. Figure (10.1), however, indicates the essential features of the device. Data is available to describe the University of Illinois gyro. The figures given below are considered to be typical for devices of this type.

The rotor is accurately centered within the electrodes by servo controlled high voltage. An acceleration of 4 g on a 25 gram rotor is supported by 3800 volts RMS with an electrode gap of 0.025 cm. This gives a field intensity of 150,000 volts per centimeter and a field emission current of 0.5 micro-amperes.

For readout two pairs of photomicroscopes observe a zig-zag pattern as described in Section (10.2).

The sphere is made from aluminum. Wall thickness is 0.020 in. thickened at the equator to 0.100 in. to increase the moment of inertia and define the spin axis of the ball. The rotor is hollowed out through 1/2 in. holes at the poles. The holes are then closed with plugs. Mating surfaces are gold plated to create a vacuum tight joint which prevents leakage of gas trapped in the ball during assembly. Sealing is necessary as the time to evacuate the ball would be prohibitive.

10.4 LEVIATION CIRCUITS

A.C. leviation is preferred to D. C. because it requires less complicated circuitry (6 instead of 12 electrodes for 3 axis support) and is not sensitive to D. C. stray charges trapped on the isolated rotor.

The leviation circuit shown in Figure (10.2) needs no amplifiers. It operates at a frequency near 50 K.C.

While the system works well in air without damping, in a vacuum damping is required to prevent slow buildup of oscillations. Figure (10.4) shows a damping circuit. The feedback coil modifies the inductance as a function of the levitation force.

10.5 PERFORMANCE TEST RESULTS

Performance of the existing Electrostatic Gyros is classified. The drift potential often quoted for these devices is 0.0001 deg./hr. Accuracy requirements are based on this predicted drift potential.

10.6 FREQUENCY DEPENDENCE OF OUTPUT SIGNAL

After spin up the rotor is independent of any driving circuits. It spins freely. No apparent drift signal can develop due to this action.

10.7 TEMPERATURE RESPONSE OF THE GYRO

As test data is not available, no temperature response can be quoted. It is true from basic considerations, however, that spin up generates heat in the rotor. Because of the hard vacuum environment this heat is not dissipated for about a day. The resulting aberrattions in the rotor's sphericity cause instability of gyro operation for about 24 hours.

10.8 HYSTERISIS

This phenomenon does not apply to the ESG.

10.9 ENVIRONMENTAL TESTS AND RESULTS

No data is available in the open literature.

10.10 RELIABILITY

No data is available. However, the reliability would be directly related to the reliability of the leviation power supply.

10.11 SOURCES OF SPURIOUS TORQUES

There are only four basic torque effects that can cause drift in the ESG. These results from four main causes

(1) mass unbalance in the rotor

(2) electric torques due to non-symmetrics of the electrode-rotor configuration

(3) gas drag torque from the pressures of finite molecules in the vacuum atmosphere.

(4) magnetic torques due to stray fields present in the spinning conductive sphere.

Mass unbalance effects result from non-coincidence of the rotor geometry with its center of gravity. Extreme care in construction must be exercised as these mass imbalances induce precession not only in the electric field but in the prescence of acceleration fields also.

Electric torques are caused by aberrations in the sphericity of the ball, and the tendency of the ball to become an ellipse at speed. Often the ball is designed with a prolated shape so that the desired shape is reached at speed.

Even at the pressure levels of 10^{-6} to 10^{-8} mm of mercury there are still finite molecules present which can cause rundown and precession torques.

Magnetic fields can effect the rotor which is essentially a spinning conductive sphere. For most work, however, these effects can be prevented by proper shielding and consequently neglected.

10.12 PRACTICAL PROBLEMS OF THE ELECTROSTATIC GYRO

The first main problem is one of precision. For this typical gyro described in Section (10.1), the rotor must have its center of mass within 2.6×10^{-9} inches of the geometric center to prevent static electric torques from causing an unbalance. The electrode gaps may be from 0.005 to 0.010 inches so that sphericity and speed deformations must be exactly known. Centrifugal deformation may be around 2.5×10^{-4} cm which is large compared to machining errors.

Problems of leviation and spin-up also have to be solved. Once the vacuum is obtained it must be maintained. When pressure is reduced to 10^{-7} or 10^{-8} inches of Hg in the container and the container sealed, lab tests have shown that the pressure may rise to 10^{-5} inches of Hg. This pressure drops quickly again to 10^{-8} in Hg. when an ion-getter pump is permanently attached to the container.

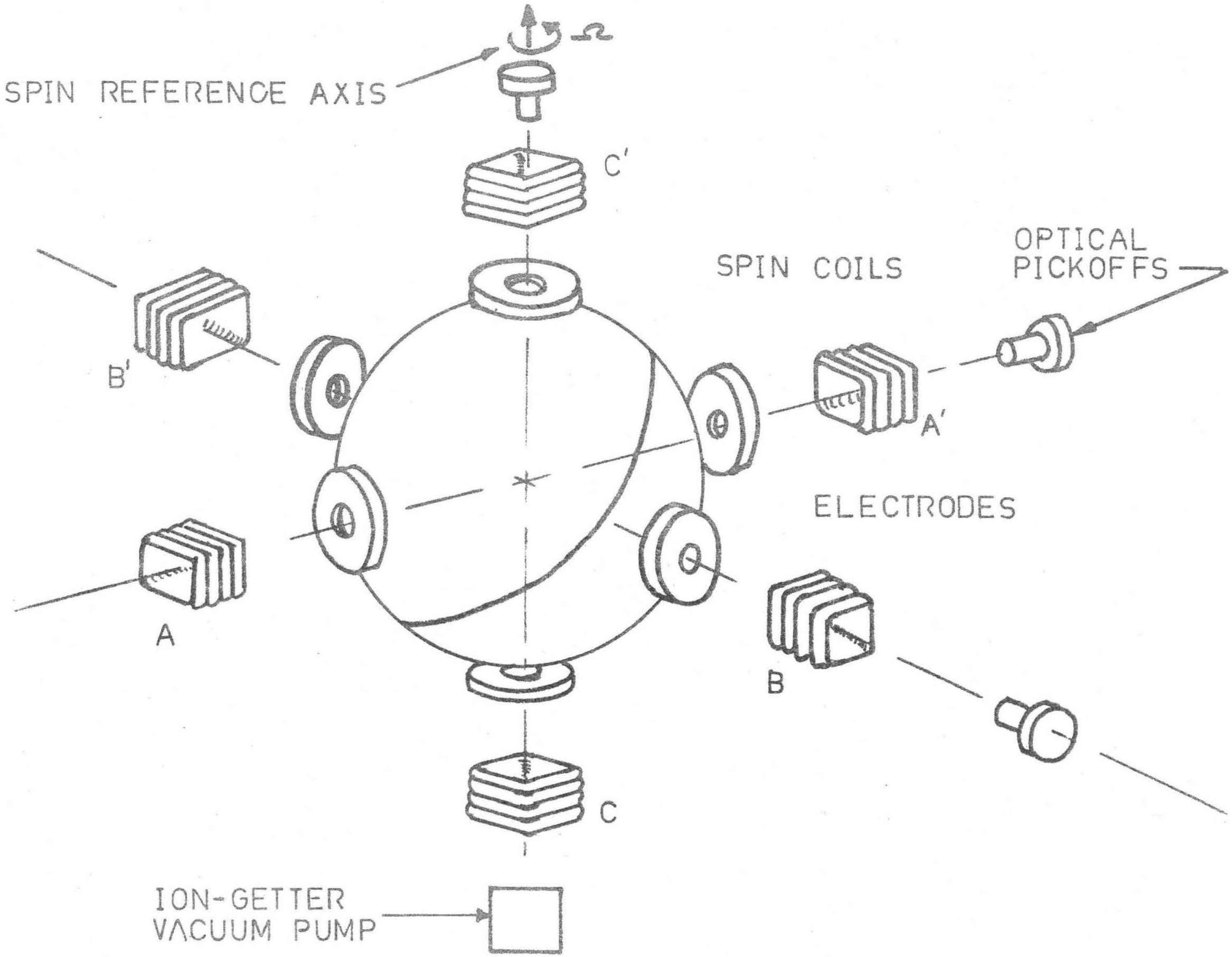

TITLE: ELECTRICALLY-SUSPENDED GYRO	
SCALE: NONE	SOURCE REF. 6.
DRAWN BY: HILL	FIGURE NO: 10-1

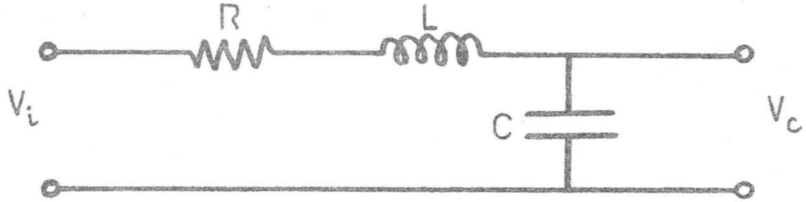

FIG 10-2A

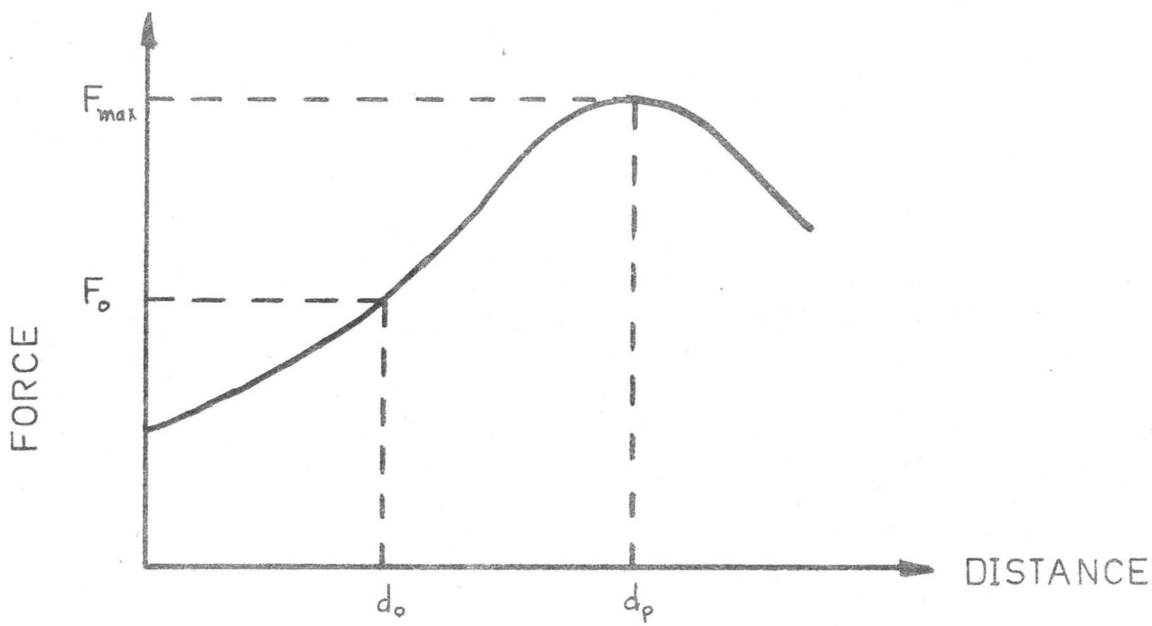

FIG 10-2B

TITLE: LEVITATION CIRCUIT	
SCALE: NONE	SOURCE: REF 3
DRAWN BY: HILL	FIGURE NO: 10-2

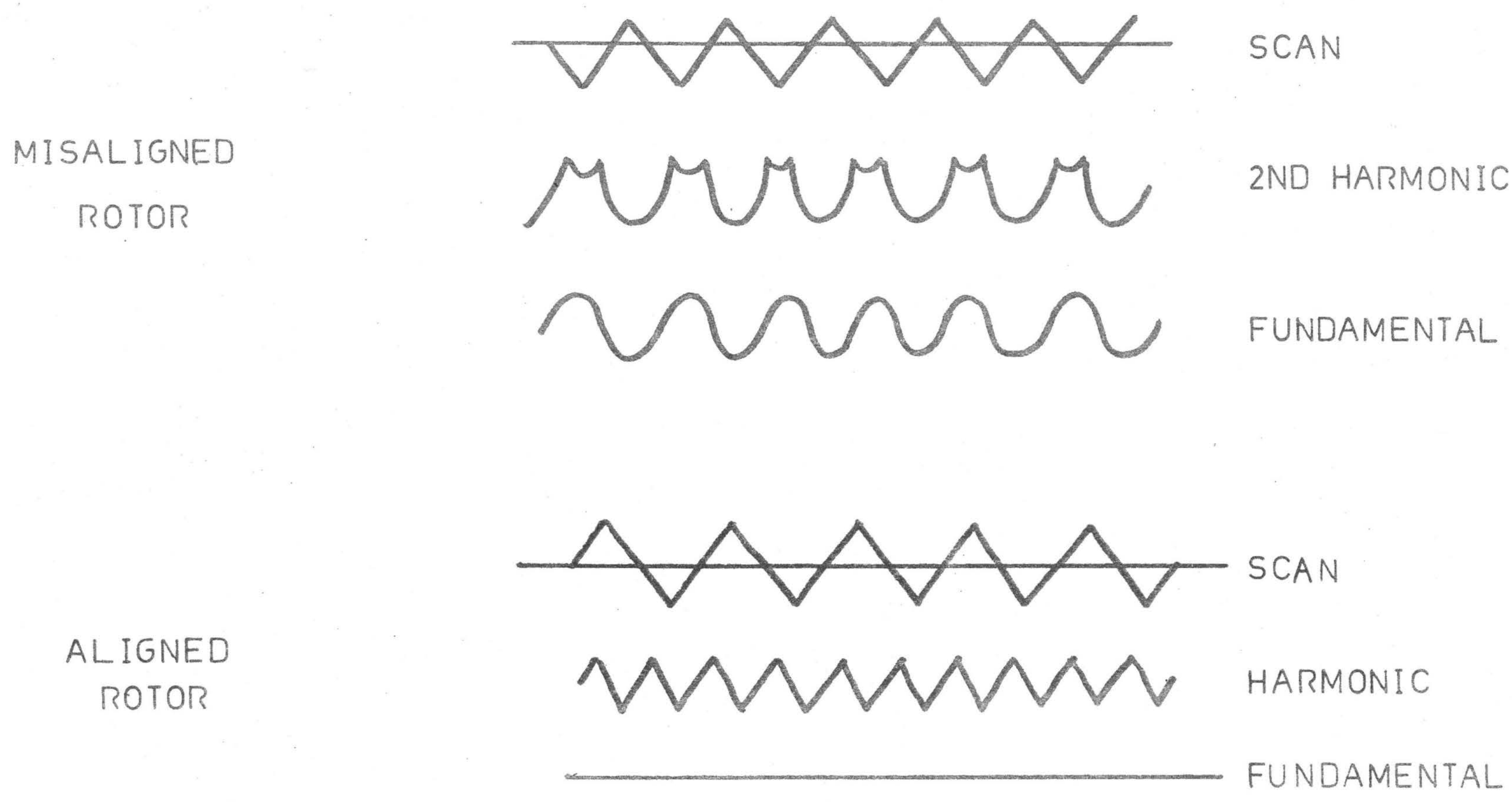

TITLE: READOUT PATTERNS	
SCALE: NONE	SOURCE: REF. 1
DRAWN BY: HILL	FIGURE NO: 10

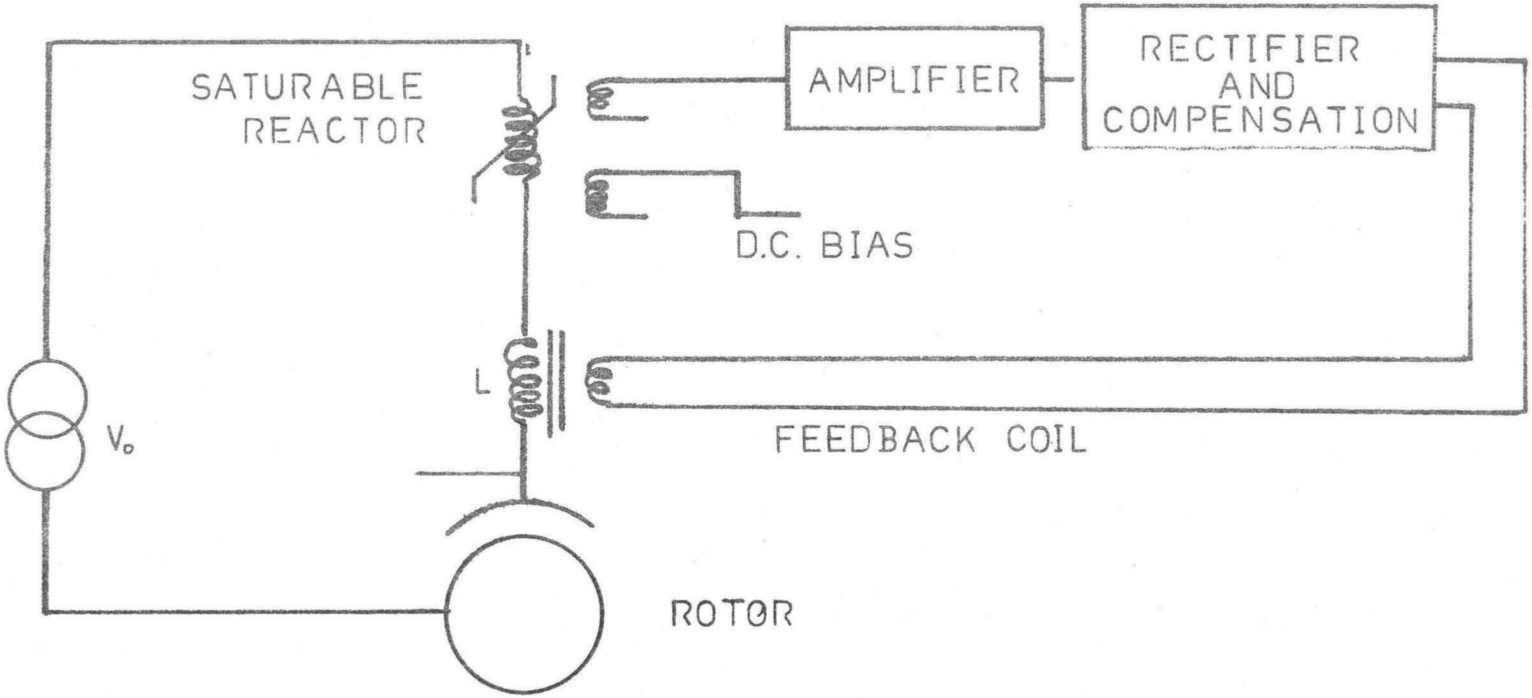

TITLE: LEVITATION SERVO	
SCALE: NONE	SOURCE: REF. 1
DRAWN BY: HILL	FIGURE NO: 10-4

REFERENCES

1. Knoebel, H. W., "The Electric Vacuum Gyro", Control Engineering, Feb. 1964, pp. 70-73.

2. Christensen, T. W., "Advanced Development of ESG Strapdown Navigation Systems", IEEE Trans. Aerospace and Electronic Systems, Vol. AES - 2 No. 2, March 1966, pp. 143-157.

3. Baker, D. H. and Harrill, I. W., "Basic Principles of Unconventional Gyros", Master's Thesis, M.I.T., May 1964.

4. Knoebel, H. W., Private Communication, July 6, 1967.

5. Lyman, E. M., "Studies Relevant to the Electrical Vacuum Gyro Programme of Electrical Breakdown in Ultrahigh Vacuum", Report R-334, Co-ordinated Science Labs. University of Illinois, Jan. 1967.

6. Langford, R. C., "Unconventional Inertial Sensors", Astronautica Acta, Vol. 12, No. 4, 1966.

CHAPTER 11

THE FLUID SPHERE GYROSCOPE

11.1 DESIGN AND PERFORMANCE SUMMARY

A gyroscope that has a rotor which is a spherical body of fluid has been successfully developed. The most noteable model is the 546-2550 developed by the Sperry Gyroscope Company. It is sensitive to rates about two axes orthogonal to the spin axis of the fluid. Specifications for this unit are listed below.

Specifications and Performance

Size	2 in dia. x 3-1/4" long
Weight	under 1 lb.
Sphere	diameter - 1 in.

Environmental		Drift Expected
Shock Loading	100 g.	
Linear Acceleation (sustained)	40 g.	0.08 deg./hr/g
Sine Vibration Tests	90 g	0.03 deg./hr/$g^{?}$

The reliability of such a unit has been shown to be very high when compared to regular floated solid rotor gyros. The reasons for this are

(1) Only two fluid gyros are needed to do the work of three floated gyros.

(2) Bearings are external to the unit. Therefore they can be larger and lubrication better maintained. Speeds are also lower for the fluid unit.

(3) The motor is external to the case. No delicate power leads are required.

There are several other advantages of the fluid sphere gyro. These will be noted later.

11.2 PRINCIPLES OF OPERATION

In the fluid sphere gyro a body of fluid is used as the rotor. The liquid is contained in a spherical cavity and is spun by rotating the cavity. Viscous coupling acts between the body of fluid and the walls of the cavity and therby causes the fluid to spin up with its container.

When spun in this manner, the body of fluid has angular momentum and thus tends to maintain a fixed direction in space. Because of the spherical shape the case can easily rotate about the spinning fluid in any direction.

The input-output relationship has been shown by Diamond [1] to be of the form

$$\frac{e_o}{e_{in}} = K \frac{\tau s}{\tau s + 1} \tag{11-A}$$

where e_o = output angle; e_{in} = input angle

τ = time constant $= \dfrac{0.381\,R}{\sqrt{\nu\Omega}}$

R = radius of cavity; ν = fluid kinematic viscosity;

Ω = cavity spin rate.

Both K and τ are functions of rotational speed, properties of the fluid, and sensor geometry. The device is thus known to behave as a free gyro at high frequency inputs and as a rate gyro at low frequency inputs.

To detect inputs which cause the misalignment between spin axes, use is made of the centrifugally induced fluid pressure at the walls of the container. In a spinning fluid body the centrifugal pressure is given by

$$P = \rho \Omega^2 R^2 \tag{11-B}$$

where

ρ = fluid density

Ω = spin rate

R = radius

Thus a change in the radial distance from the fluid spin axis to a pressure transducer on the outer cavity wall will show a pressure change.

In Figure (11.1) the two different radial distances r_1 and r_2 to the sensor pickoff parts can be seen as giving rise to a pressure difference detected by diaphragm A. Simultaneously there may be a pressure produced at diaphragm B due to rotation about the third quadrature axis. As long as a misalinqment exists (and thus as input rate) and the fluid spins at a frequency Ω, the pressure generated will be given by

$$P = \rho \Omega^2 R^2 \delta \sin(\Omega t + \phi) \tag{11-C}$$

where

δ = angular deflection in radians

ϕ = phase angle and a direct measure of the direction in space of the axis about which the rotation has occurred.

Equation (11-c) is valid for small values of δ only.

It will be seen that the output of the pressure transducers will go to zero when δ goes to zero. A pair of phase sensitive demodulators, using as references the output of a two phase alternator coupled to the spin axis, will produce voltages proportional to rotations about two orthogonal axes lying in the plane normal to the cavity spin axis.

11-3 DESCRIPTION OF TEST MODEL

The Sperry gyro is 2 inches in diameter, 3-1/4 inch long and less than 1 lb. in weight. The spin motor stator is contained within the gyro case. The case end caps have molded stators for the rotary transformer and support of the spinning inner case.

Ports through the cavity wall are at points about 45 degrees removed from the spin axis. Diaphragms arranged in the connecting passage of the ports are aluminum.

The operating speed is 6000 R.P.M.

The gyro can be designed to ensure that vibration is not a source of false pressure. The transducers, placed in diametrical opposition around the waistband of the sphere are equipped with aluminum diaphragms 0.001 inches thick that match the density of the liquid. Because of this density match the diaphragms are essentially floated and almost insensitive to vibration.

11.4 EXCITATION AND SIGNAL PROCESSING CIRCUITS

The circuitry required for signal processing is shown in Figure (11.2). Magnetic slip rings are used to transfer high frequency excitation to the spinning rotor and take signals from it. These slip rings are transformers that have ferrite cores with cylindrical air gaps in which the relative motion required for rotation occurs.

The carrier excitation from the input transforms excites four transducers in the pickoff; these are arranged in two pairs with diametrically opposed transducers in each pair. Each transducer is excited by one of the four quadrants of the output phase and the outputs of all four transducers are added. The single sideband output is derived by the modulation of the four carrier voltages phases by the four capacitative transducers. The steady state output is:

$$e_o = \omega\left\{ \sin\omega_c t \, \sin(\Omega t + \phi) + \cos\omega_c t \, \cos(\Omega t + \phi) \right\} \quad (11.0$$

where

ω = applied input rate

ω_c = carrier frequency

Ω = spin rate

ϕ = space phase of total input vector.

Equation (11-C) is the single sideband equivalent of

$$e_o = \omega \sin\phi \sin(\omega_c t + \Omega t) + \omega \cos\phi \cos(\omega_c + \Omega t) \qquad (11.D)$$

Now, since $\omega \sin\phi$ and $\omega \cos\phi$ are the inputs about orthogonal axes, if the signal is demodulated once with respect to each of two phases at sideband frequency, two d.c. voltage outputs are produced. The gyro employs a capacitative device to provide this sideband reference.

11.5 PERFORMANCE TEST RESULTS

(i) Operating Speed

Spin-speed selection is based on sensitivity, noise and stability. The optimum speed for this type of gyro (6000 r.p.m.) is relatively low as compared with wheel-type gyros. Although the generated pressure is proportional to the square of the spin speed, the time constant decreases with the square root of the speed. Also temperature gradients and vibrations are greater at a higher speed.

(ii) Hysterisis

When the displacement angle goes to zero the differential pressure sensed by the diaphragm goes to zero. Because the pressure of interest is alternating it is easily sensed and a static shift of diaphragm position produces no output signal. For this reason there is no hysterisis error.

(iii) Drift

No exact data is available. However, recent work at Sperry [3] reports random drift levels less than 0.1 deg./hour.

11.6 FREQUENCY DEPENDENCE OF OUTPUT SIGNAL

The use of a carrier signal requires that care be taken to avoid spin frequency modulation of this carrier. Such modulation could appear as bias output. However, by exciting the input transformer from a low impedance source and by working the output transformer into a low input impedance amplifier this effect can be largely eliminated.

11.7 TEMPERATURE RESPONSE OF THE GYRO

Performance of the Sperry SY6-2550 gyro was satisfactory in transient and steady state temperature tests over +60 deg. F. to +160 deg. F. without heater control.

Density of the fluid in the fluid sphere gyro is of secondary importance to its successful operation. The averaging effects of spin make diametric density gradients vanish. Centripetal acceleration forces convection currents which help to reduce axial gradients. The result is a fairly uniform fluid density which in turn means that the center of gravity of the fluid always coincides with its center of support. Mass balance is inherently possible at any temperature.

The time constant is inversely proportional to the square root of the fluid density, a fact which also reduces the importance of close temperature control. The liquid used usually has a low temperature-viscosity index.

11.8 HYSTERISIS AS A FUNCTION OF TEMPERATURE

This area is not reported in the literature as being a problem with the fluid gyro.

11.9 ENVIRONMENTAL TESTS AND RESULTS

The Sperry SY6-2550 gyro survived sustained linear acceleration to 40 g.

Drift under linear acceleration is low due to the close coincidence of the fluid center of gravity with the center of support. This is closely described in Section (11.7). Experience at Sperry has shown that an axial temperature gradient below 0.01 deg./cm. can be achieved. With such a gradient a drift of 0.8 deg./hr./g would result.

(ii) Shock Tests

The Sperry gyro survived satisfactorily 100 g shock tests.

(iii) Vibration Tests

Sine vibration tests were carried out to 90 g (peak), without difficulty.

In a 48 position sine vibration test, the g^2 sensitivity was found to be 0.03 deg./hr./g^2.

11.10 RELIABILITY

Diamond [2] shows a reliability comparison between a system using three conventional gyros versus a system using two fluid sphere gyros.

For a platform with three sensing axes, the reliability figure of merit is more than four times that obtainable with three conventional gyros.

11.11 ADVANTAGES OF THE FLUID SPHERE GYRO

In addition to the factors affecting reliability which are noted in Section (11.1), other important features are as follows.

1. In the investigation for anisoelasticity coefficient it was shown that even for an ellipsoidal cavity the drift under acceleration would be small. Thus only moderate tolerance need be achieved in sphere construction.

2. No special assembly or adjustments are needed. Construction costs are thus very low.

3. Periodic calibration during storage is not needed because the fluid is a stable fluid unchanged by long-term storage, and because the gyro is devoid of critical suspension components.

The sensitive element is completely non-magnetic and no drift results from close proximity to strong magnetic poles.

Other features such as the low vibration sensitivity, low pressure sensitivity and two axis sensitivity have been commented upon in previous portions of the text.

11.12 OTHER FLUID GYROS

There are two main classes of fluid gyros: rotating container and non-rotating types. Differences in the types of readout are the main distinguishing features between various models. The fluid sphere two diaphragm system seems to be the best to date.

Three main concepts which stand out in non-rotating container fluid gyros are now described.

Figure 11.3 illustrates one form. The rotor is a conductive liquid, such a mercury, is caused to spin by the rotating magnetic field of a conventional polyphase motor stator. The fluid rotates in the annulus. Input angular rates about the diameter of the annulus cause a pressure difference between a pair of ports at opposite ends of the annulus. The pressure difference can be considered to be caused by Coriolis acceleration.

This device is extremely simple in construction and reliability should be good. However, the value of Ω is severely limited by power input requirements and the d.c. output pressure is difficult to sense accurately at very low levels.

The vibratory column gyro is a hybrid device combining vibratory and fluid designs. See Figure (11.4). Fluid is caused to oscillate in a container by an acoustic driver. The fluid oscillates at the resonant frequency of the fluid in the tube (which acts much like an organ pipe). The device was patented by Granquist, (U.S. Patent 2,999,389) in 1961. Extreme symmetry in construction is required for low drift.

A third form of fluid gyro is the torus type. A conducting fluid is pumped around the torus by electromagnetic pumps. An effect similar to the conventional rate gyroscope is produced. Figure (11.5) shows the output axis torsion bar which is twisted when rotation about one axis of the torus causes a precession torque about an orthogonal axis. The angle of twist is a measure of the input rate.

No description other than that given by Wing [1] exists in the open literature.

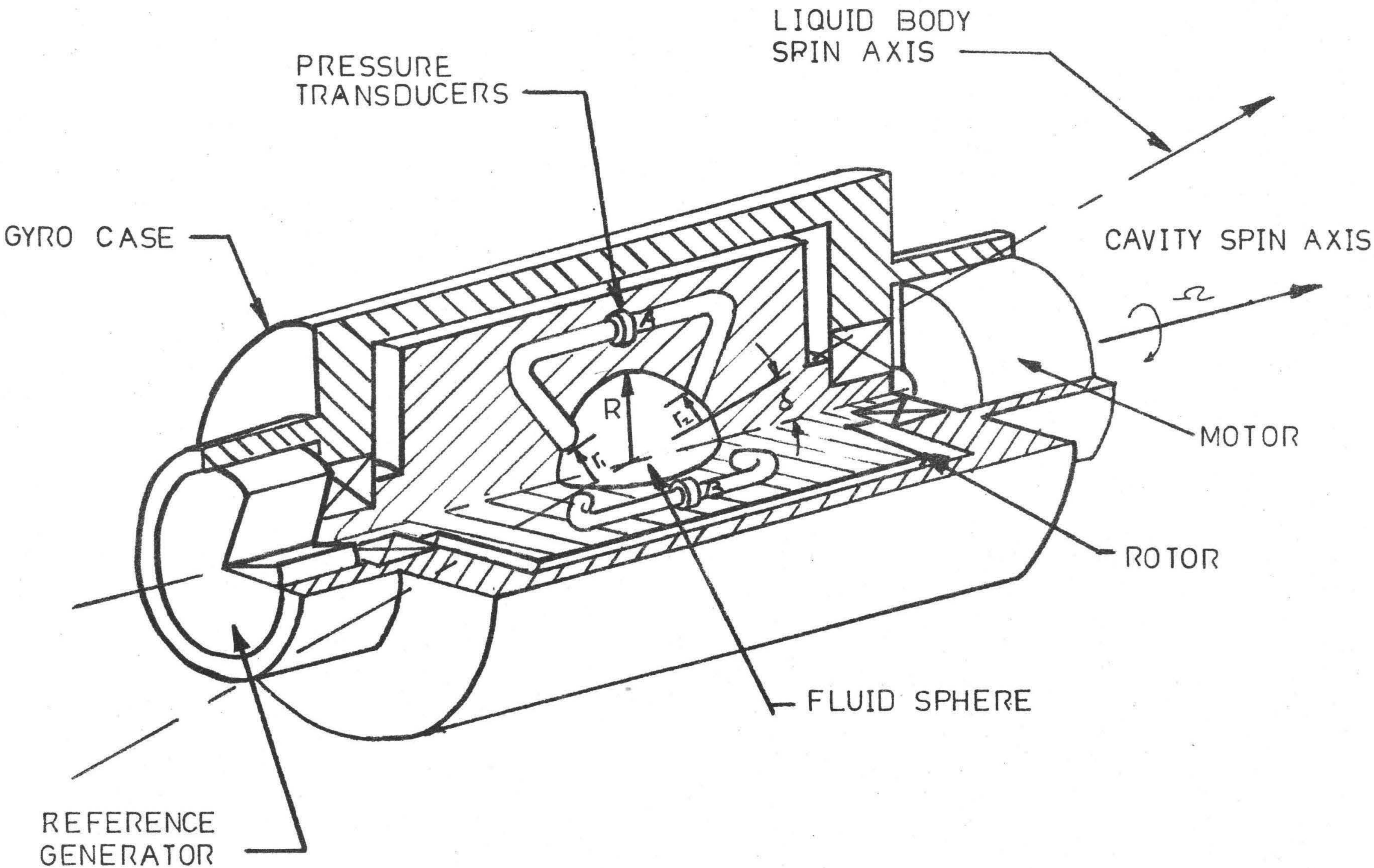

TITLE: THE FLUID GYRO	
SCALE: NONE	SOURCE: REF 1
DRAWN BY: HILL	FIGURE NO: 11-1

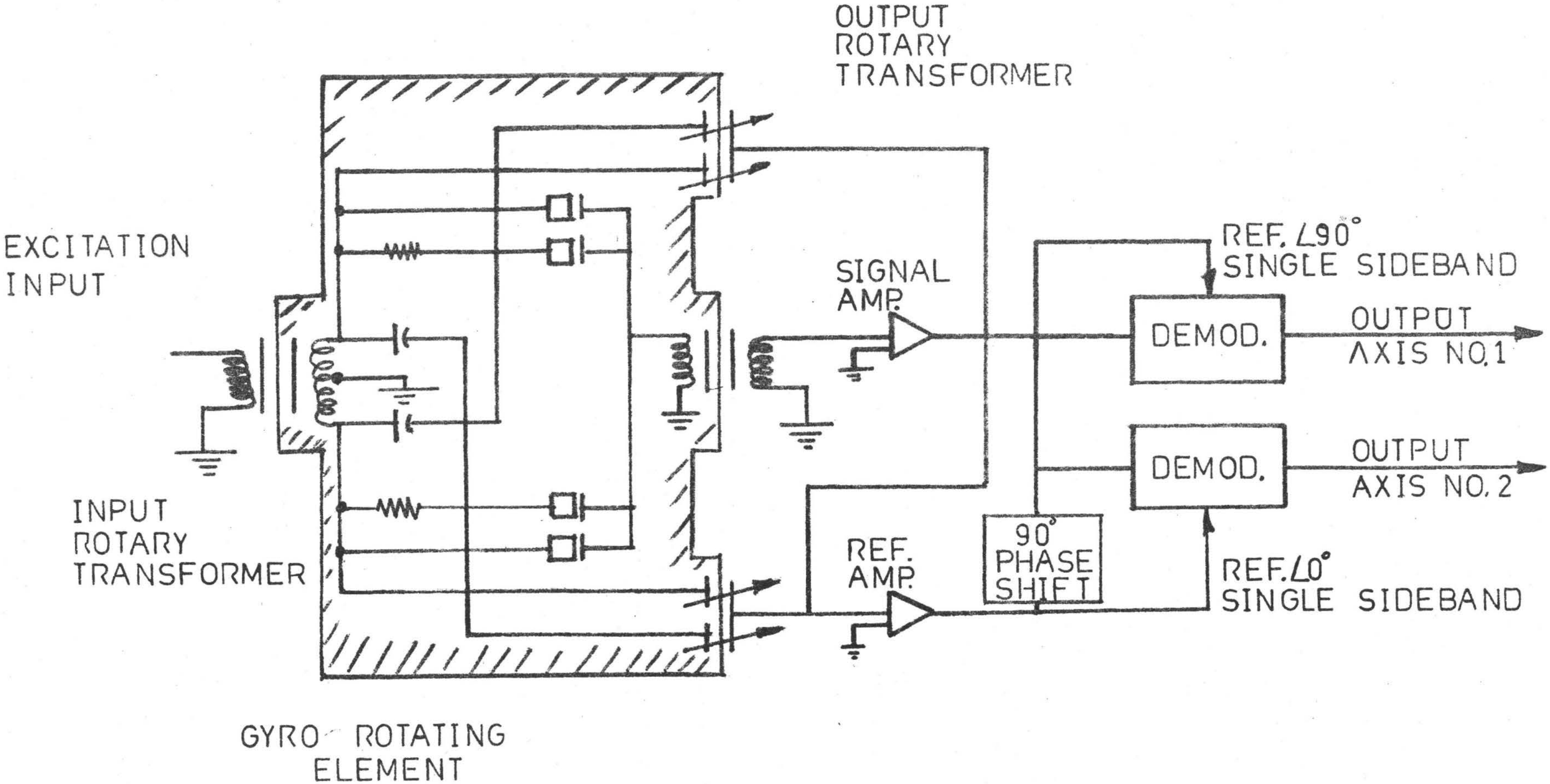

TITLE: FLUID GYRO CIRCUITRY	
SCALE: NONE	SOURCE: REF. 1
DRAWN BY: HILL	FIGURE NO: 11-2

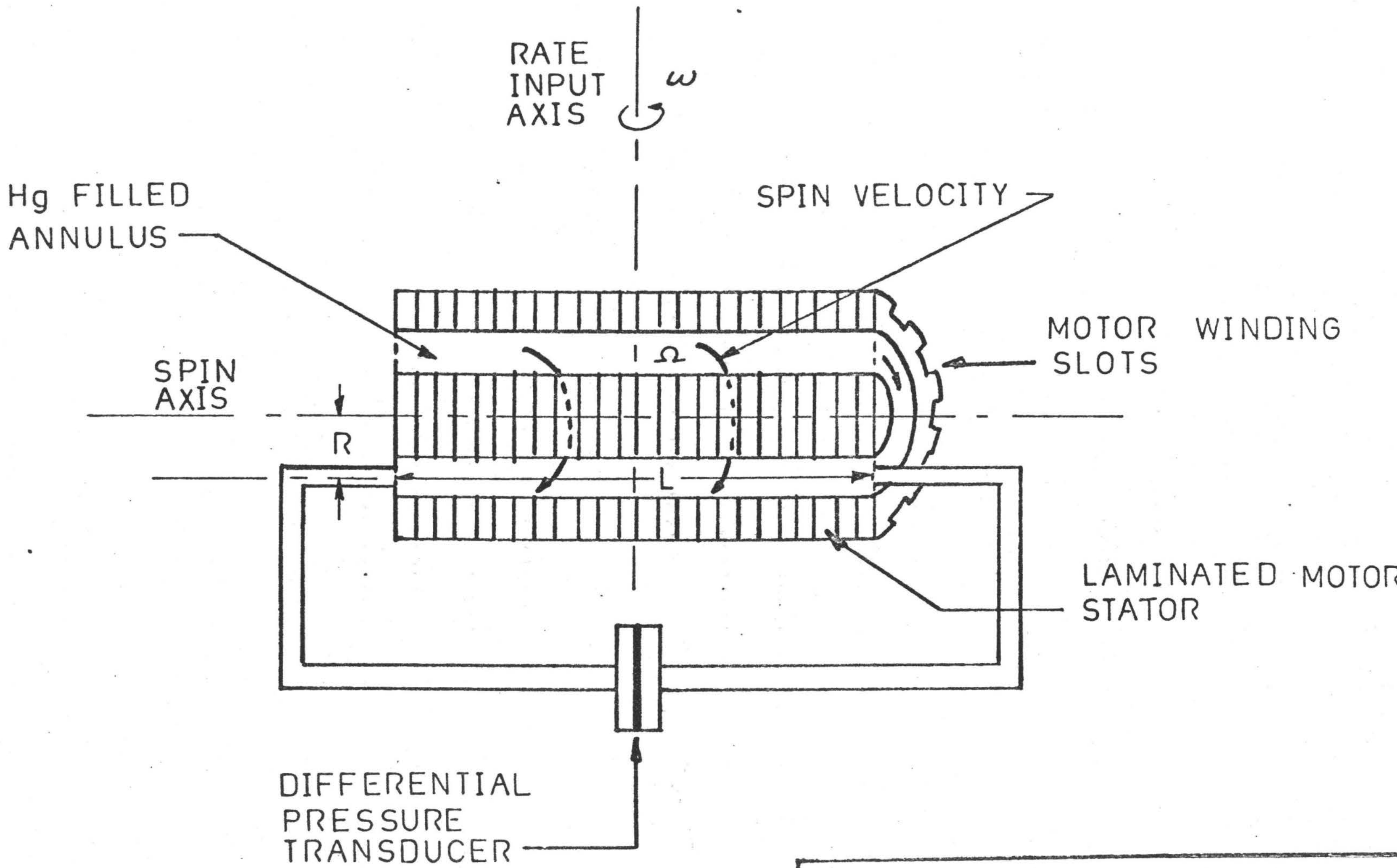

$$\Delta P = 2\Omega R L \rho \omega$$

TITLE: NON-ROTATING FLUID GYRO	
SCALE: NONE	SOURCE: REF. 1
DRAWN BY: HILL	FIGURE NO: 11-3

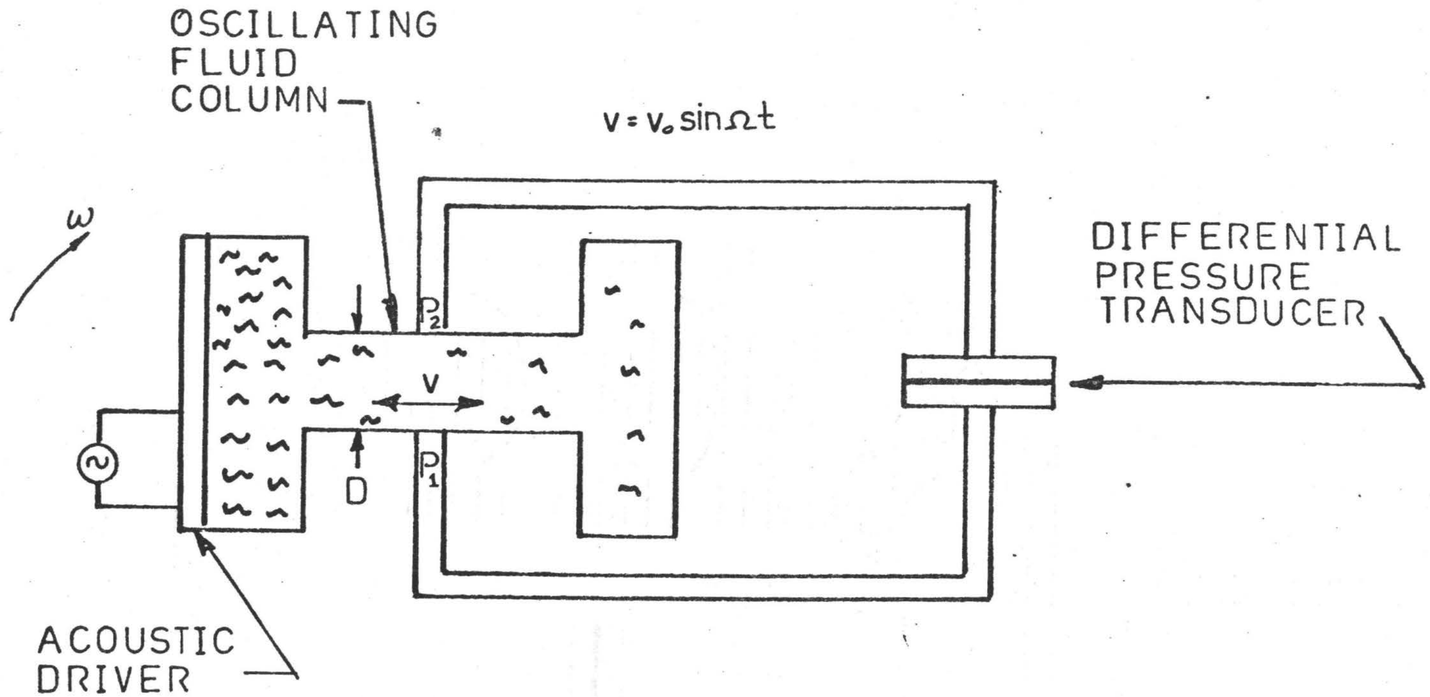

$$P_1 - P_2 = \Delta P = 2 v \rho D \omega$$

TITLE: VIBRATORY COLUMN GYRO	
SCALE: NONE	SOURCE: REF. 1
DRAWN BY: HILL	FIGURE NO: 11-4

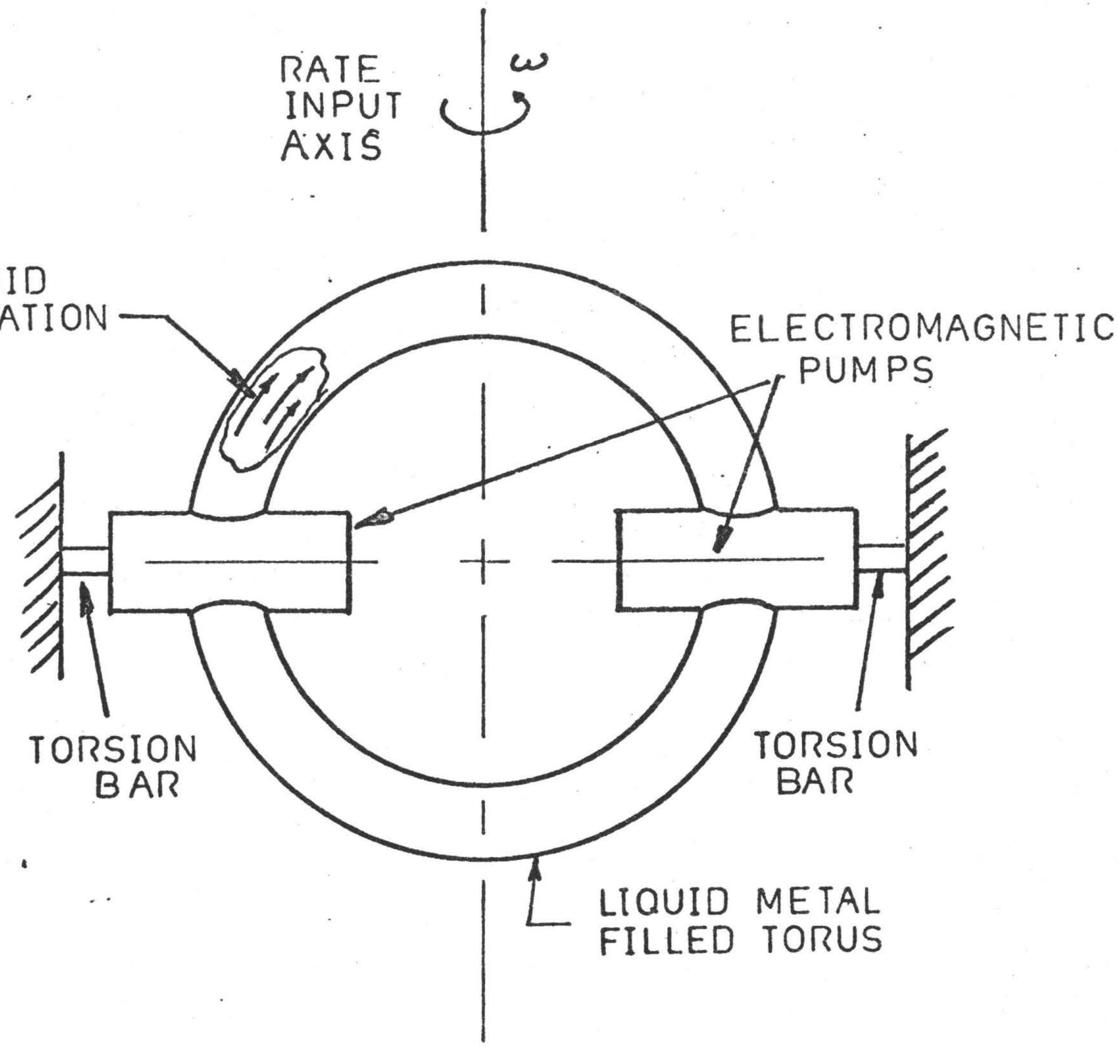

TITLE: FLUID TORUS GYRO	
SCALE: NONE	SOURCE: REF. 1
DRAWN BY: HILL	FIGURE NO: 11-5

REFERENCES

1. Wing, W. G., "Pros and Cons of Fluid Rotor Gyros", *Control Engineering*, March 1963, p. 105-109.

2. Diamond, H. R., "The Fluid Sphere Gyro", *Sperry Engineering Review*, summer, 1967.

3. Langford, R. C., "Unconventional Inertial Sensors", *Astronautica Acta*, Vol. 12, No. 4, 1966.

CHAPTER 12

THE LASER GYRO

12.1 DESIGN AND PERFORMANCE SUMMARY

The laser gyro combines the properties of the optical oscillator, the laser and general relativity to produce an integrating rate gyroscope.

Exact performance data and physical dimensions are not available in the open literature. For general information, however, Honeywell [1] has given capability characteristics that have either been achieved or will be achieved in the near future.

(i) Physical:

Weight . . . . 2 to 10 pounds

Volume . . . . 10 to 200 cubic inches

Power . . . . 2 to 4 watts

(ii) Drift:

Random . . . . 0.1 to 0.01 deg./hour

g sensitive . . negligible

g^2 sensitive . negligible

(iii) Scale Factors:

Stability . . . . one part in 10^5

Linearity . . . . one part in 10^6

Readout is in digital form with pulses coming at the rate of 2^{13} to 2^{19} counts/radian.

The laser gyro has no rotating mass no sensitive torquing element, no mechanical null point, no problems of mass unbalance and no temperature-sensitive flotation fluids. The ready-time is, extremely short, being less than 10^{-3} seconds.

12.2 PRINCIPLES OF OPERATION

The ring laser gyro operates on the basic principle that the laser is a light amplifier. The manner in which a gas laser works will be described first. The laser gyro will be considered as an extension of the basic device. The papers of Baker and Harrill [3] and Killpatrick [4] are excellent references for the theory of laser gyros.

The laser can be considered as a source of monochromatic coherent light. In its simplest form the gas laser can be considered as a modified gas-filled discharge tube. To obtain lasing action, two conditions must be fulfilled. First there must be a gain or amplification medium in the system to overcome energy losses. The gain medium consists of a tube filled with a mixture of helium and neon at a low pressure. A voltage is applied across a metallic anode and cathode as seen in Figure (12.1A). This voltage ionizes the contained gas, excited helium atoms collide with neon atoms transferring energy to the neon atoms and raising them to higher energy levels for a short time. A few of these high energy neon atoms emit a photon as they drop back to their normal energy level. These photons strike other excited neon atoms, causing other photons to be emitted, which in turn strike other neon atoms and so on. A multitude of photons is produced in all directions.

The second condition required to obtain lasing is a resonant cavity. If mirrors are located at each end of the tube, the photons travelling parallel to the axis of the tube will be reflected many times. The mirrors are the elements producing the positive feedback necessary to sustain oscillation. The cavity is resonant at a large number of frequencies since the cavity length is a large multiple of the optical wavelength of the emitted radiation. Most of these frequencies do not receive sufficient gain to achieve oscillation.

When a resonant frequency does receive sufficient gain to oscillate, the radiation intensity will build up to a steady-state value and be emitted through the mirrors which may be designed to allow transmission of a fraction of the light (around 0.2 percent).

The ring laser differs from the conventional laser in having three or more mirrors so placed as to cause the light to travel around a closed path as seen in Figure (12.1B). The ring laser is not different from the parallel mirror form. The possible oscillation frequencies are determined by having an integral number of wavelengths around the entire path. Because of the closed nature of the path, there can be two separate beams of light involved, one travelling in each direction.

For rotation sensing, the important characteristic of the ring laser is that the effective distance around the closed path changes when the assembly is rotated. This phenomena was explained best by Landau and Lifshitz [6]. They investigated the propagation of light in a closed loop. The shape of the loop was arbitrary. Their work was summarized by Baker and Harrill as follows.

The difference in transit time for this beam in a rotating loop from that with no rotation is given as

$$\delta t = \frac{1}{c^2} \int \frac{\omega r^2 \, d\phi}{1 - \left(\frac{\omega r}{c}\right)^2}$$

$$= \frac{\omega}{c^2} \int r^2 \, d\phi$$

$$= \pm \frac{2\omega A}{c^2} \qquad (12.A)$$

where δt = transit time difference

ω = angular velocity of the loop = $\dot{\phi}$

c = speed of light

r = radius of the loop

A = area of loop (normal to axis of rotation)

If the circumference of the loop is L, the actual time of transit is given by

$$t = \frac{L}{c} \pm \frac{2\omega A}{c^2}$$

$$= \frac{L}{c^2}\left(c \pm \frac{2\omega A}{L}\right) \qquad (12.B)$$

Thus, the conclusion is that the apparent speed of light is

$$c_{app} = c \pm 2\omega \frac{A}{L} \qquad (12.C)$$

Therefore, the two beams of light will have frequencies given as

$$f_1 = \frac{c_{app}}{\lambda} = \frac{c - 2\omega A/L}{\lambda} \qquad (12.D)$$

$$f_2 = \frac{c_{app}}{\lambda} = \frac{c + 2\omega A/L}{\lambda} \qquad (12.E)$$

The frequency difference is thus

$$\delta f = f_1 - f_2 = \frac{4\omega A}{\lambda L} = \frac{4 A f_s \omega}{c L} \qquad (12.F)$$

where f_s = frequency of the light source.

It can be seen that the difference in frequencies is proportional to the angular rate of the assembly. To use this property, samples of clockwise and counter-clockwise beams are mixed and applied to a photocell detector. The total light intensity seen by the photo detector will vary at the difference frequency and its electrical output will have this same frequency.

12.3 DESCRIPTION OF TEST MODEL

The design and construction of the laser gyro varies with application, with time (as technology advances) and with laboratory. The Honeywell gyro is described extensively in references [1,4] and because of the comparative wealth of information available on this device, it will be described here.

The Honeywell Laser Integrating Gyro, shown in Figure (12.2) is made from a solid block of high quality fused quartz. Holes are drilled in the block for the light path, fill ports, and anodes and cathode.

Mirrors are made by vacuum depositing very thin films of dielectric materials in multiple layers on pieces of quartz. The mirrors back surfaces are polished optically flat and held in place by molecular attraction, or a so-called "optical contact".

The interior of the block is cleaned, evacuated and filled with a gas mixture of 10 parts helium to 1 part neon at a pressure of about 5 mm. of Hg. A voltage (around 1000 vdc) is applied between the anode and cathode. Lasing action occurs if proper alignment of the mirrors is attained.

12.4 EXCITATION AND SIGNAL PROCESSING

Excitation has been described. It simply requires the application of a d-c voltage across the anode and cathode to initiate and maintain the ionization of the helium.

The output readout technique is essentially an optical one using prisms and photo cells. A diagram of the laser beam paths is shown in Figure (12.3).

A small amount of the laser energy is transmitted through the mirror. The transmitted energy is uniquely related to the frequency and phase of the energy in the cavity. The two transmitted beams are combined to produce a fringe pattern of alternate interference. If the phase between the two oscillators remains fixed, the fringe pattern remains fixed. Should the phase between the two oscillators change (i.e. there is a frequency difference between the two oscillators) the fringe pattern will appear to move to the right or left. The direction of motion will depend on the direction of the phase change (which oscillator is at the higher frequency) and the magnitude is measured by the number of fringes.

The output sensing devices are two photo detectors mounted at the readout prism and placed about a quarter of a wavelength apart. With this spacing, their outputs are phased so that the direction, as well as magnitude of the fringe motion can be monitored. When the gyro is rotated clockwise the fringe pattern moves in one direction;

when the input is reversed, the pattern motion is reversed.

The signal from each detector is amplified and used to trigger digital counters that monitor plus and minus counts. For rotations in one direction the counts are identified as positive. The number of pulses is used to determine the magnitude of the angle turned through. The angular size of each count is dependent upon the gyro relation between input rate and output frequency difference.

For example, consider an input rate of 1 deg./hour. This rate will produce typically a frequency change of 1 Hz. Now one degree per second is 1 arc second per second. Therefore, each second an inertial angle of one arc second is generated and an output phase change of one cycle is produced. Thus each count has a weight of one arc second. Turning the gyro through 360 degrees would produce 1,296,000 pulses.

12.5 PERFORMANCE TEST RESULTS

(i) Operating Frequency:

The Honeywell laser gyro uses two optical oscillators operating at 3×10^{14} Hz. [4].

(ii) Linearity:

The variation of output frequency with rotation rate is almost ideally linear for rates measured as high as 1000 deg./second. Refer to Figure (12.4). At extremely high input rates (10^8 deg./hour) the output deviates from the ideal by one part in 10^6.

(iii) Hysterisis:

This phenomena does not appear to be a problem.

(iv) Drift:

Exact figures are not published. Generally the magnitudes of random drift are from 0.1 to 0.01 deg./hour, [1].

(v) Threshold:

The minimum detectable input rate is now around 0.1 deg./hour [4]. Theoretically the gyro should be able to measure rates down to zero. This limit may not be reached because of fundamental problems such as "lock-in" which will be discussed later.

12.6 FREQUENCY DEPENDENCE OF THE OUTPUT SIGNAL

There is no problem with frequency control of a power supply. There is a problem with the frequencies of the two apposing laser beams called frequency "lock-in". It is a different phenomena than would be expected here, and thus will be covered in the special problems section.

12.7 TEMPERATURE RESPONSE OF THE GYRO

The laser gyro performance is not affected by temperature.

12.8 ENVIRONMENTAL TESTS

(i) Acceleration:

Ultimate performance limits are not known. However, the Honeywell quartz laser gyro has been spun on a centrifuge to a linear acceleration of 23 g's. There was absolutely no deterioration in the gyro's linearity of response as shown in Figure (12.4).

(ii) Shock and Vibration:

Because of the very nature of the gyro's operation there are no g or g^2 sensitive elements to affect its output. Ultimate environmental conditions will depend on how well the gyro body can maintain its alignment. Because the gyro is a solid block, this limit should be very high indeed.

12.9 SPECIAL PROBLEMS OF THE LASER GYRO

(i) Lock-In:

"Lock-in" refers to the coupling of the two oscillators. At a very low input rate the frequency difference between the two oscillators will fall to zero before the input rate goes to zero. The input rate at which this lock-in zero difference frequency occurs is called the lock-in rate. Lock-in is caused by scattering or back reflections of energy from mirrors or from other objects in the light path. These back reflections couple energy from one beam with energy from another. The effect on the input-output relation is shown in Figure (12.5).

The input rate where lock-in starts is given by the relation

$$\text{Lock-in Input Rate} = \frac{k(\text{wavelength})^2(\text{scattered losses})^{1/2}}{(\text{enclosed area})\ (\text{beam diameter})}$$

In practise the magnitude of the lock-in rate is typically 100 deg./hour for a ring of about 0.1 m^2 enclosed area.

(ii) Null Shift:

The null shift is an error in the output which occurs when the input-output zero is shifted (see Figure 12.6). This effect is caused by the direct current used to excite the laser gyro. The mechanism is as follows.

When a gas discharge is maintained with a direct current, the gas flows in the discharge cavity. The flow is established by such effects as wall collisions, charge distribution on the wall and the electric field along the discharge. The result is a flow of gas toward the cathode in the center of the discharge and a flow back toward the anode in a region close to the cavity walls. The laser energy is concentrated in the center portion of the cavity and therefore passes through gas that is flowing toward the cathode. The flow produces a shift in the index of refraction that depends on the relative directions of the laser energy and the gas flow. Therefore, the cavity will appear longer in one direction than the other, and will cause an apparent null shift in the input rate sensed by the gyro.

This effect can be reduced by constructing the gyro in a balanced fashion with two anodes and one cathode as shown in Figure (12.7). Energy travelling around the cavity now passes through gas travelling both with and against the laser energy. By balancing the two anode currents the null shifts due to this effect can be greatly reduced.

By balancing the two anode currents the null shifts can be greatly reduced, If only one anode is used apparent input rates of several hundred degrees per hour are introduced. This effect can be used to advantage either to cancel other null shift terms or to introduce known input rates purposely.

(iii) Multimode Effects:

There can be problems when two or more modes of about the same intensity are present and the difference frequency between clockwise and counter-clockwise beams of one mode is 180° out of phase with the difference frequency of the other mode.

Two undesirable effects are noted. First, there is interference at the detector, causing noise. Secondly, there is interference in the cavity, also causing noise.

Proper design can eliminate all modes except one. Generally it is possible to either reduce gain or to increase the losses in the unwanted mode so that no lasing occurs at those unwanted wavelengths.

12.10 BIASING TECHNIQUES

One method of overcoming the lock-in problem is to introduce another known or effective, input rate to the gyro. This biasing moves the operating point of the laser gyro away from very low rates where lock-in occurs, to much higher rates where ideal operation is approached. The total input rate is now the sum of the input rate and the bias rate. The true input can be found by merely subtracting the known bias from the gyro output.

The most practical method of producing this bias is to introduce into the laser cavity an optical element having an index of refraction dependent upon the direction in which the radiation is passing through the element.

The magnitude and direction of this index difference can be controlled by the magnetic field in a Faraday Cell. A schematic is shown in Figure (12.8). Since the subsequent light path is larger in one direction than the other, the laser gyro is biased (see Figure (12.9)) away from the lock-in region.

Figure (12.9) shows the results of a fixed bias technique. This approach requires strict bias stability (e.g. an internal bias of 10^6 deg./hour must be stable in one part in 10^8 to measure rates of 10^{-2} deg./hour [3]).

An approach to avoid the bias stability requirement is to oscillate the bias from positive to negative. Varying the magnetic field of the Faraday Cell will do this. Since the gyro is an integrating rate gyro only the net rotation angle appears at the output.

12.11 PRACTICAL PROBLEMS OF THE LASER GYRO

While many of the important operational problems have been discussed and the methods of solution have been outlined, other problems have yet to be solved for the laser gyro. Performance has not yet reached the level attained by conventional gyros. Present size is not yet competitive but great strides are being made in this direction [2].

The main limits to the gyros ultimate performance presently seen are construction, cleanliness, and bias techniques [2].

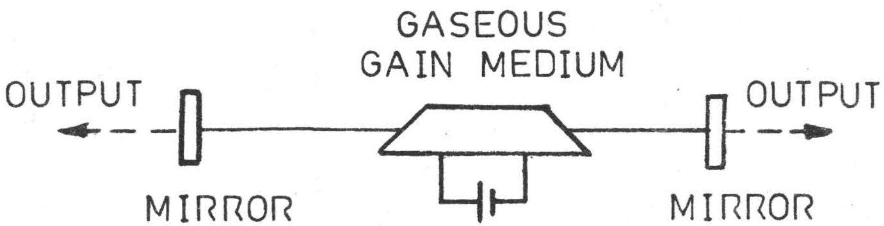

(A)

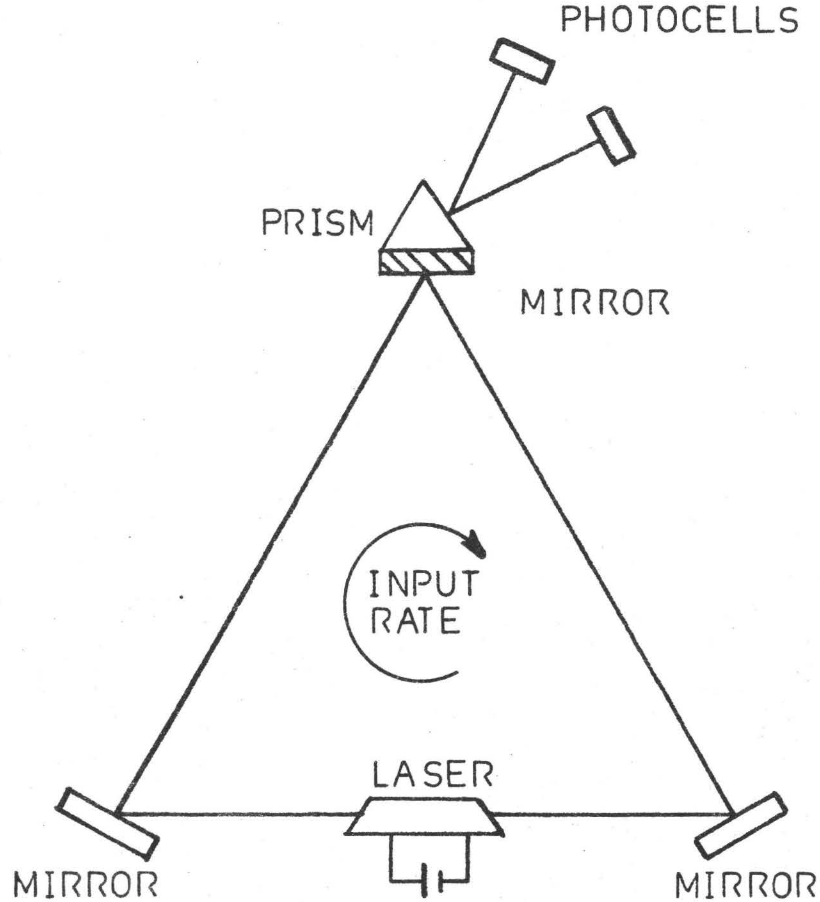

(B)

TITLE: FUNDAMENTALS OF OPERATION	
SCALE: NONE	SOURCE: REF. 4
DRAWN BY: HILL	FIGURE NO: 12-1

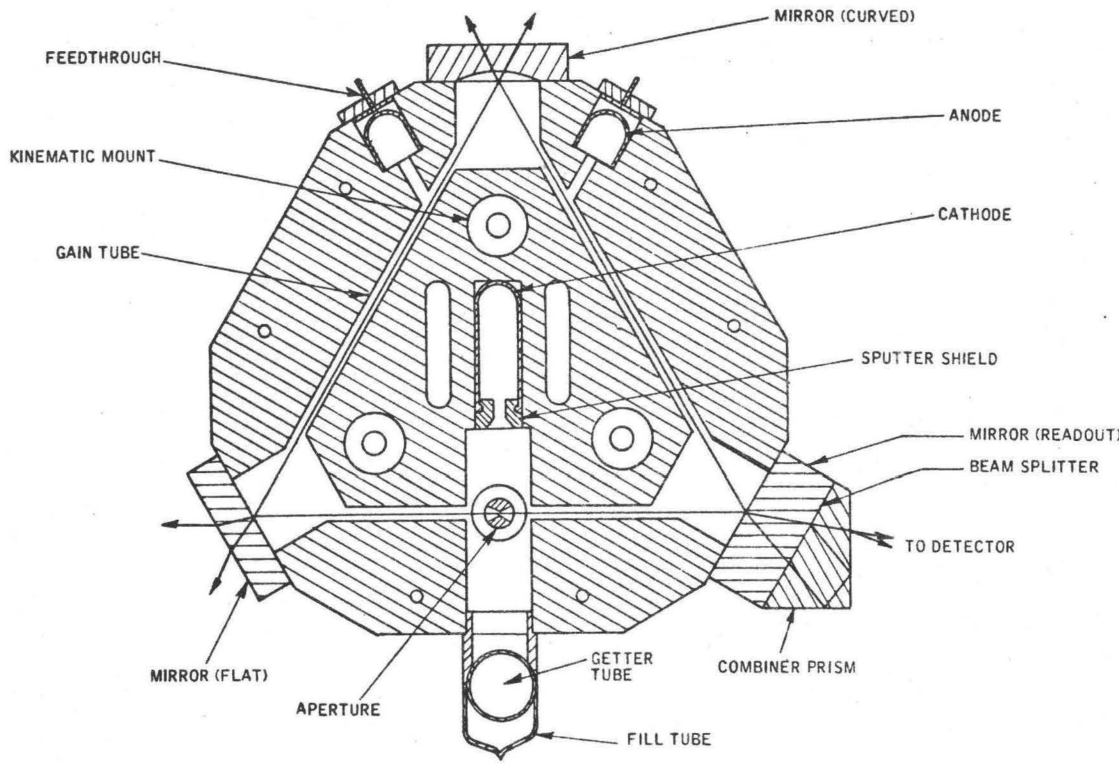

TITLE: QUARTZ BLOCK LASER GYRO	
SCALE: NONE	SOURCE: REF. 1
DRAWN BY:	FIGURE NO: 12-2

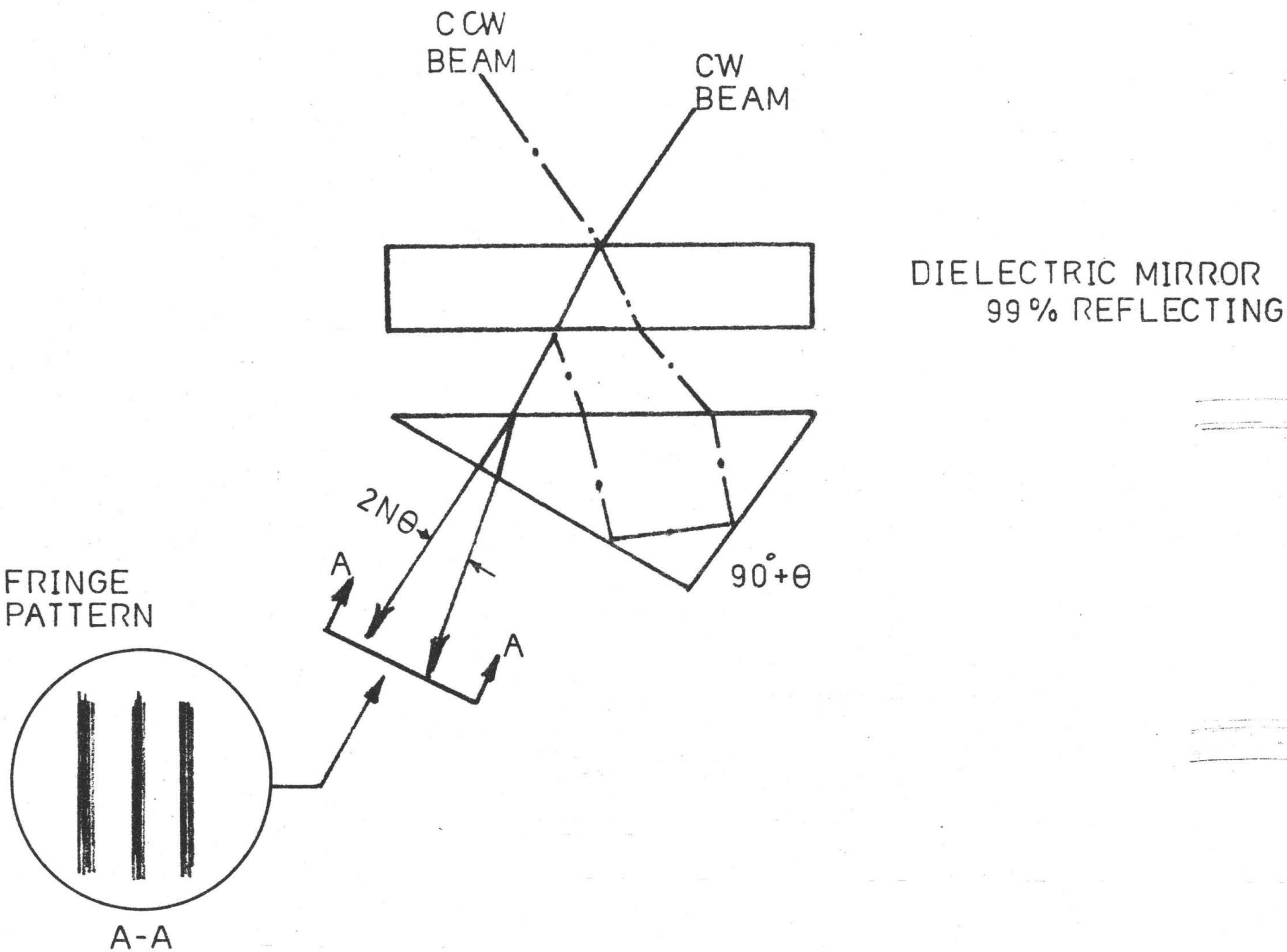

TITLE: OPTICAL READOUT TECHNIQUE	
SCALE: NONE	SOURCE: REF.
DRAWN BY: HILL	FIGURE NO: 12-3

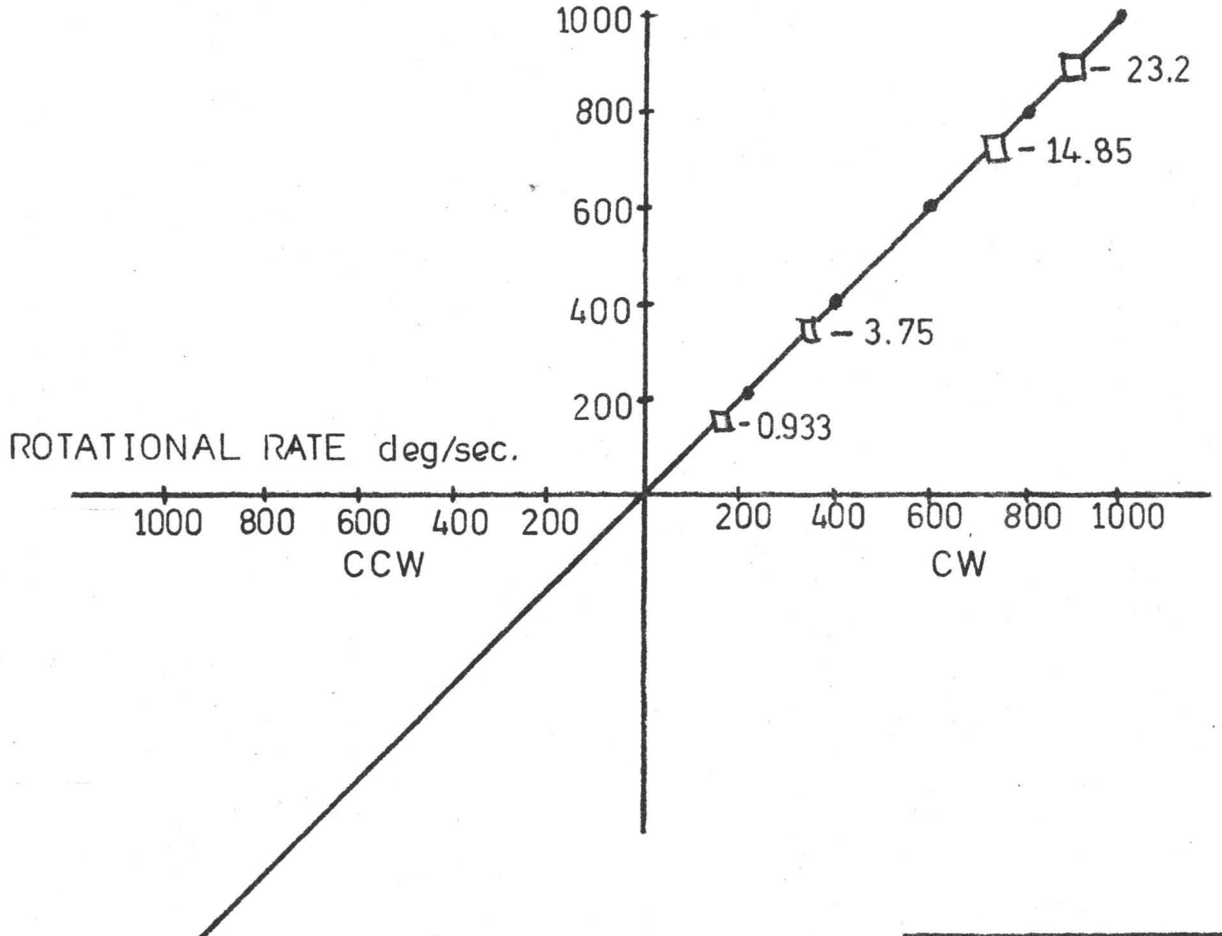

TITLE: LINEARITY GRAPH	
SCALE: AS SHOWN	SOURCE REF.
DRAWN BY: HILL	FIGURE NO: 12-4

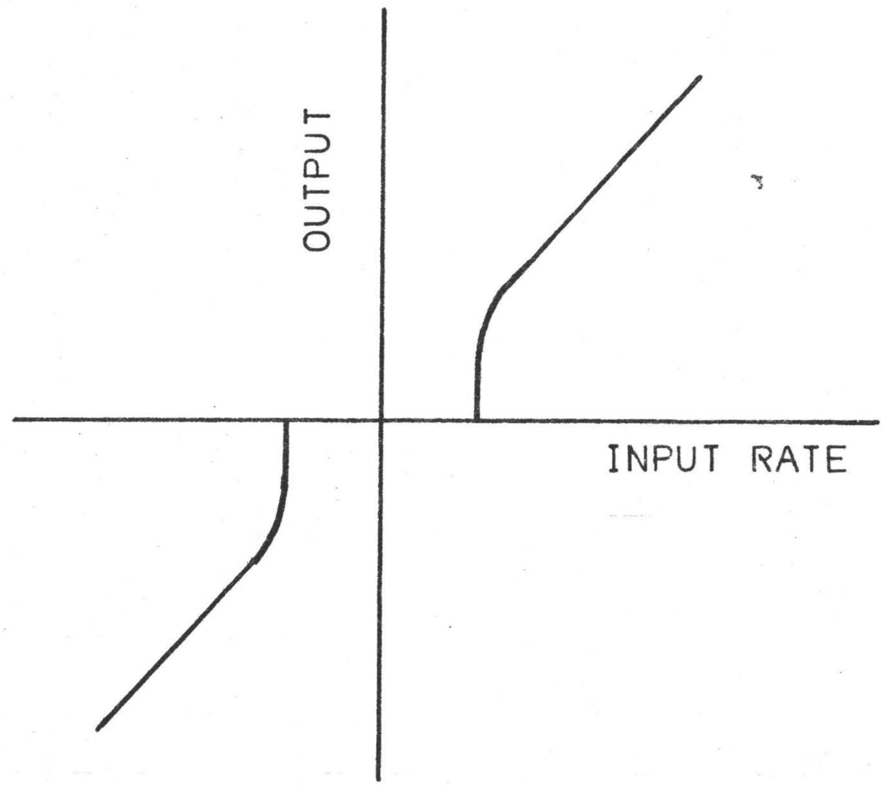

TITLE: EFFECTS OF LOCK-IN	
SCALE: NONE	SOURCE: REF.
DRAWN BY: HILL	FIGURE NO: 12-5

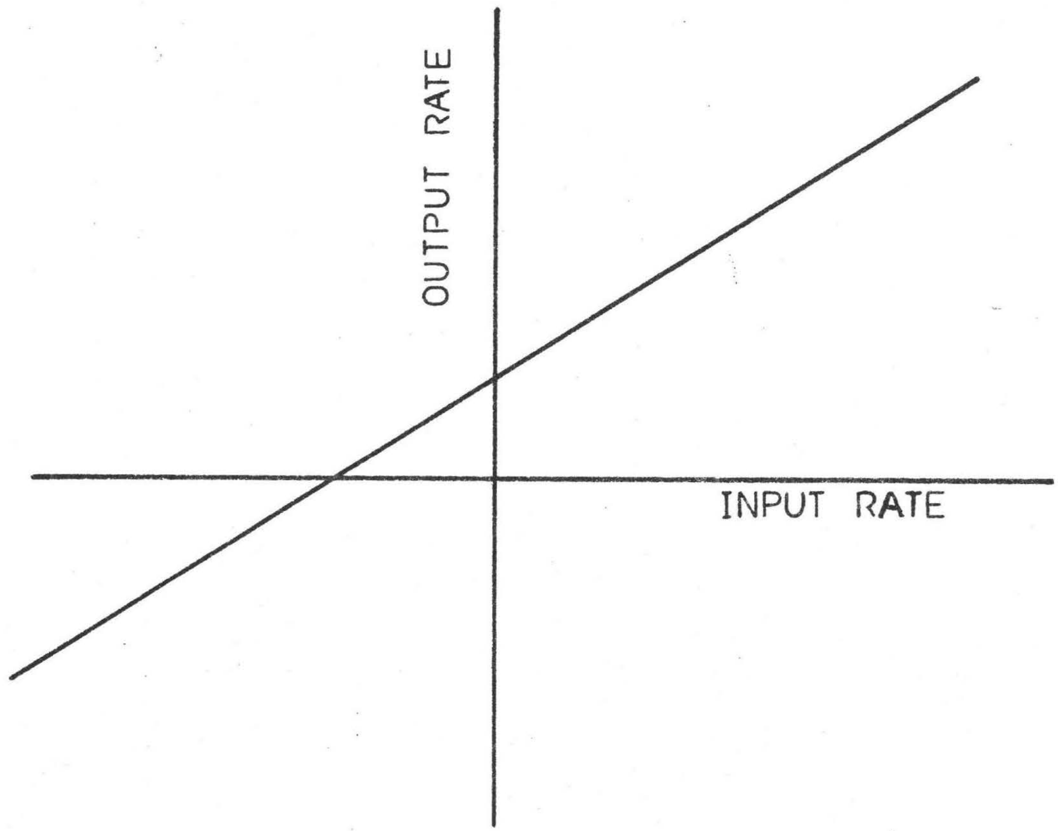

TITLE: GYRO NULL SHIFT	
SCALE: NONE	SOURCE: REF.
DRAWN BY: HILL	FIGURE NO: 12-6

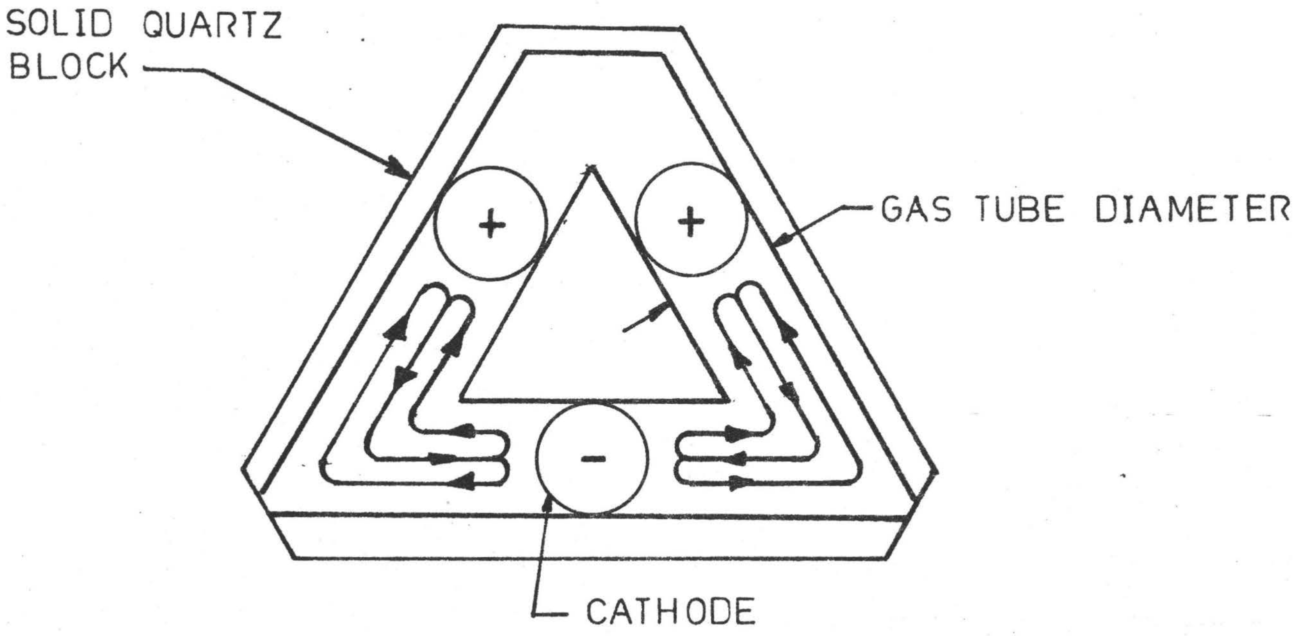

TITLE: NULL SHIFT REDUCTION	
SCALE: NONE	SOURCE: REF.
DRAWN BY: HILL	FIGURE NO: 12-7

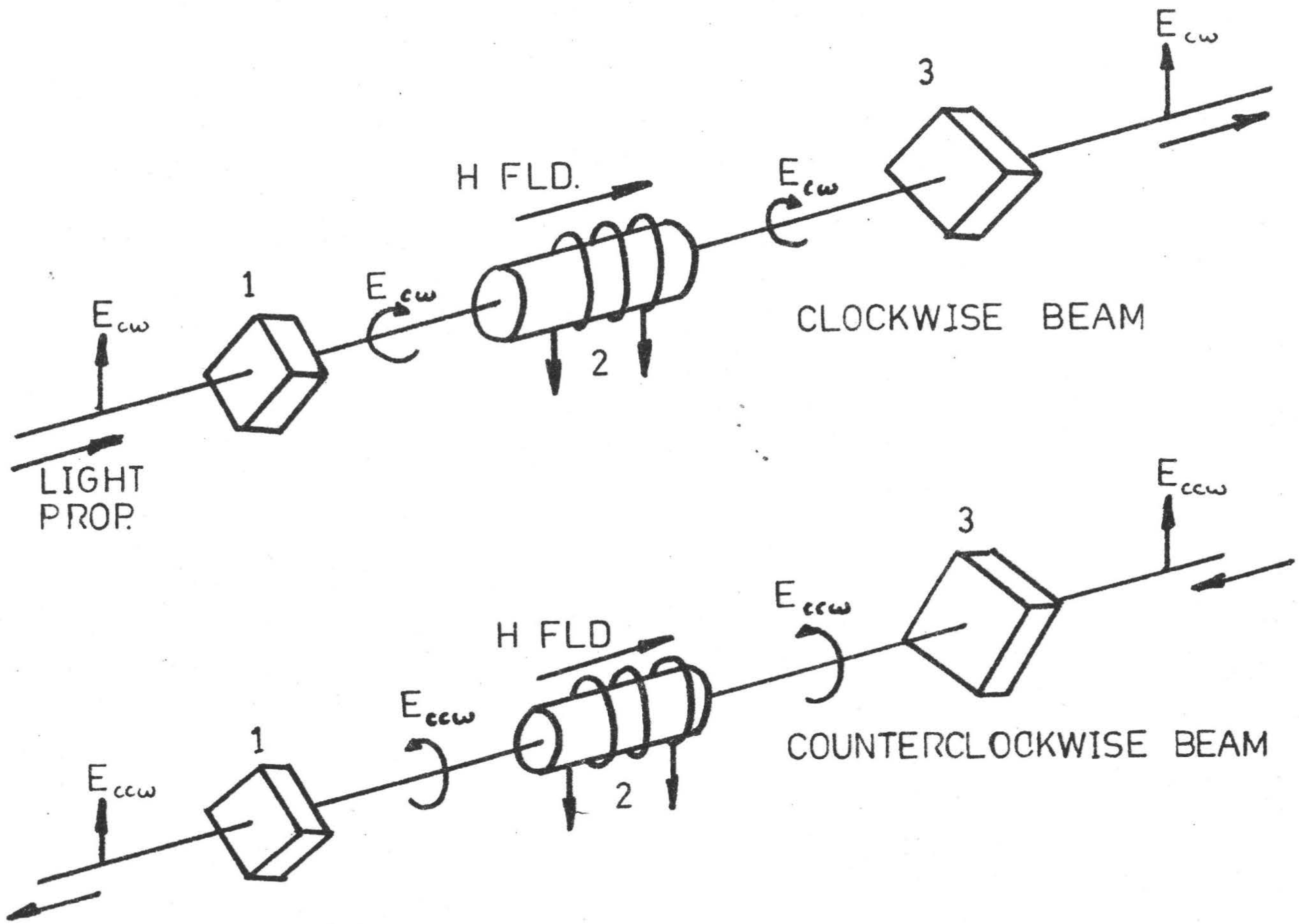

1,3 1/4 WAVE PLATES
2 FARADAY CELL

TITLE: FARADAY ROTATOR BIAS CELL	
SCALE: NONE	SOURCE: REF. 2
DRAWN BY: HILL	FIGURE NO: 12-8

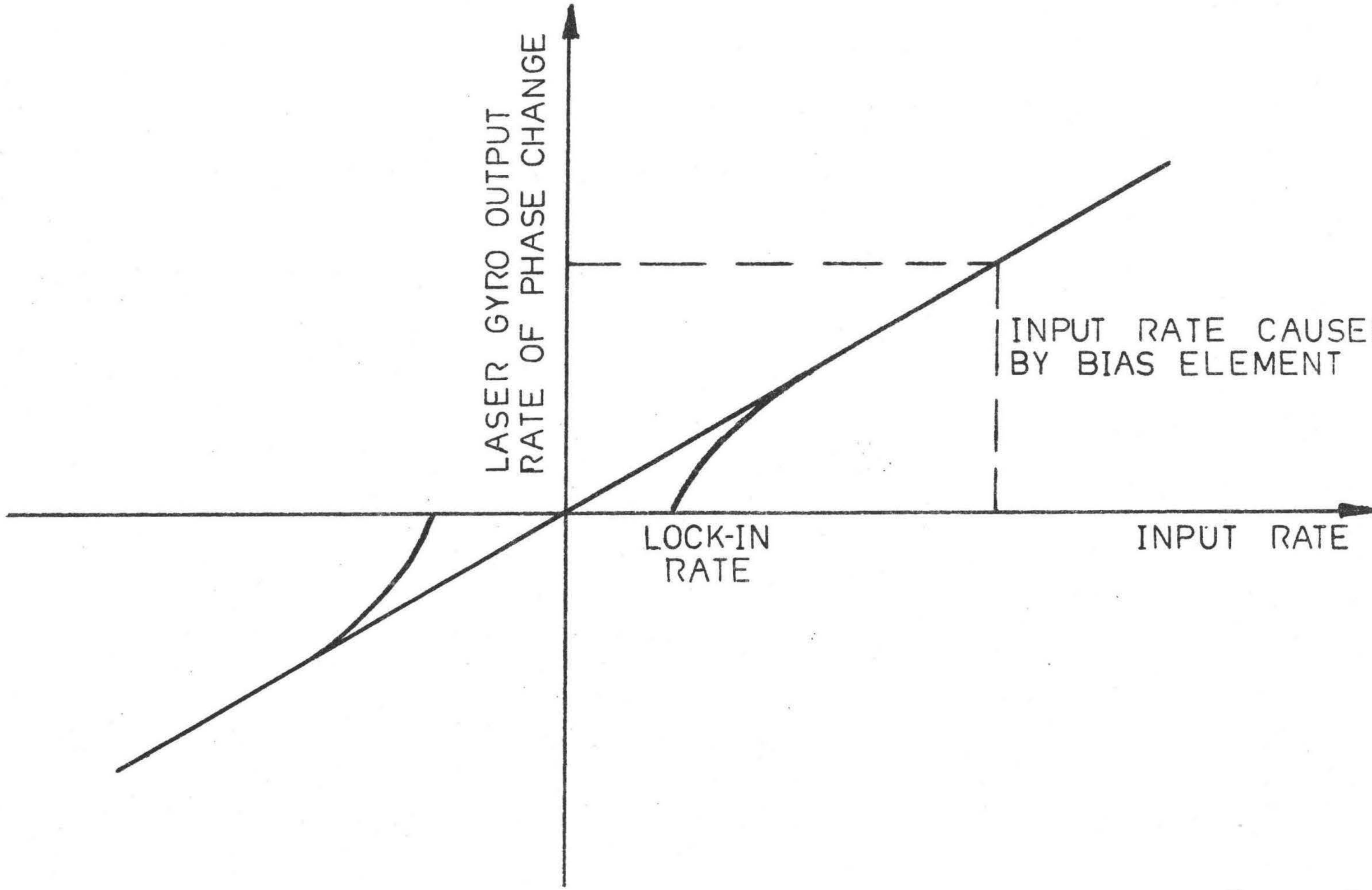

TITLE: LASER GYRO FIXED BIAS	
SCALE:	SOURCE: REF. 4
DRAWN BY: HILL	FIGURE NO: 12-9

REFERENCES

1. Honeywell Systems and Research Division, "The Laser Gyro", Report 6D-E-504.

2. Langford, R. C., "Unconventional Inertial Sensors", Astronautica Acta, Vol. 12, No. 4, 1966.

3. Baker, D. H. and J. W. Harrill, "Basic Principles of Unconventional Gyros", Master's thesis, M.I.T., 1964.

4. Killpatrick, J., "The Laser Gyro", IEEE Spectrum, October, 1967, pp. 44-45.

5. Knapp, R. S., "The Laser Gyroscope", New Scientist, 15 July, 1965, pp. 149-151.

6. Landau and Lifshitz, Classical Theory of Fields, Chapter 10, Pergamon Press and Addison Wesley, 1962.

CHAPTER 13

THE SOLID STATE VIBRATORY GYROSCOPE

13.1 DESIGN AND PERFORMANCE SUMMARY

To date, several feasibility models have been built and tested. The performance has been found to be adequate for short-duration applications of moderate accuracy.

The design goals and the actual achievements for the gyro developed in 1964 for the U.S. Air Force are shown in the table below by Buckley, Roese and Shearer [1].

DESIGN GOALS AND ACHIEVEMENTS

	Design Goal	Achievement
Size	0.5 cu. in.	0.43 cu. in.
Weight	6.0 oz.	0.67 oz.
Power Req'd	0.5 watts	0.32 watts
Threshold (Steady State)	0.1 deg./sec.	0.5 deg./sec.
Max. Rate	$\pm$ 100 deg/sec.	$\pm$ 500 deg./sec.
Sensitivity	n/a	1.5 mv deg. sec.
Excitation Voltage	n/a	45 volts D. C.
Long Term Drift	n/a	0.25 deg. sec. min.
Short Term Drift	n/a	2 to 5 deg. sec. Random

The large threshold figure is due solely to the drift of the zero rate signal. The drift of this signal is primarily the result of the apparent temperature sensitivity of the ceramic sensor, the variable mass inbalances which act on the sensor, and asymmetrical forces acting within the gyro element due to its lack of homogeneity.

The theory and basic technology for this device is fundamentally sound and significant improvements in performance await the development of better materials. The most outstanding problem, the null drift can be solved as the commercial attainability of improved piezoelectric ceramic bodies comes about.

13.2 PRINCIPLES OF OPERATION

The solid state or piezoelectric gyro is a vibratory device. The theory of solid state gyros can be understood by reference to Figure (13.1). Vector notation is used.

The velocity of a particle m about a point 0 moving along a path C in the plane of the paper as shown in Figure (13.1A), and at a distance r from 0 can be described in terms of its radial and transverse components. With unit vectors $\vec{r}$ and $\vec{s}$ in the directions shown, the velocity is

$$\bar{v} = \dot{r}\bar{r} + r\Omega\bar{s} \qquad (13.A)$$

where Ω is the angular velocity. The acceleration is then

$$\bar{a} = \dot{\bar{v}} = (\ddot{r} - r\Omega^2)\bar{r} + (r\dot{\Omega} + 2\Omega\dot{r})\bar{s} \qquad (13.B)$$

showing, in order, the radial, centripetal, angular and Coriolis acceleration terms. The reaction force capable of producing a torque about any axis through 0 is simply

$$\bar{F} = -m(r\dot{\Omega} + 2\Omega\dot{r})\bar{s} \qquad (13.C)$$

or if Ω is constant

$$\bar{F} = -2m\Omega\dot{r}\bar{s} \qquad (13.D)$$

Thus F is due only to the Coriolis component of acceleration

The torque developed about point 0 is then

$$\vec{T} = \vec{r} \times \vec{F_o} = -2rm\Omega\dot{r}\vec{i_\Omega} \qquad (13.E)$$

where $\vec{i_\Omega}$ is unit vector in direction of $\vec{\Omega}$.

In the solid state gyroscope the sensor is a thin-walled cylinder of polycrystalline ceramic. The cylinder is selectively polarized so that each end can be electrically driven in a circumferential mode of vibration in phase opposition with the other end. The converse piezoelectric effect is utilized to achieve this motion.

The cylinder may be considered as composed of many small masses m. It is seen in Figure (13-1B) that as elements at the top of the cylinder have a velocity radially outward, those at the bottom have velocity radially inward.

If the element is rotated about axis XX' with angular velocity Ω, torques due to Coriolis acceleration would be developed at the top and bottom of the element, but in opposite directions. If the radial motion can be described by

$$r = R + \Delta R \sin \omega_v t \qquad (13.5)$$

it can be shown that, neglecting small double frequency terms the torque is given by

$$T = 2 m \Delta R \omega_v \Omega \cos \omega_v t \qquad (13.6)$$

where ω_v is the frequency of vibration. The result of the oppositely directed torques is a torsional vibration with the same frequency as the circumferential modes as shown in Figure (13.2). Both modes of vibration have a common nodal line around the periphery of the center portion of the cylinder. The cylinder is attached to the case at this common node. Since the torsional oscillation of each end is 180° out of phase with the other, each end reacts against the case. The dimensions of the cylinder are chosen such that the circumferential and torsional vibrational modes are tuned to the same resonant frequency. This is done to achieve a resonant condition to produce the highest gain possible within the sensitive element.

The ends of the cylinder are used as the reactive element in a piezo-oscillator which maintains the circumferential mode of vibration at the fixed resonant frequency. The output is obtained from the torsional mode of vibration. Use is made here of the direct piezoelectric effect. The amplitude of the torsional oscillation is proportional to the magnitude of the input angular velocity. The phase of the torsional vibration, referenced to the circumferential mode, indicates the direction of the input angular rate.

13.3 DESCRIPTION OF THE FEASIBILITY MODELS

Figure (13.3) is an outline drawing of a finished feasibility model. Figure (13.4) is a longitudinal cross-section and shows the simplicity of the design. The piezoelectric sensor is held along the nodal line by a Viton "A" rubber O-ring. Using Figure (13.3) for reference, note that connectors 1 and 2 are used to excite the driven circumferential mode of vibration, while 3 and 4 are for the output signal.

All machined metal parts are anodized aluminum, while the base, to facilitate soldering of the connectors, is brass.

The piezoelectric solid state gyroscope sensor is cylindrical in shape and is machined to the dimensions shown in Figure (13.5). The material is a polycrystalline ceramic made of lead zirconate-lead titanate.

Electrode configurations are either patterns "C" or "L-4", which are shown in Figures (13.6) and (13.7). The basic difference in these patterns is the finished electroding. In pattern L-4 conductors are plated on the surface in nonpolarized regions so that connections to the output electrodes can be made to the sensor at the nodal mounting line and the adverse effects of variations in mass unbalances due to movement of lead wires are reduced to a minimum.

A technique known as metallizing of non conductors by chemical reduction has been successfully used to electroplate the sensor. This process applies a coating of copper about 20 millionths of an inch in thickness. The sensor is first given a vapour blast to prepare the surface and then it is completely metallized. Then selected areas are masked with Mylar tape and the unmasked areas etched away leaving the desired electrode pattern. Modifications in the polarizing electrodes to produce the operational electrodes can be achieved by a second masking and metallizing step. The oxidation of the copper is retarded by depositing a thin film of nonporous gold of about 20 millionths of an inch thickness on the copper. This deposition of gold is by an immersion process. Since it does not adhere to the ceramic no masking is required.

Leads can be attached to the electrode by precision soldering or thermal pressure bonding. Precision soldering produces a strong conductive joint capable of withstanding steady-state acceleration in excess of 9000 g. More advantages of this metallizing technique are listed in the report.

13.4 EXCITATION AND OUTPUT SIGNAL PROCESSING CIRCUITS

The fundamental electronic components required to make the piezoelectric gyro operate are shown in block form in Figure

(13.2) and in circuit diagram form in Figure (13.8). The main elements required are a driving oscillator, an amplifier and a demodulator.

Buckley, Roese and Shearer [1] found that to obtain a stable null with the ceramic material then being employed, frequency control in the oscillator on the order of one part in 10^7 was necessary.

13.5 PERFORMANCE TEST RESULTS

(i) Operating Frequency:

In the course of examining nulling techniques and cross-coupling reduction, the Westinghouse research team found that there are certain frequencies for different crystal mounting positions which could be called the best points for extracting the rate intelligence. The best rate signal amplitude with respect to the cross-coupling signal occurred when the cross-coupling signal was 270° out of phase with the driving signal. There, the cross-coupling signal was rejected by the demodulator and the rate intelligence was in phase (or 180° out) with respect to the reference phase. The most desirable operating frequency was thus NOT the motional resonance frequency, because the cross-coupling amplitude was a maximum at that frequency. For this particular example, resonant frequency was 92457 cps whereas minimum cross-coupling occurred at 92948 cps.

Thus the mounting position and the operating frequency should be co-ordinated.

(ii) Linearity:

The curves relating Rate Output Signal to Rate Input were considered (Figure 13.9). They would be vastly improved, however, if drift could be controlled.

(iii) Hysterisis:

Hysterisis loops for Zero Rate Output Signal vs. Rate Input were plotted, as in Figure (13.10). While drift affected accurate measurements, the main conclusion was that hysterisis is less than the observable threshold level of the instrument.

(iv) Drift Tests:

Tests have shown a short term drift of 2 to 5 deg.sec. and a long term drift of 0.25 deg./sec./min.

(v) Dynamic Threshold:

In this case the lowest possible input rate was 0.07 deg./sec.

(vi) Steady State Threshold:

This is the minimum unidirectional input that causes a detectable change in output. Several tests indicated this parameter was of the order of 0.5 deg./sec.

13.6 FREQUENCY DEPENDENCE OF OUTPUT SIGNAL

The variation of driving frequency causes amplitude and phase shifts of the cross coupling signal as well as the rate output signal. The overall result was an apparent rate signal drift.

The frequency dependence of the gyro zero rate signal varies from unit to unit. Since a gyro zero stability of less than 0.1 deg./sec. has been specified, this requirement dictates a frequency stability maintained to within 3 parts in 10^8. For this, either a quartz-controlled oscillator is mandatory or a decided improvement in piezoelectric ceramics is required.

13.7 TEMPERATURE RESPONSE OF THE GYRO

The more accurately the driving frequency is controlled, the more susceptible the gyro became to slight temperature variations. Changes in the amplitude of the applied drive voltage caused a resonant frequency shift due to the temperature rise within the piezoelectric body which was directly attributable to the increased power dissipation. Oven tests show that the average temperature drift is several hundred deg./sec. rate signal drift/degree centigrade. The temperature sensitivity was believed to be the major contributor to the short-term erratic drift. By comparison the contributions of mass unbalance or driving amplitude are thought to be much less significant.

13.8 HYSTERISIS AS A FUNCTION OF TEMPERATURE

The frequency of minimum impedance at different temperatures was taken for each vibrational mode as the temperature was cycled from 25°C to 120°C to 25°C. These hysterisis loops indicated that the two modes of vibration do not precisely track each other and do not show a good repeatability. Thus, either an improved material or temperature control or both are required.

13.9 ENVIRONMENTAL TESTS AND RESULTS

Only the Acceleration, Shock and Vibration tests of the standard military test procedure will be reported here as temperature sensitivity has already been covered.

(i) Acceleration Tests:

The solid state gyroscope was placed on a centrifuge and subjected to a one-minute steady-state acceleration of 14 g's, in turn, in each direction along its three orthogonal axes.

With the input axis parallel to the axis of rotation of the centrifuge, the high angular rates saturated the electronic circuitry. The acceleration tests along the other two orthogonal axes showed that the linear acceleration sensitivity of the present design is 1.0 degree / second / g. A visual and a performance check indicated no sensor damage as a result of these tests.

(ii) Shock Tests:

The gyroscope was subjected to 18 impact shocks of 15-g acceleration, along each of the three orthogonal axes.

Again, both visual examination and before and after performance tests indicated no degradation of the device.

(iii) Vibration Tests:

The vibration schedule was as follows:

5 to 10 cps	0.08 inch double amplitude
10 to 17 cps	$\pm$ 0.41 g's
17 to 74 cps	0.36 double amplitude
74 to 500 cps	$\pm$ 10 g's

No resonant modes were found in the 5 to 500 cps frequency range, along any of the three axes. The frequency was cycled between 5 and 500 cps in 15 minute cycles at an applied amplitude of 0.36 inch or an applied acceleration of $\pm$ 10 g's for a period of 3 hours along each axis.

The standard visual and performance checks indicated no basic changes.

13.10 RELIABILITY

In the three years or more that the gyro has been under development, not one single operational failure of a sensor was experienced. The small size and mass, as well as the monolithic configuration of the sensor, enhances the capability of the solid state gyro to survive the combined adverse environmental effects of high acceleration, shock and vibration.

In the abscence of any rate of failure data, it must be assumed that the mean time between failure is determined by the associated electronic package.

13.11 SOURCES OF ZERO ANGULAR RATE SIGNALS

The most significant problem encountered in the development of the solid-state gyroscope is closely associated with the forces which are generated to drive the gyroscopic element in a prescribed vibrational mode relative to its reference frame.

In the practical case, small assymetries permit the unwanted coupling of the input and output modes. This cross coupling from input to output produces extremely large zero signals which completely overshadow the portion of the output signal containing the rate intelligence.

Mass imbalances in the sensor are caused by:

(a) lack of homogeneity in the sensor ceramic

(b) nonsymmetrical poling and electrode configurations

(c) sensor wiring and mounting

(d) dimensional tolerances

The elimination of the cross coupling signal, called nulling, by the techniques listed below has not been entirely satisfactory because of the temperature and frequency dependence of the phase and amplitude of the unwanted signal relative to the reference.

13.12 TECHNIQUES FOR NULLING THE ZERO RATE SIGNAL

(i) Mechanical:

Three different mechanical approaches were tried and evaluated.

(1) addition of balancing masses

(2) change of Nodal Mount Position

(3) Kinetic Nulling Technique

While all three of the above approaches were effective, the first two had severe inherent difficulties and would be impossible to use in the practical case, especially after full assembly of the gyro case. The kinetic technique was judged the best of the mechanical approaches.

This nulling method utilizes forces and the resultant torques which are a function of the mass imbalances to cancel the cross coupling torques. The forces are developed by the proper placing of springs as shown in Figure (13.11).

There has been no indication that the rate sensitivity of the gyroscope has been affected by the kinetic nulling technique. The stability of the null achieved by this approach is equal to that obtained by electronic "bucking" techniques.

13.13 PRACTICAL PROBLEMS OF THE PIEZOELECTRIC GYRO

At present drift rates are extremely high being of the order 2 to 5 deg./sec. for short term drift. This drift may be reduced by using new ceramic materials with improved temperature related characteristics and by controlling temperature more closely. With the present material to obtain a gyro zero rate signal stable to within 0.1 deg./sec. drift rate would require the stabilization of temperature to within approximately one-thousandth of a degree centigrade.

The sensor is a polycrystalline material which is neither homogeneous nor isotropic. Because these properties are lacking a non symmetrical motion of the sensor in the driven mode results. Cross coupling between the input and output mode takes place. Materials research will have to provide a more homogeneous material to eliminate this zero rate error source.

In addition to these fundamental problems, troubles in the mounting of sensors and in mounting electrodes to the sensors will have to be overcome. While the feasibility of this approach has been proven, its full potential is far from realized.

VIEW OF SENSOR ELEMENT SHOWING MOTION OF ELEMENTARY PARTICLES

A)

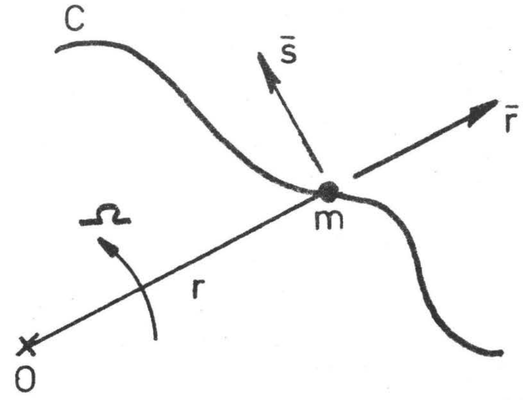

RADIAL AND TRANSVERSE COMPONENTS OF MOTION FOR AN ELEMENTARY PARTICLE

B)

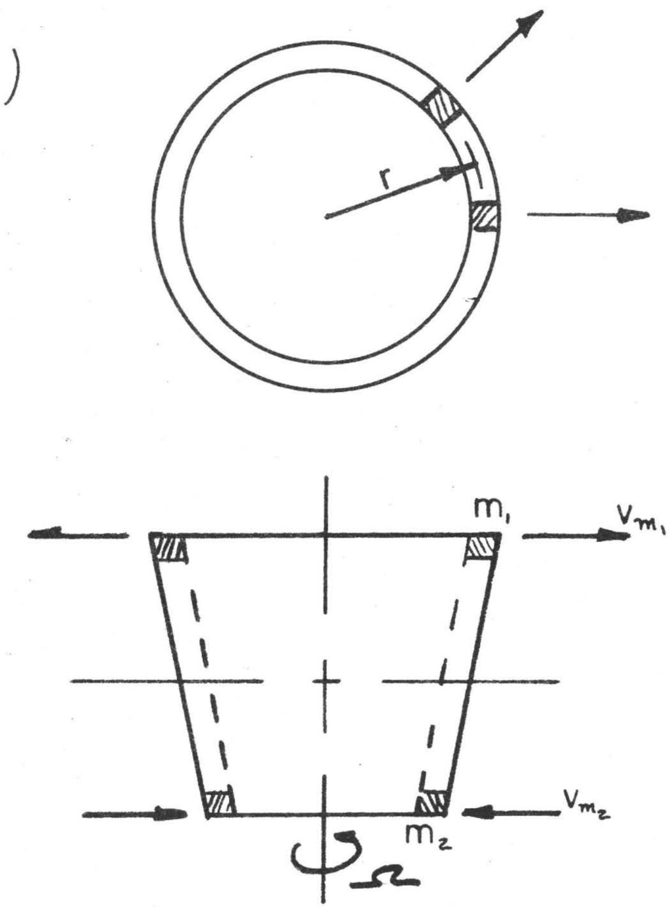

TITLE: BASICS OF SENSOR OPERATION	
SCALE: NONE	SOURCE: REF. 2
DRAWN BY: HILL	FIGURE NO: 13-1

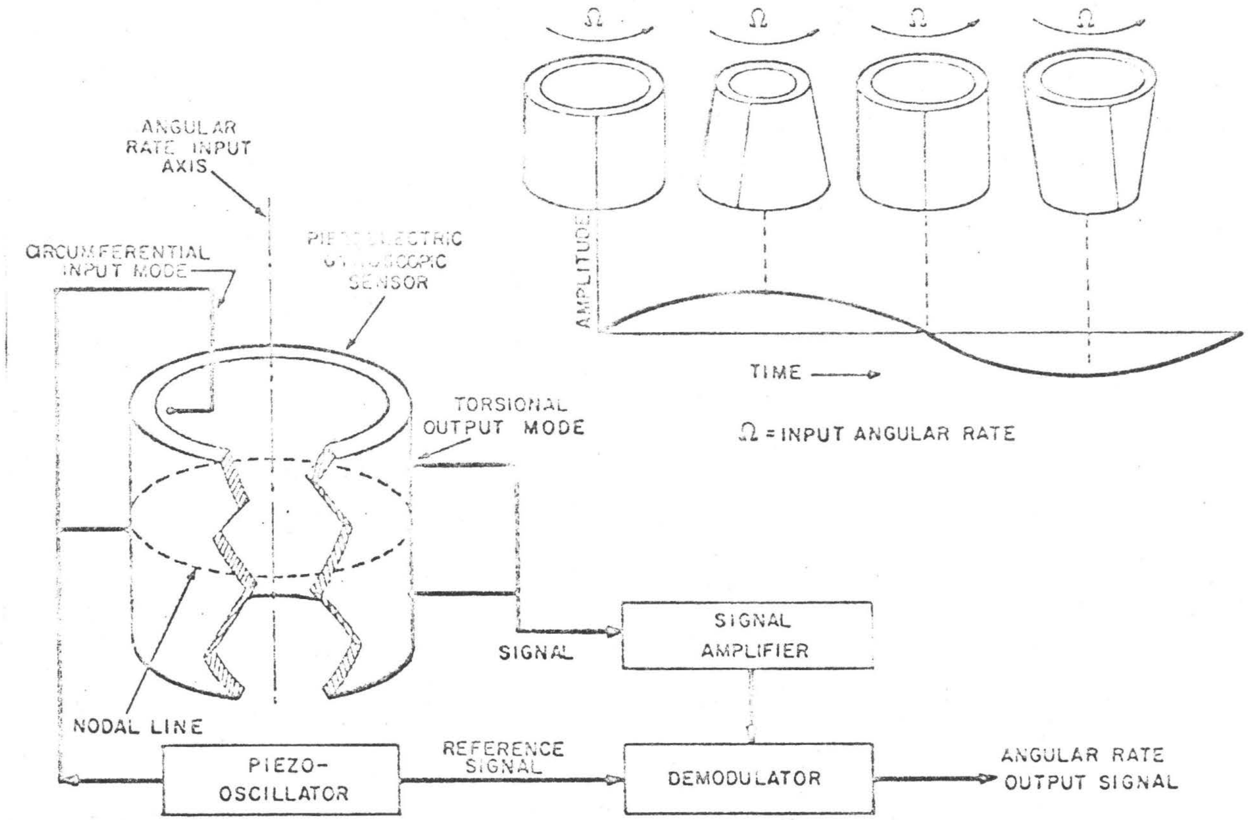

TITLE: FUNCTIONAL BLOCK DIAGRAM	
SCALE: NONE	SOURCE: REF. 1
DRAWN BY:	FIGURE NO: 13-2

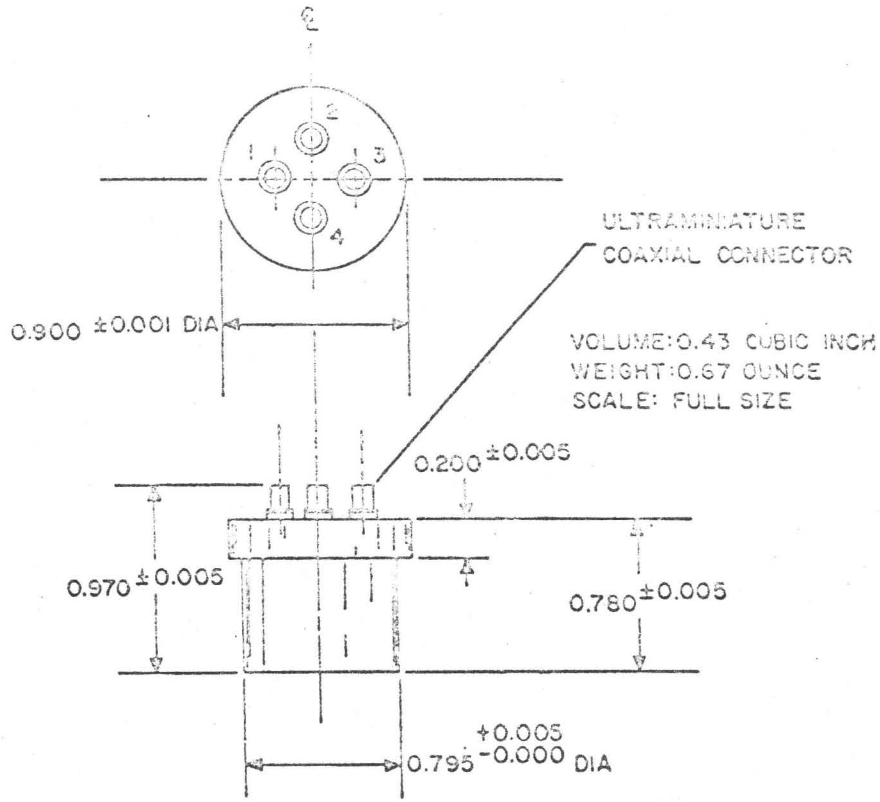

TITLE: GYRO OUTLINE DRAWING	
SCALE: NONE	SOURCE: REF. 1
DRAWN BY:	FIGURE NO: 13-3

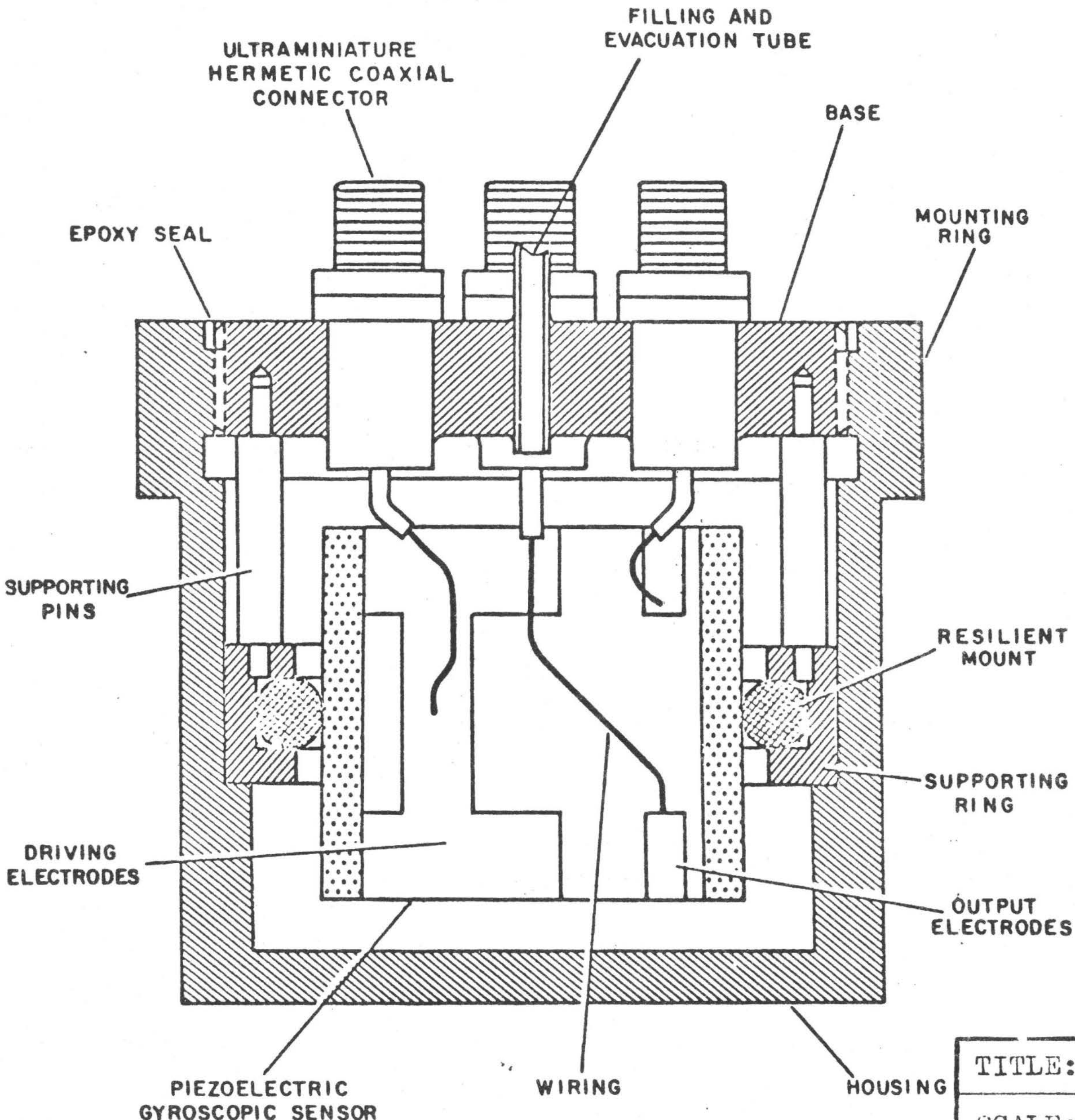

TITLE: GYRO CROSS SECTION	
SCALE: NONE	SOURCE: REF. 1
DRAWN BY:	FIGURE NO: 13-4

MATERIAL: CERAMIC, LEAD ZIRCONATE – LEAD TITANATE

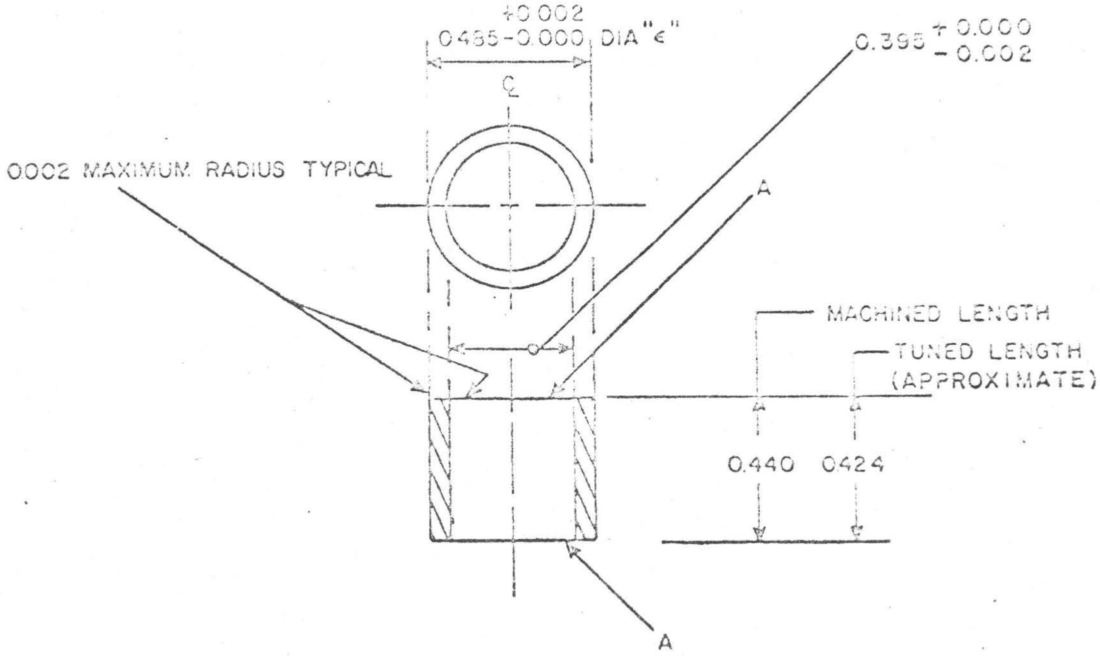

NOTES

a. DIAMETERS MARKED "ε" TO BE CONCENTRIC WITHIN 0.0002 T.I.R.

b. 0.0001; MAXIMUM DEVIATION FROM A TRUE CYLINDER

c. END SURFACES MARKED "A" WILL BE PARALLEL WITHIN 00005 T.I.R.

d. END SURFACES MARKED "A" WILL BE PERPENDICULAR TO CENTERLINE WITHIN 0.0005 INCH PER INCH

e. 16√ FINISHED ALL OVER

CAUTION

MATERIAL IS HARD AND BRITTLE. IT FRACTURES EASILY AND MUST BE HANDLED WITH CARE

TITLE: GYRO SENSING ELEMENT	
SCALE: NONE	SOURCE: REF. 1
DRAWN BY:	FIGURE NO: 13-5

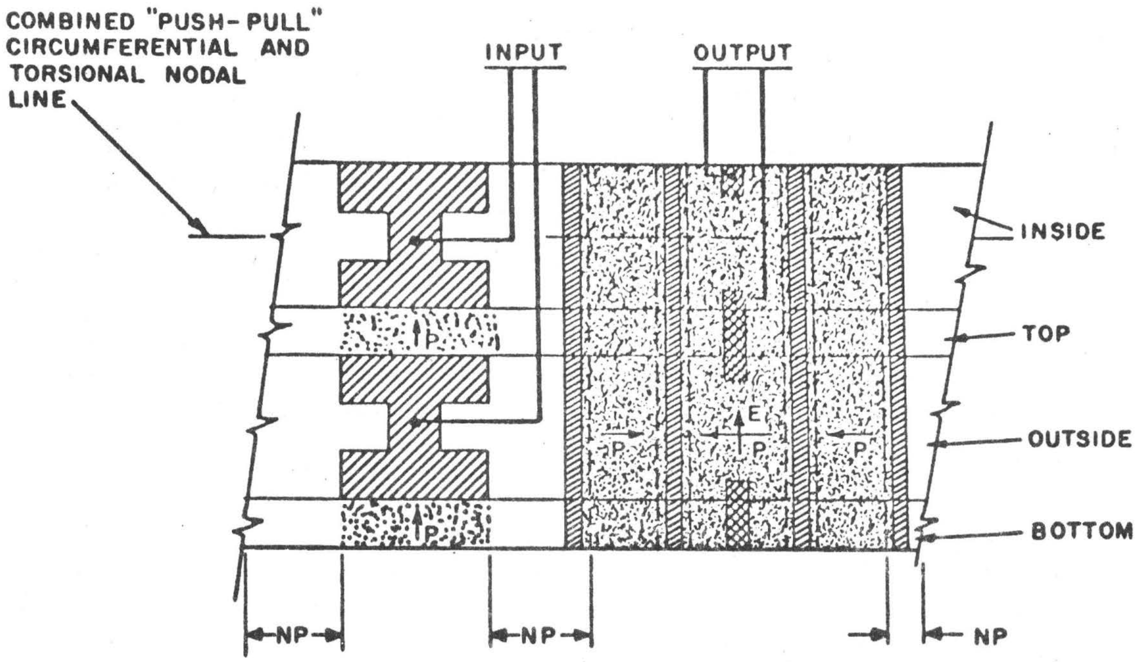

NOTES:

(clear box)	CLEAR AREA NOT POLARIZED
(dotted box)	DOTTED AREA POLARIZED
(hatched box)	PLATED CONDUCTORS USED FOR POLING
(hatched box)	INPUT DRIVING ELECTRODES
(cross-hatched box)	SIGNAL OUTPUT ELECTRODES
NP	REGIONS NOT POLARIZED
↑P	DIRECTION OF POLARIZATION VECTOR
↑E	DIRECTION OF ELECTRIC VECTOR

1712A-VB-7

TITLE: ELECTRODE CONFIGURATION "C"	
SCALE: NONE	SOURCE: REF. 1
DRAWN BY:	FIGURE NO: 13-6

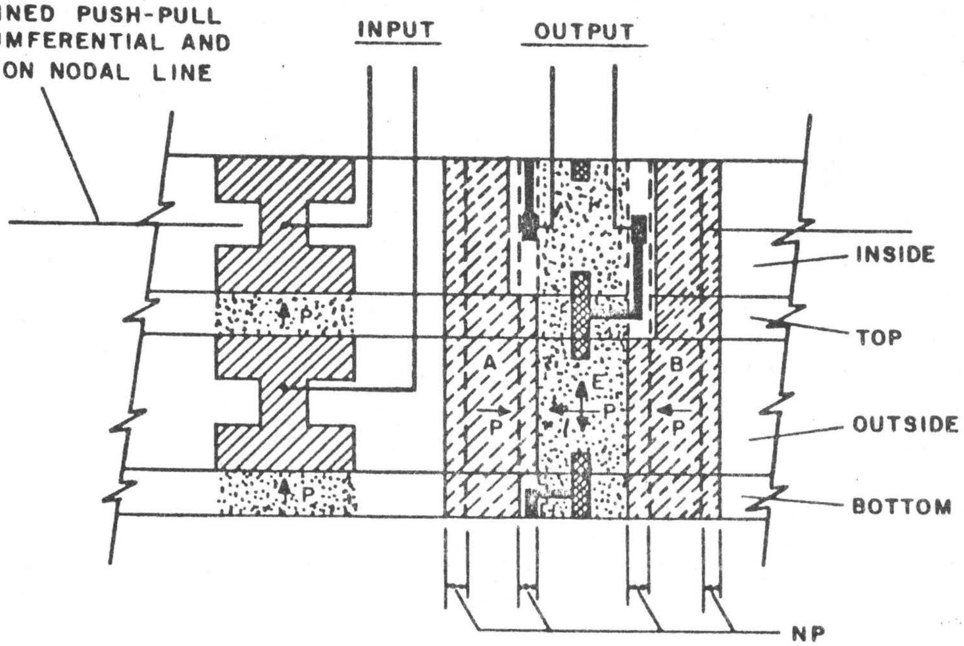

CLEAR AREA NOT POLARIZED

DOTTED AREA POLARIZED

PLATED CONDUCTORS

INPUT DRIVING ELECTRODES

SHORTING ELECTRODES

SIGNAL OUTPUT ELECTRODES

NP REGIONS NOT POLARIZED

↑P DIRECTION OF POLARIZATION VECTOR

↑E DIRECTION OF ELECTRIC VECTOR

TITLE: ELECTRODE CONFIGURATION "L4"	
SCALE: NONE	SOURCE: REF. 1
DRAWN BY:	FIGURE NO: 13-7

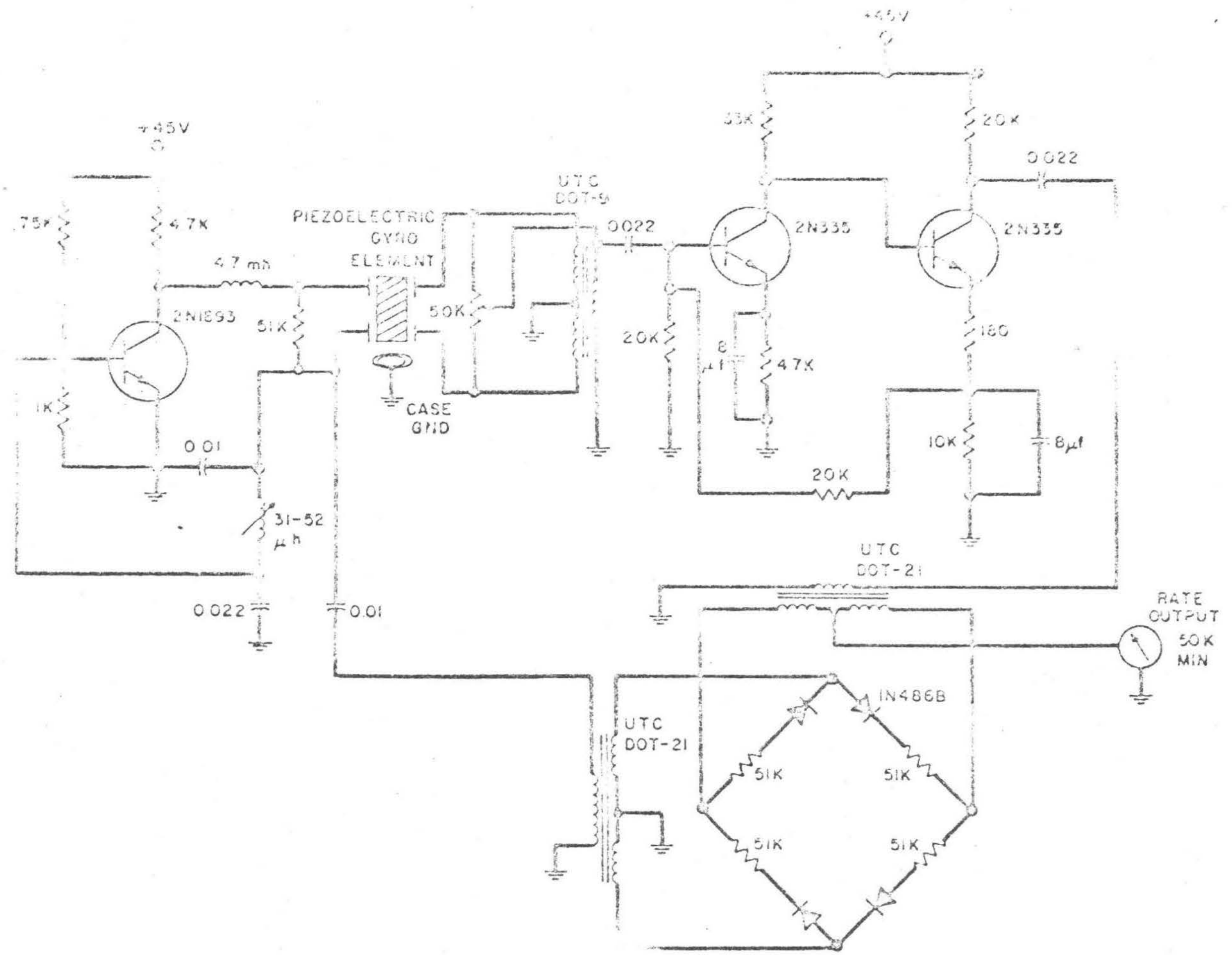

TITLE: EXCITATION & OUTPUT CIRCUITRY	
SCALE: NONE	SOURCE: REF. 1
DRAWN BY:	FIGURE NO: 13-8

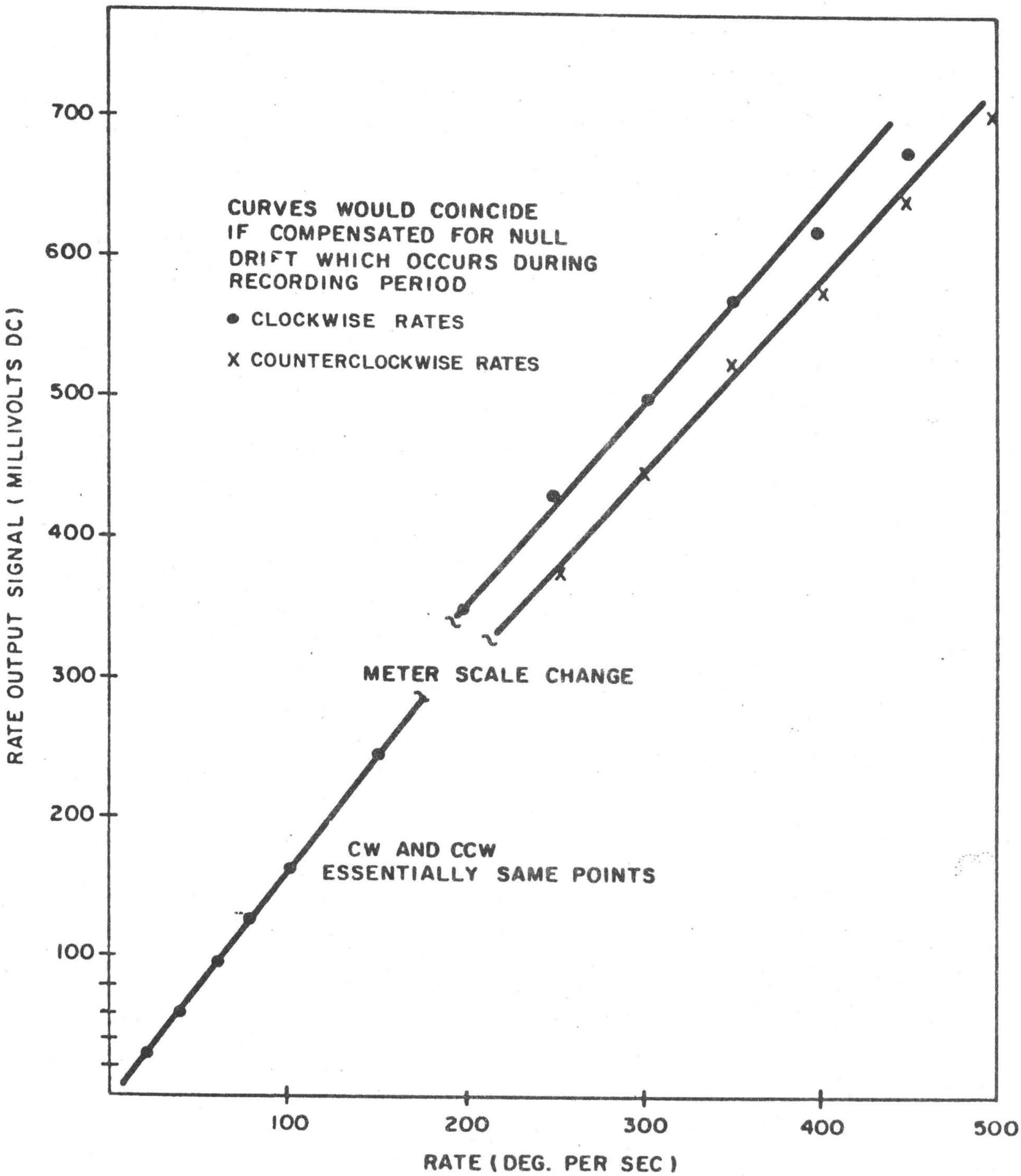

TITLE: LINEARITY CURVE	
SCALE: NONE	SOURCE: REF. 1
DRAWN BY:	FIGURE NO: 13-9

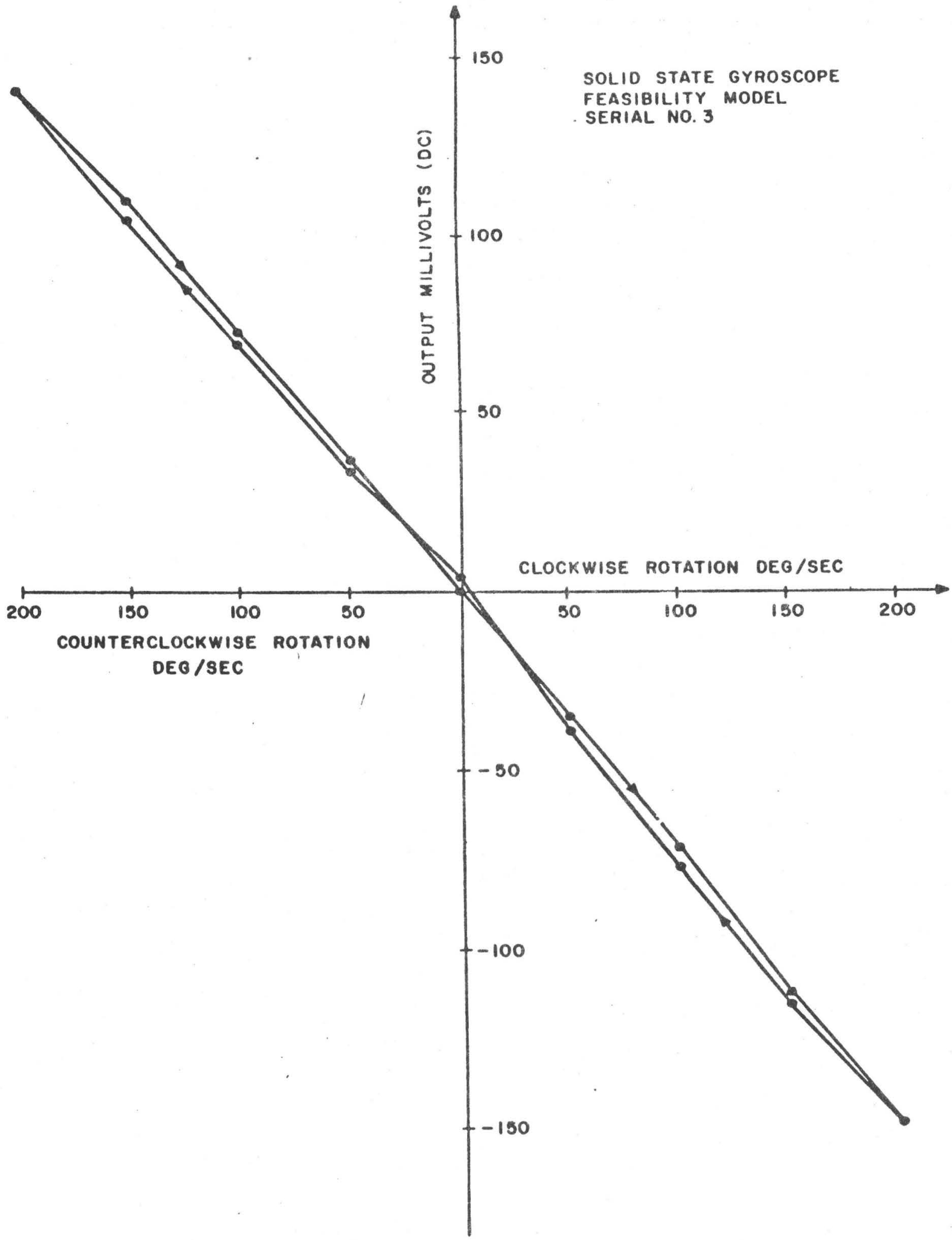

TITLE: HYSTERISIS LOOP	
SCALE: AS ABOVE	SOURCE: REF. 1
DRAWN BY:	FIGURE NO: 13-10

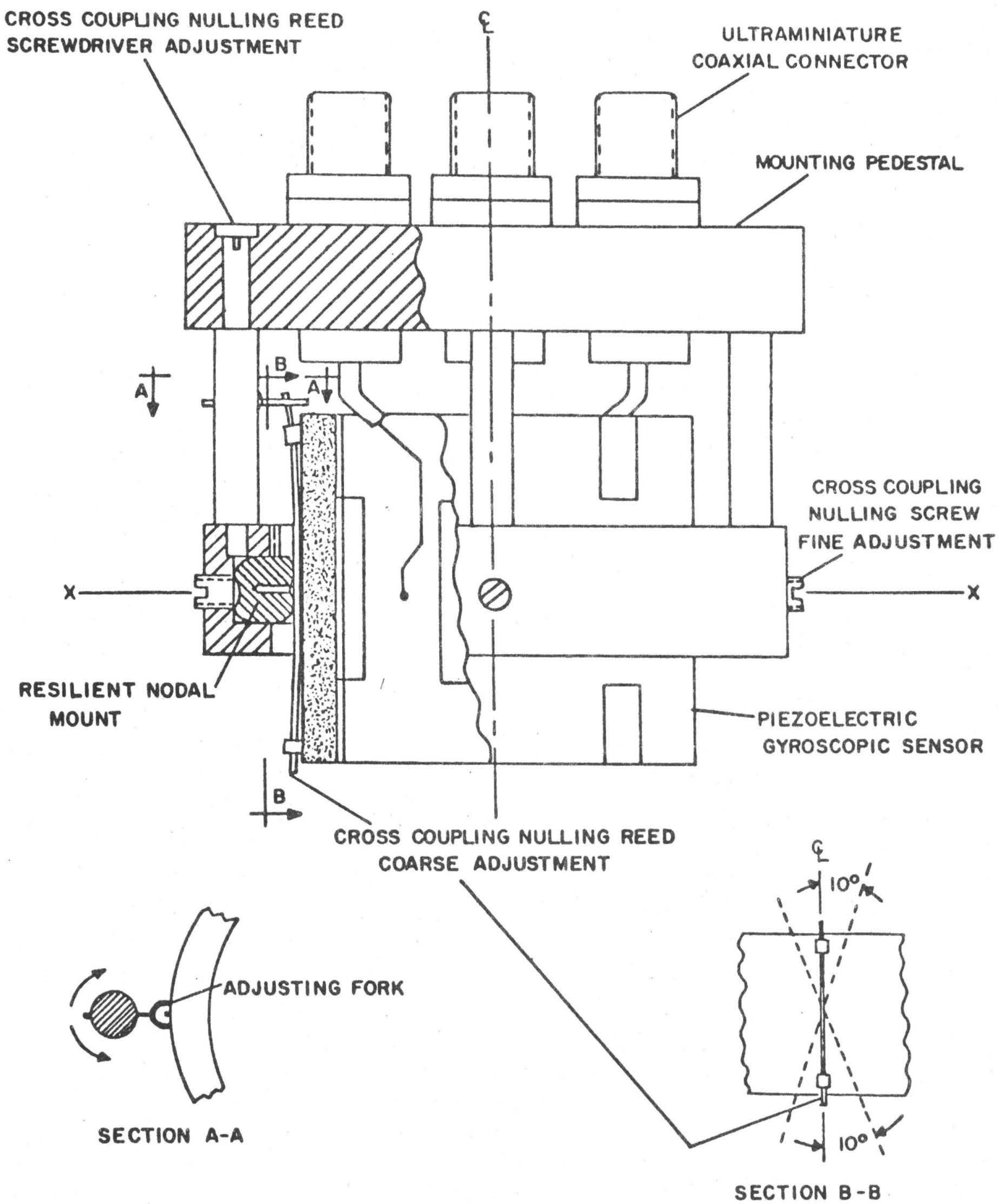

TITLE: MECHANICAL NULLING METHOD	
SCALE: NONE	SOURCE: REF. 1
DRAWN BY:	FIGURE NO: 13-11

REFERENCES

1. Buckley, J. J., D. W. Roese and J. W. Shearer, "Solid State Vibrating Gyroscope Technique Study", Report No. TDR-64-101, Flight Dynamics Laboratory, Wright-Patterson Air Force Base, Ohio, October 1962.

2. Chatterton, J. B., "Fundamentals of the Vibratory-Rate Gyro", ASME Paper No. 55-S-25.

3. Fearnside, K. and P. Briggs, "The Mathematical Theory of Vibrating Angular Tachometers", Proc. I.E.E.E., 105, (Part C), 1958.

CHAPTER 14

THE TUNING FORK GYROSCOPE

14.1 DESIGN AND PERFORMANCE SUMMARY

The Tuning Fork Gyroscope (T.F.G.) has been successfully built and tested in the United States and Great Britain. Test have shown this configuration to be quite feasible but subject to certain errors which are now under study.

The performance achieved by the most representative models is shown below. As the object of these tests up to the present has been the providing of the concept's feasibility and investigating the accuracies obtainable, only the Sperry instrument has been subjected to environmental testing.

Example #1 Sperry Gyrotron IA

Performance:

Range 15 to 2.6×10^{6}°/hour

Stability and Uncertainty - 15°/hour for an 8 hour period (after initial warmup)

Linearity - 1% up to 0.65×10^{6}°/hour, 13% at 1.3×10^{6}°/hour, 20% at 2.6×10^{6}°/hour. Linearity can be maintained at 1% over the entire range with amplitude control.

Environmental Tests -

Shock Resistance - 30 g in all directions

Vibration - 10 - 55 gps at 0.06"

Operating Temperatures -65° to + 80°C

General -

Length (Housing) 7"

Body Diameter 3"

Weight 4 pounds

Life of Sensing Element - unlimited

Temperature Control Heater - 2 amp at 26.5 VDC.

Example #2 Royal Aircraft Establishment T.F.G.

Performance:

Stability - Constant Acceleration Conditions

Long Term (20 hour periods) - 0.5°/hr.

Short Term (6 min. periods) - 0.07°/hr.

Varying Acceleration Conditions

The variations in residual error signal were of the order of 12°/hr/g (in phase).

Vibratory type gyros and particularly the tuning fork configuration have been investigated rather extensively by Chatterton [1], Newton [2], Morrow [3] and Fernside and Briggs [4]. Morrow [5,6] and Hobbs [8] have investigated the error sources in these devices.

Sensitivity of the tuning fork is not as good as that of the conventional rotor gyro, and linearity is shown to decrease with sustained high rates of turn. The response to input rates is definitely confined to one axis, however.

Zero rate signals are the most serious performance drawback and are due to several factors. Output signals can be produced by the direct torsional effect of mass unbalance, torsional vibration produced from lateral vibration, axial vibration, gravity effects and the generation of zero signals by the drive unit.

Careful control of the temperature of the fork and the alignment of the drive forces also have a considerable effect on the sensor performance.

The problems identified above, however, all have solutions and laboratory tests have shown that a production model is realizable. The accuracy achievable, combined with its robust design, make it an attractive device.

14.2 PRINCIPLES OF OPERATION

While more detailed and extensive descriptions exist, a brief summary is included here to provide a reference for the work that follows.

The output signal of the tuning fork gyro for an impressed rate of turn is a torsional vibration at the frequency of the tuning fork. This vibration is produced by Coriolis Force acting on the tines. Figure (14.1) shows a simple comparison between rotor gyros and the tuning fork. Figure (14.2) shows the basic elements of the tuning fork. This first diagram should assist those more familiar with conventional gyros.

Referring to Figure (14.1) two counter rotating gyroscope rotors exhibit precessional or Coriolis forces under applied rate. T e oscillating masses of the tuning fork exhibit the same action. However, since the fork motion periodically reverses, direction the precessional forces do the same. The theory of Section (13.2) describing the operation of the piezoelectric gyro could also be applied here. This oscillating precessional couple acts about the central axis of the fork and is proportional in magnitude to the applied rate. In practice, the oscillating torque causes relative motion between the fork and its base through a torsionally tuned member. The magnitude of the rate of turn determines the velocity of the torsional oscillation.

If it is assumed that the gyro consists of a suspended mass M_0 with a base of infinite mass and rigidity, and

(a) Rotational Inertia of Mass = $I = M_0 R^2$
(b) Radius of Gyration of Mass = $R = R_0(1 + \Delta R/R_0) \cos 2\pi f_s t$
(c) Amplitude of Vibration of Mass = ΔR
(d) Distance from Mass to Input Axis of Rotation = R_0
(e) Angular Velocity of Assembly (Input) = ω_b

The problem is then to find $\omega_g = \omega - \omega_b$

where ω_g = output vibration (with respect to base)
ω_b = input vibration
ω is taken with respect to inertial space.

The system is considered to have, about the axis of

Rotational Stiffness = s_R
Rotational Resistance (damping) = r_R

Then by summing the torques acting on the suspended inertia

$$\frac{d}{dt}(I\omega) + r_R(\omega - \omega b) + s_R(\theta - \theta b) = 0 \tag{14.B}$$

we obtain

$$M R_o^2 \Big[\left(1 + \frac{\Delta R}{R_o} \cos 2\pi f_s t\right)^2 D(\omega_g + \omega b) \\ - 4\pi f_s (\omega_g + \omega b)\left(1 + \frac{\Delta R}{R} \cos 2\pi f_s t\right) \sin 2\pi f_s t \Big] \\ + r_g \omega_g + s_R \omega_g / D = 0 \tag{14.C}$$

where $\dfrac{d}{dt} = D$

For constant base motion $D\omega b = D\omega b_o = 0$

Simplifying the torque equation and attempting a solution of the form

$$\omega_g = A \cos 2\pi f_s t + B \sin 2\pi f_s t \tag{14.D}$$

we must define the torsional resonant frequency

$$f_R = \frac{1}{2\pi}\left(\frac{s_R}{M_o R_o^2}\right)^{1/2} \tag{14.E}$$

Making the driving frequency equal to the fork frequency tunes the system and give us

$$\omega_g = (2\,\varphi_R\,\Delta R/R_0)\,\omega b_0 \sin 2\pi f_f t \qquad (14.F)$$

with $\varphi_R = 2\pi f_f\, M_0 R_0^2 / r_R$

14.3 DESCRIPTION OF TEST MODEL

The Royal Aircraft Establishment's T.F.G. will be described in detail here. Little mechanical sophistication is shown as this was a feasibility model only, but the basic principles and the possible high performance is illustrated clearly .

Description of Existing Models

Mechanical:

Figure (14.3) shows a cross section of the Royal Aircraft Establishment's model. The tuning fork and output torsion systems, together with their supporting frame, are integrally machined from one piece of high carbon tool steel having low internal hysterisis properties. An overall accuracy of $\pm$ 0.5 x 10^{-3} inches was required for this design.

Drive System:

The forces used to maintain the motion of the tuning fork are those which occur when a varying potential is applied between plates of a condenser. In this case one plate which is at earth potential is the flat surface at the end of each tine while the high potential plate is an electrode which is brought near the fork.

If the electrode potential is $(A + B \sin \omega t)$ volts, a convenient driving method is to have an A.C. voltage at fork frequency with $A \neq 0$. Peak force is then proportional to 2AB. With large values of A, the required force can be achieved without large areas or small gaps for the electrodes.

The electrode air gap was 5×10^{-2} cms. which, with a plate area of 3.6 sq. cms. a polarizing voltage of 400 v.D.C., and A.C. voltage with peak values of 120V, gave an oscillatory force at fork frequency with a peak magnitude of 60 dynes. The corresponding tine amplitude at the free end was 15×10^{-3} cms.

To maintain constant amplitude of vibration some limiting is required in the A.C. amplifier which connects tine pickoff to drive electrodes; this amplifier must have zero phase shift since force has the same phase as the signal from the pickoff which is velocity sensitive. In this example a linear A.C. amplifier with zero phase shift completed the A.C. path whose output controlled the D.C. polarizing voltage applied to the drive electrodes to give amplitude control.

The tine pickoff signal is used to provide the reference voltage at 590 cps for the output signal demodulator.

The torsional motion is sensed by variable reluctance transducers. Alternating torques occurring in the base either from Coriolis torque or those due to asymmetries in the vibrational motion will cause the base to oscillate and produce oscillatory displacements of two armatures carried on the fork base. The remaining magnetic circuitry is maintained on the fork outer frame.

After amplification the total A. C. output voltage from the torsional motion pickoffs is compared in phase with the A. C. voltage obtained from the tine motion pickoffs to separate torques due to mass asymmetries from those indicating rate of turn or error torques having the phase of the tine velocity.

14.4 ELECTRICAL CIRCUITRY

The electrical circuitry required varies with the design of the instrument. Electronic bucking of zero rate signals could be used. Electromagnetic damping could be used instead of material or fluid damping.

A block diagram of a tuning fork using bucking and electromagnetic damping is shown in Figure (14.4). If these techniques are not used then their signal paths are simply deleted from the design.

A further design refinement for reducing cross coupling errors, called Double Modulation, is reviewed in a later section. The circuitry required for this design is more complicated then that described above.

14.5 PERFORMANCE TEST RESULTS

(1) Operating Frequency:

The gyro is usually designed so that the driving frequency is equal to the resonant frequency of the torsional vibrating system. The R. A. E. gyro had a fork frequency of 590c/s.

By selecting an appropriate torsional damping ratio the magnification factor for resonance can be controlled. This magnification factor will control the amount of twist given to the torsion stem by the force generated when the vibrating fork is rotated.

Fearnside and Briggs [4] have shown by a thorough mathematical analysis from a stability approach that the best magnification doesn't occur when the torsional resonant frequency equals the driving frequency. The resonant frequency should be designed to be somewhat below the driving frequency. For simplicity, however, linear theory is usually used in gyro design and an exact frequency match between input and output is made.

(ii) Linearity:

The Sperry Gyrotron has a reported linearity of 1 % up to 0.65×10^6 deg./hour, 13 % at 1.3×10^6 deg./hour and 20 % at 2.6×10^6 deg./hour. Linearity could have been maintained at 1 % or better over the entire range with a fork amplitude control added to the fork drive circuit.

Solution of the equations governing tuning fork motion have given torsional oscillation frequency as

$$\omega_g = (2\,\varphi_R\,\Delta R/R_o)\,\omega b_o \sin 2\pi f_s t \qquad (14.G)$$

Thus the vibration is proportional in magnitude to the rate of turn ωb_o and has a phase which reverses with direction of turn. The sensitivity remains constant as long as the ratio $\varphi_R \Delta R/R_o$ remains constant, where Q_R is the torsional Q, R_o is the average radius of gyration and ΔR is the amplitude by which the radius of gyration is modulated.

In practise it is sometimes easier to run the fork at constant supplied power rather than constant amplitude. Under this condition, a decrease in sensitivity occurs for sustained high rates of turn due to absorption of power from the tuning fork by the torsion system. The rotation of the base cannot supply any power to the torsion system.

If constant power is used to drive the tuning fork, application of a large rate of turn will cause the effective amplitude to decrease from an initial value ΔR_o to a new value ΔR.

For rates of turn small enough so that $\Delta R = \Delta R_o$, the decrease in sensitivity is expressed as

$$\frac{\Delta R_0 - \Delta R}{\Delta R} = \frac{\varphi_f \varphi_R}{2\pi^2 f_f^2} \omega b_0^2 \qquad (14.H)$$

This decrease in sensitivity occurs only during and immediately after sustained rapid rates of turn, and the amount of it can be controlled by design. This is a steady phenomenon and will not appear instantly on application of a rate of turn.

(iii) Amplitude and Phase Response to Oscillatory Inputs:

When there is an oscillation as an input rather than a steady rate-of-turn the amplitude and phase response are not constant.

Since the output signal of the tuning fork is a torsional vibration (or a corresponding alternating voltage) at the frequency of the fork itself, and since the envelope of this signal is related to the magnitude of the rate of turn, the signal voltages at the fork frequency may be considered a carrier whose modulation expresses the measured rates of turn. Indeed, it is a suppressed carrier, since the amplitude goes to zero when there is no rate of turn.

In practical applications, especially in some servo systems, the rates to be measured will not be steady nor of high frequency. The amplitude and phase of the carrier envelope are then of importance in designing for servo loop stability.

For a tuned system the amplitude and phase relationships can be shown to be:

$$\text{Amplitude} = \sigma = \frac{2 Q_R \, \Delta R \, \omega_{b0}}{R_0 2\pi f_f} \cdot \frac{f}{\left(1 + \frac{4 f_R^2 Q_R^2}{f_f^2}\right)^{1/2}} \qquad (14.I)$$

$$\text{Phase} = \phi = \tan^{-1} 2 f_b Q_R / f_f \qquad (14.J)$$

Graphs of typical variations are shown in Figures (14.5A) and (14.5B).

The approach used above enables time constants and cut-off frequencies to be calculated. To be noted also is the fact that due to the difference in Q factors for torsion system and fork unit, it is possible to design for independently specified linearity and time constant.

(iv) Drift Test:

The Sperry Gyrotron had a drift rate of 15 deg./hour for an 8 hour period.

The R.A.E. gyro, using electromagnetic bucking and close temperature control ($\pm$ 0.1°C) had a long term drift (over 20 hour periods) of 0.5 deg./hour and a short term drift of around 0.07 deg./hour.

(v) Threshold:

The minimum input rate detectable by the Sperry Gyrotron was 15 deg./hour.

14.6 FREQUENCY DEPENDENCE OF OUTPUT SIGNAL

Investigation of this phenomenon has not been reported upon. Because of the basic similarity between the tuning fork device and the piezoelectric gyro, the frequency problems described in Section (13.6) may also apply here.

14.7 TEMPERATURE RESPONSE OF THE GYRO

As mentioned earlier in Section (15.5, iv) for the low drift rates mentioned temperature control within $\pm$ 0.1°C was required. It is thought that drift rates can be significantly lowered with the advent of improved thermostats.

14.8 HYSTERISIS AS A FUNCTION OF TEMPERATURE

This phenomenon has not been reported upon.

14.9 ENVIRONMENTAL TESTS AND RESULTS

(i) Acceleration Tests:

The drift rates for constant acceleration conditions were reported in Section (15.5,iv). For a variable 1 g field, toppling experiments on the R.A.E. gyro showed a residual error signal of 12 deg./hour/g.

(ii) Shock Tests:

The limit is not known. The Sperry Gyrotron withstood 30 g. in all directions in preliminary tests.

(iii) Vibration Tests:

The only data is reported by Sperry:

10-55 cps at 0.06 inches excursion.

14.10 RELIABILITY

The design has an inherent long life expectancy. There should be no gradual deterioration of stability with time. No failures have yet been reported.

14.11 SOURCES OF ZERO ANGULAR RATE SIGNALS

(i) Zero Rate Signals:

Whereas the primary causes of zero signals in the conventional rate gyroscope are mass imbalances of the gimbal in the presence of the earth's gravitational field (or an acceleration) and pickoff unbalance, the tuning fork gyro, on the other hand, being entirely vibratory in principle, can have no first order effects due to steady forces. Its zero signal comes primarily from the effect of asymmetries and dynamic unbalances upon vibration of the fork.

Three major spurious vibrations can be produced in the turning fork; a torsional vibration, a lateral vibration parallel to tine motion which can be converted to torsion if the support is asymmetrical and an axial vibration which can be converted to torsion by subtle asymmetries in the support.

(ii) Lateral Vibrations:

Lateral vibration of the base has two main sources. One is the case when the tines have different effective masses; the other is when the tines have non parallel directions of motion.

As theory shows, the principal coupling between translational and angular motions of the base occurs through static unbalance of the base or asymmetric linear damping. The former will produce a torsion output in quadrature with a rate of turn signal and is not of concern, whereas the latter introduces an output signal which cannot be distinguished from a rate of turn signal. Thus minimization of translational motion is a very important consideration in design and development.

(iii) Torsional Motion:

Even when the tines are balanced and no translation occurs, a torsional motion may be produced because of fork asymmetries about the plane of vibration. This situation is not considered serious as the signal's phase is in quadrature with the output signal.

(iv) Axial Motion:

Usually the point of support of a tuning fork is not nodal for bending of the tines. In addition the tine equilibrium position may be inclined to the XX axis giving a component of the fundamental motion parallel to XX. As a result, some axial motion of the base parallel to the sensitive axis may be present at the fundamental frequency.

The result, due to complex coupling effects, may be translational motion in the X or Z directions and hence angular motion, or angular motion may be produced directly.

In practise, axial motion comes as a result of large manufacturing inaccuracies. These very rarely occur in test equipment.

(v) <u>In Phase Residual Angular Motion:</u>

In phase signals can be produced by acceleration forces from tine unbalance in the prescence of certain asymmetries in the base. The driving system may also introduce an in-phase torque directly by misaligned electrodes.

The variation of air temperature in the air gap between tine and electrode introduces a variable air damping factor into the output. Acoustic radiation and reflection from obstructions near the fork or from the thermostat walls are such that in-phase signals greater than 250°/hr. can occur with the introduction of a reflecting surface near the fork.

14.12 ELIMINATION OF ZERO RATE SIGNALS

(i) <u>Double Modulation:</u>

Double modulation refers to the introduction of a second modulation of the Coriolis torque through modulation of the angular rates to be measured. The first modulation is associated with the vibratory velocities imparted by the basic drive member. The additional modulation is introduced by rotating or oscillating the basic drive member about one of its rate insensitive axes. A complete theoretical treatment is given by Bush and Newton [6].

Improvements realized in the performance of the gyro with double modulation are shown below. Results were sought with an without temperature control.

PERFORMANCE

	Without Double Modulation	With Double Modulation
Standard Deviation of Short Term Drift	6 eru	6 eru
Standard Deviation and Long Term Drift	44 eru	Not Observable
Magnitude of Zero Rate Signal	5650 eru	60 eru
Phase Shift Sensitivity	100 eru/deg.	1 eru/deg.

(NOTE: 1 eru = 1 earth rate unit = 15°/hour)

Conclusions reached in the investigation were:

(a) Improvement in zero rate error attributed to non-acceleration dependent cross-coupling by a factor of at least 100 has been achieved by double modulation. This result has been obtained in spite of a high level of double modulation bearing noise that tends to bias the result in favour of the test without double modulation.

(b) Zero rate error attributed to acceleration dependent cross-coupling is not affected by double modulation.

(c) Double modulation spin axis bearings do not appear to be critical.

It should be noted that the results obtained were from a tuning fork whose torsional unbalance was larger than the unbalance of the best tuning gyros by a factor of 500.

14.13 EQUATIONS OF DOUBLE MODULATION

It can be shown using the vector approach that the Coriolis force exerted by a moving mass is given by

$$\bar{F}_c = 2m(\bar{v} \times \bar{\Omega}) \tag{14.K}$$

where $\bar{v}$ = velocity of the mass

Ω = angular rate of the frame of reference

If simple harmonic motion is assumed for the mass, its displacement v from its rest position is given by

$$v = v_m \sin \omega_d t \tag{14.L}$$

where v_m = amplitude of the motion

ω_d = radial frequency of the driving vibration

The Coriolis torque about the sensing axis can then be found as

$$M_c = -4 m R v_m \omega_d \Omega_{yf} \cos \omega_d t \tag{14.M}$$

where Ω_{yf} = input angular rate = rate about sensitive axis.

The next step is to determine the torques caused by cross-coupling effects. The cross coupling force is the sum of the reaction forces on the central member of the tuning fork required to balance the acceleration force of the mass m in its simple harmonic motion and the driving force required to overcome losses.

It is best to write the total torque as an equation in which direct and quadrature components of the cross coupling torque have been combined. The total cross coupling is then separated into two components.

(a) an acceleration sensitive component represented by the equivalent rate Ω_a at a phase angle θ_a

(b) a non-acceleration sensitive component Ω_n at a phase angle θ_n.

The acceleration term arises from non symmetrical bending of the tines under an acceleration load whereas the non-acceleration dependent term is a function of time and temperature.

The major contribution to the acceleration component will come from acceleration $a_{z\zeta}$ along the Z axis of the fork. Thus one could write

$$\Omega_a \cong K_a a_{z\zeta} \tag{14.N}$$

where K_a = the acceleration sensitivity.

By referring to Figure (14.2) one can note the axes for the Double Modulation discussion. If the tuning fork is rotated about the $x\zeta$ axis at a constant angular rate ω_m, the angular rate about the sensitive axis is given by

$$\Omega_{yf} = \Omega_y \cos\omega_m t + \Omega_z \sin\omega_m t \tag{14.O}$$

where Ω_y = the angular rate about the y axis of the doubly modulated instrument

Ω_z = the angular rate about the Z axis

Thus, under conditions of Double Modulation, the acceleration along the Z axis of the fork becomes

$$a_{zf} = -a_y \sin\omega_m t + a_z \cos\omega_m t \tag{14.P}$$

Placing the equations for acceleration, (N) and (P) and the expression (O) for angular rate into an equation for total torque, such as

$$M_s = -K_{mc}\left[\Omega_{yf}\cos\omega_d t + \Omega_n(\cos\omega_d t + \theta_n) + \Omega_a(\cos\omega_d t + \theta_a)\right] \tag{14.Q}$$

where $K_{mc} = 4 m R v_m \omega_d$ (14.R)

then the expression for the total torque about the sensing axis becomes

$$M_s = M_{s+} + M_{sd} + M_{s-} \tag{14.S}$$

i.e. The torque signal has three components at frequencies

(1) $\omega_+ = \omega_{drive} + \omega_{modulation}$,

(2) $\omega_d = \omega_{drive}$

(3) $\omega_- = \omega_{drive} - \omega_{modulation}$

These are

$$M_{s+} = -\frac{K_{mc}}{2}\left[(\Omega_y + K_a a_y')\cos\omega_+ t + (\Omega_z + K_z a_z')\sin\omega_+ t\right] \tag{14.T}$$

$$M_{sd} = -K_{mc}\,\Omega_N \cos(\omega_d t + \theta_n) \tag{14.U}$$

$$M_{s-} = -\frac{K_{mc}}{2}\left[(\Omega_y + K_a a_y'')\cos\omega_- t - (\Omega_z + K_a a_z'')\sin\omega_- t\right] \tag{14.V}$$

Note that the primed and double-primed accelerations refer to accelerations projected on axes rotated relative to the instrument axes in the positive direction about the X axis by angles of $\frac{\pi}{2} + \theta_a$ and $\frac{\pi}{2} - \theta_a$ respectively.

By suitable signal processing it is possible to have the overall instrument respond to either the upper or lower sideband to the exclusion of the other two components.

The sideband torque components both contain acceleration dependents that cannot be distinguished from rate signals. This can be allowed for to the extent that K_a can be calibrated for an individual instrument.

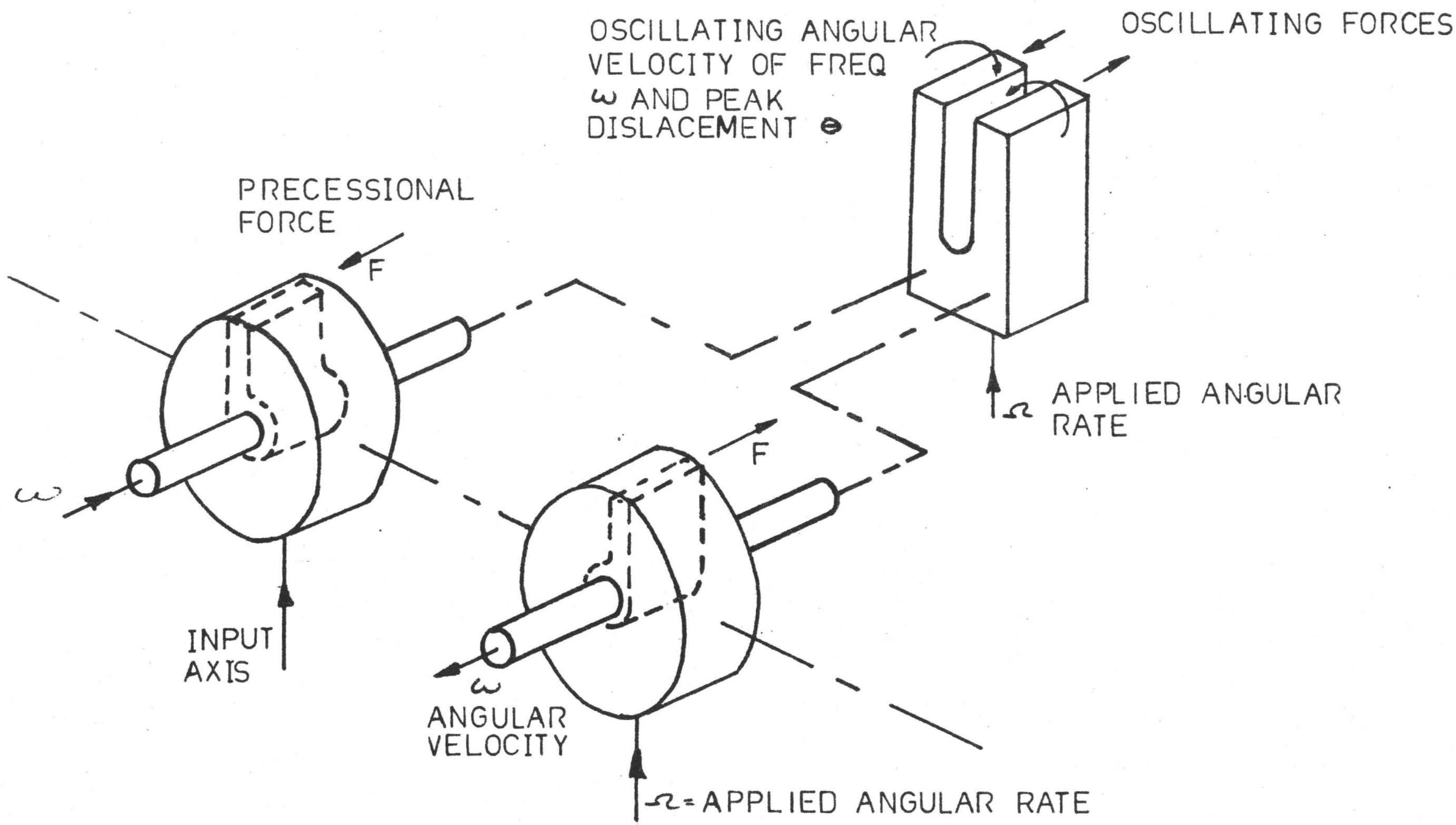

TITLE: GYRO COMPARISON	
SCALE: NONE	SOURCE:
DRAWN BY: HILL	FIGURE NO: 14-1

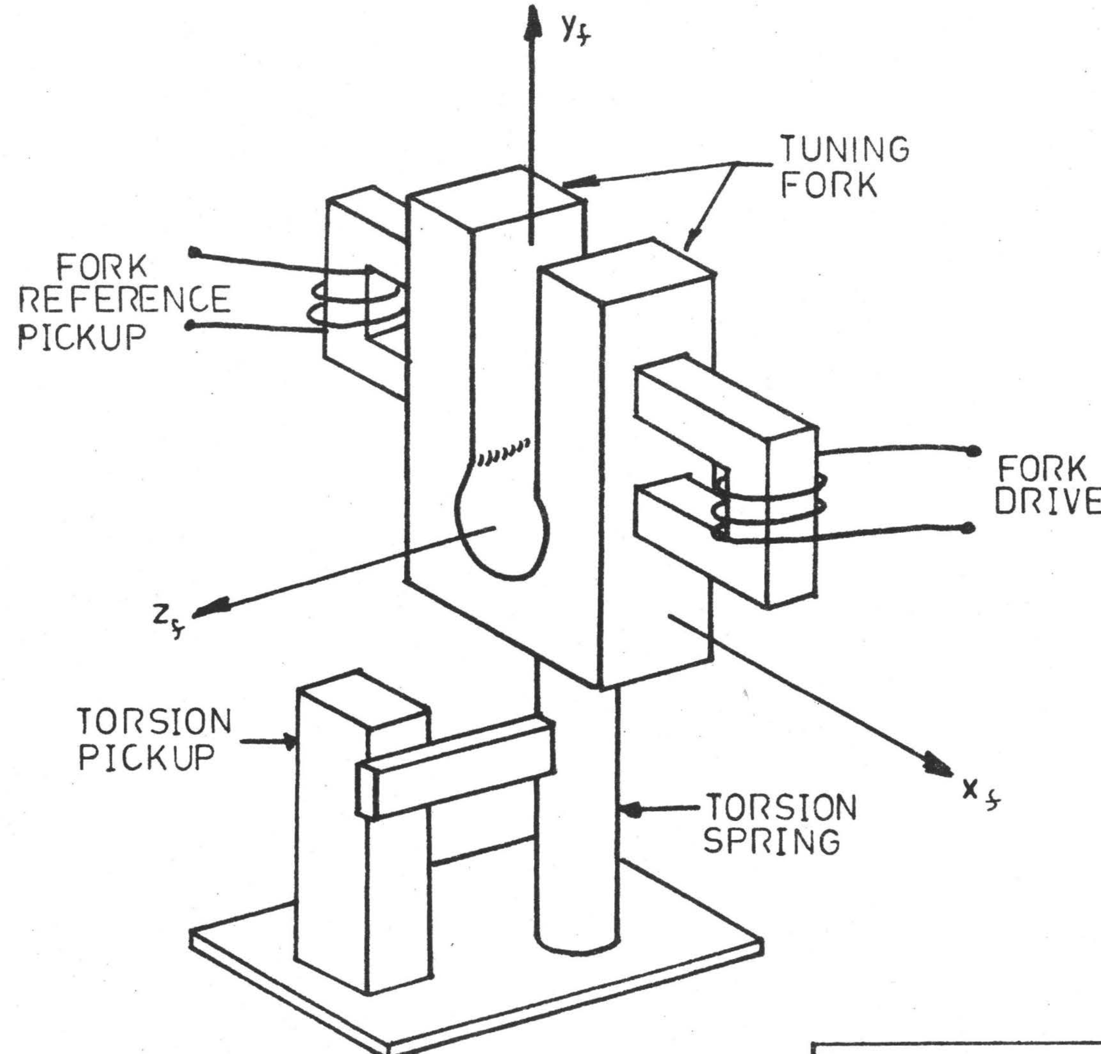

TITLE: TUNING FORK GYRO MODEL	
SCALE: NONE	SOURCE: REF. 3
DRAWN BY: HILL	FIGURE NO: 14-2

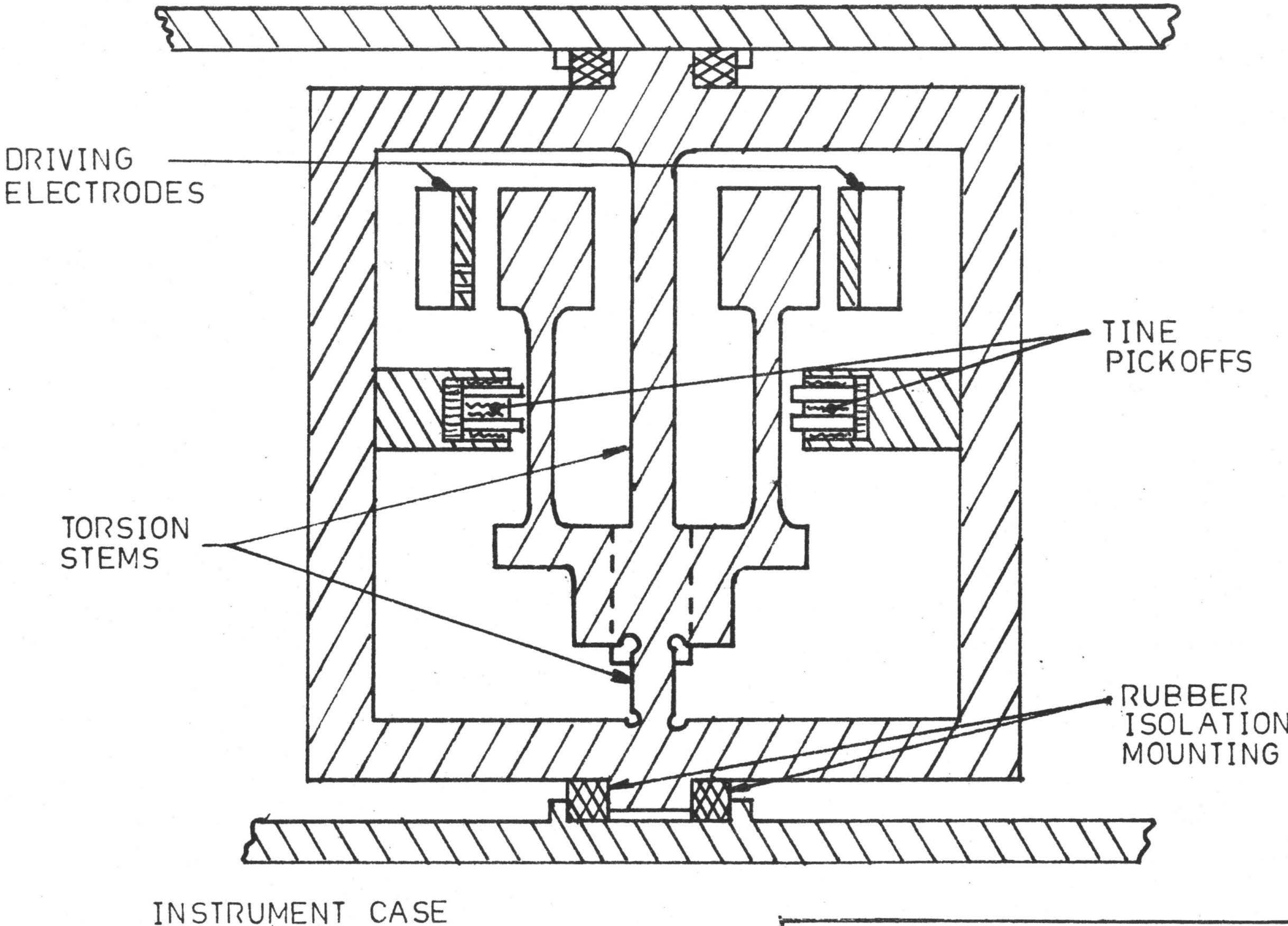

TITLE: TUNING FORK GYRO EXAMPLE	
SCALE: NONE	SOURCE: REF. 8
DRAWN BY: HILL	FIGURE NO: 14-3

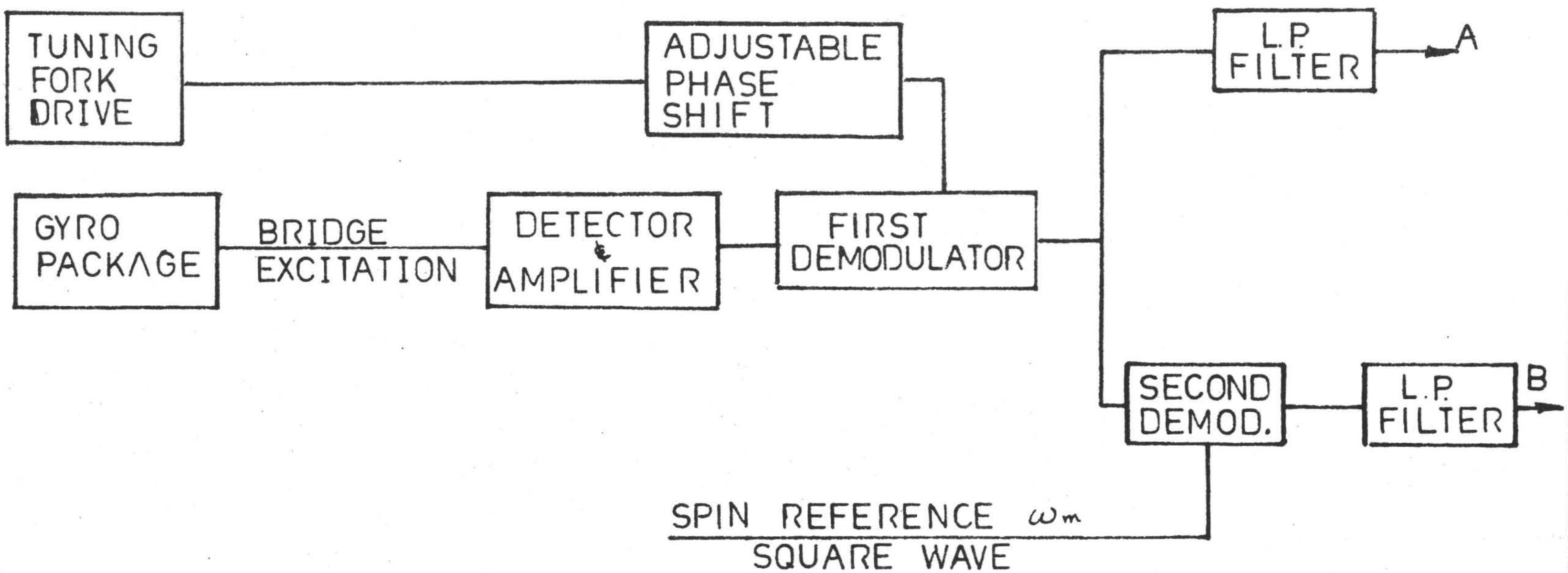

A = OUTPUT WITHOUT DOUBLE MODULATION
B = " WITH " "

TITLE: ELECTRONIC CIRCUITRY	
SCALE: NONE	SOURCE: REF. 2
DRAWN BY: HILL	FIGURE NO: 14-4

PHASE RESPONSE AS A FUNCTION OF FREQUENCY

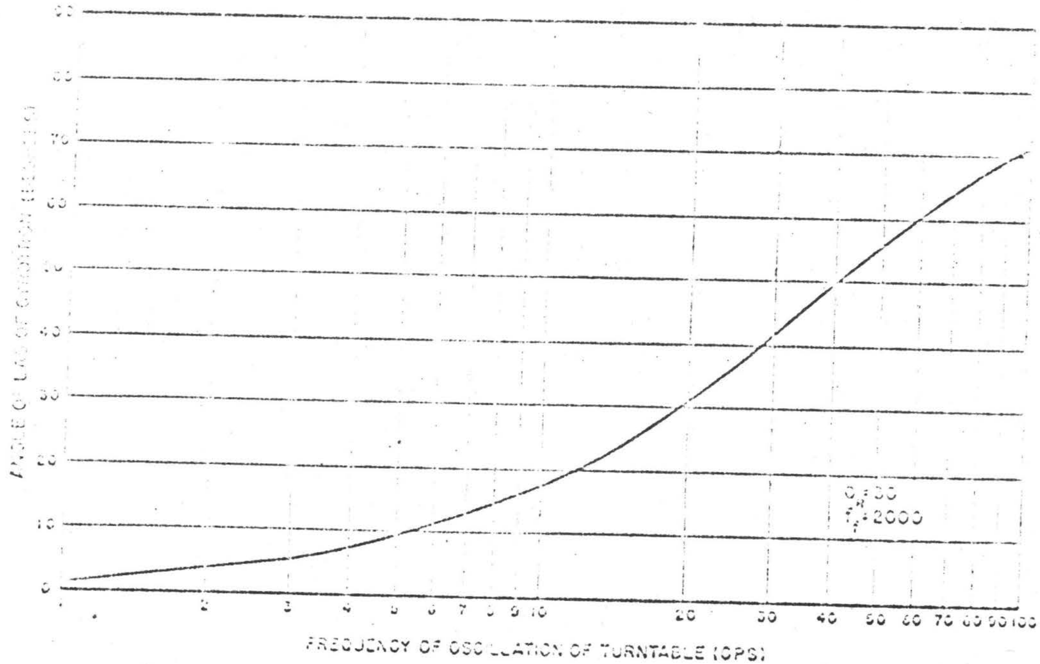

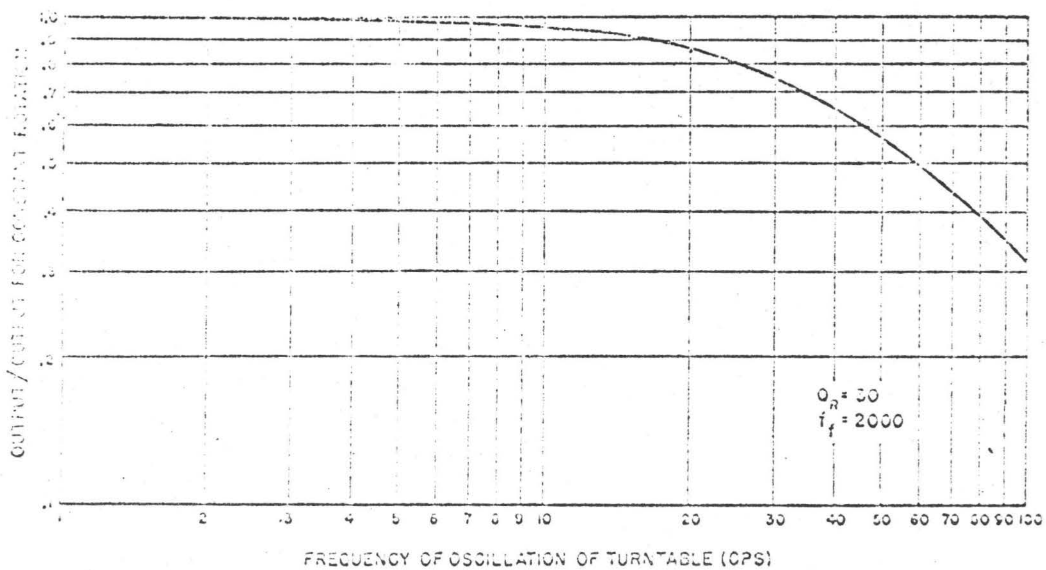

AMPLITUDE RESPONSE AS A FUNCTION OF FREQUENCY

TITLE: AMPLITUDE PHASE RESPONSE	
SCALE: NONE	SOURCE: REF. 3
DRAWN BY: HILL	FIGURE NO: 14-5

REFERENCES

1. Chatterton, J. B., "Fundamentals of the Vibratory Rate Gyro", ASME Paper No. 55-5-25.

2. Newton, G. C., "Theory of Practise in Vibratory Rate Gyros", Control Engineering, June 1963, pp. 95-99.

3. Morrow, C. T., "Steady State Response of the Sperry Rate Gyrotron", J. of Acoust. Soc. of America, Vol. 27, No. 1, 1955.

4. Fearnside, K. and P. Briggs, "The Mathematical Theory of Vibrating Angular Tachometers", Proc. of I.E.E.E., 105, (Part C), 1958

5. Morrow, C. T., "Response of the Sperry Rate Gyrotron to Varying Rates of Turn", J. of Acoust. Soc. of America, Vol. 27, No. 1.

6. Morrow, C. T., "Zero Signals in the Sperry Tuning Fork Gyrotron", J. Acoust. Soc. of America, Vol. 27, No. 3, 1955.

7. Kopytov, V. I. Studenikin, "Floating Vibratory Gyroscope", Izvestiya Uuzov, No. 3, 1966.

8. Hobbs, A.E.W., "Some Sources of Error in the Tuning Fork Gyroscope", R.A.E. Tech. Note No. IAP1139, April 1962.

9. Bush, R. W. and G. C. Newton, "Reduction of Errors in Vibratory Gyroscopes by Double Modulation", MIT Electronic Systems, Laboratory, 1964.

PART 6

SUMMARY AND CONCLUSION

CHAPTER 15

SENSOR ASSESSMENT

15.1 SENSOR ASSESSMENT FORMAT

The concepts and devices described in the preceding chapters will now be evaluated for their suitability for gun launch. The design constraints developed in Part 1 of this report will be restated first. These constraints will then be paired with the capabilities of each device.

The general format of the comparison will be a table listing the design criterion number, the prospect of suitable operation (favourable, unfavourable or questionable) and comments on the state of the sensor.

The chapter will conclude with a table of the relative ratings of each device with respect to the design requirements.

15.2 DESIGN CRITERIA RESTATED

The design criteria developed in Part 1 are given below.

*1. Sensor must withstand gun launch (7,000g) without loss of sensitivity.

*2. The device must function in a spinning vehicle.

*3. The device must be able to function at any hour of the day or night.

*4. The device chosen should have a proven feasibility and use proven components and proven design techniques as much as possible. Design and development of new highly specialized components should be kept to a minimum.

5. Operation time need not exceed 15 minutes. Thus only very high drift rates will be rejected.

6. Acceleration sensitive drifts should be small as the device operates during the boost phase.

7. Initial system alignment should be simple and easy to accomplish (especially during flight).

8. Weather conditions (up to the capability of the vehicle itself) should not affect the attitude sensors operation.

9. Support equipment must be capable of surviving gun launch in operating condition.

10. Sensors and related equipment must be compact and light in weight to increase payload (i.e. less than 10 lbs. and less than 200 cu. in. volume).

* It should be noted that failure of a scheme to meet any one of criteria 1,2,3, and 4 will be sufficient reason for rejecting it.

15.3 HORIZON SENSOR EVALUATION

The horizon sensor capabilities are now discussed, point by point, against the design criteria. Because of the nature of the horizon sensor concept it can be used only for sensing of the vertical, and thus for pitch attitude reference. Horizon sensing methods will thus be evaluated in this context.

Criterion No. 1 Favourable

Tests have been conducted by Aviation Electric Limited [1] on a thermistor bolometer type of device built by Barnes Engineering. The type of support for the germanium windows required for the sensor have been simulated using glass which has the same properties. Gun launch at 7,000 g caused no problems when the windows were edge supported and bonded in place using four grades of semi-flexible expoxy.

A machined aluminum housing for the sensors has withstood a 9,700 g peak acceleration successfully.

Criterion No. 2 Favourable

The horizon sensor concept requires a scanning mechanization for its operation. In usual designs a mechanical drive assembly is employed to rotate the sensor through its scanning motion. In a spinning vehicle, however, the sensors may be rigidly mounted to the vehicle frame. The vehicle's spin accomplishes the scan.

Criterion No. 3   Favourable

If the horizon sensor detects infared radiation, it can operate day or night. The 15 micron Carbon Dioxide radiation band is favoured for infared horizon sensing because it displays the smallest diurnal variation of intensity and distribution

Criterion No. 4   Favourable

Horizon sensing methods for the determination of the local vertical near a planet have been successfully used on various earth satellites. Manned space vehicles of the Mercury and Gemini types have used horizon scanners for attitude determination. Hardware is highly developed for sensing radiation up to about 30 microns wavelengths. As mentioned earlier, under Criterion No. 1, these devices show great promise for survival of the gun launch shock.

Criterion No. 5   Favourable

While horizon sensor accuracy varies with time, these variations, in phenomena to be sensed, are on a yearly or daily basis. A 15 minute period is thus negligible.

Criterion No. 6   Favourable

The horizon sensing concept has no active components which are acceleration sensitive. No drift can then occur because of acceleration.

Criterion No. 7 Favourable

The concept needs no initial alignment scheme. The sensor detects the on and off points of the earth's radiation and takes the midpoint of this pulse as the center of the disk of the earth.

Criterion No. 8 Favourable

No clouds exist above 18 km. altitude [2]. The second stage operation begins at approximately 35 km. The drop off in radiance of carbon dioxide occurs near the altitude also. (See Figure 4.2). Thus the vehicle should be out of range of cloud blocking effects and upper atmosphere radiation which would cause a continuous scanner output.

Criterion No. 9 Favourable

Tests on transistors, diodes, resistors and capacitors were carried out by Aviation Electric Limited [1]. Certain brand name components were found in each of these categories which successfully withstood gun launch accelerations. A listing of them is given in [1].

Criterion No. 10 Favourable

The sensors themselves can be less than 5 inches long and 2-1/2 inches in diameter. The electronic modules can be approximately the same size. Weights of these devices would hardly be greater than 5 lbs.

15.4 CELESTIAL SENSING EVALUATION

Celestial sensors have had favourable results in satellites and interplanetary space probes in recent months. It is also quite probable that sun and star sensors could be designed to meet the restrictions placed on them by the criteria for launch acceleration survival, size, weight, and operation times. This is particularly true of the photocell detectors, which have already been tested and proven by Aviation Electric [1]. There are certain fundamentals of operation which prevent celestial sensors from satisfying criteria 2 and 3, however.

Criterion No. 2 Questionable

Whether or not the sensor can operate in a spinning vehicle depends on the sensor mechanization. The photocell detector which senses the differential brightness of the sun as a function of vehicle yaw angle operates satisfactorily on a period pulse from the radiation source. The magnitude of this periodic pulse is sufficient to determine the yaw.

Systems which acquire a specific star and subsequently check vehicle orientation with respect to this star would not work in a spinning vehicle. These systems (either gimballed or television tube type) must be approximately aligned before being activated. They are usually mounted on a stable platform device to check its alignment periodically. Intermittent scanning in a random orientation is definitely not a possible mode of operation.

Criterion No. 3 Unfavourable

The photocell device, which can be used satisfactorily to sense large luminous objects such as the sun can operate only at specific hours of the day, as stated in Chapter 5, Section 5.3.

It should be noted, however, that since the sensors would be operating above 35 km altitude clouds, with a maximum altitude of 18 - 20 km would not obscure the reference.

If distant stars were to be sensed instead, a goal which has been achieved in daylight, sophisticated narrow aperature devices would have to be used. This type of sensor must be prealigned by its gimbal system. As mentioned earlier, this is not feasible in a spinning vehicle. The effect of the atmosphere, extending out to 50 km causes the stars to twinkle, and thus produce sensing uncertainties.

If one is prepared to accept the limitations of restricted hours of operation for orbit injection or tactical applications, than the photocell sun sensor may prove satisfactorily. In general, however, this limited utility is not acceptable.

15.5 EVALUATION OF GRAVITY FIELD SENSORS

Gravity field sensing has not yet reached the practical stage. More importantly, it is not feasible for defining the vertical from moving vehicles. Any acceleration detector placed in this vehicle would measure an acceleration which is the resultant of the earth's gravity field and the vehicle accelerations along its path. Because the gradient is so small within the atmosphere, it cannot be discerned by methods presently known.

Because gravity gradient sensing is not in fact possible, it can only be rejected.

15.6 EVALUATION OF MAGNETIC FIELD SENSING

Magnetic field sensing will be evaluated with respect to the most promising designs for overall attitude determination systems.

Criterion No. 1 Favourable (by design)

The complete lack of moving parts and the proven design of basic electrical components such as resistors and capacitors makes the successful survival of the magnetometer highly possible.

Criterion No. 2 Favourable

The magnetometer attitude reference system considered in this report was designed specifically for a spinning vehicle.

Criterion No. 3 Questionable

Further information is required before a definite ruling can be made here. If the system is to operate with a sun sensor as a phase reference then its ultility is restricted. If a system of three magnetometers was used a large amount of data would be required in addition to large computing facilities.

Criterion No. 4   Favourable

Actual test flights by Conleys group [1] have shown that the concept is indeed a feasible one for conventional sounding rockets.

Criterion No. 5 and 6   Favourable

No problems should be experienced here, as there are no acceleration sensitive drifts invloved.

Criterion No. 7   Favourable

There is no need to align the system. The magnetometer is surrounded by the field it is to sense. What is needed is some phase reference for the resulting sinusoidal signal. For Conley's system, this is easily provided by the sun vector. If an approximate vehicle alignment at system start-up is known, it can be used as the first approximation for the attitude iteration calculations. The solution of one iteration is then used as the starting point for the next iteration.

Criterions 8, 9 and 10   Favourable

Based on past experience no problems are expected here.

15.7 EVALUATION OF CONVENTIONAL SENSORS

Conventional gyros will be evaluated with respect to the developed design criteria.

Criterion No. 1 Questionable

The most sophisticated solid rotor gyro available, the single-degree-of-freedom floated gas bearing gyro, is not capable of withstanding acceleration rates greater than 100 g's [3]. The Whittaker Corporation markets a spring energized gyro Type SP1.11 which has the inner and outer races of its gimbal bearings bonded in place by thermosetting resin. The shock that this unit can withstand is 325 g for 20 milliseconds.

Other two-degree-of-freedom gyros are available of the floated type using ball bearings for the rotor and gimbals and synchro pickoffs and torques on each gimbal axis. These units, such as the Whittaker FF10 can withstand up to 250 g shocks.

Thus while the shock capacities of present is quite sufficient for present aircraft and missile applications, they are not of the same order of magnitude for gun launch shocks. Dinter of Honeywell [4] feels that there will also be a problem of finding materials strong enough to resist permanent deformation in sections light enough to permit floatation and to maintain low values of mass imbalance.

Criterion No. 2 Questionable

Strap-down systems to date have been intended for satellites or aircraft where radical changes in attitude were not expected. While no references exist in the open literature on the application of strap-down systems to spinning vehicles, there appears, on preliminary examination, to be no reason for the system not be to applicable.

Criterion No. 3 Favourable

No external references are needed for the inertial sensor.

Criterion No. 4 Questionable

While conventional gyros are the standard of the gyro field, their behaviour in very high shock environments is not known. While researches in the field, such as Dinter [4] feel that the ultimate limit of a gyro designed specifically for shock would be 1000 g, only actual design and testing will prove the feasibility of this unit.

Criterion Nos. 5 and 6 Favourable

If a gyro such as the Whittaker Spring energized unit were used for yaw sensing (with the spin axis set parallel to the intended trajectory plane), a drift rate of 0.5 deg./minute characteristic of this unit was accepted, an orbit injection error as great as 10 degrees could be expected. More accurate gyros can be obtained but with a lower shock rating.

Criterion No. 7 Unfavourable

Initial system alignment is not possible without some external reference information.

Criterion No. 8 Favourable

No problems here.

Criterion No. 9 Favourable

Tests on electronic components by Aviation Electric [1] indicate that no problems should arise in this area if proper precautions are taken.

Criterion No. 10 Favourable

Compact gyro units (3 inches long x 2 inches diameter, weight, 1 lb.) and present electronic technology would provide a sensing unit well with the design limits.

15.8 EVALUATION OF THE ELECTRICALLY SUSPENDED GYRO

Criterion No. 1   Unfavourable

Because of the long settling time of the unit after spin-up, the gyro would have to be already running at the time of gun launch. This, therefore, would require that the levitation of the spinning ball be maintained during the high "g" acceleration. Presently available figures show that this is not possible.

Knoebel [5] reports that the highest voltage gradient that could be sustained was 10^6 volts/cm. The present state of the art in high voltage breakdown research by Lyman [6] indicates a maximum gradient of 2×10^6 volts/cm.

Basic theory shows that if we assume one electrode does all the lifting and that we have a plane parallel plate, the acceleration in g's would be

$$g = \frac{F}{980m} = \frac{1}{980m} \frac{NAE^2}{2}$$

where

F = lifting force

m = mass of rotor = 15 gm

A = electrode area = 10 cm^2

N = permittivity of space = $\frac{1}{4\pi}$

E = voltage gradient = $\frac{2 \times 10^6}{300} = 6.6 \times 10^3 \frac{\text{stat. volt}}{\text{cm.}}$

The above figures are those for a typical gyro. The voltage gradient is the maximum obtainable within the state-of-the-art.

Substituting:

$$g = \frac{10 \times 4.4 \times 10^2}{980 \times 15 \times 2 \times 4\pi} = 1200$$

This value is considerably less than 7,000. The results of these calculations are further tempered by the fact that it has been difficult to design for a reliable 30 g for military applications.

The electrically suspended gyro is thus unsuitable.

15.9 EVALUATION OF THE FLUID SPHERE GYRO

The fluid sphere gyro could be used best for yaw rate sensing, although it could be used for pitch angle determination as well. For the evaluation considered here, the gyro would be a rate gyro mounted with its spin axis parallel to the spin axis of the vehicle. The inner rotating cylinder is supported during launch such that no "axial thrust" on the spin bearings is permitted. A proposed design is shown in Appendix A.

Criterion No. 1 Questionable

While the fluid sensing element would not be harmed by the gun launch, the survival of the bearings and the motor-pickoff elements is open to speculation. It is very difficult to support the relative soft iron structures and conductors. Without actual test firings no exact pronouncement can be made.

Criterion No. 2 Favourable

By mounting the gyro so that its spin axis is parallel to the vehicle's spin axis, the use of a roll stable platform could be avoided. A servo loop would be necessary to control the spin speed, however, as the vehicle spin speed increases or decreases.

Criterion No. 3 Favourable

Being independent of any external phenomenon no limitation is experienced.

Criterion No. 4 Favourable

Test models have been built and tested. Performance (See Section 11.1) has been good. The device has been considered good for missile applications where accelerations are quite high.

Criterion No. 5 Favourable

Using the expected drift rate of 0.1 deg./hr. for the Sperry fluid sphere gyro, and the values of 10 minutes duration of the boost phase, the error in yaw would be around 0.02 deg.

Criterion No. 6 Favourable

The sensitivity of this gyro to acceleration dependent or $(\text{acceleration})^2$ errors is extremely low.

Criterion No. 7 Questionable

Initial system alignment is not possible without some external reference information.

Criterion No. 8 Favourable

Not dependent on external references.

Criterion No. 9 Favourable

All support equipment is electronic. This problem can be solved.

Criterion No. 10 Favourable

The gyro unit can be only 3 inches long by 2 inches in diameter and weigh less than 1 lb.

15.10 EVALUATION OF THE LASER GYRO

The laser gyro, like all inertial devices in this report, will be considered as best applied to yaw sensing.

Criterion No. 1 Favourable

While no tests have been made, the complete abscence of moving parts in the gyro and its solid block design make its adaptation a very likely possibility.

Criterion No. 2 Favourable

While no treatment of the spinning vehicle problem and signal demodulation has done it is thought by Honeywell that this adaptation could be made.

Criterion No. 3 Favourable

An inertial device experiences no problem here.

Criterion No. 4 Unfavourable (at present)

The laser gyro has been reduced in size greatly in the last few years to a solid quartz block about 11 inches across. However, much development work remains to be done before the laser becomes an accepted inertial device. Because of its low state of development, this device will have to be rejected.

The laser gyro is very much the inertial sensor of the future and one which should be carefully reconsidered for gun launched rockets at some future date.

15.11 EVALUATION OF THE SOLID STATE GYRO

The solid state gyro is a rate gyro useful for yaw rate sensing applications. A method of supporting the sensitive element during launch was designed and is described in Appendix B.

Criterion No. 1 Questionable

The sensor ceramic is a brittle device easily broken if dropped.

However, a support system for the element was designed (see Appendix B) that is simple to construct and, by its simplicity inherently reliable. Success during gun launch is an open question, however.

Criterion No. 2 Favourable

The solid state gyro should be capable of being strapped down in the vehicle and allowed to spin with it. The concept of Double Modulation, discussed in relation to the Tuning Fork gyro could be applied and the appropriate rate signal obtained.

Criterion No. 3 Favourable

An inertial device needs no external reference.

Criterion No. 4 Favourable (to date)

Test models have been built and their performance has indicated the feasibility of this design. However, manufacture of the sensitive element is a difficult process. Balance, alignment and temperature control are present limitations. Material research is being carried out to find an improved sensor ceramic.

Criterion No. 5 Unfavourable

Present drift rates are extremely high. If yaw angle in a spinning,coning vehicle is found by integrating the yaw rate through time, the long term drift of the gyro will integrate out to zero. The short random drift, a plus or minus quantity about the null appears as a rate signal of 2 to 5 deg./sec. Since it is random though and one vehicle revolution takes only 1/5 of a second, the error should sum to zero.

Criterion No. 6 Questionable

A linear acceleration sensitivity of 1 deg./sec./g is extremely high when compared to the fluid sphere gyro (0.8 deg./hour/g) and the tuning fork gyro (12 deg./hour/g). The drift due to this source during the boost phase could be minimized by the integration procedure though.

Criterion No. 7 Questionable

System alignment during flight is difficult.

Criterion No. 8 Favourable

No problems here.

Criterion No. 9 Favourable

No problems here.

Criterion No. 10 Favourable

No problems here. The sensor package can be less than 1-1/2 inches in diameter by 1 inch long.

15.12 EVALUATION OF THE TUNING FORK GYRO

The tuning fork gyro is a vibratory rate gyro device, best employed for yaw rate sensing.

Criterion No. 1 Favourable (by design)

The very concept and design of the tuning fork gyro is inherently rugged. From the theory it can be seen that sensitivity does not require a delicate construction. The complete abscence of bearings or rotating parts, even in the readout devices reduces many of the potential problems that are present in conventional designs. Tests would have to be conducted before any positive statement could be made.

Criterion No. 2 Favourable

The concept of Double Modulation permits the gyro to be strapped-down to the vehicle frame and proper signal demodulation to obtain the desired yaw rate signal.

Criterion No. 3 Favourable

Inertial devices need no external references.

Criterion No. 4 Favourable

Several models of the tuning fork gyro have been built and tested with great success. Performance and environmental capabilities have compared favourably well with other gyros. See

Section (14.1).

Criterion No. 5 Favourable

While the drift rate of around 15 deg./hour would cause a small misalignment error for a running time of less than a quarter of an hour, the scheme of integrating over the coning motion would minimize the drift errors.

Criterion No. 6 Favourable

Acceleration sensitive drift would be no problem for an integrated signal, providing the acceleration was not wildly erractic.

Criterion No. 7 Questionable

System alignment is difficult.

Criterion No. 8 Favourable

No problems here.

Criterion No. 9 Favourable

No problems here.

Criterion No. 10 Favourable

While existing test models have been rather large (7" long x 3" diameter - twice the size of the fluid sphere gyro, 3 times the size of a floated conventional gyro) the concept lends itself to miniaturization.

15.13 SUMMARY OF SENSOR ASSESSMENTS

The following table is a summary of the material in the preceding sections of this chapter. There were ten design criteria. One point was given to a sensor or sensor class for each "favourable" characteristic. Those classifications which were not suitable are stated as such. The result is a graph of the relative suitabilities of various sensors or sensing schemes for sensing attitude in a gun-launched spinning rocket. It must be noted that this is an open literature survey, of present sensors. The validity of this survey could be altered drastically at any time.

From the table it can be seen that those sensors which appear most suitable for consideration, based on the material available for this survey are horizon sensors and the tuning fork gyroscope.

15.14

RELATIVE MERITS OF SENSORS FOR GUN-LAUNCHED ROCKETS

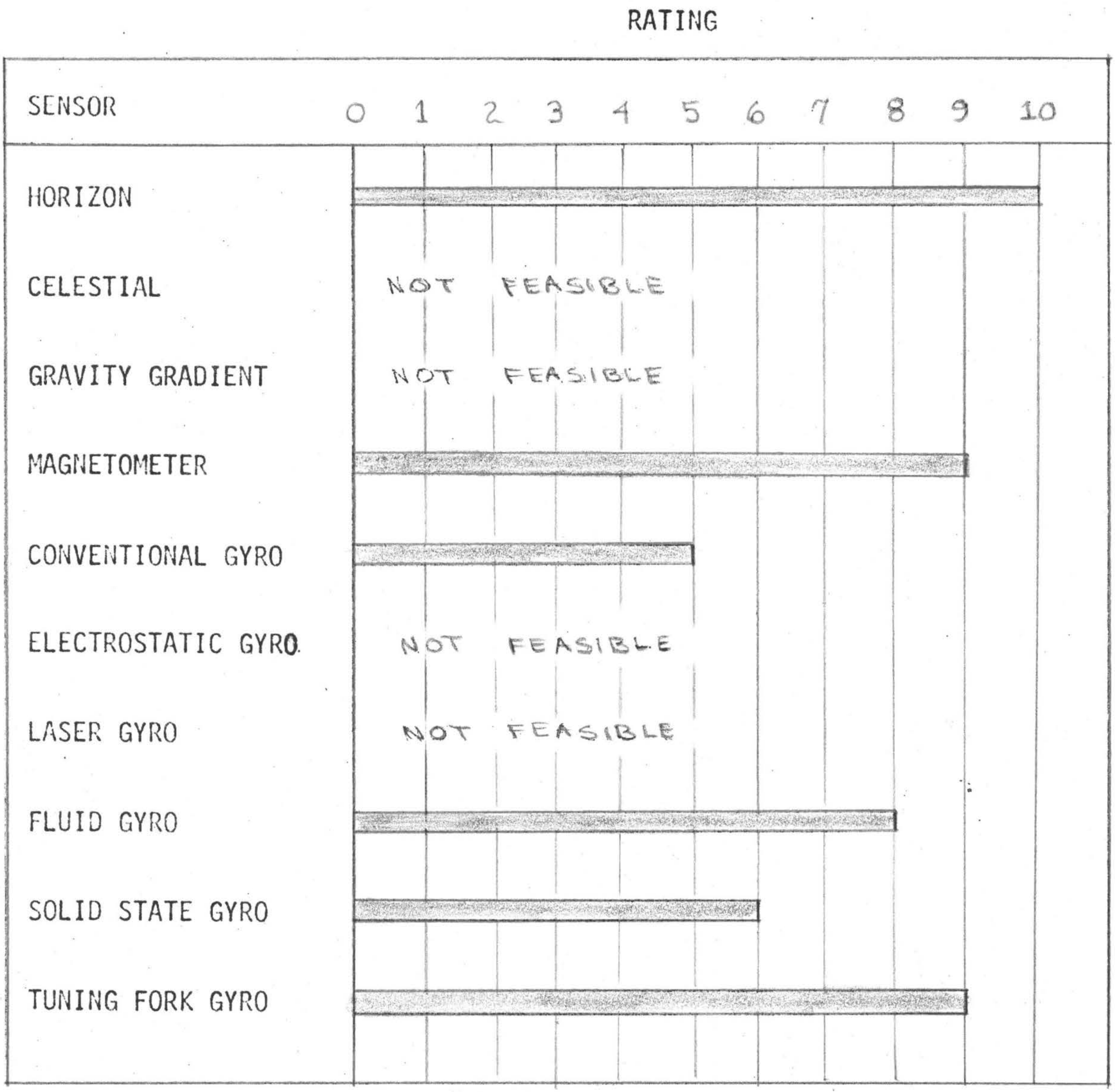

REFERENCES

1. Aviation Electric Limited, "Progress Report No. 4, Orbit Injection Control", AETR 13565, August 30, 1965.

2. Carroll, W. J., "Horizon Sensor Phenomenalogy", Sperry Engineering Review, Vol. 18, No. 3, Fall, 1965.

3. Lund, P. S., "The Changing Emphasis and Future Trends in Navigational Gyros", SAE Trans., Paper No. 650586, 1966.

4. Dinter, H. A., Minneapolis Honeywell Corp., Private Communication, August 1966.

5. Knoebel, H. W., Private Communications, July 6, 1967.

6. Lyman, E.M., "Studies Relevant to the Electrical Vacuum Gyro Programme of Electrical Breakdown in Ultrahigh Vacuum". Report R-334, Coordinated Science Labs, University of Illinois, January 1967.

CHAPTER 16

FINAL SYSTEM PROPOSAL

16.1 THE SYSTEM

The attitude reference sensing scheme proposed for gun-launched spinning rocket vehicles consists of two major components:

(1) Two infared horizon sensors to determine vehicle orientation about the pitch axis.

(2) A tuning fork vibratory gyroscope for determining vehicle orientation about the yaw axis.

It has been shown that these devices best meet the requirements for attitude sensors used in orbit injection control systems for the particular case of gun-launched rocket vehicles.

The merits of these devices is apparent because of the following items:

(1) Complete abscence of bearing surface or rotating parts.

(2) Simplicity of operation.

(3) Economy of parts and operation.

(4) The high degree of durability that can be designed into them without affecting their sensitivity in any way.

(5) The horizon sensors can be used to generate not only pitch error signals but an earth center pulse which acts as phase reference for signal demodulation.

16.2 OPERATION OF THE PROPOSED SYSTEM

The main components of the proposed system are shown in Figure (16.1).

(i) Horizon Sensors

As indicated in the diagram the horizon sensors detect the radiation difference between earth and space. The output signals from the two sensors will be unequal if the vehicle has a finite pitch angle. By determining the rate of scan and the difference in duration between the sensor output signals, the pitch of the vehicle can be determined by relating the sensor difference pulse to an earth center pulse.

If a pitch error exists, a signal is sent to the valve trigger circuitry to cause a pulse force to be applied to the vehicle. This pulse produces a torque about the spinning vehicle's center of gravity. The vehicle is thus made to precess or re-orient itself about a third axis orthogonal to the spin and torque axes. The circuitry must determine the proper timing of the pulse so that the torque and thus the precession will occur about the proper axis.

The circuitry required for such a system is not exceptionally complicated. Figure (16.2) shows the elements required for the horizon sensor logic circuitry. This circuit is patterned after one designed by Aviation Electric for the Martlet IV vehicle. It has the characteristics of a sampled data system.

The horizon sensor signals are amplified and squared by a Schmidt trigger circuit. The signal is then fed to OR gate A and to gates G1 and G2.

For Cycle Number 1, the data storage cycle, flip-flop terminal z is active and it opens gates G1 and G2 to the pulse signals. In addition the pulses go the the comparator and to OR gate B. Information on the length of the output pulse from B is stored as a voltage in the Earth Pulse Hold Circuit. In other words, the length of time that a voltage is allowed to build up on the earth pulse hold capacitor is the length of time the sensor is scanning the earth's disk. Half of this observation time would bring an observer to the center of the earth's disk, and thus the local vertical. Since the system uses squared signals, the magnitude is not important. What makes the earth pulse hold work is the proper selection of resistor R_2 so that the discharge time constant is 1/2 the charging time constant.

The comparator generates an error signal and closes either circuits S2 or S3 depending on the sign of the error signal. A capacitor in these circuits is charged to a voltage which is proportional to the total error signal duration ($t_1 + t_2$) (see Chapter 4). The system has thus gathered and stored information on the length of the earth pulse and the magnitude of the error. This information is stored until Cycle Number 2, the Control cycle is initiated.

When the sensors cross the horizon and new earth pulses are generated, Cycle Number 2 is initiated. Terminal 1 of the flip-flop becomes active, thus gates G1 and G2 are closed. When terminal 1 is turned "on" switch S1 closes and the earth pulse voltage decreases linearly to value zero in time T/2. The decrease in voltage to zero initiates the earth center pulse. Switching circuits S4 and S5 are activated and a comparison between the stored error voltage and the reference voltage E_2 is made. If the difference of these voltages exceeds a fixed threshold signal, the reactive control system is activated.

(ii) The Tuning Fork Gyro

The Tuning Fork Gyro is fixed to the frame of the vehicle. Because it is spinning it can sense rate about both the pitch and yaw axes. However, by proper signal demodulation, the yaw rate signals can be determined using the earth center pulse as a phase reference. (i.e. the yaw signal is 90° ahead or behind the earth center pulse).

If the yaw signal is integrated over time it will provide the angular drift or displacement of the vehicle from time of start-up. If the vehicle has a "coning" motion of its axis of symmetry about the flight path, the signal will integrate to zero. If the vehicle is straying off the trajectory or the vehicle is made to precess about the yaw axis, the rate signals will become unequal. The integral will then be some finite value other than zero.

By comparing the gyro's integrated signal with a reference signal at different times during flight the orientation of the vehicle can be determined with respect to some desired trajectory. Again, if errors exist, a signal will be sent to the valve trigger circuitry to apply a precession torque at the proper time.

A diagram of the logic circuitry that would be required for the sampled data yaw control system is shown in Figure (16.3). The tuning fork demodulator circuits are not considered here. The output rate signal from the second demodulator is the input signal for the logic circuitry.

For this system as well there are two operational cycles: data storage and system actuation. The data storage cycle can be initiated by the horizon sensor circuits as shown in Figure (16.3).

During Cycle No. 1, (data storage) yaw rate signals will come from the demodulator. Two signals will be produced per revolution, one for a yaw rate to the right of the trajectory plane (viewed from the rear of the vehicle) and one for a yaw rate to the left. These signals could be made positive and negative respectively. The signals would be doubly integrated and stored, the positive signal in Data Hold No. 1, the negative signal in Date Hold No. 2.

When the Actuation Cycle is initiated by the horizon sensors the earth center pulse is triggered as described earlier. The earth center pulse is used to trigger not only the pitch error logic circuit but the yaw circuit as well.

The earth center pulse is fed to a time delay circuit. Using the known spin speed of the vehicle, the timing circuit delays the earth pulse by one quarter of the period of spin. This retarded signal switches the holding circuits 1 and 2 and an error determination is made with comparators C_3 and C_4 and reference values E_3 and E_4. An error signal, if it exists ,actuates the control jets.

One outstanding problem concerned with the accuracy of such a guidance system is that it would not normally come into operation until second stage ignition. By that time the first stage could have strayed appreciably off course. The only solution is to have the gyro operating as soon after launch as possible and continuously computing the yaw deviation of the vehicle. The gyro could function quite easily in this situation and even operate during the second stage boost. The problem, however, is concerned with obtaining a suitable phase reference for demodulation. The horizon sensors are not available for the vertical reference.

Since the first stage would be spinning very slowly if at all (the spin is applied aerodynamically by the fins) it would be possible to employ a spin rate sensor of the type shown in Figure (16.4). This device would be oriented vertically in the vehicle before launch such that a positive signal was obtained. Then as the vehicle rotated slowly during the first phase of its flight an alternating signal would be generated at the frequency of the spin. The spin is expected to be low enough so that centrifugal force does not lock the vibrating mass in one position.

Yaw rate signals would be monitored during the first flight phase and stored in the Data Hold of the yaw logic circuit. Thus when the control system was activated at booster stage ignition, the initial misalignment would be known. When the second stage was brought into operation, the high spin speed of the rocket would make this device inoperative. It would be switched out of service and an oscillator would be employed instead.

16.3 DESCRIPTION OF HORIZON SENSORS

A schematic diagram of a typical infared horizon designed for this application is shown in Figure (16.5). The infared detector consists of two 1 mm x 1 mm thermistors mounted in sapphire blocks and a coated germanium window which acts as a high pass filter. The mass of the thermistors is small and it is easy to shock-proof them in the launch direction by supporting the sapphire blocks in expoxy. The windows have survived simulation tests satisfactorily by bonding them in their edge-supported state with semiflexible expoxy.

Section 15.3 discusses in detail tests conducted on devices of this type. It is not expected that the horizon sensors will be a large problem.

Since horizon sensors can be designed to survive gun-launch, their design problems need not be investigated further.

16.4 DESCRIPTION OF VIBRATORY GYROSCOPE

(i) General

The Tuning Fork Vibratory Gyroscope (T.F.G.) is a device that has the unique capability of being able to function as a gyro without the usual gimbals or bearings being required. Unlike to other gyros, it may be employed in a strapped down configuration even though the vehicle is spinning. The principle of Double Modulation permits this action to take place. The instrument may also be designed to any desired level of sensitivity without sacrificing either ruggedness or sensitivity.

The T.F.G. has been treated fairly well in the literature and several operational models have been constructed. The concept has thus been shown to be feasible and practical. Extensive development work has not been undertaken, however, because at the time of the original investigations, applications of this device were not evident.

A summary of the operation of this device and the pertinent design equations are given in Chapter 14.

(ii) Merits

The several unique features and advantages of this instrument are:

(1) No rotating parts

(2) Self-Generated A-C output

(3) Inherent ruggedness and shock resistance

(4) No response to cross axis accelerations and velocities

(5) Rapid response characteristics

(6) Wide range of rate measurements

These points will become more obvious as the details of the gyro's construction and theory of operation are obtained from the material that follows.

(iii) Design Description

A Tuning Fork Vibratory Gyroscope has been designed to withstand a 7000 g acceleration rate and to detect angular rate up to a maximum of 2.6×10^6 deg./hr. The electrical design of the pickoff components and support electronics has been eliminated as this is beyond the scope of this report. The required components and alternatives available are indicated, and many important design considerations applicable to each of them are listed.

Figures (14.6) and (14.7) show the details of a sample design for a T.F.G.

Design details are as follows:

Total Weight - 2 lbs. Tine Element (2) - 0.24 lbs. total

Torsion Bar - 0.25 in.D. Inner Cyclindr - 2" D. x 2-1/4" long

Damping Gap - 0.065 in.

Tines-1/4 in. thick x 1 in. wide x 3/4 in. long.

(iv) Description of Sensitive Element

The sensitive element actually consists of an inner cylinder (concentric with the outer case) to which is attached the tuning fork base and the pickoff components. Viscous damping takes place in the gap between the inner cylinder and the gyro case.

(v) Materials and Construction

The Tuning Fork masses and tines are machined from 4140 alloy steel. The base, which is separate, is also made from the same steel, as is the torsion rod. The tines and the torsion rod are held in position by an "expanded" fit i.e. the tines and rod are cooled in liquid oxygen before being assembled. On heating the ambient temperature, they expand and lock into position.

Beryllium Copper 25 has also been suggested for the torsion rod because of its strength and excellent stability.

The inner and outer cylinders can be made from Aluminum. The possibility of making the inner from a 356 Aluminum casting should be investigated as this would avoid difficult machining problems.

The damping fluid is Dow Corning 200 Silicone fluid. A viscosity of 20 centistrokes is used for this sample design.

(vi) Drive Elements

The tines are driven by the varying force which developes between two plates of a capacitor. One plate is the tine face and it is kept at zero potential. The other plate is mounted on the inner surface of the inner cylinder. This plate is mounted in an insulation mounting. Leads are provided to the rear of the plates. Power is brought through the top pivot via the contact point illustrated in the drawings.

(vii) Pickoffs

Three pickoff devices are suggested for use with this design. They are:

(1) Capacitative pickoff

(2) E-Bar variable reluctance pickoff

(3) Rotary Differential Transformer

In the capacitative pickoff, one plate is attached to the inner oscillating cylinder while the other is fixed to the outer stationary one. The variable area of the plates which results from the oscillation causes a capacitance change.

In this unit, provision for a lead to the inner plate would have to be made.

High frequencies, in the order of 5000 to 10,000 c.p.s. are suggested for a device of this type.

The support network can be either a resonant circuit, where frequency change is proportional to displacement, or a bridge circuit in which the unbalance is proportional to displacement.

Guarding against stray capacitances in such a circuit is difficult, but a very important factor in the successful operation of the device.

For the E-Bar type variable reluctance pickoff, no extra leads inside the inner cylinder would be required. A short length of soft iron would be fixed to the inner cylinder. The E section, with its coils, would be fixed to the outer case. The oscillations of the inner cylinder would vary the reluctance in the two opposing flux paths of the E element and on unbalance voltage proportional to displacement would be produced.

The Rotary Differential Transformer is another inductive-type pickoff consisting of a rotor and a wire-wound stator. The stator appears similar to that of a motor with teeth and slots except that the slots are abnormally wide. The primary and secondary windings of a two-phase motor, one displaced 90 electrical degrees around from the other. The rotor has the same number of teeth as the number of poles of either the primary or secondary and appears somewhat similar to the rotor of a reluctance motor except that the teeth are sharp concerned and just wide enough to reach from the center of one stator tooth to the center of the next.

In utilizing this pickoff a rod to carry the rotor would have to be attached to the base. One idea would have the torsion rod a hollow tube and the pickoff rod passing through the center of this rod. The transformer unit would then be attached to the bottom of the gyro case. A commercially available unit might be employed here.

(viii) Dampers

Damping of the resonant vibration is accomplished in this design by using the viscous action provided by a fluid in the gap between inner and outer cylinders.

Other damping means that could be employed are electromagnetic dampers or viscoelestic torsion springs on the output axis. The viscous damping approach was considered to be the most straightforward for the high g application. Volume is kept to a minimum as in the number of parts and power leads. Nonlinearities are also avoided.

16.5 SENSING ELECTRONICS

For a non-rotating tuning fork, the total torque acting about the output (and the sensing) axis is the sum of the Coriolis torque and cross-coupling torques. The Coriolis torque depends only on the rate about the input axis and is independent of the rates about the other two axes.

When the insturment is rotated about one of these rate insensitive axes, however, torque components about the output axes occur not at just the resonant frequency as for the non-rotating case, but at three frequencies. That is,

$$M_{s} = M_{s+} + M_{sd} + M_{s-}$$

where

M_{s} = total torque

M_{s+} = torque at frequency

M_{sd} = torque at frequency

M_{s-} = torque at frequency

By proper signal processing it is possible to have the instrument respond to either the upper or lower sideband signals to the exclusion of the other two.

In the proposed system the additional rotation of the fork is accomplished by the spinning vehicle. The frequency of this signal modulation is the spin frequency of the vehicle.

Further mathematical details of this mechanism of double signal modulation are given in Chapter 14, Section (14.13). A sample electronics network block diagram is shown as Figure (14.8) of this section. This network will sort out the required input rate.

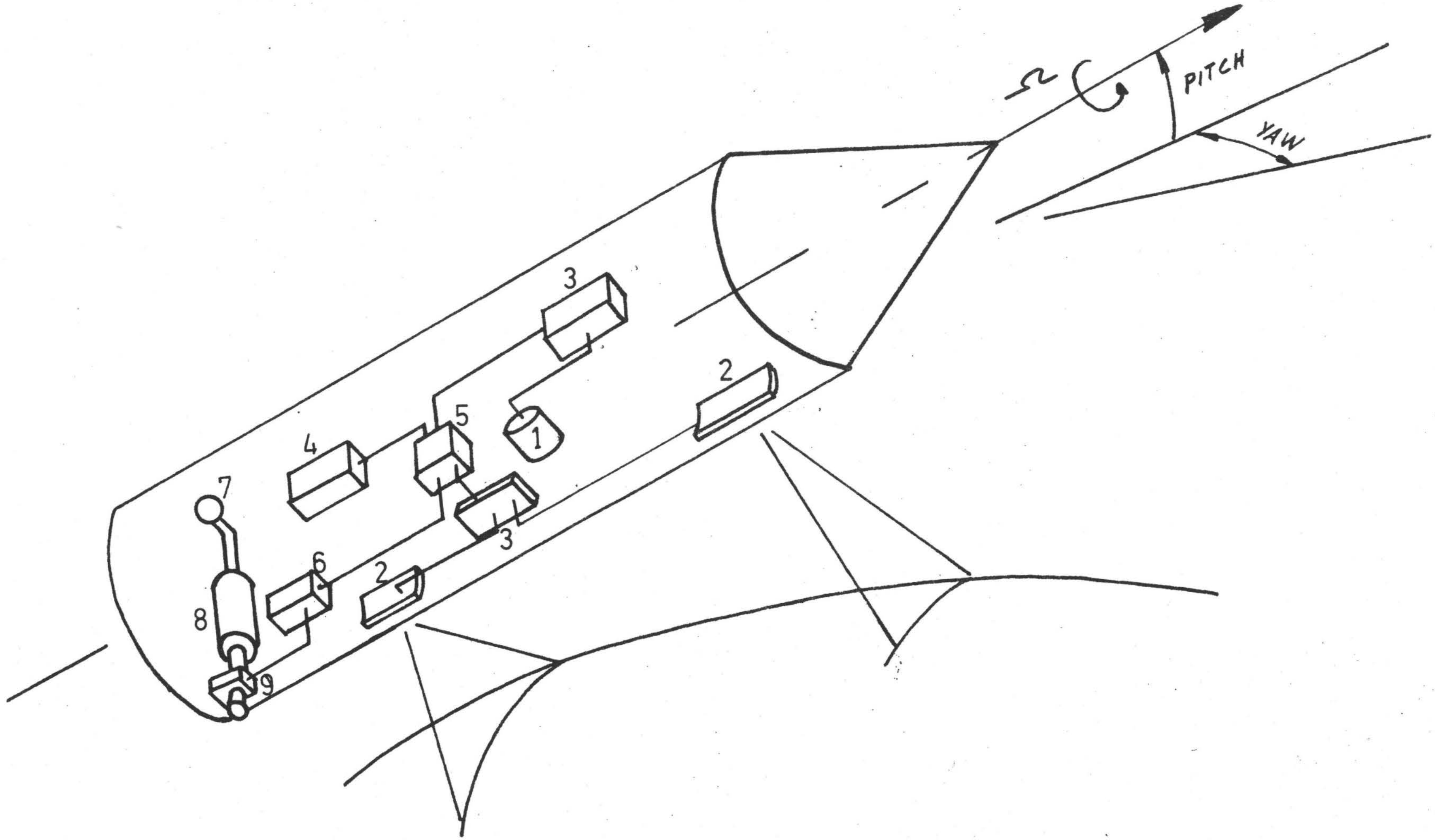

1 VIBRATORY GYRO
2 INFARED SENSORS
3 SIGNAL PROCESSING ELECTRONICS
4 REFERENCE SIGNAL STORAGE
5 ERROR SIGNAL ELECTRONICS
6 VALVE SIGNAL ELECTRONICS
7 GAS RECEIVER
8 PRESSURE REGULATOR
9 SOLENOID NOZZLE VALVE

TITLE: CONTROL SYSTEM SCHEMATIC	
SCALE: NONE	SOURCE:
DRAWN BY: HILL	FIGURE NO: 16-1

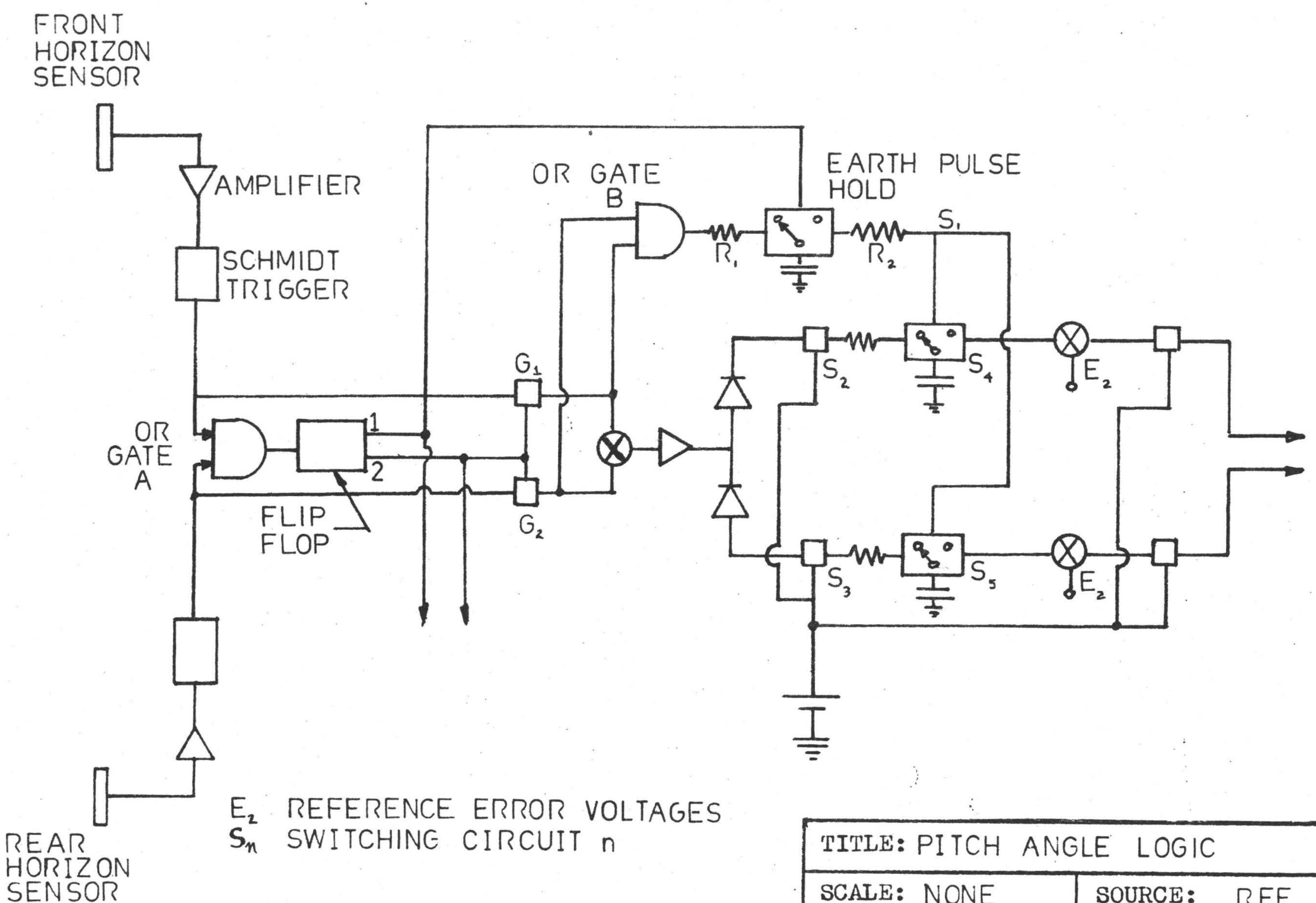

E_2 REFERENCE ERROR VOLTAGES
S_n SWITCHING CIRCUIT n

TITLE: PITCH ANGLE LOGIC	
SCALE: NONE	SOURCE: REF.
DRAWN BY: HILL	FIGURE NO: 16-2

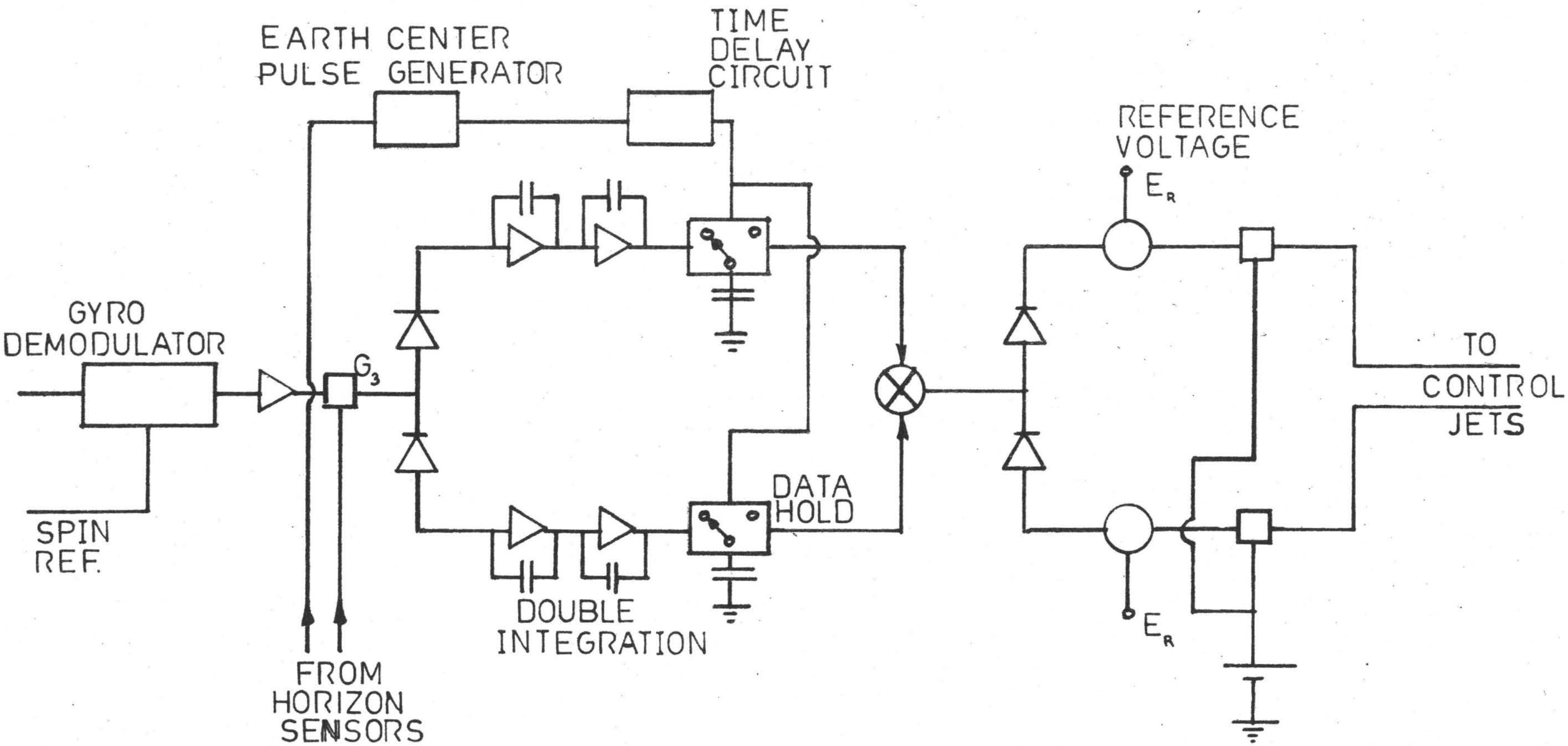

TITLE: YAW ERROR LOGIC	
SCALE: NONE	SOURCE:
DRAWN BY: HILL	FIGURE NO: 16-3

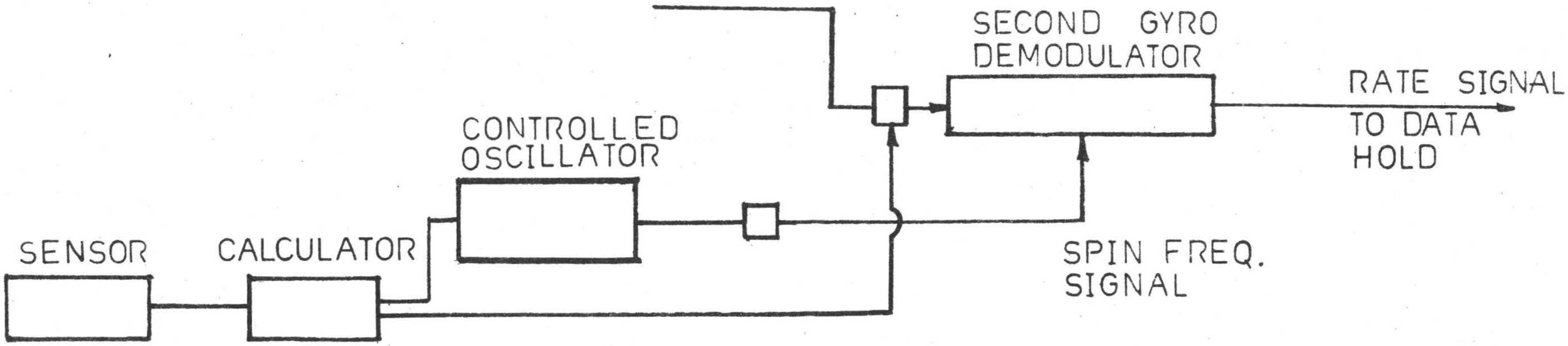

NOTE: CALCULATOR FINDS AVERAGE FREQUENCY OVER N PERIODS AND CONTROLS OSCILLATOR ACCORDINGLY. IF FREQUENCY OF SPIN DETECTED BY SENSOR VARIES OUTSIDE OF SET LIMITS, THE CALCULATOR STOPS THE DEMODULATION AND RESETS THE OSCILLATOR TO A NEW AVERAGE FREQUENCY.

SPIN SENSOR

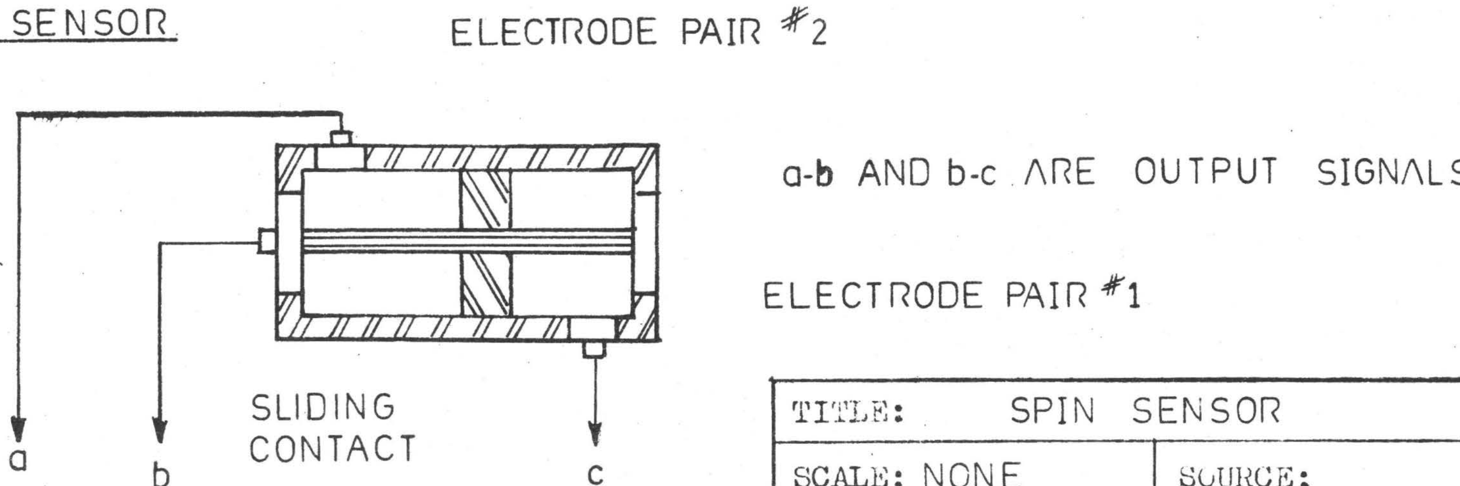

TITLE: SPIN SENSOR	
SCALE: NONE	SOURCE:
DRAWN BY: HILL	FIGURE NO: 16-4

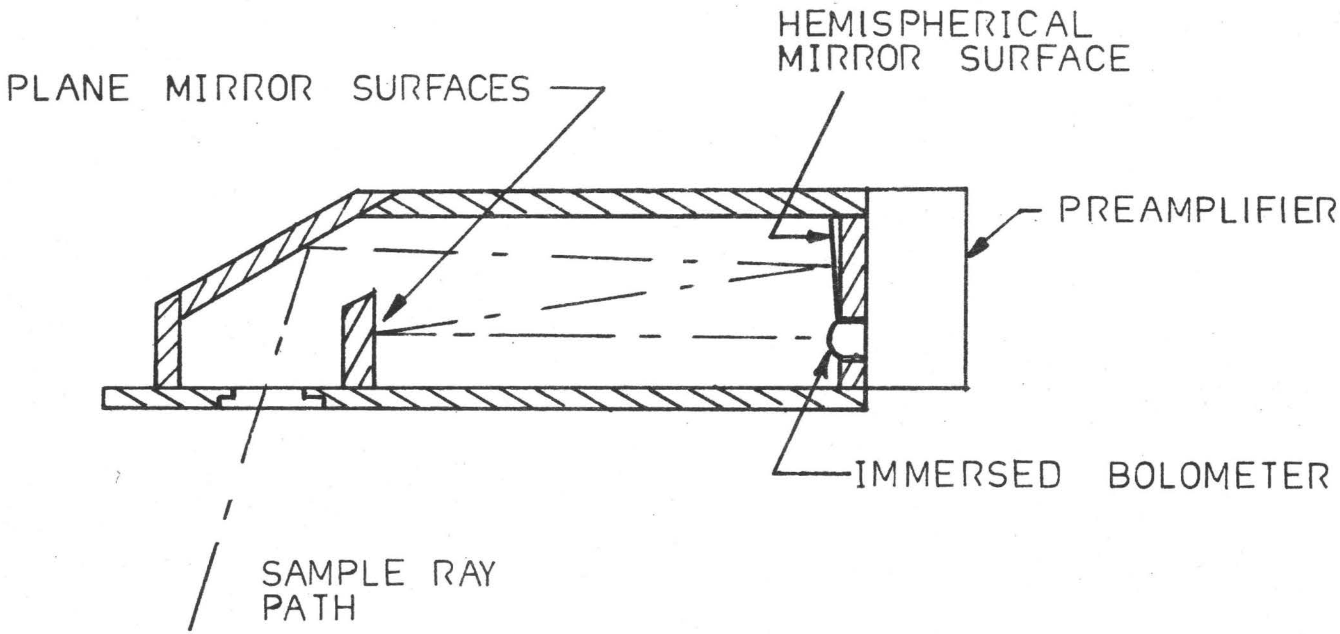

TITLE: INFARED HORIZON SENSOR	
SCALE: NONE	SOURCE:
DRAWN BY: HILL	FIGURE NO: 16-5

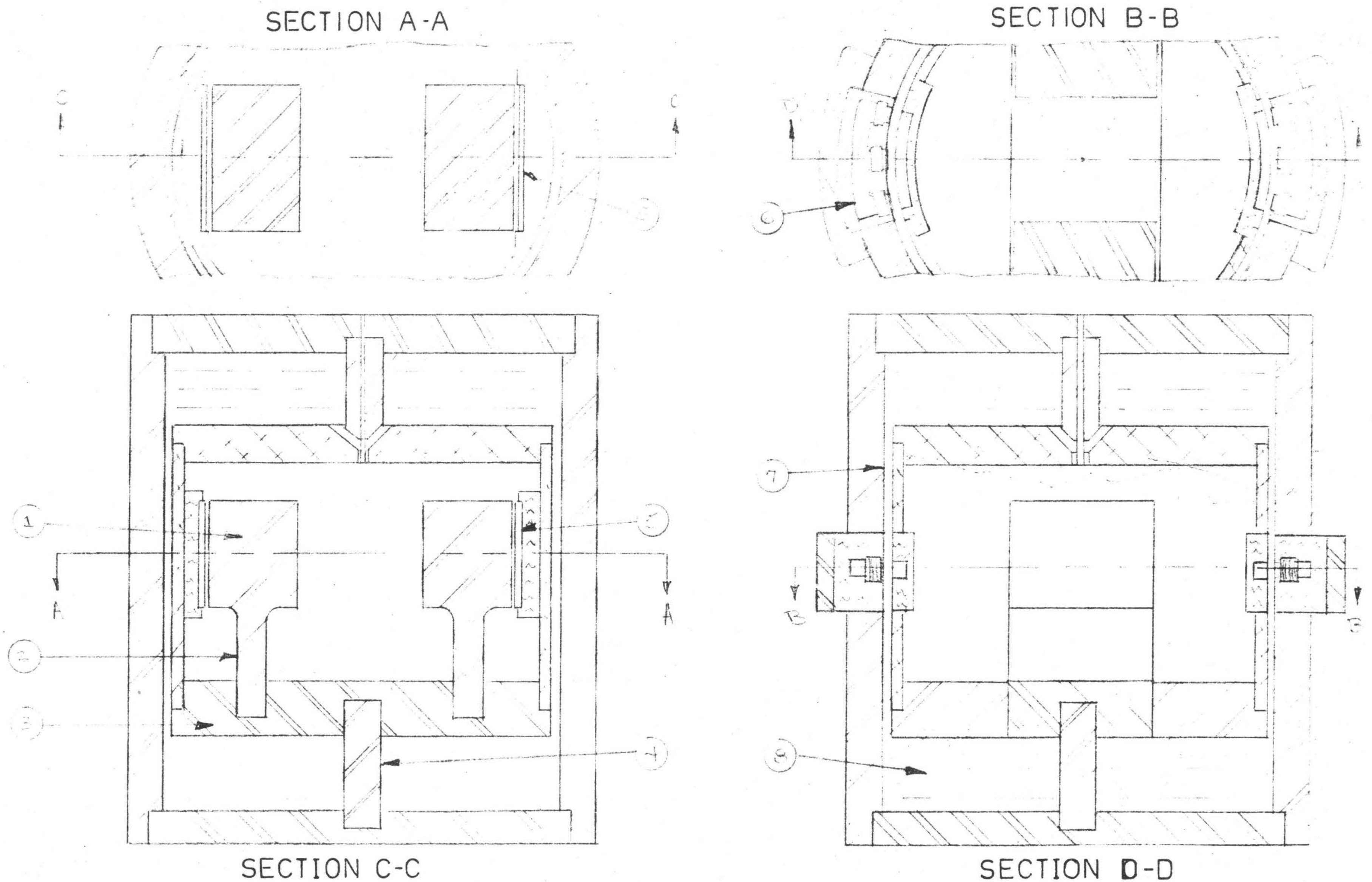

1 MASSES
2 TINES
3 BASE
4 TORSION SPRING
5 DRIVING ELECTRODES
6 E-I PICKOFF
7 DAMPING GAP
8 DAMPING FLUID

TITLE: DETAIL DRAWING OF GYRO	
SCALE: NONE	SOURCE:
DRAWN BY: HILL	FIGURE NO: 16-6

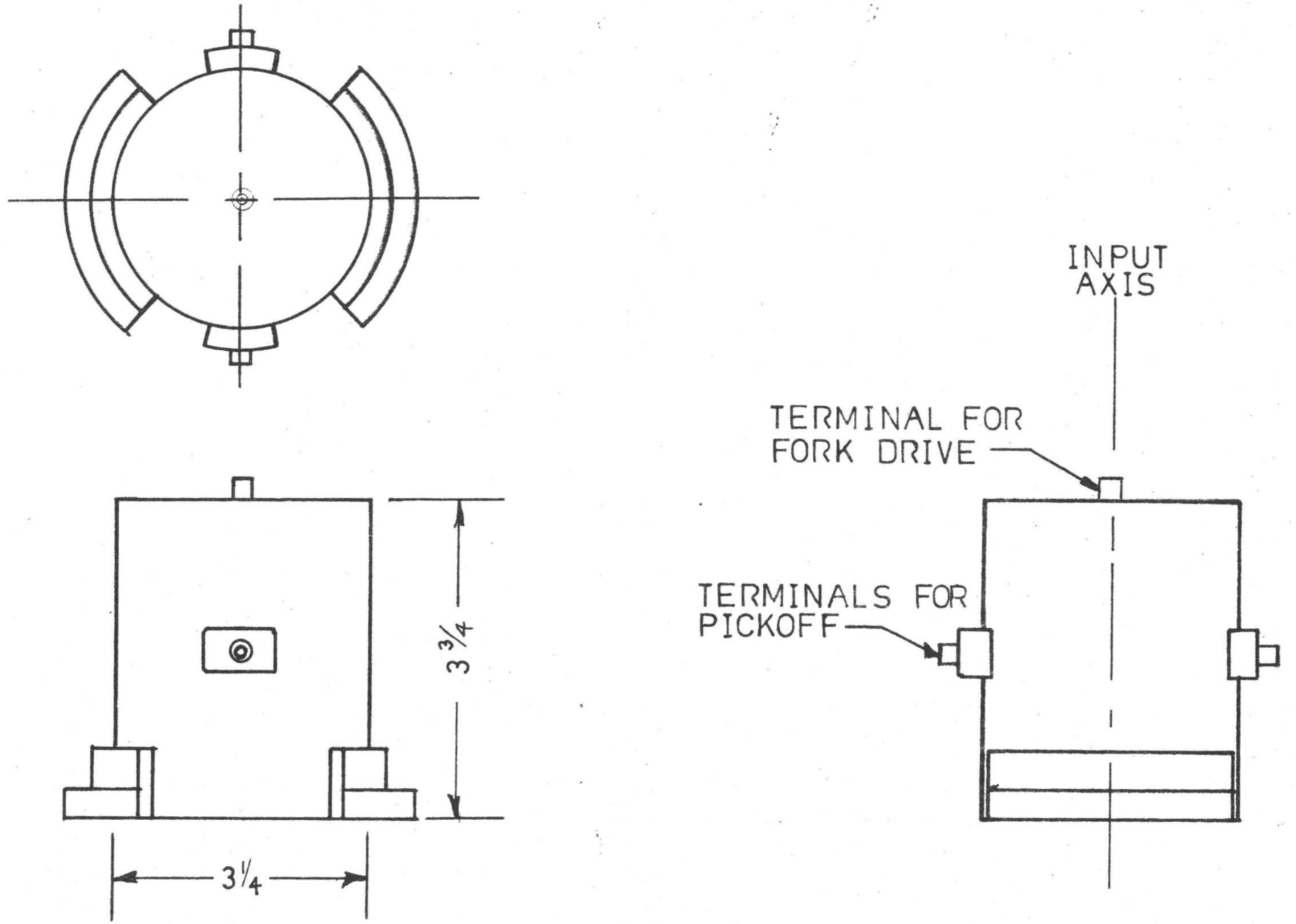

TITLE: OUTER CASE OF GYRO	
SCALE: NONE	SOURCE
DRAWN BY: HILL	FIGURE NO: 16-7

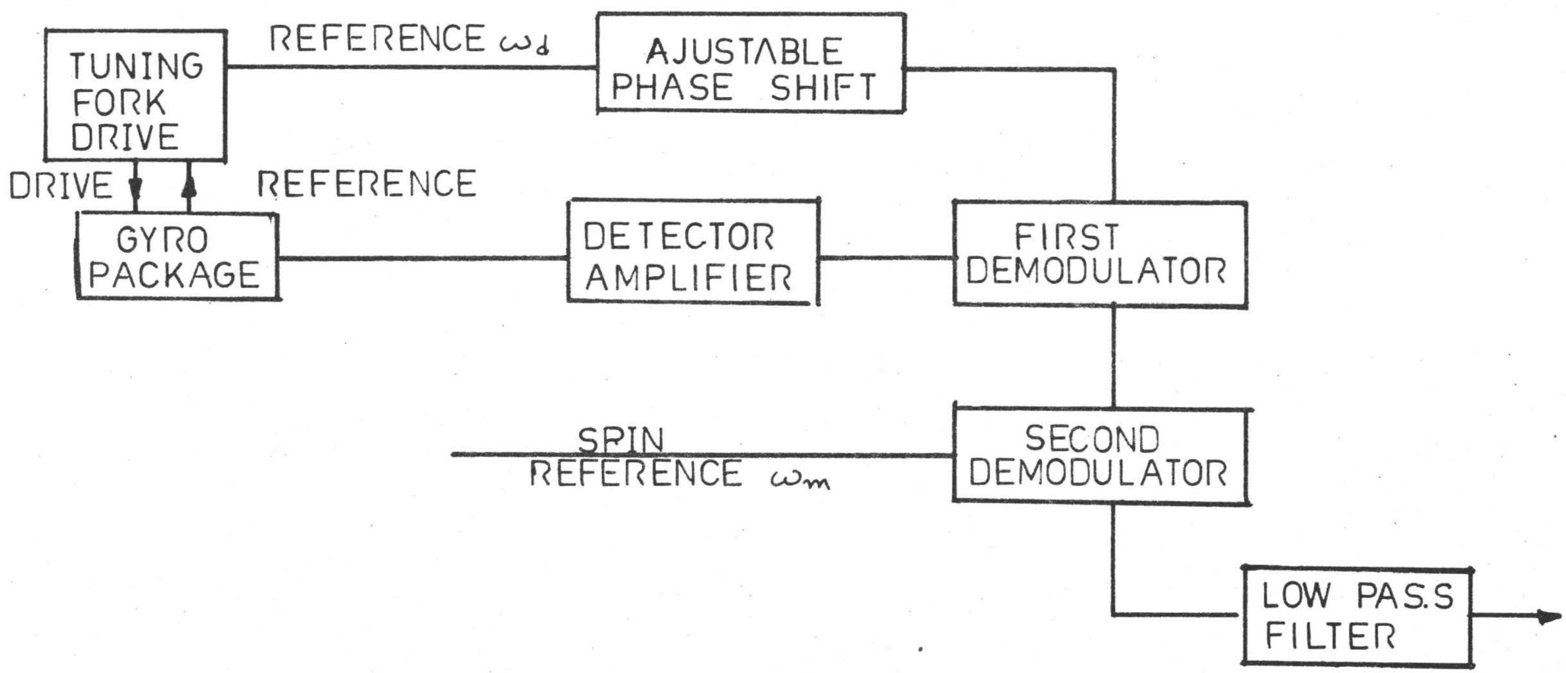

ω_d = TUNING FORK FREQUENCY
ω_m = DOUBLE MODULATION

TITLE: DOUBLE MODULATION CIRCUIT	
SCALE: NONE	SOURCE:
DRAWN BY: HILL	FIGURE NO: 16-8

REFERENCES

1. Aviation Electric Limited, "Martlet IV Orbit Injection Control System", Proposal No. 9290, Aviation Electric Ltd., Montreal, Canada, June 12, 1964.

2. Tse, F. S. and I. Morse and R. T. Hinkle, Mechanical Vibrations, Allyn and Bacon, Boston, 1963.

3. Savet, P. H., Gyroscopes, Theory and Design, McGraw-Hill, New York, 1961.

4. Thomson, W. T., Introduction to Space Dynamics, Wiley and Sons, New York, 1961.

5. Leondes, C. T., Guidance and Control of Aerospace Vehicles, McGraw-Hill, New York, 1963.

APPENDIX A

FLUID SPHERE GYRO ROTOR SUPPORT SYSTEM

APPENDIX A

FLUID SPHERE GYRO ROTOR SUPPORT SYSTEM

A-1 GENERAL

A support system for the rotor of the fluid sphere gyro was proposed and is shown in Figure A-1. The diagram illustrates the conditions for normal operation (lower half of diagram) and with the rotor support in place (upper half).

The system consists simply of several wedge blocks which fill the space between the ends of the case and the rotor.

A-2 OPERATION

(i) During Launch

The support blocks prevent the rotor case from moving along the spin axis during launch thereby preventing the bearing from an axial shock loading. (Which could cause its destruction).

(ii) After Launch

Electromagnets located around the outside of the core are energized and they lift the wedge blocks clear of the space they are filling. The normal operating condition shown in the bottom half of the diagram is thus regained.

A-3 COMMENTS

The system is simple and easy to operate. However, it requires extra power and increases the weight and volume of the gyro substantially.

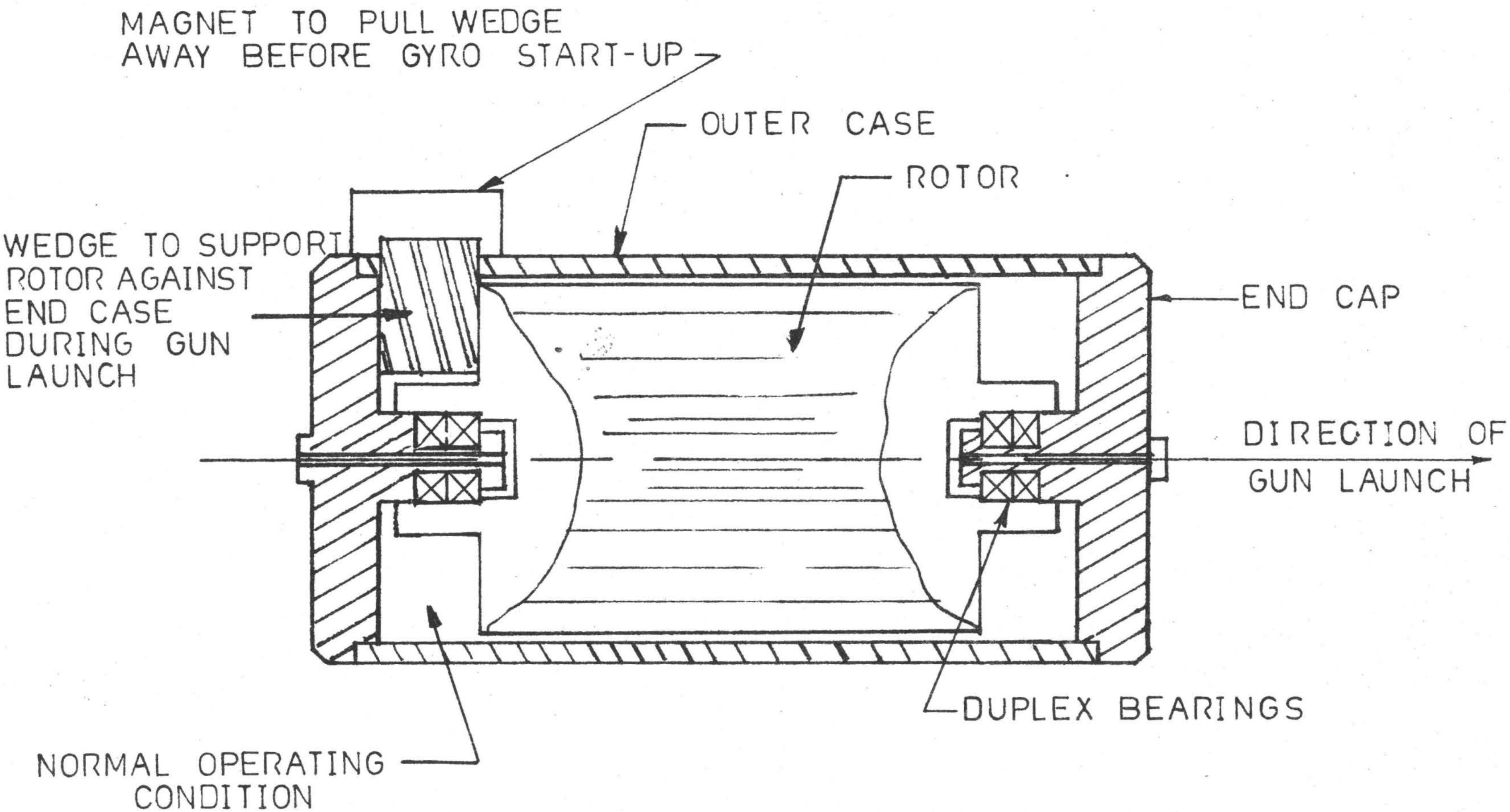

NOTE: ONLY ONE WEDGE IS SHOWN
3 OR 4 WOULD PROBABLY
BE REQUIRED

TITLE: FLUID GYRO SUPPORT	
SCALE: NONE	SOURCE:
DRAWN BY: HILL	FIGURE NO: 15-2

APPENDIX B

SOLID STATE GYRO SUPPORT SYSTEM

APPENDIX B

SOLID STATE GYRO SUPPORT SYSTEM

B-1 GENERAL

A support system for the sensitive element of the solid state gyro was designed and is shown in Figure B-1. The diagram illustrates the system condition both before launch (on the left half of the diagram) and after launch (on the right).

The system is composed of a gas supply, a gas flow control, the support blocks and a means of restraining the support blocks after gyro start-up.

B-2 OPERATION

(i) During Launch:

The support element is fitted over the ends of the cylindrical sensing element and held in place by a snap ring. The snap ring serves also as a seal for the gases that later enter the confines of the gyro case. In this first position, the support block prevents the gyro element from moving in the direction parallel to the launch direction (shown in the diagram).

(ii) After Launch:

The high threshold acceleration switch closes when subjected to gun launch acceleration and opens the solenoid valve, permitting high pressure gas to flow from storage into the gyro case. The gas (shown by the arrows) pushes against the face of the supports and pushes them to the extreme end of the gyro case. The snap rings then close in and lock the supports away from the gyro element. The gyro is then free to operate in its normal manner.

B-3 COMMENTS

The system is simple, has no moving parts and therefore should be reliable. However, it requires extra components external to its case which increases both the weight and volume of the unit.

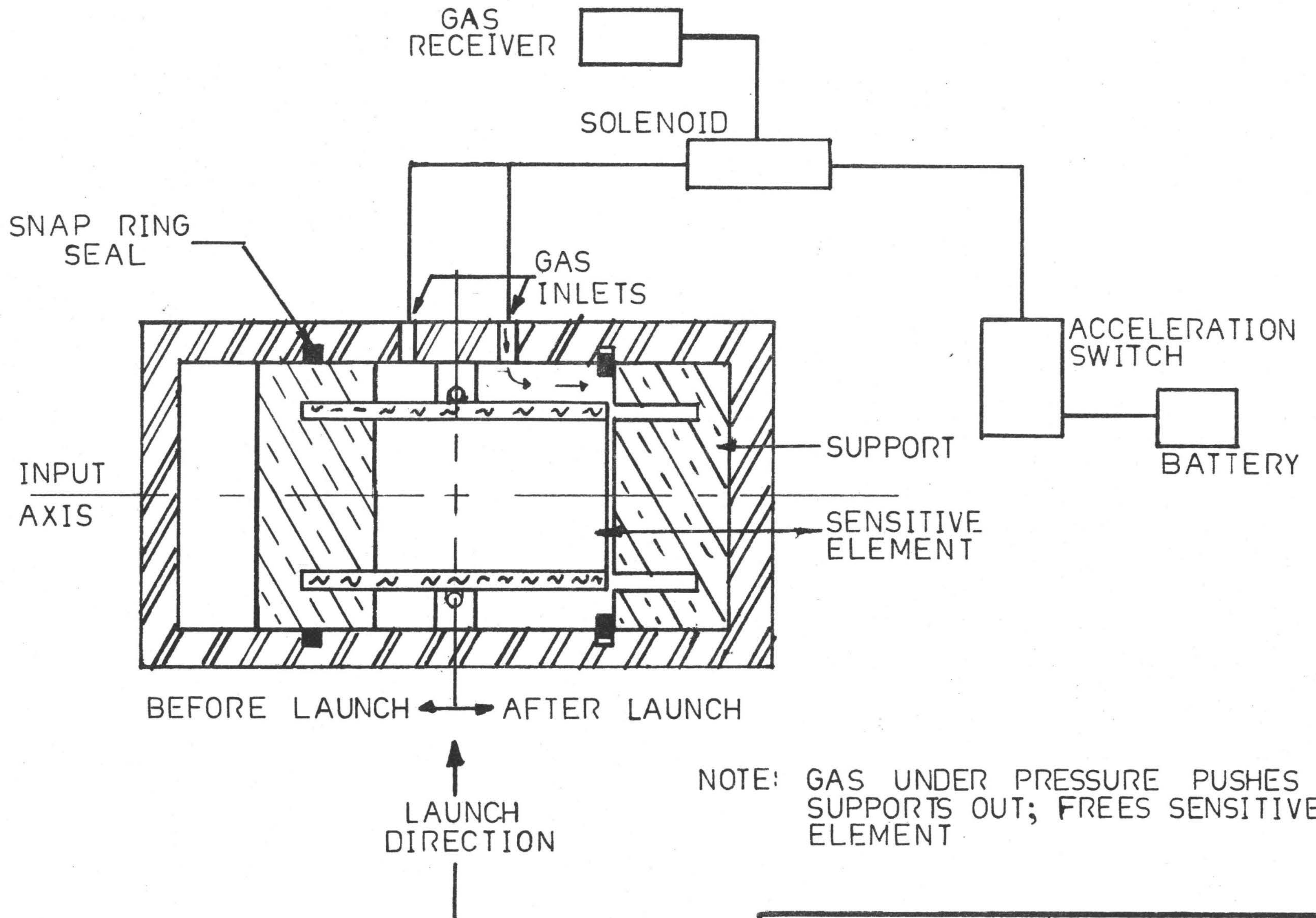

TITLE: SOLID STATE GYRO SUPPORT	
SCALE: NONE	SOURCE:
DRAWN BY: HILL	FIGURE NO: 15-1

APPENDIX C

SELECTED BIBLOGRAPHY

ON

ATTITUDE REFERENCE SYSTEMS

ATTITUDE REFERENCE SYSTEMS

The problem of sensing position and direction in space is a many sided one, with as many answers as there are systems. The following list of material has been compiled as a brief summary field of endeavour. The list is by no means complete but the material cited was found helpful to the author in his work on attitude reference systems. It is hoped that this list may be useful to others beginning work in this general area.

WORKS ON GENERAL THEORY OF ATTITUDE CONTROL SYSTEMS

1. Woestemeyer, F. B., "General Consider in the Selection of Altitude Control Systems", SAE Transactions, Paper #650591, 1965, 20 pp.

2. Langford, R. C., "Guidance and Control", Astronautics and Aerospace Engineering, Nov. 1963, 4 pp.

3. Keeler, R. J. and C. W. Benfield, "Injection Guidance", Astronautics, Nov. 1961, 4 pp. References.

4. DeLisle, J. E., B. M. Hildebrant and I. D. Petranic, "Attitude Control of Spacecraft", Astronautics, November 1961, 4 pp.

5. Otten, D. D., "Altitude Control for an Orbiting Observatory", Control Engineering, December 1963, 5 pp.

6. Gates, C. R., J. R. Scull and K. S. Watkins, "Space Guidance", Astronautics, November 1961, 11 pp.

7. Lillistrand, R. L. and J. E. Carroll, "Horizon Based Satellite Navigation Systems", IEEE Transactions on Aerospace and Navigational Electronics, September 1963, 24 pp.

8. Naqui, A. M. and R. J. Levy, "Some Astromonical and Geophysical Considerations for Space Navigation", IEEE Transactions on Aerospace and Navigational Electronics, September 1963, 26 pp. References.

9. Puckett, A. E. and S. Ramo, <u>Guided Missile Engineering</u>, McGraw-Hill, New York, 1961.

10. Leondes, C. T. (ed). <u>Guidance and Control of Aerospace Vehicles</u>, McGraw-Hill, 1963.